Formal Intramolecular Photoredox Reactions of Anthraquinones Mediated by Water

by

Yunyan Hou
B.Sc., Jilin University, 1995
M.Sc., Jilin University, 1998

A Dissertation Submitted in Partial Fulfillment
of the Requirements for the Degree of

DOCTOR OF PHILOSOPHY

in the Department of Chemistry

Supervisory Committee

Formal Intramolecular Photoredox Reactions of Anthraquinones Mediated by Water

by

Yunyan Hou
B.Sc., Jilin University, 1995
M.Sc., Jilin University, 1998

Supervisory Committee

Dr. Peter Wan, (Department of Chemistry)
Supervisor

Dr. Natia Frank, (Department of Chemistry)
Departmental Member

Dr. Alexandre G. Brolo, (Department of Chemistry)
Departmental Member

Dr. Michel Lefebvre, (Department of Physics and Astronomy)
Outside Member

Abstract

Supervisory Committee

Dr. Peter Wan, (Department of Chemistry)
Supervisor
Dr. Natia Frank, (Department of Chemistry)
Departmental Member
Dr. Alexandre G. Brolo, (Department of Chemistry)
Departmental Member
Dr. Michel Lefebvre, (Department of Physics and Astronomy)
Outside Member

The formal intramolecular photoredox reaction initially discovered for the parent 2-(hydroxymethyl)-9,10-anthraquinone (**HMAQ**) in aqueous solution was extended to a variety of anthraquinone derivatives **2.1-2.9**, biphenyl anthraquinones **3.1-3.4** and acenequinones **4.1-4.4**. The purpose of the study was to explore the generality of the unique photochemical reaction involving **HMAQ**, understand the mechanism of the reaction and develop potential applications.

All the anthraquinones studied (except for **2.4**) undergo the formal intramolecular photoredox reaction with a range of quantum yields (Φ = 0.02-0.7). Mechanistic studies based on the parent compound **HMAQ** were carried out by product studies, isotope effects, solvent deuterium isotope effects, pH effect, triplet quenching studies, and laser flash photolysis. It was found that the formal intramolecular photoredox reaction involves a highly polarized triplet excited state in which the electron density of the benzylic CH_2OH moiety is transferred to the central anthraquinone ring. This highly polarized triplet excited state is subsequently trapped adiabatically by protonation at the anthraquinone carbonyl oxygen.

Designed anthraquinones **2.2**, **2.3, 2.5** and **2.6** successfully photoreleased "protected" alcohol, aldehyde, or ketone with good yields (80-90 %), respectively, and shows that the anthraquinon-2-yl chromophore is potentially useful for photocaging in aqueous solution. In addition, diketone **2.9** undergoes an analogous photoredox reaction but only in acid ($\Phi = 0.003$, pH < 1), to give the formal redox product diphenylisobenzofuran **2.29**, thereby demonstrating that other aromatic diketones can react in an analogous fashion.

Biphenyl and terphenyl analogs **3.1-3.4** in which the oxidizable benzyl alcohol group is significantly further away from the anthraquinone moiety were designed to explore the effect of the distance between CH_2OH and carbonyl group on the efficiency of the intramolecular photoredox reaction. All of these compound undergo a clean and efficient formal intramolecular photoredox reaction in water catalyzed by acid ($\Phi = 0.1$-0.6). Triplet quenching studies and laser flash photolysis support a mechanism involving reactive triplet excited states. Laser flash photolysis also detected a long-lived and pH dependent transient which might be assigned to an enol intermediate.

A number of acenequinones were also designed to explore the intramolecular photoredox reaction for higher benzannelated systems. In particular, we were interested in whether the photoredox reaction could be applied to 2-(hydroxymethyl)-6,13-pentacenequinone (**4.1**) which would result in 2-formyl-6,13-dihydroxypentacene (**4.5**) and hence offer a photochemical method for synthesizing a pentacene derivative. Whereas a number of related acenequinones displayed a range of photoredox reactivity, photolysis of **4.1** in acidic aqueous solution (pH < 3) resulted in a clean intramolecular Photoredox reaction, via an enol intermediate, to give **4.5** (green compound; $\Phi \sim 0.2$ at pH 1). Thus the photoredox reaction is reasonably general for acenequinones.

Table of Contents

List of Tables

List of Figures

List of Schemes

List of Numbered Compounds-Names

HMAQ	2-(hydroxymethyl)-9,10-anthraquinone
DHA	2-formyl-9,10-dihydroxyanthraquinone
FAQ	2-formyl-9,10-anthraquinone
HMAQ-αD	α-D-2-(hydroxymethyl)-9,10-anthraquinone
HMAQ-a	2-methyl-9,10-anthraquinone
2.1	2-(1-hydroxyethyl)-9,10-anthraquinone
2.2	2-(ethoxymethyl)-9,10-anthraquinone
2.3	2-(1-methoxyethyl)-9,10-anthraquinone
2.4	2-(acetoxymethyl)-9,10-anthraquinone
2.5	9-phenyl-7,11-dihydro-8,10-dioxa-cyclohepta [b]anthracene-5,13-dione
2.6	9-methyl-9-phenyl-7,11-dihydro-8,10-dioxa-cyclohepta [b]anthracene-5,13-dione
2.7	2,3-di(hydroxymethyl)-9,10-anthraquinone
2.8	2-[1,3]dioxolan-2-yl-9,10-anthraquinone
2.9	1,2-dibenzoyl-4-methylbenzene
2.11	2-acetyl-9,10-anthraquinone
2.14	1-hydroxy-1,3-dihydro-anthra[2,3-*c*]furan-5,10-dione
2.16	3*H*-anthra[2,3-*c*]furan-1,5,10-trione
2.18	9,10-dioxo-9,10-dihydroanthracene-2-carboxylic acid 2-hydroxy-ethyl ester
2.29	1,3-diphenyl-isobenzofuran-5-carbaldehyde
2.30	1,2-dibenzoyl-4-formylbenzene

2.34	2-formyl-9,10-diacetoxyanthracene
2.35	2-(hydroxymethyl)-9,10-diacetoxyanthracene
3.1	2-(*o*-hydroxymethylphenyl)-9,10-anthraquinone
3.1a	2-(*o*-methylphenyl)-9,10-anthraquinone
3.2	2-(*m*-hydroxymethylphenyl)-9,10-anthraquinone
3.2a	2-(*m*-methylphenyl)-9,10-anthraquinone
3.3	2-(*p*-hydroxymethylphenyl)-9,10-anthraquinone
3.3a	2-(*p*-methylphenyl)-9,10-anthraquinone
3.4	2-(*p*-hydroxymethylbiphenyl)-9,10-anthraquinone
3.4a	2-(*p*-methylbiphenyl)-9,10-anthraquinone
3.8	2-(*o*-formylphenyl)-9,10-anthraquinone
3.9	2-(*m*-formylphenyl)-9,10-anthraquinone
3.10	2-(*p*-formylphenyl)-9,10-anthraquinone
3.11-OAc	2-(*p*-formylbiphenyl)-9,10-diacetoxyanthracene
3.14	2-(*p*-formylphenyl)-9,10-diacetoxyanthracene
4.1	2-(hydroxymethyl)-6,13-pentacenequinone
4.1a	2-methyl-6,13-pentacenequinone
4.2	6-(hydroxymethyl)-1,4-naphthoquinone
4.2a	6-methyl-1,4-naphthoquinone
4.3	6-(hydroxymethyl)-1,4-anthraquinone
4.3a	6-methyl-1,4-anthraquinone
4.4	2-(hydroxymethyl)-5,12-naphthacenequinone
4.6	2-formyl-6,13-pentacenequinone

4.7-OAc 6-formyl-1,4-diacetoxynaphthalene

4.8 6-formyl-1,4-naphthoquinone

4.9 6-formyl-1,4-anthraquinone

List of Numbered Compounds-Structures

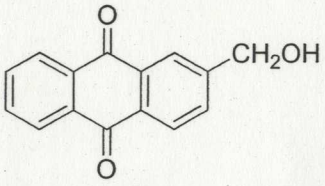

HMAQ

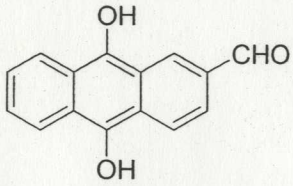

DHA

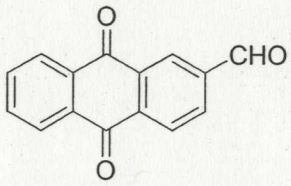

FAQ

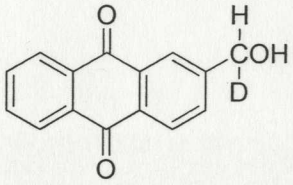

HMAQ-αD

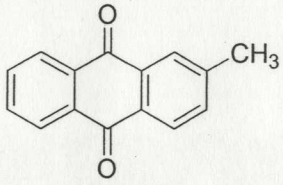

HMAQ-a

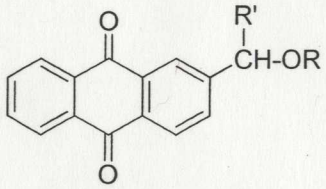

2.1 R = H; R' = CH_3
2.2 R = CH_2CH_3; R' = H
2.3 R = R' = CH_3
2.4 R = $COCH_3$; R' = H

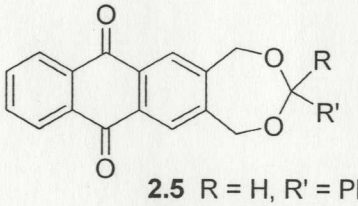

2.5 R = H, R' = Ph
2.6 R = CH_3, R' = Ph

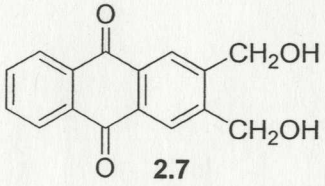

2.7

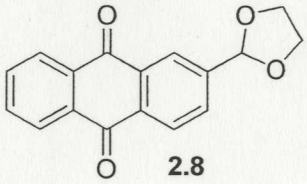

2.8

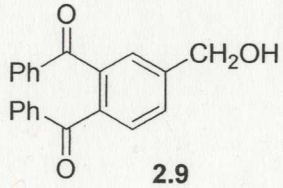

2.9

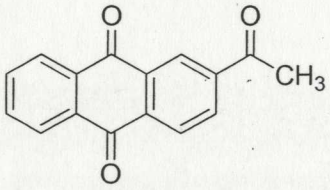

2.11

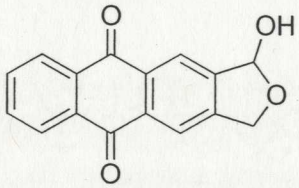

2.14

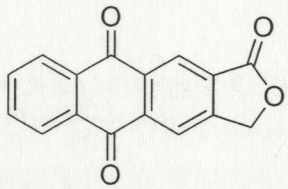

2.16

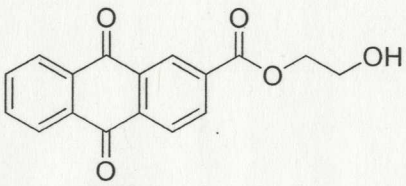

2.18

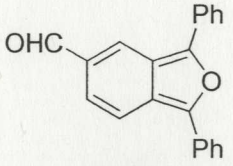

2.29

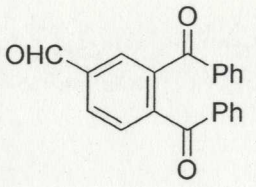

2.30

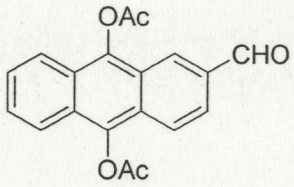

2.34

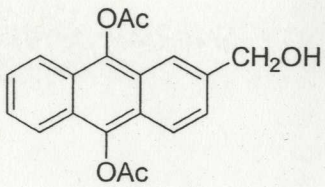

2.35

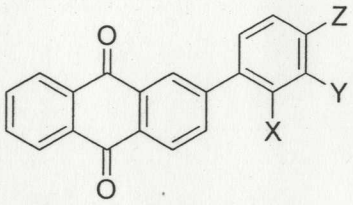

3.1 X = CH_2OH; Y = Z = H
3.1a X = CH_3; Y = Z = H
3.2 X = Z = H; Y = CH_2OH
3.2a X = Z = H; Y = CH_3
3.3 X = Y = H; Z = CH_2OH
3.3a X = Y = H; Z = CH_3
3.8 X = CHO; Y = Z = H
3.9 X = Z = H; Y = CHO
3.10 X = Y = H; Z = CHO

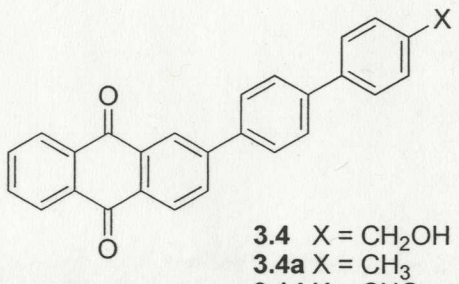

3.4 X = CH_2OH
3.4a X = CH_3
3.14 X = CHO

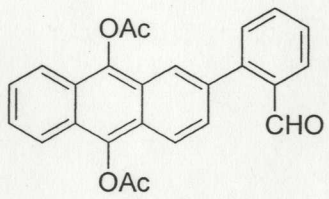

3.11-OAc

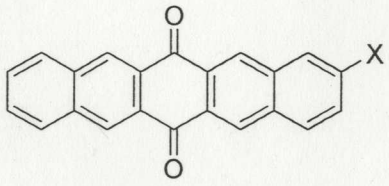

4.1 X = CH_2OH
4.1a X = CH_3
4.6 X = CHO

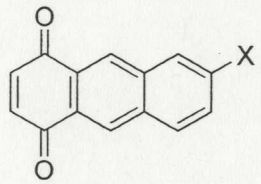

4.3 X = CH_2OH
4.3a X = CH_3
4.9 X = CHO

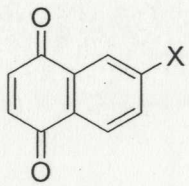

4.2 X = CH_2OH
4.2a X = CH_3
4.8 X = CHO

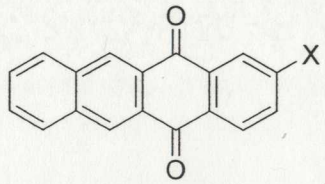

4.4

List of Abbreviations

A	absorbance
AQ	9,10-anthraquinone
Ac_2O	acetic anhydride
cm^{-1}	units of wavenumber
conc.	Concentrated
DME	dimethylethane
DMSO	dimethylsulfoxide
EtOAc	ethyl acetate
eV	electron volt
g	gram
h	hours
HOMO	highest occupied molecular orbital
HRMS	high resolution mass spectrometry
Hz	Hertz
IR	infrared
ISC	intersystem crossing
J	coupling constant
LUMO	lowest unoccupied molecular orbital
m	meta
M^+	molecular ion
mg	milligram

min	minutes
mL	milliliter
mmol	millimoles
M	molarity
MO	molecular orbital
mp.	melting point
MS	mass spectrometry
m/z	mass per charge
nm	nanometer
NBS	*N*-bromosuccinimide
NMR	nuclear magnetic resonance
p	para
Ph	phenyl
ppm	parts per million
q	quartet (NMR descriptor)
t	triplet (NMR descriptor)
THF	tetrahydrofuran
TLC	thin layer chromatography
UV-Vis	ultraviolet-visible
°C	degree Celsius
δ	chemical shift in parts per million
λ_{max}	maximum absorption wavelength
λ_{ext}	excitation wavelength

λ_{em}	emission wavelength (fluoresecene)

Acknowledgments

I would like to express the deepest gratitude to my supervisor, Dr. Peter Wan, for his encouragement, patience, guidance and support from the initial to the final stages of my studies at the University of Victoria. I am impressed by his prudence in science and enthusiasm in research. As a result, my research life has been smooth and rewarding.

All the lab workers in Dr. Wan's group (past: Nicola Basaric, Erin Dallin, Devin Mitchell; current: Niloufar Behin Aein, Alfredo Franco Cea) made a friendly and convivial environment to work in. I especially thank Dr. Nikola Basaric for his help and inspiration in my study and research.

A special thank goes to Dr. Cornelia Bohne, her group members and Luis Netter for their technical support on LFP and fluorescence measurements. I would also like to thank Dave McGillivary for MS and Chris Greenwood for NMR.

Finally, thanks to my family for their encouragement and support.

Dedication

To my mother and my husband

1. Introduction

1.1 Redox Reactions

Oxidation-reduction (also called redox reaction), a simple and important chemical process, involves the loss and gain of electrons within molecules that result in their overall oxidation and reduction. Redox reactions are very common and essential to life. They occur frequently, such as in the rusting of iron, combustion of coal, and in the photosynthesis of plants. In organic synthesis, redox reactions are widely employed to prepare a large variety of organic compounds.[1] Redox reactions also play an important role in biological processes for the storage and release of energy.[2]

Due to the importance of the redox reaction, it is not surprising that there is great interest on the details of this process and countless papers have been published. A number of reviews[3] have also been published on the redox process, either initiated thermally, e.g. enzyme or metal catalyzed, or photochemically. For example, methanol is not harmful, but ingestion of methanol could result in blindness. This is because the oxidation of methanol catalyzed by alcohol dehydrogenase (an enzyme) generates toxic formaldehyde[4]. The biochemical process involves oxidization of methanol via an important coenzyme-NAD^+ (oxidizing reagent) catalyzed by dehydrogenase, to produce formaldehyde (eqn. 1.1). To treat methanol ingestion, ethanol[5] or fomepizole[6] is given to the patient by intravenous injection. Alcohol dehydrogenase has a much bigger affinity for ethanol or fomepizole than it has for methanol. Thus, there is less of a chance for methanol to be oxidized due to the fact that most of alcohol dehydrogenase will be loaded with ethanol or fomepizole.

$$CH_3OH + NAD^+ \xrightarrow[\text{dehydrogenase}]{\text{alcohol}} HCHO + NADH + H^+ \quad (1.1)$$

1.2 Basic Photophysical and Photochemical Processes

An organic molecule might undergo photophysical and/or photochemical processes after excitation to an electronic excited state. Photophysical processes result in no net chemical change and are further classified as a radiative or radiationless transition. As shown in Figure 1.1 (simplified Jabłonski diagram),[7] a molecule in the ground state (S_0) absorbs a photon and is promoted to an excited singlet state (S_1 S_2……)(→) at different vibrational levels. The electronic excited state undergoes an isoenergetic radiationless process, internal conversion (IC)(⇝) followed by vibrational relaxation to arrive at the lowest level S_1 (⇝). The molecule in the S_1 state may then undergo internal conversion followed by vibrational relaxation or radiative emission (fluorescence) back to the ground state S_0. The former emits heat (⇝) and the latter emits light (⇢). A change in spin multiplicity on the excited state results in transformation from the singlet excited to the triplet excited state (T_1, T_2……) via intersystem crossing (ISC)(⇝). The triplet excited state (T_1) relaxes to the ground state (S_0) via phosphorescence (⇢) or intersystem crossing (ISC) followed by vibrational relaxation (⇝).

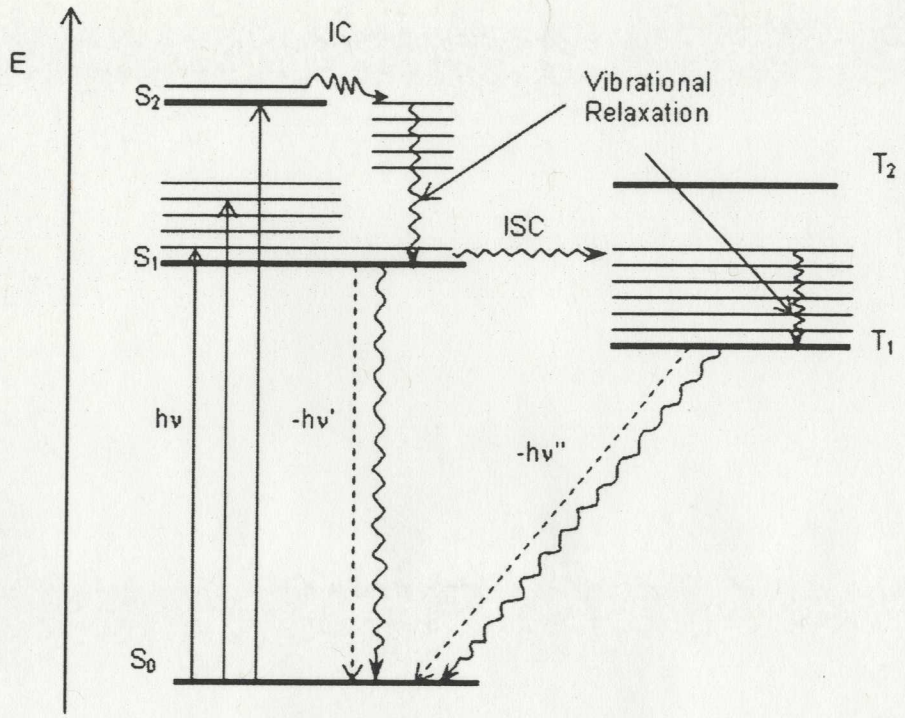

Figure 1.1 Photophysical processes as shown in a simplified Jabłonski diagram

Different from photophysical processes, photochemical processes result in net chemical change due to formation of photoproducts. The reactant in the ground state (**R**) absorbs photons to create an electronic excited state (***R**) which transforms to products (**P**)(eqn. 1.2). Due to the operation of photophysical processes that compete with the photochemical pathway, in order to observe photochemistry, the photochemical processes must be faster (as measured by their respective rate constants) than the sum of all deactivative photophysical processes, $k_p > \Sigma k$ (k_p: the rate constant for formation of products, Σk: the sum of all the rate constants for photophysical decay). Many photochemical reactions proceed from triplet excited states rather than singlet excited states because the former is much longer lived than the latter, although singlet excited states can be photochemically reactive as well.

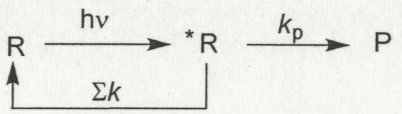

(1.2)

Chemists are also interested in how photochemical processes occur by understanding mechanisms of reactions. Photochemical processes may involve many possible pathways to form products, and many of these involve formation of intermediates such as radical pairs, biradicals, carbenes, zwitterions, etc.

Studying a photochemical reaction may include preparative irradiations as well as mechanistic studies. Preparative irradiation requires light sources and photochemical reactors. Light sources such as mercury arc lamps, deuterium lamps, and xenon lamps emit over certain wavelengths. The proper irradiation wavelength is chosen by measuring the absorption spectra of compounds.

A photochemical reactor consists of lamps, a reaction vessel, a cooling system and a degassing system. The reaction vessel should be transparent to the wavelength of excitation. A cooling system is used to prevent any competing thermal reaction. A degassing system is used for the removal of oxygen which is known to quench triplet excited states and react with free radicals and other intermediates.[8]

Photoproducts generated by preparative irradiation are directly characterized by NMR, IR, UV-Vis spectroscopy and mass spectrometry.[9] Mechanistic studies involve measuring quantum yields, and studying various pH and solvent effects.[9] In addition, direct information regarding mechanism, including the possibility of a reactive triplet excited state and existence of short-lived intermediates, may be gathered by time-resolved spectroscopy such as nanosecond laser flash photolysis (LFP).[9] Additional information

about triplet state reactions may also be obtained by using triplet quenching and sensitization experiments.[9]

1.3 Photoredox Reactions

Redox reactions initiated by electronic excitation are called photoredox reactions. The most important example is photosynthesis. The Earth is a huge chemical factory and most of its energy is derived from solar irradiation. In this huge chemical factory, photosynthesis is the most important process that produces two essential compounds for living organisms: oxygen and carbohydrates. Photosynthesis involves the well-known photochemical redox reaction in which electron transfer induced by light results in the oxidation of H_2O and the reduction of CO_2. The former generates O_2 and the latter generates carbohydrates (glucose).[10]

An electronic excited molecule is more reactive than its ground state because of the promotion of an electron from the HOMO to a higher energy LUMO. Occupancy of the LUMO results in a lower oxidation potential (P_{ox}) and a larger reduction potential (P_{red}) in the excited state than in the ground state (Fig. 1.2). Consequently, the electronically excited molecule is both easier to lose or gain an electron than its ground state. Thus, it is not hard to understand that electronic excited molecules are both strong oxidants and reductants and in principle can readily undergo photoredox reactions.

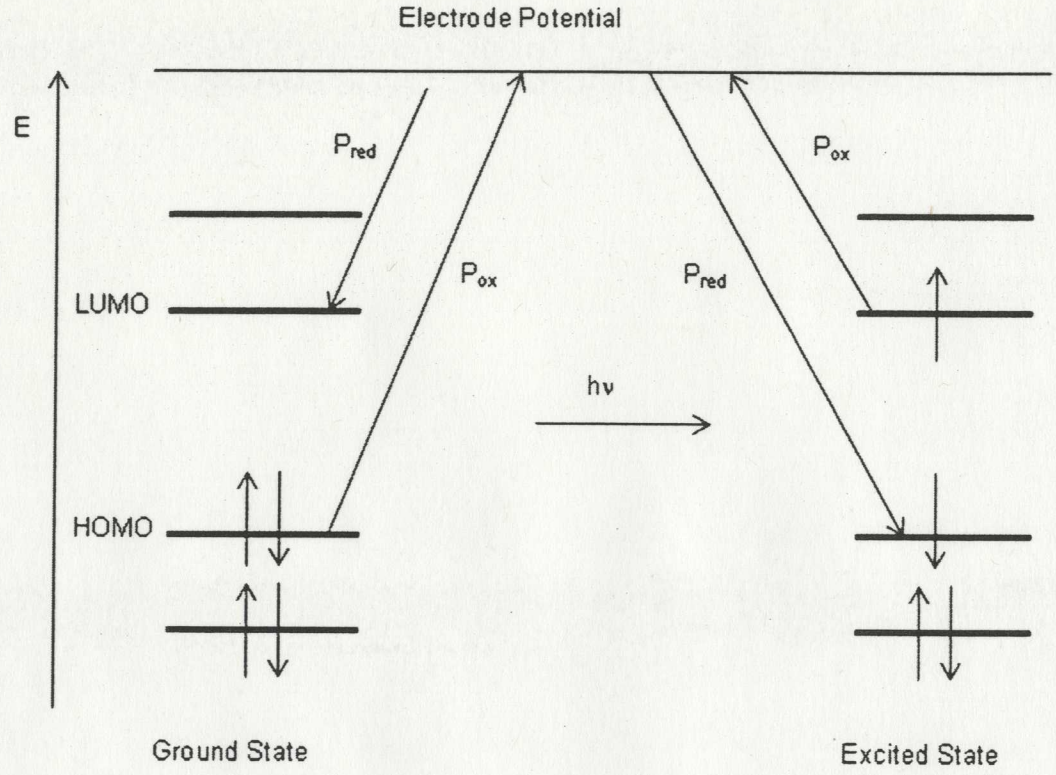

Figure 1.2 Redox potentials in ground and excited states

This Thesis focuses on intramolecular photoredox reactions which involve oxidation of one functional group and reduction of another functional group on the same molecule. To accomplish this, a molecule should have both an oxidizing moiety (electron acceptor) such as NO_2 or C=O, and a reducing moiety (electron donor) such as NH_2 or OH.

1.4 Photoredox Reactons of Nitroaromatic Compounds

Nitroaromatic compounds have played very important roles in organic synthesis and are also important precursors of dyes and explosives.[11] Although the first paper of photoinduced reactions of nitroaromatic compounds was published more than one century ago, studies on their photoactivity have gradually increased since 1960s due to the unique character and utility of the nitro group in organic photochemistry.[12]

The nitro group provides low-lying triplet excited states which enhance intersystem crossing.[12] Consequently, many of photochemical reactions of nitroaromatic compounds proceed via triplet excited states, of either π-π^* or n,π^* configuration.[13]

The intramolecular photoredox reaction of nitroaromatic compounds is a class of reactions resulting in the overall reduction of the nitro group, to give nitroso, and the oxidation of another functional group in the same molecule. Most of the known examples[13,14,15] involve ortho substituted nitrobenzyl derivatives and their primary mechanistic step is believed to involve hydrogen atom abstraction by the triplet excited nitro group (usually of the n,π^* configuration).

The well-known intramolecular photoredox reaction of *o*-nitrobenzaldehyde (**1.1**) gives *o*-nitrosobenzoic acid (**1.4**) in neat acetonitrile ($\Phi \sim 0.5$).[16] The proposed mechanism involves an intramolecular hydrogen atom transfer from the aldehyde in the triplet excited nitro group, to generate ketene **1.2**. Cyclization of **1.2** gives **1.3** which eventually undergoes rearrangement to lead to an overall reduction of the nitro group and oxidation of the aldehyde, to form the final photoredox product *o*-nitrosobenzoic acid (**1.4**) (Scheme 1.1). Picosecond LFP studies of **1.1** showed that the triplet excited state has a lifetime of 0.6 ns and that the intermediate ketene **1.2** has an absorption band centered at 440 nm.[16]

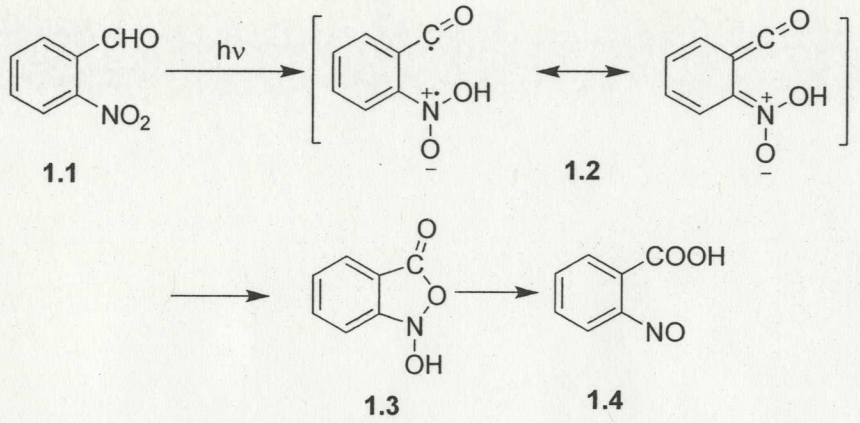

Scheme 1.1 Proposed mechanism for the intramolecular photoredox reaction of **1.1**

Consistent with the above mechanism, both meta- and para-substituted isomers were not expected to undergo photoredox reaction because the two functional groups are too far away to react via hydrogen atom abstraction and this is indeed the case when organic solvents are used. However, *p*-nitrobenzaldehyde (**1.5**) is the first example of a nitroaromatic compound that is not ortho-substituted but still undergoes a formal intramolecular photoredox reaction, but only in water. In the presence of water, photolysis of **1.5** gave *p*-nitrosobenzoic acid (**1.9**) ($\Phi \sim 0.034$ in 99:1 H_2O-CH_3CN) with the quantum yield dependent on the concentration of water.[17] The proposed mechanism (Scheme 1.2) involves electron transfer from water to the nitrophenyl triplet n,π* state, to generate the radical ion pair **1.6**, which undergoes quick proton transfer to generate the radical pair **1.7**. Subsequent hydrogen abstraction from the aldehyde hydrogen results in formation of quinoid ketene intermediate **1.8**, which ultimately gives the photoredox product *p*-nitrosobenzoic acid (**1.9**).[18]

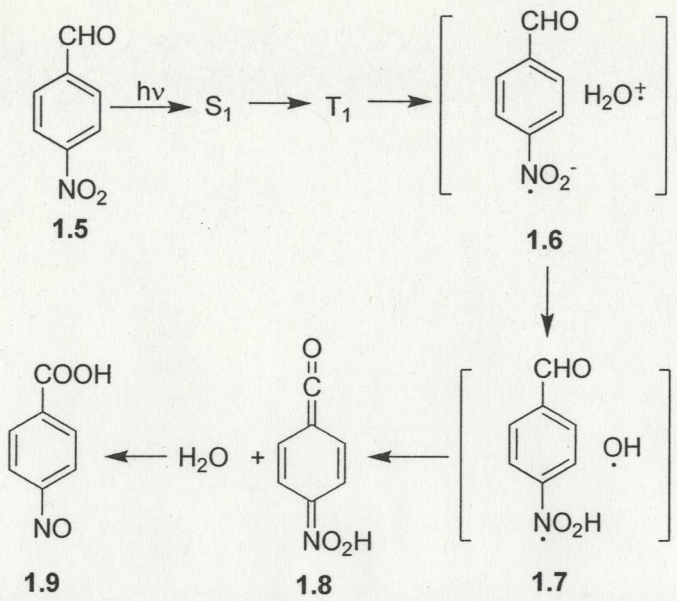

Scheme 1.2 Proposed mechanism for the photoredox reaction of **1.5**

It is well-known that the electron donating or withdrawing ability of functional groups attached to benzene and other aromatic rings can be considerably enhanced on electronic excitation.[19] Therefore, it is perhaps not surprising for meta- and para-nitrobenzyl alcohols to undergo intramolecular photoredox reaction since the benzyl alcohol moiety is readily oxidized. For instance, *p*-nitrobenzyl alcohol (**1.10**) in basic aqueous solution undergoes intramolecular photoredox reaction to form *p*-nitrosobenzaldehyde (**1.13**) ($\Phi <$ 0.01, pH 14).[20] The mechanism involves benzylic C-H bond deprotonation of triplet excited **1.10** by hydroxide ion with proton transfer from solvent water to the nitro group oxygen, to generate aci-nitro intermediate **1.11**, which undergoes ketonization to give hydrated nitroso **1.12**, which upon final loss of water gives **1.13** (eqn. 1.3).

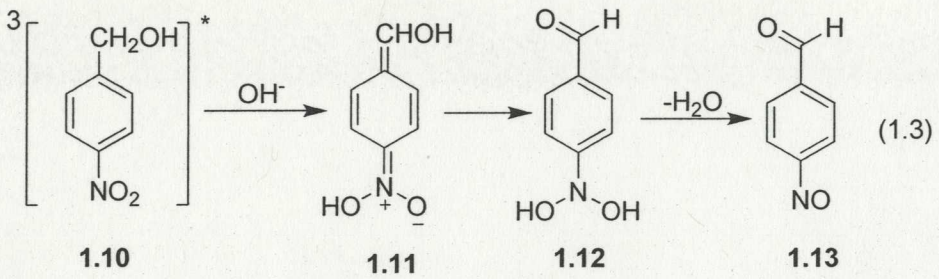

1.10 **1.11** **1.12** **1.13** (1.3)

The mechanism of intramolecular photoredox reaction of meta-nitrobenzyl alcohol (**1.14**) is more complicated. Photolysis of **1.14** produces two products: meta-nitrobenzaldehyde **1.15** ($\Phi \sim 0.25$, pH -1.4) and meta-azoxybenzaldehyde **1.16** ($\Phi \sim$ 0.079, pH -1.4), via intramolecular photoredox reaction, without detectable formation of *m*-nitrosobenzaldehyde (eqn. 1.4).[20] The photochemical reaction requires water and is dependent on pH. The authors proposed a mechanism similar to that of the para isomer in the initial steps. Deprotonation of the benzylic carbon by water of triplet excited **1.14*** excite generates intermediate **1.17**, which subsequently gives rise to the initial unstable photoredox product **1.18**. Products **1.15** and **1.16** are proposed to arise by subsequent dark reactions. Disproportionation of two molecules of **1.18** generates nitrobenzaldehyde **1.15** and the hydroxylamine **1.19**. The latter then reacts with with **1.18** to give observed azoxy product **1.16** via a condensation reaction (Scheme 1.3).

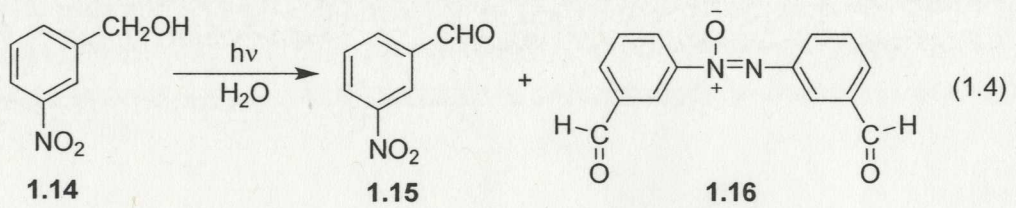

1.14 **1.15** **1.16** (1.4)

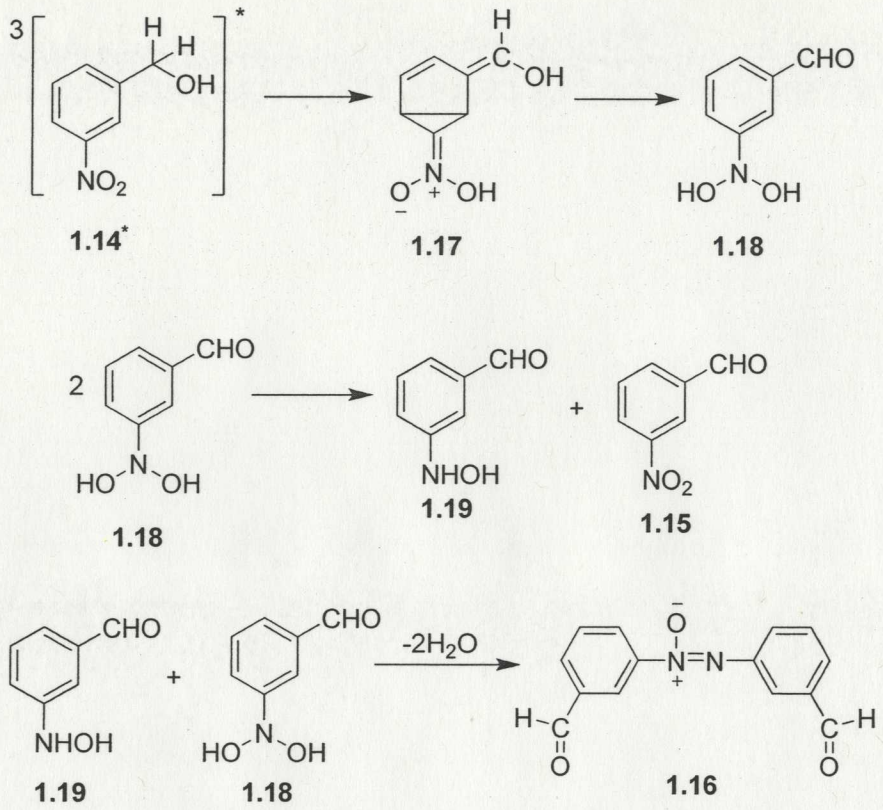

Scheme 1.3 Proposed mechanism for the intramolecular photoredox reaction of **1.14**

The authors commented that both reactions proceeded via π,π* triplets instead of n,π* triplets. Generally, simple nitrobenzenes are believed to have the lowest n,π* triplets which are not known to activate the benzene ring. However, the above reactions clearly involve activation of the benzene ring. A reasonable explanation is that π,π* triplets are involved.[20] The above reactions are only observed in water but not in common organic solvents. It is known that solvents of high dielectric constant stabilize π,π* and destabilize n,π* configurations. Water has a higher dielectric constant (ε = 80) than all the common organic solvents (ε ≤ 40). Thus, in water, the lowest triplets might be of π,π* character which would lead to the above reactions.

1.5 Classical Photochemistry of Aromatic Ketones

As this Thesis focuses on the photochemistry of aromatic ketones, it is necessary to discuss general photochemical properties of the carbonyl chromophore. Thus, a brief review of the photochemistry of aromatic ketones is provided below.

In organic photochemistry, compounds bearing the carbonyl (C=O) chromophore are the most widely and intensively investigated. It is well-known that in thermal chemistry, the carbonyl group is easily attacked by nucleophiles at the carbonyl carbon. However, in photochemistry, completely different behaviour is observed.

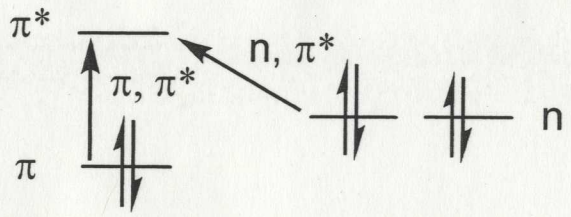

Scheme 1.4 Simplified n,π* Transitions of the carbonyl chromophore

The oxygen in the carbonyl group has two non-bonding electron pairs in non-bonding molecular orbitals (Scheme 1.4). An electron in the non-bonding molecular orbital (n) is excited to the lowest anti-bonding orbital (π*) to form the lowest energy excited state. Consequently, the electron in the π* orbital is shared between both carbon and oxygen atoms, which results in lower electron density at the oxygen atom than in the ground state. This electronic feature readily leads to the species **1.20** as the representative of the excited state, which is resemblant to alkoxy radicals. Therefore, it is not surprising that electronically excited carbonyl compounds undergo the following reactions:

a) Photoreduction via hydrogen abstraction to form ketyl radicals **1.21**;[21]

b) α-Cleavage or Norrish Type I reaction to form radicals **1.22**;[22]

c) Norrish Type II elimination reaction via 1,4-biradicals **1.23** which are formed via 1,5-hydrogen abstraction;[23]

d) Photocyclization via intramolecular hydrogen abstraction.[24]

e) [2 + 2] Photocycloaddition to form oxetanes (eqn. 1.5), via one of **1.24**, **1.25**, or **1.26**.[25]

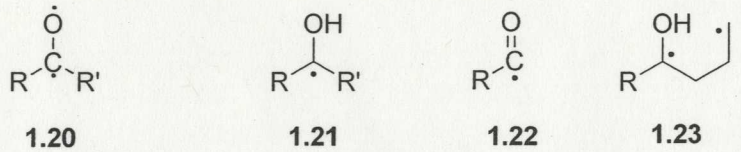

1.20 **1.21** **1.22** **1.23**

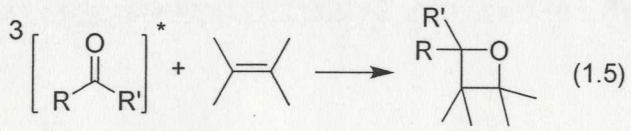

(1.5)

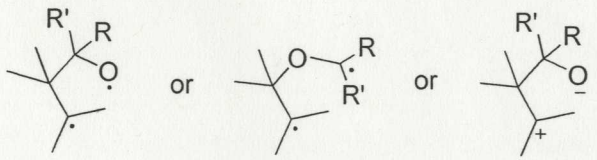

1.24 **1.25** **1.26**

Compared with the aliphatic ketones, aromatic ketones exhibit somewhat different features. For example, aromatic ketones such as benzophenone do not undergo Norrish Type I (α-cleavage). Vibrational energy for the bond cleavage must come from the electronic excitation energy. Thus, in order to cleave a bond, the initial electronic energy must be high enough. However, electronically excited benzophenone, due to its lower triplet (and singlet) energy, has less available electronic excitation energy to be converted to vibrational energy for bond breaking than aliphatic ketones such as acetone.[26]

Norrish Type II photoelimination of aliphatic ketones proceeds via hydrogen abstraction to generate 1,4-biradical **1.23**, followed by γ-cleavage to give rise to alkenes

and enols, the latter being readily converted to ketones (Scheme 1.5). However, aromatic ketones such as **1.27** can only undergo the initial hydrogen abstraction from the alkyl group at the ortho postion, but not the subsequent elimination since that would lead to fragmentation of the aromatic ring. The overall result is photoenolization.[24a,27]

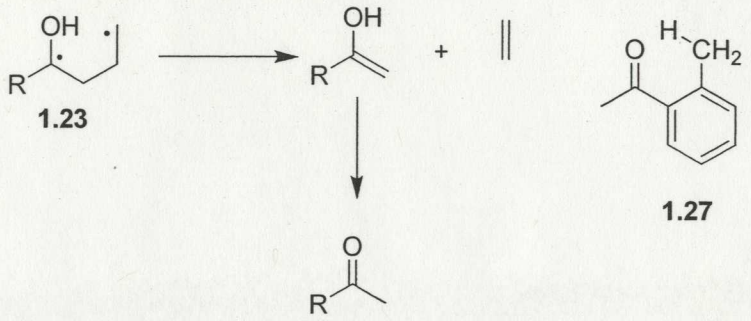

Scheme 1.5 Norrish Type II photoelimination of aliphatic ketones

One of most common pathways of reaction of photoexcited aromatic ketones is hydrogen atom abstraction. The process may occur in a bimolecular or unimolecular reaction, to generate semi-pinacol radicals resulting in overall reduction of the carbonyl group. The reactive excited state can be either singlet or triplet.[28]

Upon photolysis, aromatic carbonyl compounds with an alkyl group in the ortho position are known to readily produce the corresponding enols. The mechanism involves the triplet excited state **1.29** that generates a triplet biradical $^3\boldsymbol{E}$ via intramolecular hydrogen abstraction. Subsequently, $^3\boldsymbol{E}$ leads to formation of two isomeric enols, ***E*** and ***Z***. Singlet excited state **1.28** produces only enol ***Z***. The short-lived ***Z*** is quickly converted back to starting molecule **1.27**. The longer-lived ***E*** isomer has a lifetime of up to seconds (for ketonization)(Scheme 1.6).[29]

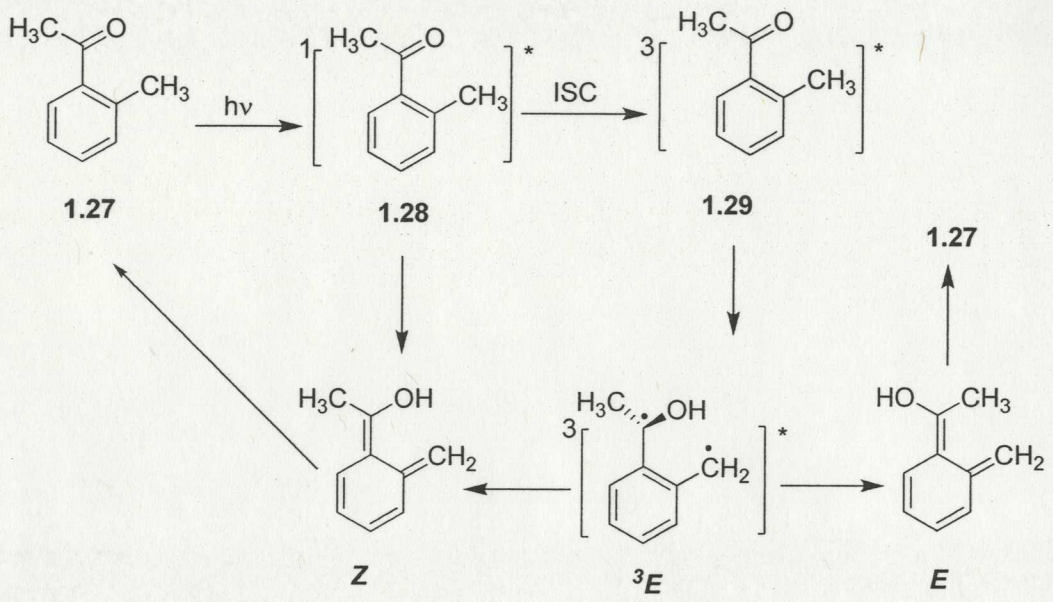

Scheme 1.6 Proposed mechanism for photoreduction of **1.27**

In the presence of a trapping reagent such as a dienophile, the long-lived enol ***E*** can undergo Diels-Alder reaction. Meador and coworkers reported the synthesis of phenanthrene **1.34** via the initial photoenolization of 3,6-dibenzoyl-*o*-xylene (**1.30**) followed by subsequent Diels-Alder trapping.[30] In the photochemical preparation, **1.30** in nitrogen saturated benzene was irradiated (450 W medium pressure Hg lamp equipped with a Pyrex filter) and the enols trapped with *N*-phenylmaleimide (**1.31**), to give rise to bisadduct **1.32** in good yield (65%). Subsequently, phenanthrane **1.34** was synthesized by initial acid-catalyzed dehydration of **1.32** followed by aromatization of **1.33** with DDQ (Scheme 1.7). The key step in the synthesis is the hydrogen abstraction by the carbonyl oxygen of **1.30**, to generate triplet biradical **1.35** which undergoes enolization to give o-xylylenol **1.36** (eqn. 1.6).

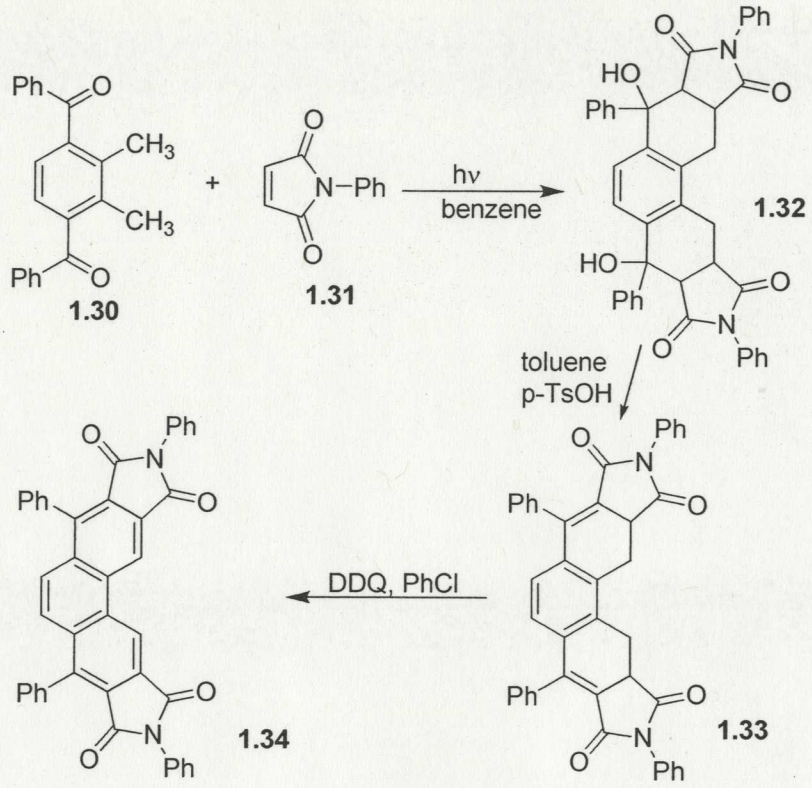

Scheme 1.7 Synthesis of **1.34** via an initial photoenolization of **1.30**

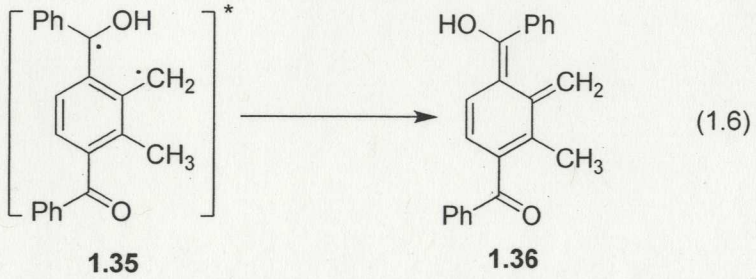

If there is a good leaving group such as a carboxylate at an appropriate position, the long lived enol ***E*** can undergo elimination to release a caged group such as an alcohol[31] or a carboxylic acid.[32] Thus, photoenolization can be widely used for photodeprotection. For example, the 2,5-dimethylphenacyl chromophore serves as a good photodeprotecting group for carboxylic acids. The carboxylate leaving group, on the α-carbon of the 2,5-

dimethylphenacyl compound **1.37**, is photoreleased to form indanone **1.38** via the enol ***E'*** ($\Phi \sim 0.2$) (eqn. 1.7).[32]

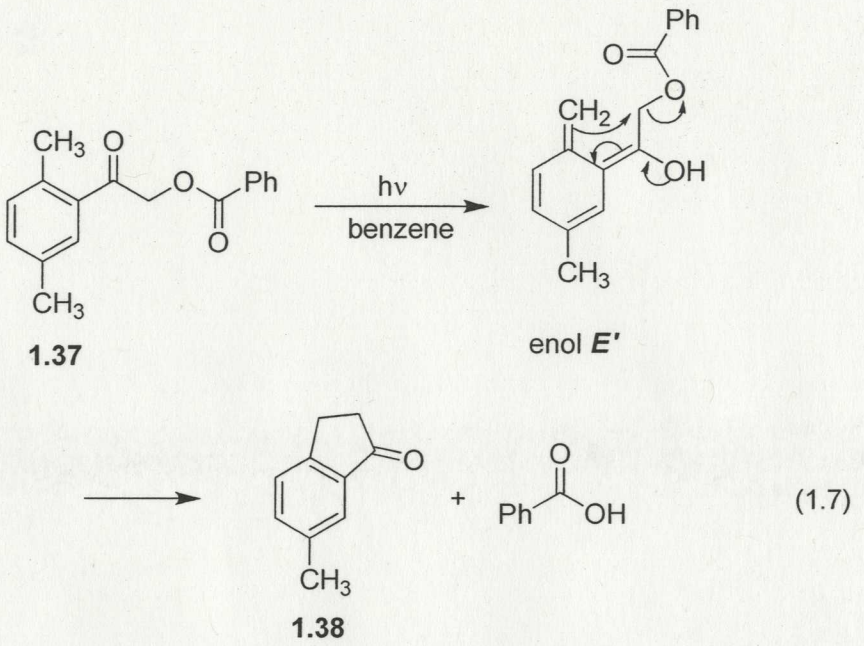

(1.7)

1.6 Excited State Acid-Base Properties of Aromatic Compounds

Just as Section 1.3 noted that redox behaviour of molecules changes significantly on going from ground to excited states, the acid-base properties of molecules also change considerably. A simple explanation is that there is significant migration of electron density in molecules upon electronic excitation. This affects acid-base properties of molecules.[33,34,35,36] Thus, it is not surprising that some electronically excited molecules readily undergo proton transfer but the corresponding ground state molecules do not.

Phenols are known to be more acidic in the S_1 state than in the S_0 state. The enhancement of acidity may be simply explained with an energy level diagram involving the different electronic states of the phenol (HA) and its conjugated base (A^-), as shown in the Förster Cycle (Figure 1.3).[20] Note that phenols (HA) in general have a higher energy (ΔG_{HA}) for the HA-HA* transition than for the A^-- A^{-*} transition of the

conjugated base (ΔG_{A^-}). Thus, the dissociation of HA^* is more favourable than that of HA. In another words, HA^* is more acidic than HA.

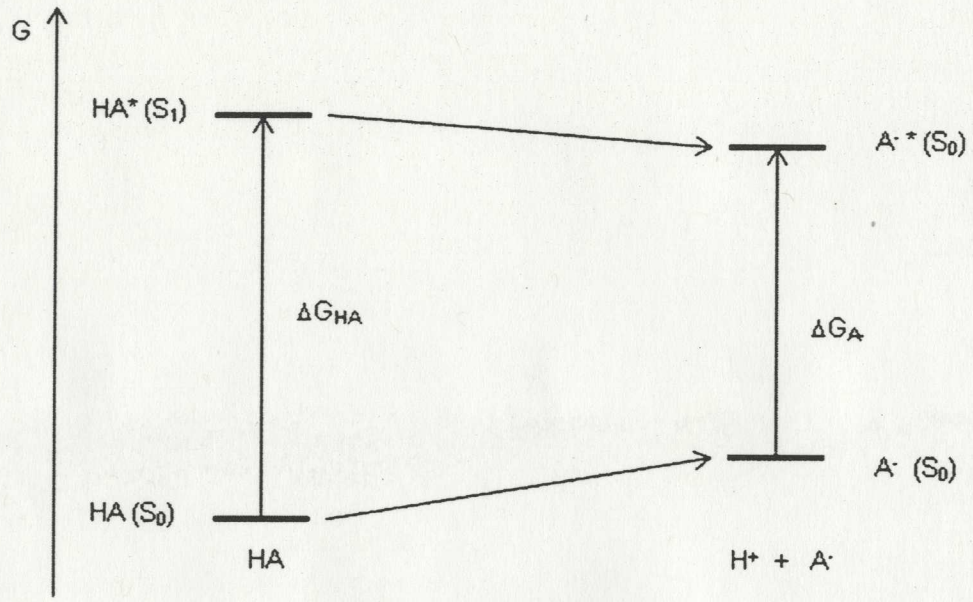

Figure 1.3 Förster Cycle

Benzyl alcohol **1.39** undergoes photodissociation (loss of hydroxide ion) to generate benzyl cation **1.40** (eqn. 1.8).[37] Photodissociation of *o*-hydroxybenzyl alcohol (**1.41**) ($\Phi \sim 0.3$) is 5 times more efficient than **1.39**. This is rationalized by the higher acidity of the phenol of **1.41** in S_1 ($pK_a^* \sim 3$), which leads to a concerted intramolecular proton transfer pathway that results in the elimination of water (eqn. 1.9). The first step leads to photodehydration, to generate *o*-quinoemethide **1.42**, which then undergoes methanolysis to give **1.43**.[38]

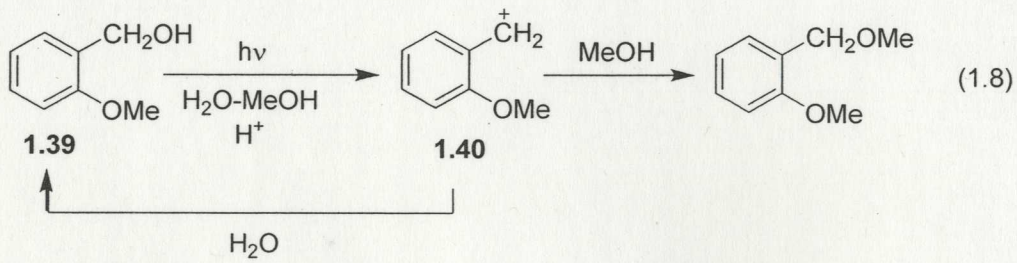

(1.8)

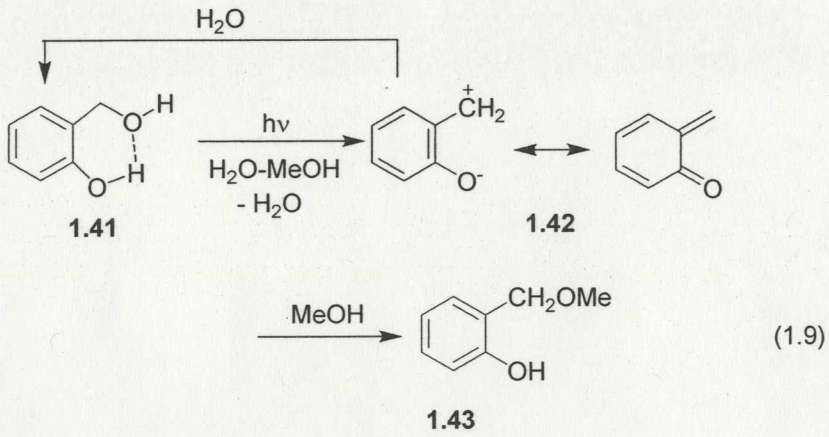

(1.9)

Suberene (**1.44**) is the first example of an excited state carbon acid.[39] Photolysis of **1.44** in D_2O-CH_3CN results in deuterium exchange at the benzylic position ($\Phi \sim 0.035$), to give **1.46** via carbanion **1.45** (eqn. 1.10). The mechanism involves the deprotonation at the 5-position by water acting as the general base, which is consistent with the much higher acidity of **1.44** in S_1 ($pK_a^* \sim -1$) than that in the ground state ($pK_a \sim 31$-38).

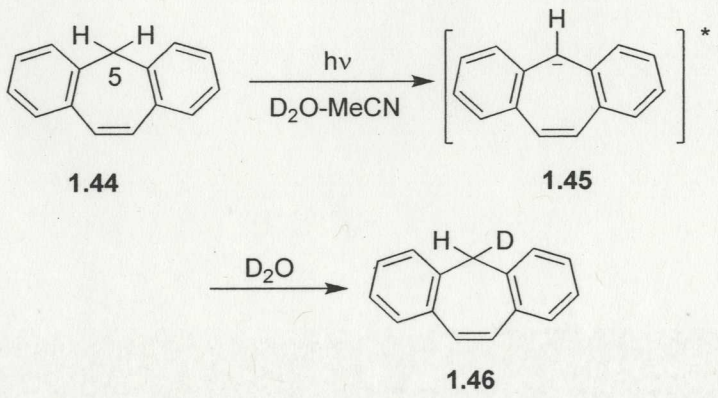

(1.10)

Aromatic ketones also exhibit significantly different acid-base properties in the excited state. As opposed to phenols or suberene, electronically excited aromatic ketones are more basic.[40] For example, benzophenone **1.47** in the triplet excite state is more basic than in the ground state. This has been experimentally verified by measurement of the pK_a of protonated benzophenone **1.48**, in the triplet excited state, pK_a (T_1) ~-0.4 whereas

in the ground state, pK_a (S_0) = -5.7.[41] Additionally, the reactive triplet states in these protonations are believed to be of π,π* character rather than n,π* character. Consequently, triplet excited benzophenone **1.47** undergoes adiabatic proton transfer to oxygen, resulting in the formation of triplet excited conjugate acid **1.48**.

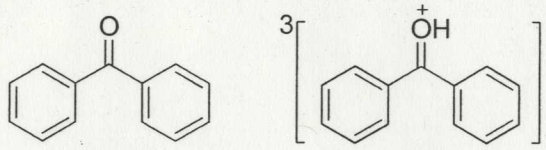

1.47 **1.48**

Indeed, Wirz and co-workers have reported the photohydration of benzophenone via this type of proton transfer.[41] Triplet excited benzophenone **1.47** undergoes initial protonation of the carbonyl oxygen in the presence of acid, to generate triplet excited **1.48** which has substantial positive charge at the ortho and meta positions of the benzene ring (Scheme 1.8. In this and future schemes, for simplicity, not all open shell structures are explicitly shown except in representative cases). Attack by water at these positions leads to the transiently observed unusual hydration products **1.49** and **1.50**. Both hydration products readily return to **1.47** by dehydration.

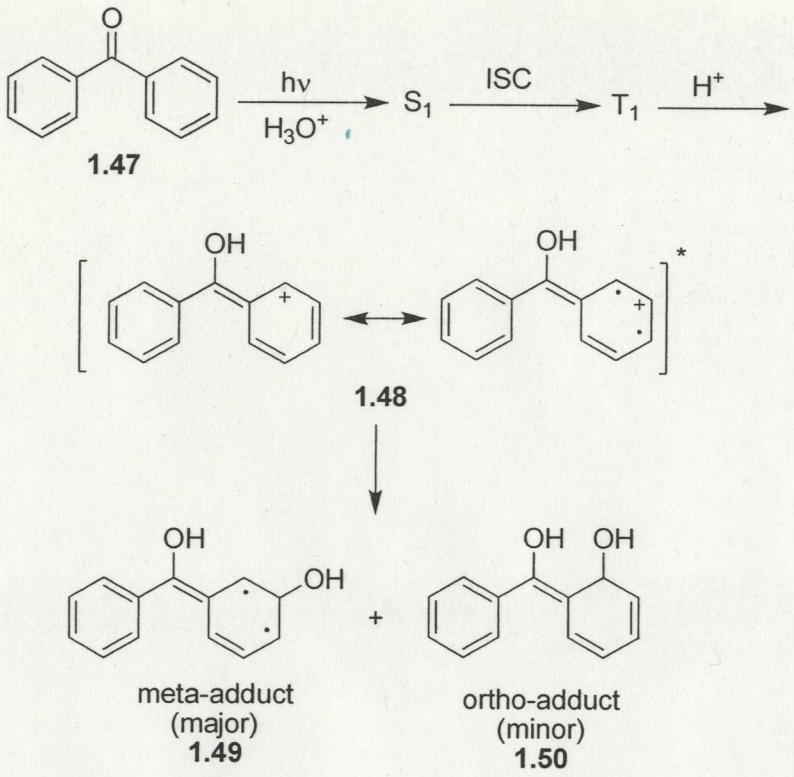

Scheme 1.8 Proposed mechanism for the photohydration of benzophenone **1.47**

1.7 Photoredox Reactions of Benzophenones

With respect to photochemistry, benzophenone is one class of aromatic ketone that has been studied most widely.[22a,23a,42,43,44] Benzophenone (**1.47**) undergoes efficient intersystem crossing[45] and hence has a non-fluorescence and very short-lived (10^{-11}s) singlet state.[44] In addition, benzophenone has a higher triplet energy than many compounds. The above properties make benzophenone and derivatives useful as triplet sensitizers.

Like most aromatic ketones, the most common primary photochemical reaction of benzophenone and its substituted derivatives is photoreduction via hydrogen atom abstraction in the presence of hydrogen donors.[46,47,48] However, recently, an unusual intramolecular photoredox reaction involving the benzophenone chromophore was reported by Wan and coworkers.[49] In neutral aqueous solution,

3-(hydroxymethyl)benzophenone (**1.51**) undergoes only photoreduction. Under acidic conditions, an intramolecular photoredox reaction was observed. The reaction requires water and is very efficient in the presence of acid ($\Phi \sim 0.6$, pH <3, H_2O-CH_3CN), to generate the formal photoredox product **1.52** (eqn. 1.11). Nanosecond laser flash photolysis of **1.51** showed two absorption bands (λ_{max} = 325 nm and λ_{max} = 525 nm) assignable to triplet excited benzophenone with a lifetime of 0.6 μs.

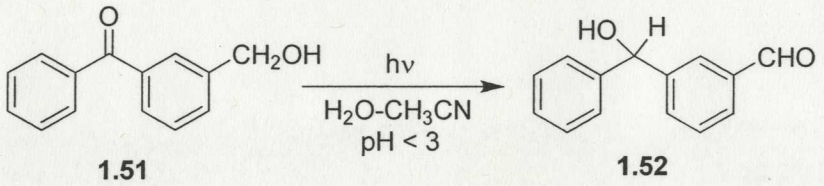

1.51 **1.52** (1.11)

When the hydroxymethyl group is replaced by a methyl group, under the above experimental conditions, no photoredox reaction was observed.

The proposed mechanism involves an excited state carbocation **1.53** and is very similar to the acid-catalyzed photohydration of benzophenone **1.47** previously explored by Wirz.[41] Protonation of the carbonyl oxygen of triplet excited **1.51** gives rise to **1.53** in which the positive charge is strongly localized at the *meta* position. This enhances the acidity of the benzylic C-H bond (of the CH_2OH moiety) sufficiently that it is deprotonated by solvent water, giving rise to a biradical dienol **1.54**. The dienol **1.54** undergoes intersystem crossing and electron pairing, to give a zwitterionic intermediate **1.55** that subsequently results in an overall intramolecular photoredox reaction (Scheme 1.9).

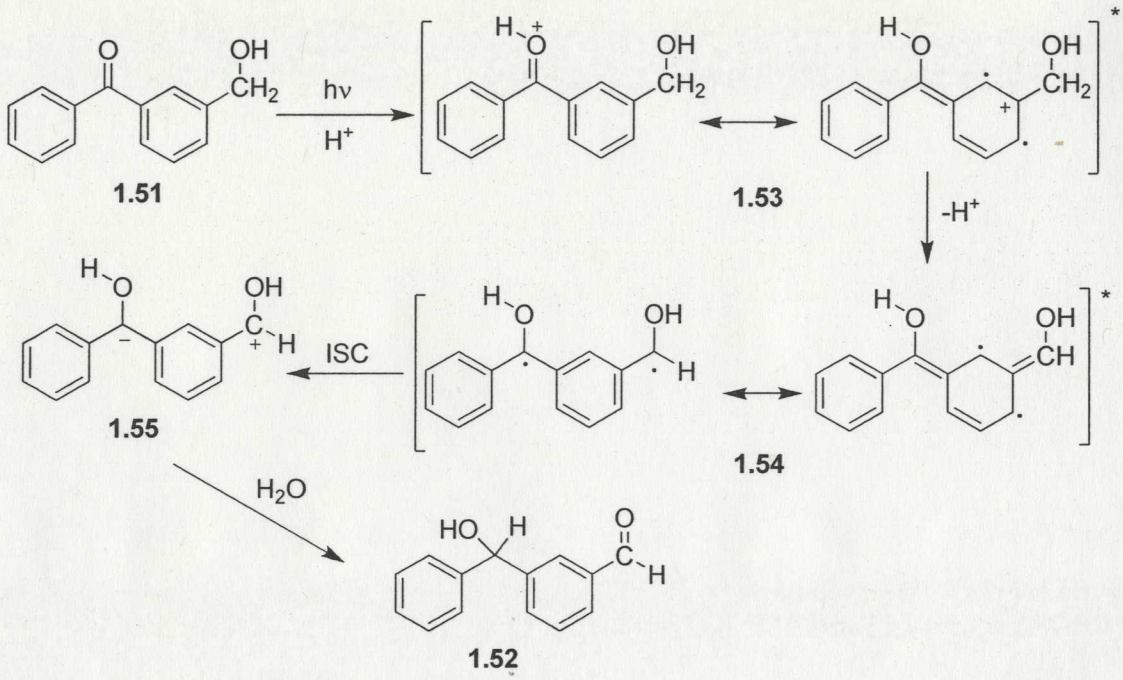

Scheme 1.9 Proposed mechanism for the intramolecular photoredox reaction of **1.51**

1.8 Photochemistry of Anthraquinones

As this Thesis primarily studies anthraquinones, a subset of aromatic ketones, it is necessary to briefly review the general applications and photochemistry of anthraquinones. In nature, anthraquinones are found in plants (e.g. rhubarb), and in some fungi and insects (e.g. coccids). All of these anthraquinones serve as the basic skeleton for pigments.[50] In industry, many anthraquinone derivatives are used as dyes. Alizarin, which is exctacted from the root of the madder plant, is the first natural pigment to be synthesized from anthracene by Graebe and Liebermann in 1869.[51] Anthraquinones are also used as catalysts for the production of wood pulp to enhance fiber potency.[52] They are also used as effective bird repellents on seeds.[53] In addition, in the manufacture of H_2O_2, the autoxidation of anthraquinones is the first and still a major method.[54] In this process, 2-ethyl-9,10-dihydroxyanthracene (**1.56**) is autoxidized in air to generate H_2O_2

and anthraquinone **1.57**, which is reduced back to the dihydroxy compound using hydrogen gas with metal catalysts (Scheme 1.10).

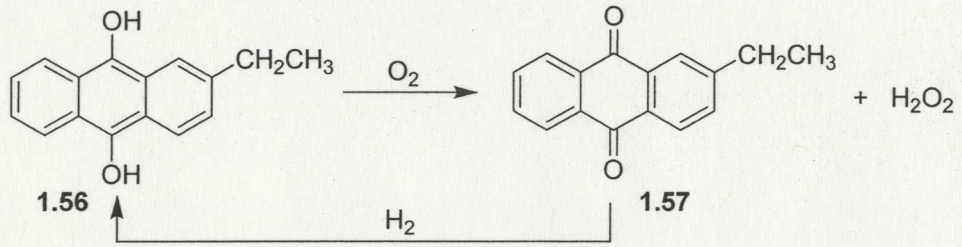

Scheme 1.10 Manufacture of H_2O_2 via the autoxidation of anthraquinone **1.56**

The photochemistry of anthraquinones has been extensively investigated due to their widespread use as photosensitizers and antennas for solar energy conversion.[55] Anthraquinones undergo efficient intersystem crossing ($\Phi_{ISC} \sim 0.9$), to form a long-lived triplet excited state, which can lead to efficient photochemical reaction competing with physical radiative and radiationless decay.[56,57] Anthraquinones are also good electron acceptors and efficient hydrogen abstractors (via the carbonyl oxygen).[56] Thus, electronically excited anthraquinones may undergo photoreduction and photoinduced electron transfer, some of which will be further elaborated below.

1.8.1 Photoreduction

The well-known photoreduction of anthraquinone was reported by Wilkinson and coworkers.[58] Photoexcited anthraquinone **1.58** is reduced by isopropanol (hydrogen donor), to dihydroxyanthracene **1.60** via hydrogen atom abstraction. More recently, the mechanism has been investigated in detail using time-resolved transient spectroscopy by Görner.[59] These studies suggest that hydrogen abstraction by the carbonyl oxygen of triplet excited anthraquinone **1.58** gives rise to the corresponding semi-quinone radical **1.59** ("ketyl") ultimately leading to reduced anthraquinone **1.60** (Scheme 1.11).[59] This

reaction involves the addition of external hydrogen atoms and hence involves an overall bimolecular process.

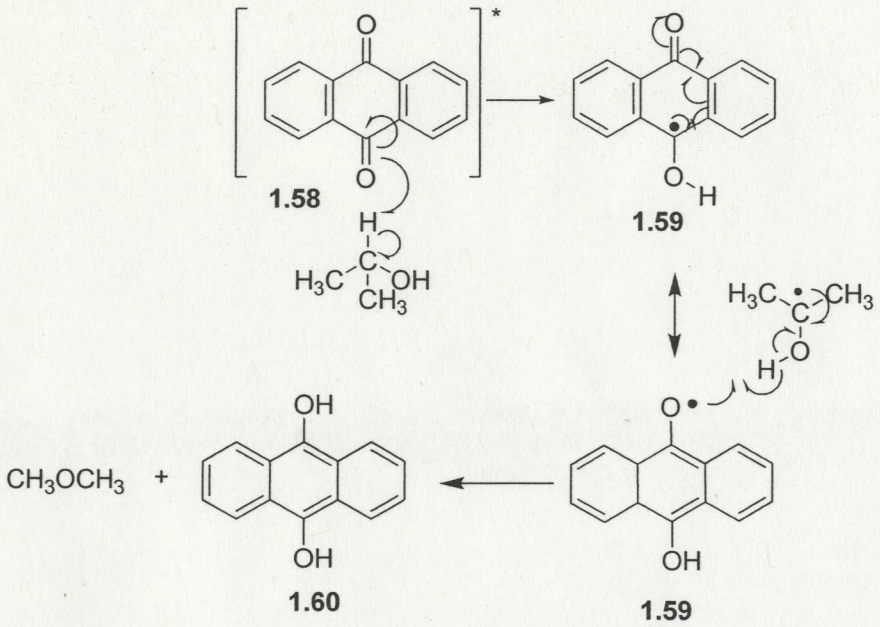

Scheme 1.11 Proposed mechanism for photoreduction of anthraquinone **1.58**[59]

1.8.2 Photoinduced Electron Transfer

Pal and coworkers reported bimolecular photoinduced electron transfer in an anthraquinone-amine system.[60] The proposed mechanism involves photoinduced electron transfer from the amine donor (**1.61**) to the singlet excited anthraquinone acceptor (**1.62**). The process was observed by time-resolved fluorescence quenching. The intensity of fluorescence of the singlet excited anthraquinone is significantly quenched by aromatic amines ($k_q \sim 2.4 \times 10^{10}\ M^{-1}s^{-1}$). The free energy change (ΔG_{et}) for the photoinduced electron transfer reaction is -0.964 eV.

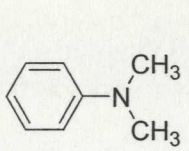

1.61 (electron donor)

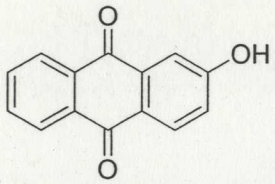

1.62 (electron acceptor)

In recent years, photoredox reactions (via electron transfer) in DNA and peptides have attracted considerable attention. Schuster and coworkers[61] reported selective oxidative damage of DNA via photoinduced electron transfer. In a complex of an anthraquinone conjugated to a duplex DNA, the DNA base is an electron donor and electronically excited anthraquinone is the electron acceptor. An electron transfer from the DNA base to the excited anthraquinone results in the formation of a radical cation in the DNA. This then leads to a mutation of DNA.

1.8.3 Intramolecular Photoredox Reaction

The first intramolecular photoredox reaction involving an anthraquinone chromophore was reported by Wan and coworkers.[62] 2-(Hydroxymethyl)anthraquinone (**HMAQ**) undergoes a highly efficient photoredox reaction in aqueous solution ($\Phi \sim 0.8$) (eqn. 1.12).[62] Photolysis of **HMAQ** in neutral aqueous solution gave an orange 2-formyl-9,10-dihydroxyanthracene (**DHA**), which is oxidized to give 2-formyl-9,10-anthraquinone (**FAQ**) when exposed to air. When the hydroxymethyl group was replaced by a methyl group, no photoredox reaction was observed, even upon prolonged irradiation. The reaction requires water and no reaction was observed in neat acetonitrile. The observed concentration (10^{-6}-10^{-4} M) independence of the substrate on quantum yield of reaction suggests that the photoredox reaction is unimolecular in anthraquinone. A detailed mechanism of this reaction will be presented in Chapter 2 of this Thesis since a number of related substrates will be studied as part of continuing work on this reaction.

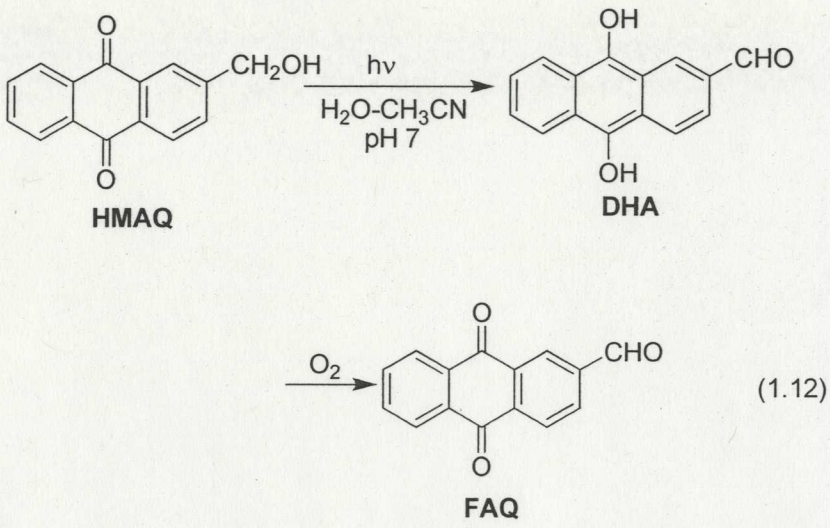

(1.12)

1.9 Photodeprotecting Groups

Photodeprotecting groups have attracted considerable interest due to their wide application in organic synthesis[63] and biochemistry.[64] Photodeprotecting groups are designed to protect functional groups and to be removed by a trigger, namely light to release the protected functionality. In organic synthesis, protecting groups play an important role in chemical selectivity of reaction when two or more functional groups are present. Generally, in thermal chemistry, removal of a protecting group is carried out by acid or base, but these cannot be used for some sensitive compounds. Compared with many protecting groups that are removed thermally, photochemical deprotecting groups are more convenient and can be removed efficiently without the addition of more chemicals. This has added benefit in biology.

In the design of a photodeprotecting group, one should consider many factors, such as the synthesis of photoprotected compounds AB and the photorelease process, etc. Scheme 1.12 shows the overall process from initial syntheses to the eventual photorelease.

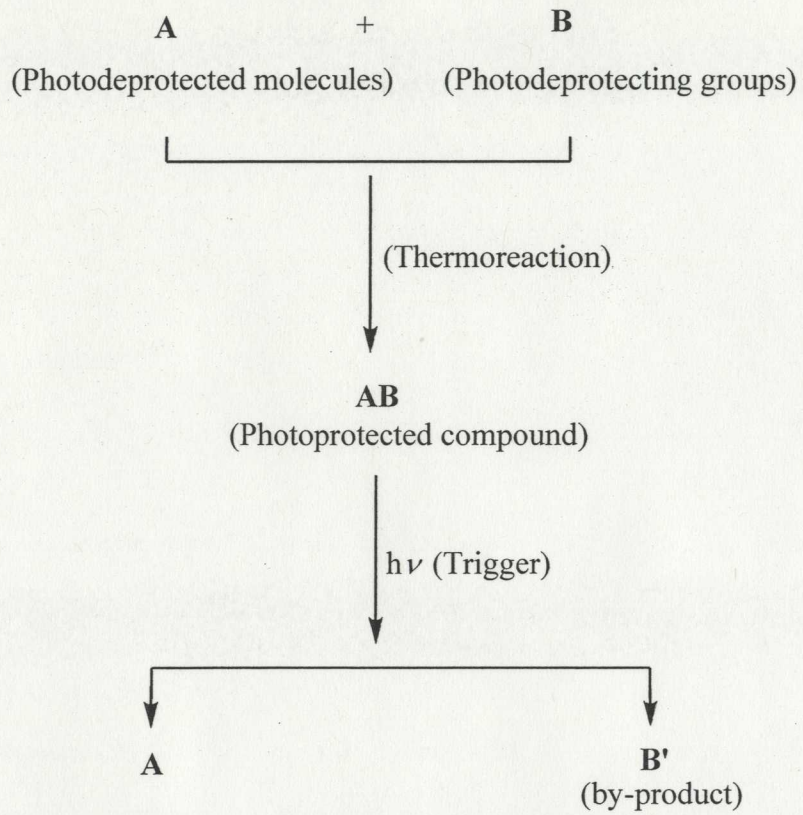

Scheme 1.12 An overall process from initial syntheses to the eventual photorelease

A good photodeprotecting group should meet the following criteria:

a) The photoprotected compound **AB** is easily synthesized in high yield;

b) **AB** should have good photosensitivity and good solubility, and especially in biology, **AB** should be water-soluble and bioinert.

c) It should be easy to remove the deprotecting group **B'**, to release the protected molecule **A** in high yield upon irradiation.

d) In biology, the excitation wavelength for **AB** should be above 300 nm in order to prevent damage to biological tissue.

e) There should be few or no by-products. The photodeprotected compound **A** should be readily recoverable.

f) The by-product **B'** should be photoinert and transparent at the excitation wavelength. In biology, the by-product **B'** should be bioinert.

The most common and also commercially avaliable photodeprotecting groups are based on *o*-nitrobenzyl derivatives. They are low cost, compatible with most functional groups and have high releasing yields.[65] Currently, *o*-nitrobenzyl derivatives are used to protect alcohols,[66] ketones (aldehydes),[67] amines,[68] carboxylic acids,[69] phosphates,[70,71] etc. The reaction mechanism involves hydgrogen atom abstraction by the nitro group, to give the *aci*-tautomers (***E*-aci** and ***Z*-aci**) as shown for the parent *o*-nitrotoluene (eqn. 1.13). The ***E*-aci** tautomer is reactive in photorelease.

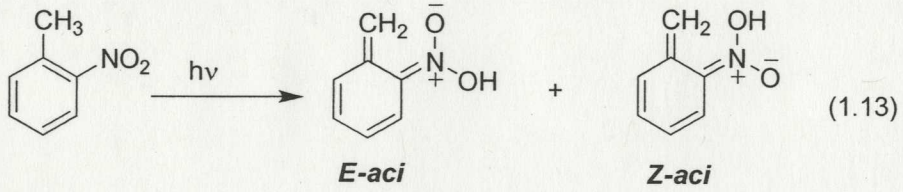

(1.13)

As an example, the 1-(2-nitrophenyl)ethyl ester of ATP **1.63** photoreleases ATP anion (RO^-) in aqueous solution in high yield ($\Phi \sim 0.63$, pH 6~10)[70,71] (Scheme 1.13). The proposed mechanism involves hydrogen atom abstraction by electronically excited **1.63**, to give *aci*-nitro form **1.64**, followed by a series of thermal steps, to give **1.65**. The ATP anion is released by elimination/ketonization of **1.65**.[72]

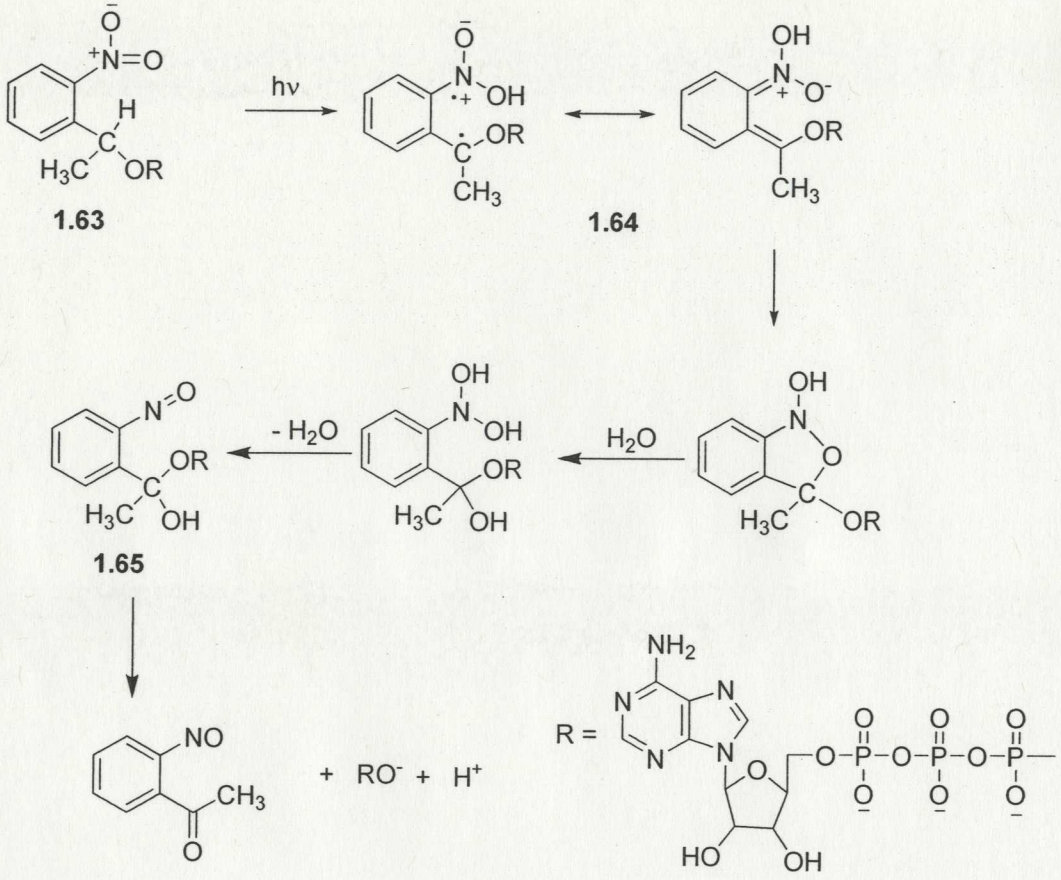

Scheme 1.13 Proposed mechanism for photolysis of *o*-nitrobenzyl derivative **1.63** to release ATP

However, nitro compounds are toxic and their photochemical by-products (nitroso compounds) compete for light absorption. Their release rate (after excitation) is relatively slow in most cases ($> 10^{-3}$ s). Consequently, other photodeproecting groups such as *p*-hydroxyphenacyl derivatives,[73] benzoin[74] and coumarinyl derivatives[75] have been developed to address these shortcomings.

Anthraquinone derivatives as a new chromophore for photodeprotection was first reported by Iwamura and coworkers.[76] Anthraquinone **1.66** photoreleases the protected galactose derivative in good quantum yield ($\Phi = 0.10$) (eqn. 1.14). However, the authors neither reported the nature of the by-products nor explored the mechanism of reaction.

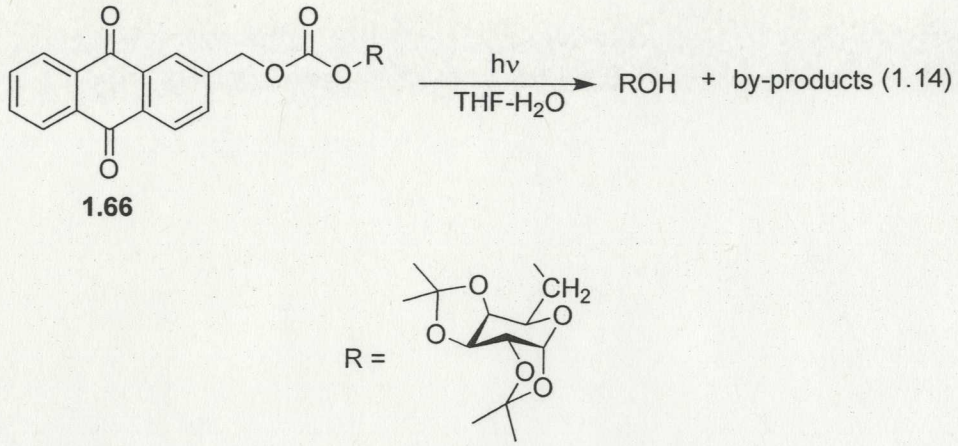

Recently, an anthraquinone photodeprotecting group for aldehydes and ketones was reported by Song and coworkers.[77] Compound **1.67** photoreleases acetophenone (Φ = 0.038 for disappearances of the caged compound) (Scheme 1.14). Besides acetophenone, two other products **A** and **B** were also formed. The authors suggested that they might be generated from the photolysis of **1.68**. The photodeprotection mechanism was proposed to arise via heterolytic bond cleavage, to generate zwitterionic intermediate **1.69**. This is subsequently trapped by water to give a hemi-acetal. Breakdown of the acetal would be expected to give acetophenone and **1.68**

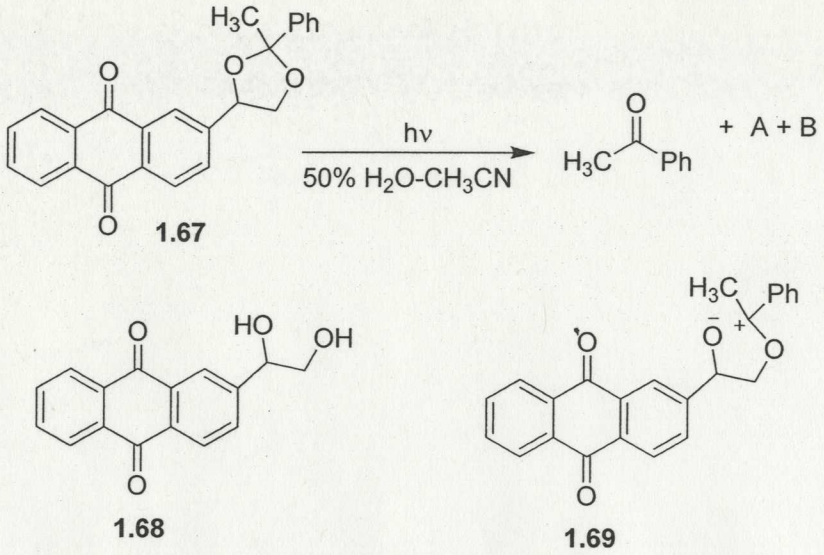

Scheme 1.14 Photolysis of anthraquinone **1.67** to release acetophenone

All of the above anthraquinone photodeprotecting groups are based on *meta* substituted compounds. Blankespoor and coworkers reported the use of *ortho* substituted anthraquinones, 1-alkoxy-9,10-anthraquinone (**1.70**) as a photodeprotecting group for aldehydes.[78] The mechanism involves intramolecular hydrogen abstraction of electronically excited **1.70**, to generate biradical **1.71**, which subsequently undergoes single electron transfer (SET), giving zwitterion **1.72**. Trapping of **1.72** by CH_3OH gives dihydroxyanthacene **1.73** (Scheme 1.15). Upon oxidation in air, anthraquinone **1.74** is produced, which upon hydrolysis in aqueous acetic acid produces 1-hydroxyanthraquinone (**1.75**) and the corresponding aldehyde in high yield (68%).

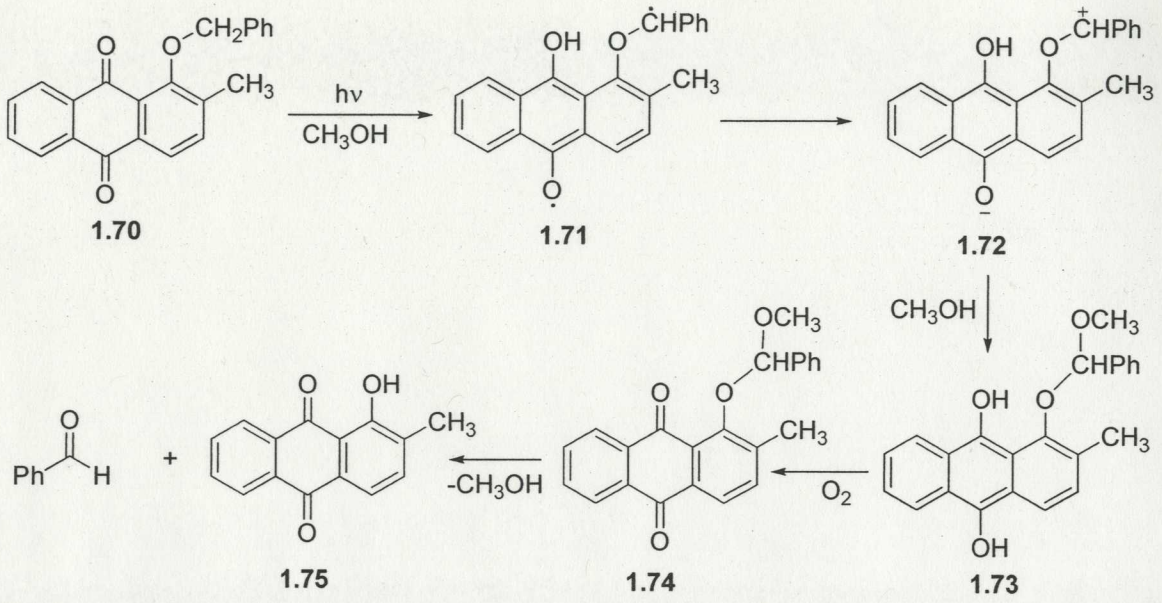

Scheme 1.15 Proposed mechanism for *ortho* substituted anthraquinone **1.70** to release benzaldehyde

1.10 Proposed Research

The initial work on the intramolecular photoredox reaction of anthraquinones such as **HMAQ** (eqn. 1.12) was reported by Wan and coworkers in 2002.[62] Prior to that, the intramolecular photoredox reactions of nitro compounds were of interest in this area.[14,16,17, 19] The work on anthraquinones may be regarded as an extension of the work on the *m*- and *p*-nitrobenzyl alcohols.[19] The goal of the present research is to further explore intramolecular reactions of aromatic ketones using the anthraquinone chromophore as the platform.

In this Thesis, the intramolecular photoredox reaction of anthraquinone **HMAQ** will be extended to a number of anthraquinone derivatives with the goal of better understanding the clean and efficient intramolecular photoredox reaction displayed by the parent compound. To study the generality of the photoredox reaction, we will design a variety of substituted derivatives on the basic backbone of the anthraquinon-2-yl moiety,

including alcohols, ethers, acetals, esters as well as related chromophores (Chapter 2), to explore whether these derivatives undergo the intramolecular photoredox reaction discussed above. In addition, a new photodeprotecting group will be designed and investigated with possibility of releasing several protected functionalities. Chapter 2 will also focus on mechanistic studies of parent compound **HMAQ** exploring isotope, solvent, pH effects as well as the use of laser flash photolysis (LFP) to investigate mechanism of reaction.

In Chapter 3, studies will explore whether or not the above formal intramolecular photoredox reaction could occur for substrates in which the benzyl alcohol moiety is far away from the anthraquinone. Thus, new anthraquinones with phenyl and biphenyl "spacers" between the two potentially reactive functional groups will be synthesized and their photochemistry investigated in detail.

The photoredox reaction will also be extended (Chapter 4) to acenequinones, by removing or adding benzene rings to the anthraquinone system but still preserving the planarity and conjugation. The designed compounds will include a naphthoquinone, an anthraquinone, a naphthacenequinone and a pentacenequinone. A photochemical method involving an intramolecular redox process to prepare a pentacene derivative will also be detailed.

2. Intramolecular Photoredox Reaction of Anthraquinones and Its Potential Utility as a Photodeprotecting Group*

2.1 Introduction

Previous studies of 2-(hydroxymethyl)anthraquinone (**HMAQ**) in water suggest a different and unusal sort of photochemical reactivity for a simple anthraquinone derivative.[62] The highly efficient reaction ($\Phi = 0.8$) of **HMAQ** is observed only in the presence of water with clean formation of the formal intramolecular redox product **DHA**. On exposure to air or oxygen, the anthraquinone chromophore is regenerated in product **FAQ**. We wondered whether this efficient photoredox reaction is only a special case reaction for **HMAQ** or it is a general one for **HMAQ** analogs.

Previous studies of **HMAQ** also suggested that the photoredox reaction might proceed via protonation of the anthraquinone carbonyl oxygen and deprotonation of the benzylic C-H.[62] In addition, the alcohol group is apparently a key substituent in the photoredox reaction because no photoredox reaction was observed for 2-methyl-9,10-anthraquinone.[62] Thus, to examine the generality of the photoredox reaction, a variety of appropriate anthraquinones (**2.1-2.8**) were designed (Chart 2.1). All of these anthraquinones have one common character: an anthraquinone or related chromophore and a "distal" substituent bearing a benzylic oxygen moiety. Diketone **2.9** was prepared to examine whether or not other aromatic diketones could react in an analogous fashion.

The design of **2.2-2.6** has a dual purpose. One is to examine the generality of the photoredox reaction as noted above; the other is to examine the possible application of

---

* [Y. Hou, and P. Wan, Formal Intramolecular Photoredox Chemistry of Anthraquinones in Aqueous Solution: Photodeprotection for Alcohols, Aldehydes and Ketones, *Photochem. Photobiol. Sci.*, **2008**, 7, 588-596.]-Reproduced by permission of The Royal Society of Chemistry (RSC) on behalf of the European Society for Photobiology, the European Photochemistry Association, and RSC.

the anthraquinon-2-yl moiety acting as a photodeprotecting group for alcohols, carboxylic acids, and ketones/aldehydes. The details of this application are presented in Section 2.3.2.

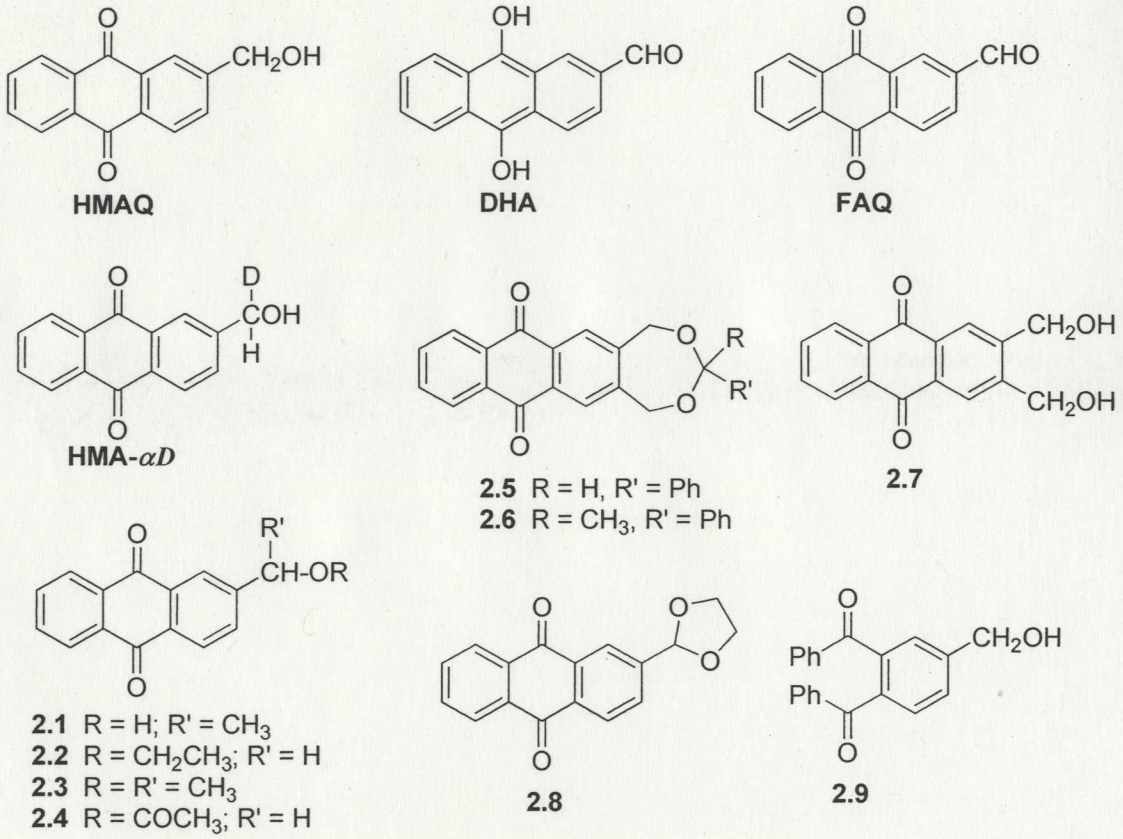

Chart 2.1

Since the photoredox reaction of **HMAQ** exhibits a significant colour change upon excitation,[62] UV-Vis spectroscopy was firstly employed to explore the possible long-lived transients and the presence of photoredox products for all the designed anthraquinone derivatives.

Since all anthraquinones (**2.1-2.8**) are an extension of **HMAQ**, **HMAQ** could be considered as a basic model for studying the photoredox reaction. However, no detailed

mechanistic studies of the photoredox behaviour of **HMAQ** had been reported. Thus, it is necessary to explore the mechanism of the photoredox reaction of **HMAQ** itself.

The photoredox reaction of **HMAQ** most likely involves the protonation of the carbonyl oxygen and the deprotonation of the benzylic C-H bond.[62] In order to examine the effect of the bond breaking on formation of the photoredox product, the α-deuterated anthraquinone **HMAQ-*αD*** was prepared, to measure the isotope effect on the deprotonation of the benzylic C-H bond. The isotope effect can be obtained by comparing the formation of deuterated or non-deuterated product yields. Protonation of carbonyl oxgen can be studied by photolysis in D_2O/H_2O and the effect of pH. Results are presented in Section 2.4.1.

Although **HMAQ** exhibits an efficient photoredox reaction in neutral aqueous solution,[62] previous studies showed that the analogous photoredox reaction of benzophenone **1.51** is pH dependent and that no photoredox reaction was observed in neutral aqueous solution.[49] In addition, the photoreduction of benzophenone **1.51** competes with its photoredox reaction.[49] It is well-known that anthraquinones also undergo photoreduction in the presence of hydrogen donors.[59] Thus, the details concerning pH effects (Section 2.4.2) and hydrogen donor solvent effects (Section 2.4.3) on the photoredox behaviour of **HMAQ** will be presented. These results reveal interesting differences between photoreduction and photoredox behaviour.

Nanosecond laser flash photolysis (LFP) will be employed to explore the nature of reactive excited states of **HMAQ** and the existence of intermediates that lead to photoredox product for the parent **HMAQ**. The results are presented in Section 2.4.4. Anthraquinones tend to react via triplet excited states due to their efficient intersystem

crossing ($\Phi = 0.9$).[57] Confirmation of triplet state reactivity for **HMAQ** photoredox chemistry will also be performed through triplet quenching methods (Section 2.4.5).

2.2 Syntheses

2.2.1 α-*D*-2-(Hydroxymethyl)-9,10-anthraquinone (HMAQ-*αD*)

Synthesis of the monodeuterated derivative **HMAQ-*αD*** was readily achieved via the reduction of **FAQ** with $NaBD_4$ in CH_3OH, and purified by column chromatography in 90% yield. **FAQ** itself was synthesized using the photochemical reaction shown in eqn. 1.12 . The presence of one deuterium at the benzylic position was confirmed in **HMAQ-*αD***, by comparison of the integration of the methylene proton signal at δ 4.86 with the aromatic proton signal with three protons at δ 7.82-7.20. A ratio of 1:3 indicated that one deuterium has been incorporated into the methylene position. The MS also indicated the required mass ($M^+ = 238$ m/z) and its purification was >98%.

2.2.2 Anthraquinone Ethers 2.2 and 2.3

The synthetic pathway of **2.2** is shown in eqn. 2.1. The commercially available starting material **HMAQ-a** was first converted to the bromo derivative **HMAQ-b**. After solvolysis in CH_3CH_2OH and purification by column chromatography, **2.2** was obtained in 56% yield. Synthesis of **2.3** followed a similar procedure via **2.1a** and **2.1b**, to give **2.3** in 74% yield.

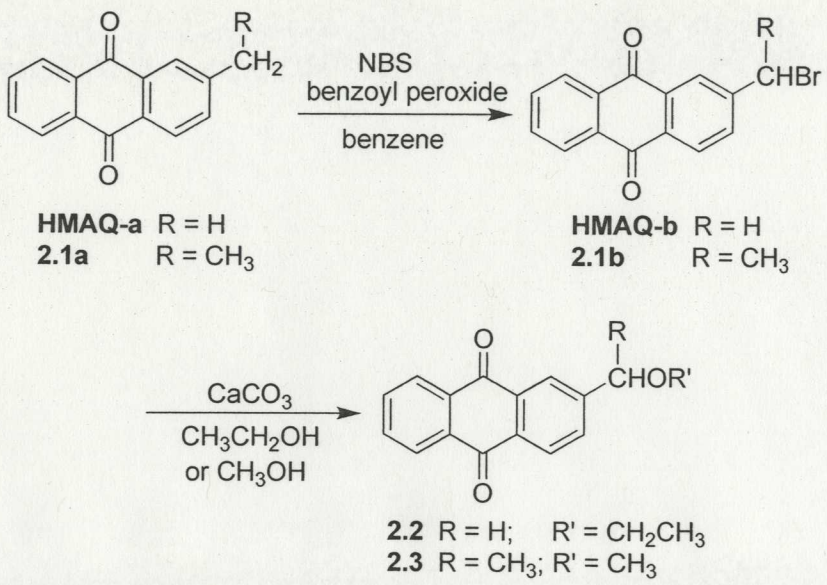

HMAQ-a R = H
2.1a R = CH_3

HMAQ-b R = H
2.1b R = CH_3

2.2 R = H; R' = CH_2CH_3
2.3 R = CH_3; R' = CH_3

(2.1)

2.2.3 Anthraquinone Alcohols 2.1 and 2.7

The synthetic pathway of **2.7** is shown in eqn. 2.2. The commercially available bismethyl compound **2.7a** was first converted to the dibromo derivative **2.7b** via NBS bromination in 90% yield. After hydrolysis, recrystallization from toluene gave **2.7** in 30% yield. Synthesis of **2.1** followed a similar synthetic protocol starting from **2.1a**, to give **2.1** in 75% yield.

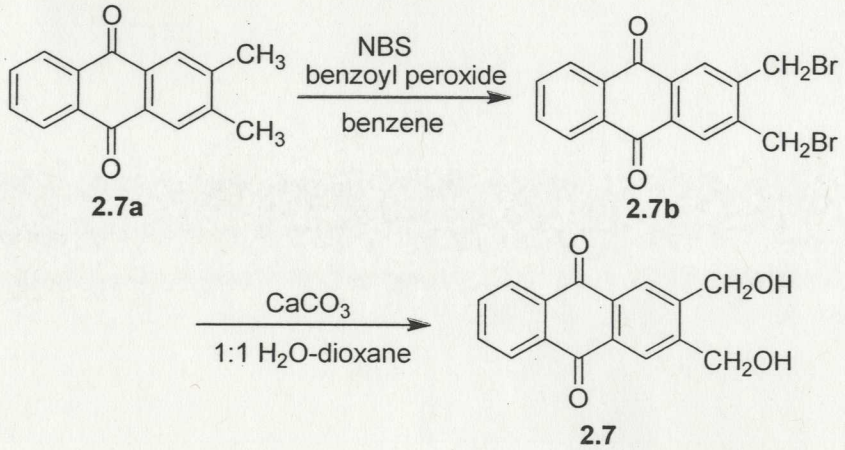

2.7a

2.7b

2.7

(2.2)

2.2.4 Anthraquinones Acetals

The synthetic procedure for acetal **2.8** is shown in eqn. 2.3. **FAQ** is reacted with ethylene glycol in refluxing toluene in the presence of H_2SO_4 catalyst (1% v/v) to give **2.8** via an overall dehydration. After column chromatography, **2.8** was obtained in 74% yield. Synthesis of acetals **2.5** and **2.6** followed a similar synthetic procedure, by reacting benzaldehyde and acetophenone (acid-catalyzed acetal formation) with diol **2.7**, to give the pure target compounds in 49% and 30% yield, respectively.

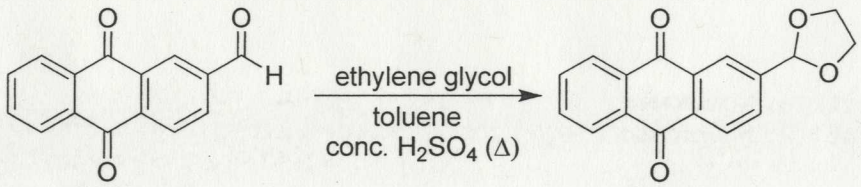

FAQ **2.8** (2.3)

2.2.5 Anthraquinone Acetate Ester 2.4 and Diketone 2.9

Acetate ester **2.4** was readily prepared by esterification of **HMAQ** with acetyl chloride in the presence of pyridine (eqn. 2.4). After column chromatography, pure **2.4** was obtained in 70% yield. Diketone **2.9** (eqn. 2.5) was readily prepared by the hydrolysis of the corresponding bromomethyl precursor, which itself was made from the known methyl derivative **2.9a**.[79] Purification by column chromatography gave an overall yield of 65% for **2.9**.

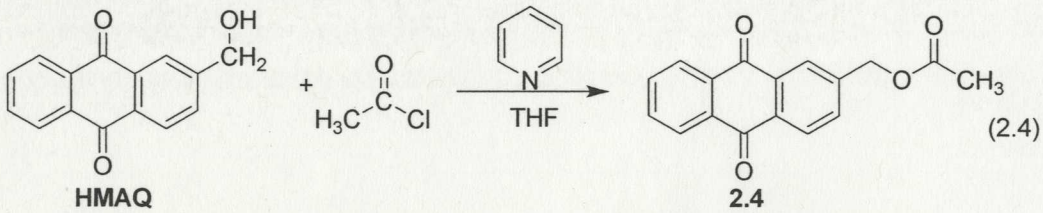

HMAQ **2.4** (2.4)

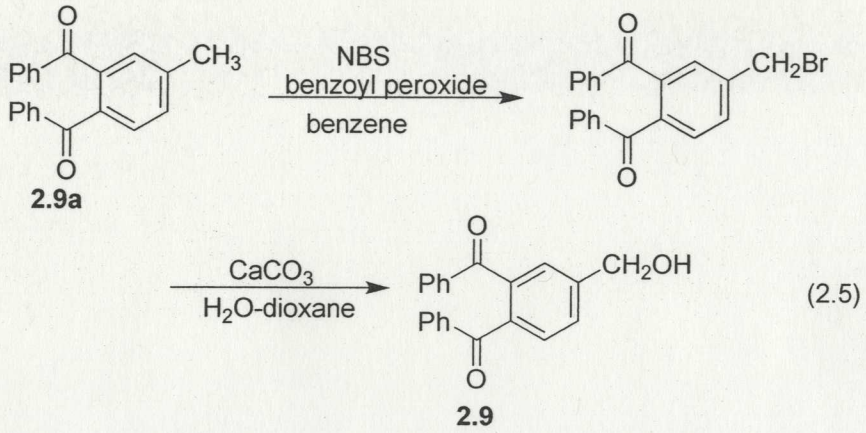

(2.5)

2.3 Product Studies

2.3.1 Photoredox Chemistry of 2.1, 2.7 and 2.8

Initial studies were carried out on anthraquinone **2.1**, **2.7** and **2.8** because these compounds may be regarded as the simplest extensions of the parent **HMAQ**, and which photoredox reaction does not result in photodeprotection of a separate molecule (which is discussed in 2.3.2).

Previous studies have shown that the photoredox reaction of anthraquinone **HMAQ** forms a new anthracene chromophore which can be readily observed by UV-Vis spectroscopy.[62] In addition, the oxygen sensitive initial photoredox product **DHA** cannot be isolated by simple experimental methods. Thus, UV-Vis spectroscopy is a very useful tool to monitor the photoredox reaction. In addition, UV-Vis spectroscopy is time-saving and solvent-saving compared to product work-up. Therefore, it was the first tool used to study the photoredox behaviour of all the anthraquinones in this Thesis.

The first studied compound was **2.1** in which the CH_2OH group of **HMAQ** was replaced by CH_3CHOH. Since the chemical structure of **2.1** is so similar to that of **HMAQ**, **2.1** was expected to undergo the photoredox reaction much like that observed for **HMAQ**. Initial UV-Vis studies were carried out for **2.1** in 1:1 H_2O-CH_3CN

(deaerated with argon). Short time exposure to 300 nm (10 s) resulted in the formation of an intense band at 281 nm and two weaker and broad bands at 396 and 433 nm, respectively (Figure 2.1). With continued photolysis (up to 50 s), these bands gradually increased in intensity. The presence of several isosbestic points indicates that all these new bands belong to the same product(s) with the absence of secondary reactions. After aeration, all of these bands disappeared quickly, to give a spectrum almost identical to that of the starting material **2.1**.

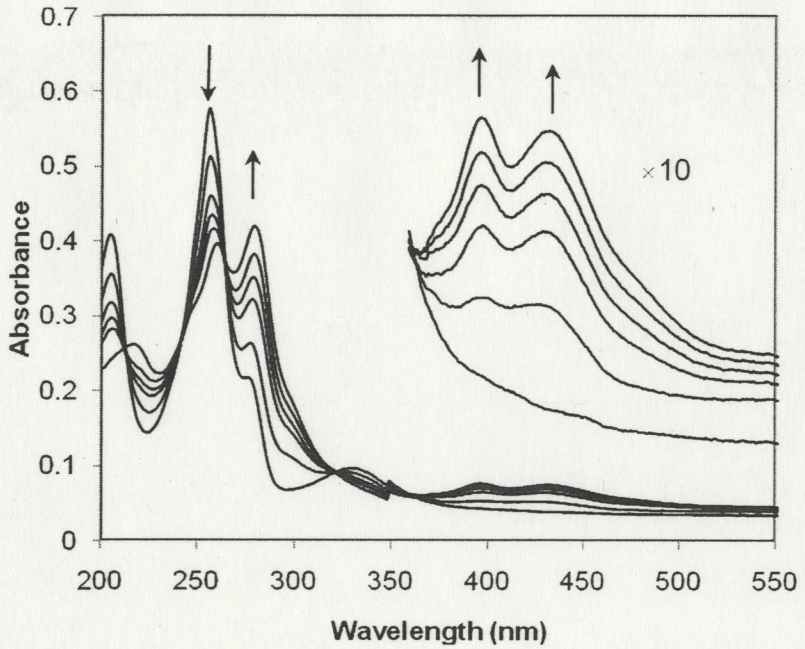

Figure 2.1 UV-Vis traces of the photoredox reaction of **2.1** in 1:1 H_2O-CH_3CN (λ_{ex} = 300 nm). Each trace represents 10 s of photolysis. Photolysis resulted in loss of absorption (due to photoreaction of **2.1**) at 257 and 326 nm with formation of **2.10** (281, 396 and 433 nm). Inset: ten-fold expansion of the long wavelength region.

All of these observations are very similar with that reported for the parent compound **HMAQ**, which suggests that **2.1** undergoes the photoredox reaction to give a UV-Vis observable product **2.10**. When the solution is exposed to air, **2.10** is readily oxidized to

the final stable compound **2.11**, which has a similar absorption spectrum with that of **2.1** (eqn. 2.6).

Direct photolysis in an NMR tube under argon was subsequently employed to study the photochemistry of **2.1** (10^{-3} M, 10% D_2O-CD_3CN, pH 7, λ_{ex} = 350 nm), so that all potential primary photoproducts could be monitored without work-up or oxidation by oxygen. This experiment showed the formation of **2.10-*OD*** (40% yield, distinctive singlet at δ 8.96 due to aromatic proton H_a and a singlet at δ 2.71 due to the methyl protons next to the carbonyl group) (eqn. 2.6). After aeration, the NMR spectrum is entirely consistent with the quantitative formation of **2.11**, with the H_a proton shifted upfield to δ 8.67 and the methyl peak upfield to δ 2.68. All of these observations indicate that **2.1** does undergo a clean photoredox reaction in aqueous solution.

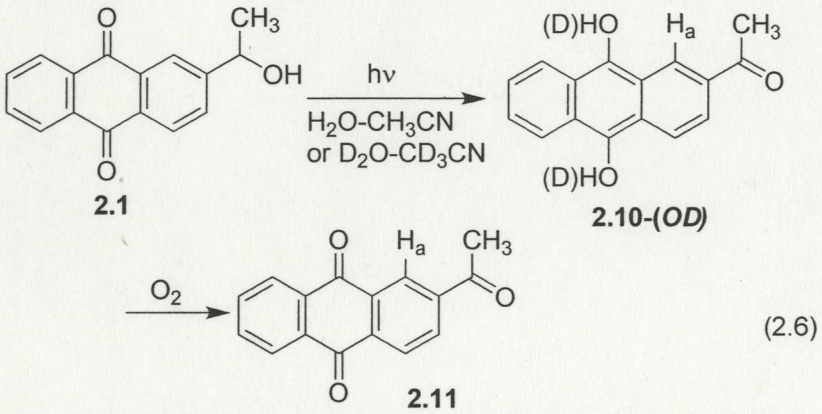

(2.6)

Semi-preparative photolyses were carried out to confirm the reactivity of all compounds (based on initial UV-Vis studies as above) and to isolate, characterize and in some cases trap initial photoproducts. Semi-preparative photolysis of **2.1** (10^{-4} M, 1:1 H_2O-CH_3CN, pH 7) was carried out in a large quartz tube. Exposure to 300 nm gave a yellow solution. When worked-up in air, the solution was bleached quickly to cleanly give **2.11** (>90%). Using the photoredox reaction reported for **HMAQ** as a secondary

actinometer (Φ = 0.8, pH 7), we estimated a quantum yield of photoredox for **2.1** to be about 0.7.

When the anthraquinone bears two CH_2OH substituents at the 2 and 3 positions, will it behave in the manner observed for **2.1** or **HMAQ**? Thus, diol **2.7** was synthesized to explore this question. Exposure of **2.7** to 300 nm excitation resulted in the formation of an intense sharp band at 268 nm with a shoulder band at 286 nm, and less intense but broad bands at 395 nm and 450 nm (Figure 2.2). Although the intense new absorption bands are different from those observed for **HMAQ**, the long wavelength bands are entirely consistent with those of **DHA**. After aeration, all new bands disappeared quickly to give a spectrum almost identical to that of **2.7**. These observations indicate that diol **2.7** gives a photoproduct bearing an oxidizable anthracene chromophore prior to aeration.

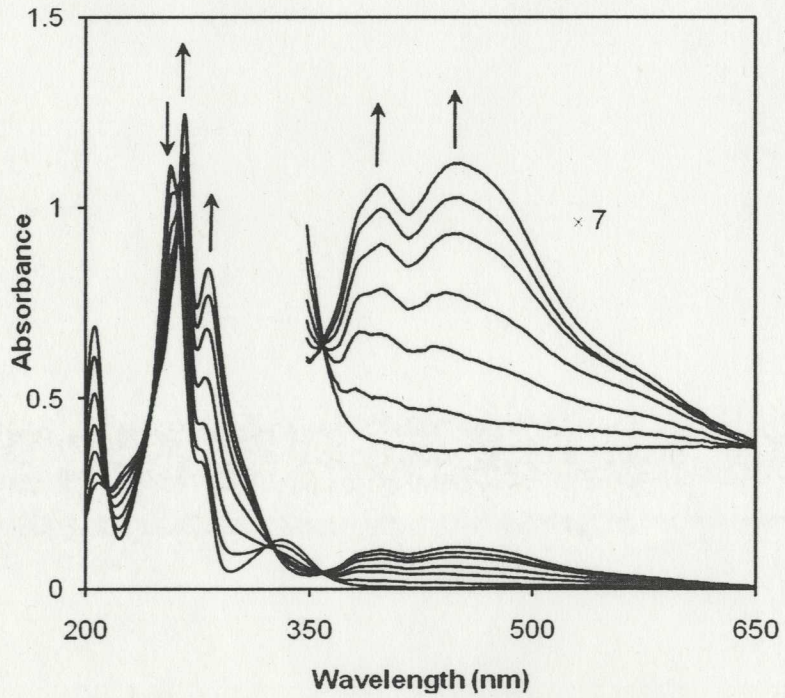

Figure 2.2 UV-Vis traces of the photoredox reaction of **2.7** in 1:1 H_2O-CH_3CN (λ_{ex} = 300 nm). Each trace represents 10 s of photolysis. Photolysis resulted in loss of absorption (due to the photoreaction of **2.7**) at 259 and 326 nm with formation of **2.13** (268 nm, 286 nm, 395 nm and 450 nm). Inset: seven-fold expansion of the long wavelength region.

Due to the low solubility of **2.7** in CH_3CN, the photochemistry of **2.7** could not be carried out in a small amount (1 mL) of D_2O-CD_3CN. Instead, semi-preparative photolysis of **2.7** (10^{-4} M, 1:1 H_2O-CH_3CN, pH 7) was employed. Photolysis of **2.7** (10^{-4}, 1:3 H_2O-CH_3CN, pH 7, deaerated with argon) was carried out in a large quartz tube (100 mL). Exposure to 300 nm gave an orange yellow solution which was bleached when worked-up in air. Finally, the major product, cyclic hemiacetal **2.14** (65%), and a minor product, lactone **2.16** (7%), were isolated (combined quantum yield, Φ ~0.5) (Scheme 2.1).

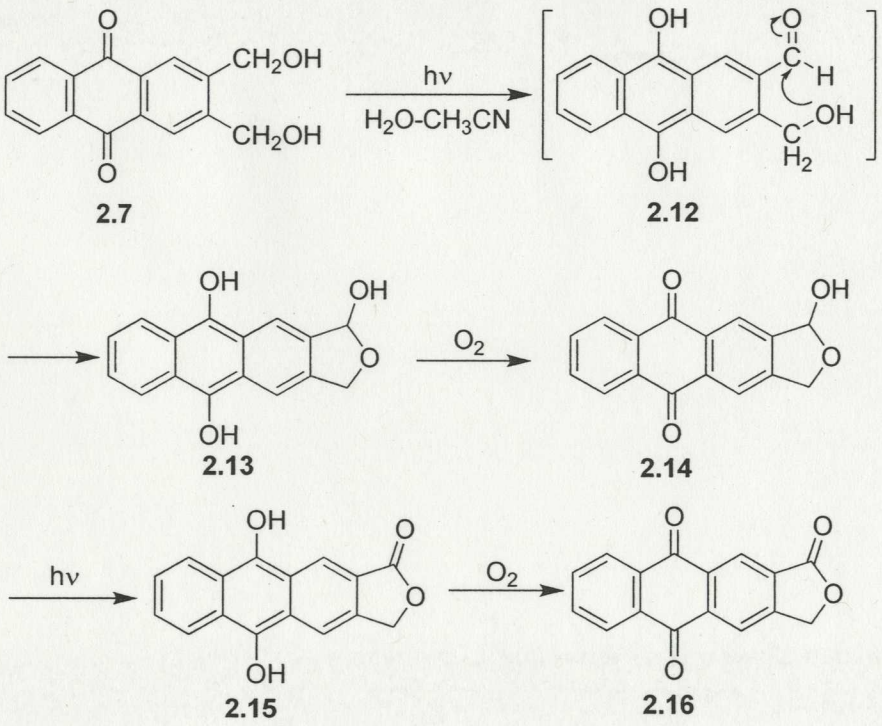

Scheme 2.1 Proposed mechanism for the intramolecular photoredox reaction of **2.7**

Although the anticipated photoredox product **2.12** was not observed, the above results are readily rationalized by the proposed mechanism shown in Scheme 2.1. Anthraquinone **2.7** undergoes an intramolecular photoredox reaction in the manner observed for **HMAQ**

or **2.1**, to generate the expected initial redox product aldehyde **2.12**, which exists as the cyclic hemiacetal **2.13**. Subsequently, **2.13** is oxidized in air to give **2.14** as the major isolated product. In the semi-preparative photolysis of **2.7**, **2.16** was also isolated albeit in low yield. One possibility is that during photolysis of **2.7**, the product **2.13** is oxidized to give **2.14** due to the presence of residual oxygen. Subsequently, **2.14** undergoes a secondary photoredox reaction, give **2.15**, which on work-up gives lactone **2.16**.

To gain further evidence for the secondary photoredox reaction of **2.14**, UV-Vis studies of **2.14** were carried out in 1:1 H_2O-CH_3CN. Exposure to 300 nm resulted in the enhancement of the intense sharp band at 258 nm and formation of a less intense but broad band at 476 nm which was assignable to **2.15** (Figure 2.3). After aeration, all new bands disappeared quickly to give a spectrum identical to that of **2.16**. These observations further show that **2.14** is photoredox active.

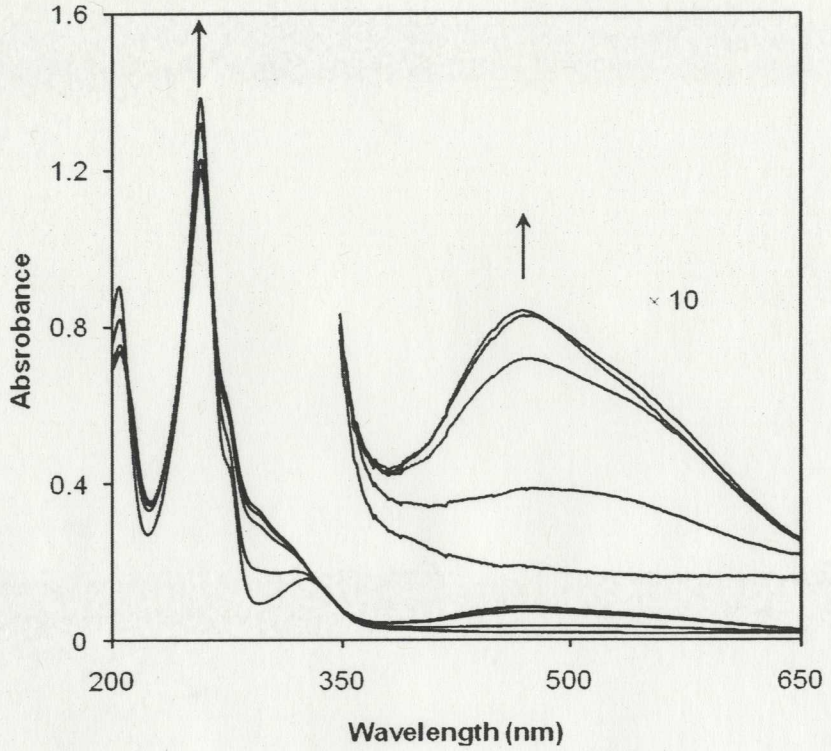

Figure 2.3 UV-Vis traces of the photoredox reaction of **2.14** in 1:1 H_2O-CH_3CN (λ_{ex} = 300 nm). Each trace represents 10 s of photolysis. Photolysis resulted formation of **2.15** (258 nm and 476 nm). Inset: ten-fold expansion of the long wavelength region.

Finally, semi-preparative photolysis of **2.14** (10^{-4}, 1:3 H_2O- CH_3CN, pH 7, deaerated with argon) was carried out in a 100 mL quartz tube. Exposure to 300 nm gave an orange yellow solution which was bleached when worked-up in air. Lactone **2.16** was isolated in 50% yield.

Cyclic acetal **2.8** has no alcohol moiety so there is no prior information as to whether a photoredox reaction would occur or not. Fortunately, UV-Vis studies of **2.8** in 1:1 H_2O-CH_3CN showed formation of a new chromophore with absorption bands at 278 nm and 455 nm (Figure 2.4). The long wavelength band is consistent with that observed for **DHA**. After aeration, all new bands disappeared quickly to give a spectrum almost

identical to that of **2.8**. These observations suggest that photolysis of cyclic acetal **2.8** gives a primary product bearing an anthracene chromophore. In addition, the presence of several isosbestic points indicates that all of these new bands belong to the same product.

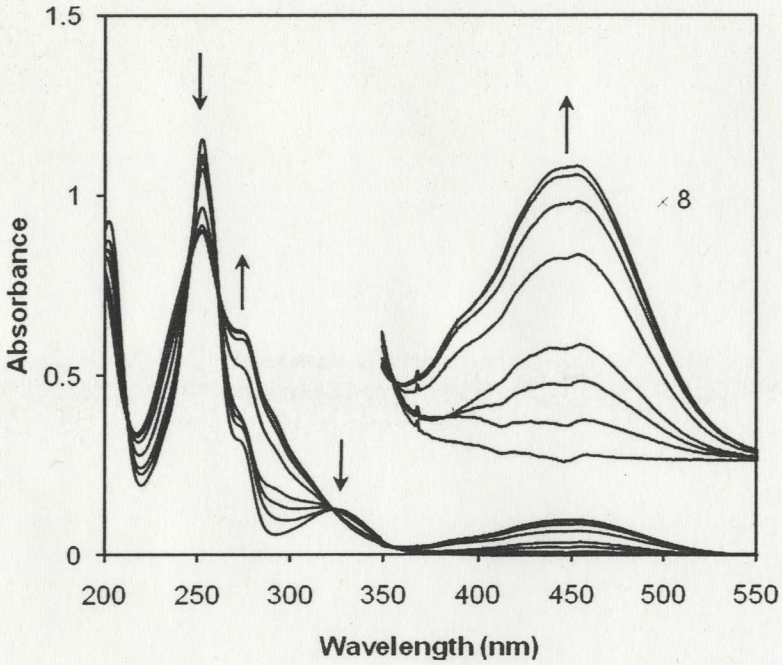

Figure 2.4 UV-Vis traces of the photoredox reaction of **2.8** in 1:1 H_2O-CH_3CN (λ_{ex} = 300 nm). Each trace represents 20 -60 s of photolysis. Photolysis resulted in loss of absorption (due to photoreaction of **2.8**) at 253 nm and 328 nm with formation of **2.17** (278 nm and 455 nm). Inset: eight-fold expansion of the long wavelength region.

Direct photolysis of **2.8** (10^{-3} M, 10% D_2O-CD_3CN, pH 7, λ_{ex} = 350 nm) in a NMR tube resulted in formation of **2.17-*OD*** (10% yield, singlet at δ 9.11 due to aromatic proton H_a). After aeration, the NMR spectrum is entirely consistent with the quantitative formation of **2.18**, with the H_a proton shifted upfield to δ 8.74 (eqn. 2.7).

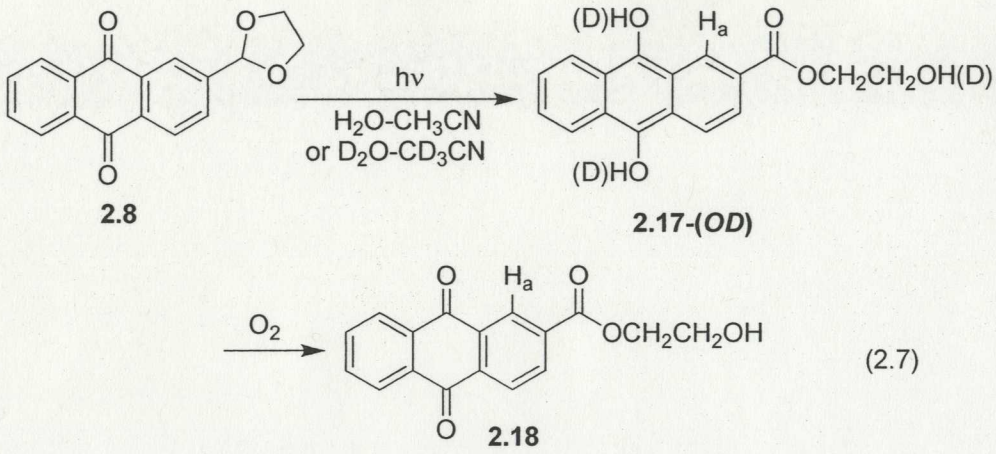

2.8 **2.17-(*OD*)** **2.18** (2.7)

Photolysis of **2.8** (10^{-4} M, 1:1 H_2O-CH_3CN, pH 7, λ_{ex} 300 nm) in a large quartz tube gave a highly coloured intermediate that is assignable to **2.17**, which on treatment with oxygen gives hydroxyester **2.18** in up to 70% yield ($\Phi \sim 0.3$). This anthraquinone system is closely related to one reported by Song and coworkers[77] for the photodeprotection of aldehydes and ketones (also in H_2O-CH_3CN) (Scheme 1.14). However, no molecular mechanisms of the photochemical reaction were given in their paper. It is assumed that the chemistry observed in their work is closely related but not identical to the intramolecular redox reaction observed for **2.8**.

2.3.2 Photodeprotection via the Intramolecular Photoredox Chemistry of 2.2-2.6

Photolabile protecting groups have received considerable attention in recent times, as attested by reviews of Pelliccioli and Wirz[65] and Bochet.[80] New systems that are efficiently photolabile only in aqueous solution with good absorption characteristics (as is inherent in the anthraquinone chromophore) in the long wavelength UV region are always of interest for application in biological systems.

Anthraquinones have been employed in the past for photodeprotection. Blankespoor and coworkers[78] have employed 1-alkoxy-substituted anthraquinones for the photorelease

of aldehydes and ketones via initial intramolecular hydrogen abstraction to generate a radical pair. Both Iwamura and coworkers[76] and Song et al.[77] have employed an anthraquinon-2-yl system for the photodeprotection of alcohols, aldehydes, and ketones. However, these latter studies make no attempts at uncovering the mechanism for the reaction, which may or may not be related to the intramolecular photoredox reaction studied in this work.

In Wan and coworkers' original report of the photoredox chemistry of **HMAQ**,[62] it was noted that when the CH_2OH side chain was replaced with CH_2OCH_3, the photoredox chemistry was still observed, with one of the products being CH_3OH, although with an attenuation in yield (the reaction was not observed with a simple CH_3 side chain).[62] Further explorations of the possibility of using the anthraquinon-2-yl moiety for the photorelease of alcohols and other functional groups (e.g., aldehydes and ketones) are warranted. Thus, anthraquinones **2.2-2.6** are designed for this purpose, all of which were anticipated to undergo intramolecular photoredox reaction with the release of alcohols (**2.2** and **2.3**), acetic acid (**2.4**), aldehyde (**2.5**) and ketone (**2.6**).

Initial UV-Vis studies were carried out for **2.2** in 1:1 H_2O-CH_3CN (deaerated with argon). Short time exposure to 300 nm (< 60 s) resulted in the formation of an intense sharp band at 260 nm and a less intense but broad band at 370 nm that absorbs up to 450 nm (Figure 2.5). When left in the dark (over a 10 min period) or with continued photolysis, this species transforms to a species with bands at 274, 392 and 451 nm which are associated with **DHA**. After aeration, all new bands disappeared quickly to give the spectrum almost identical to that of **2.2**. These observations suggest that the

intramolecular photoredox chemistry of **2.2** gives rise to an observable intermediate on the way to **DHA**. Similar behaviour was observed for **2.3**.

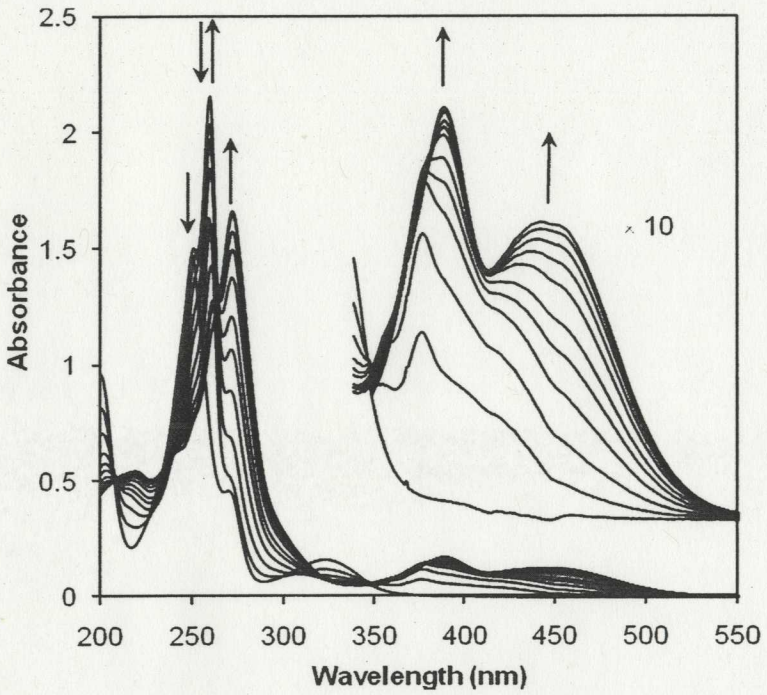

Figure 2.5 UV-Vis traces of the photoredox reaction of **2.2** in 1:1 H_2O-CH_3CN (λ_{ex} = 300 nm). Each trace represents 20s - 60s of photolysis. Early photolysis resulted in loss of absorption (due to photoreaction of **2.2**) at 250 and 325 nm with formation of an observable intermediate **2.19** (260 and 370 nm). This is subsequently transformed to **DHA** (over a 10 min period; loss of 260 nm band, formation of 274, 392 and 451 nm bands). Inset: ten-fold expansion of the long wavelength region

The photochemistry of **2.2** (10^{-3} M, 10% D_2O-CD_3CN, pH 7, λ_{ex} 350 nm) was studied by direct photolysis in an NMR tube under argon. This experiment showed formation of **DHA-*OD*** (30% yield, singlet at δ 10.07 due to the aldehyde proton and a singlet δ 8.90 due to aromatic proton H_a) as well as formation of CH_3CH_2OD (characteristic triplet and quartet at δ 1.10 (J = 7.3) and δ 3.52 (J = 7.3), respectively (eqn. 2.8). After aeration,

the NMR spectrum is entirely consistent with quantitative formation of **FAQ**, with the aldehyde proton shifted downfield to δ 10.15 and the H_a proton upfield to δ 8.67.

Similar results were obtained for **2.3**, which gave photoproduct **2.10-*OD*** (40% yield, singlet at δ 9.02 due to aromatic proton H_a and a singlet δ 2.72 due to the methyl protons next to the carbonyl group), and photoreleased the corresponding CH_3OD (characteristic singlet at δ 3.24), respectively. After aeration, the NMR spectrum is entirely consistent with the quantitative formation of **2.11**, with the H_a proton shifted upfield to δ 8.72 and the methyl protons upfield to δ 2.69.

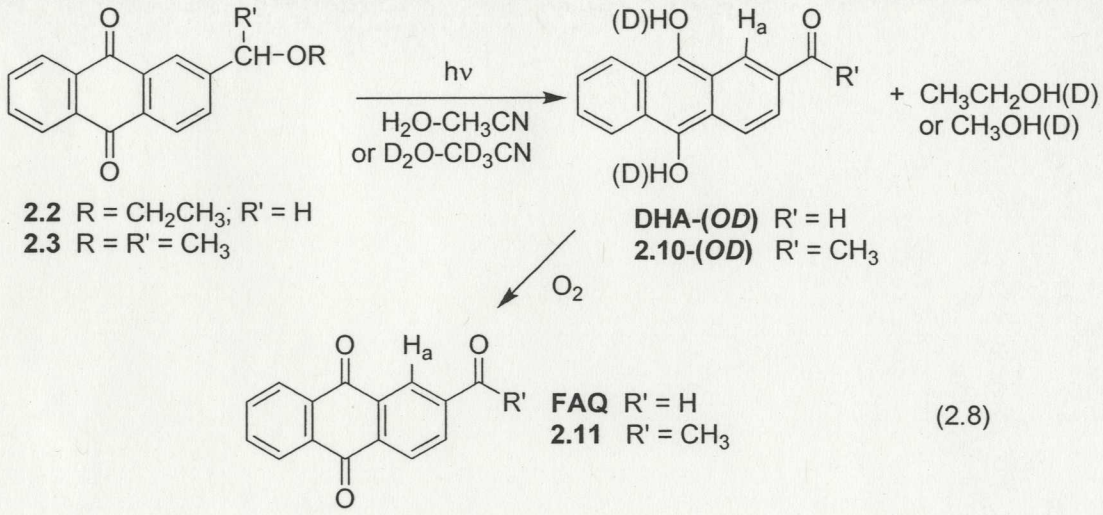

(2.8)

A proposed mechanism of reaction for **2.2** (and **2.3**) is shown in Scheme 2.2. Excited **2.2** undergoes carbonyl oxygen protonation with benzyl C-H bond deprotonation, to give a quinone dimethide intermediate **2.19** (also an enol or enol ether). Further reaction requires nucleophilic attack by water (with protonation at the remaining ketone) to generate dihydroxyanthracene **2.20**, which is expected to quickly release CH_3CH_2OH to give **DHA**, followed by transformation to **FAQ** when exposed to oxygen. Evidence for formation of **2.19** is provided in Figure **2.5** in which an intermediate absorbing at 260 nm

and 370-450 nm was observed prior to formation of **DHA**. Gritsan and coworkers[81] reported a related *o*-quinone dimethide **2.21** at 380 and 590 nm generated via intramolecular hydrogen abstraction of triplet excited 1-methylanthraquinone (it is not possible using this method to photogenerate the isomer that directly corresponds to **2.19** in which the OCH_2CH_3 is replaced by H). Since **2.19** is cross-conjugated whereas **2.21** is not (it has a longer linearly conjugated system), it is expected to have a longer wavelength absorption band. Therefore, we have tentatively assigned the observed intermediate at 260 nm and 370-450 nm as quinone dimethide **2.19**.

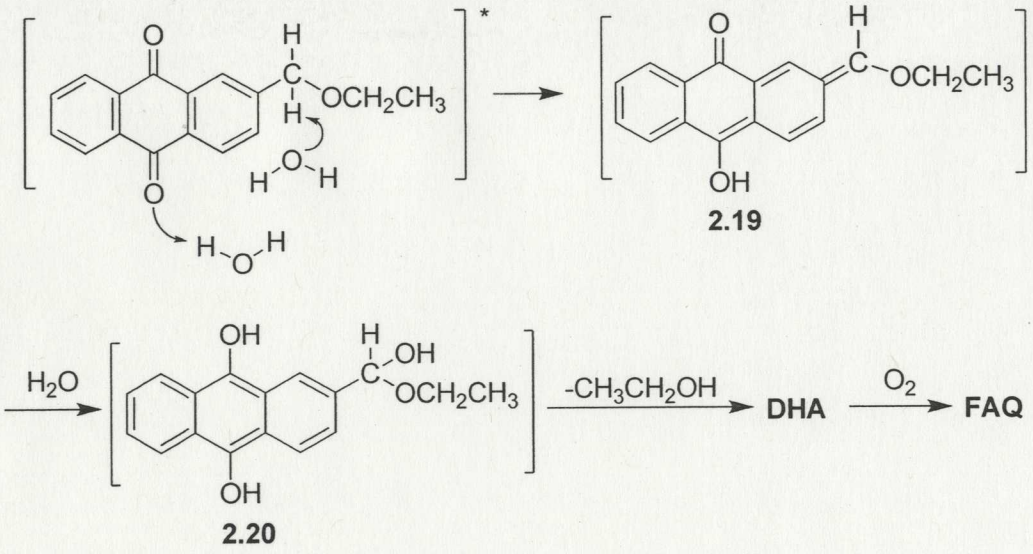

Scheme 2.2 Proposed mechanism of reaction for **2.2**

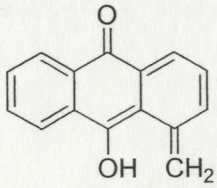

2.21 (λ_{max} 380, 590 nm)

Finally, semi-preparative photolyses of **2.2** and **2.3** were carried out in 100 mL quartz vessels (10^{-4} M, 1:1 H_2O- CH_3CN, pH 7, argon purged). Upon work-up in air, **2.11** and **FAQ** were obtained in up to 90% yield. In these runs, the formation of the corresponding photoreleased CH_3CH_2OH and CH_3OH was not observed due to the work-up procedure which involved drying under vacuum. In order to follow the photorelease of CH_3CH_2OH and CH_3OH, photolyses were carried out in 10% D_2O-CD_3CN (pH 7) using 3 mL quartz cuvettes (under argon purge) and monitored by ^1H NMR at various time intervals (Figure 2.6). The plot shows that conversions as measured by released alcohol reached up to 90%. Quantum yield measurements showed that both **2.2** and **2.3** were about equally efficient, with $\Phi \sim 0.4$ in 1:1 H_2O-CH_3CN.

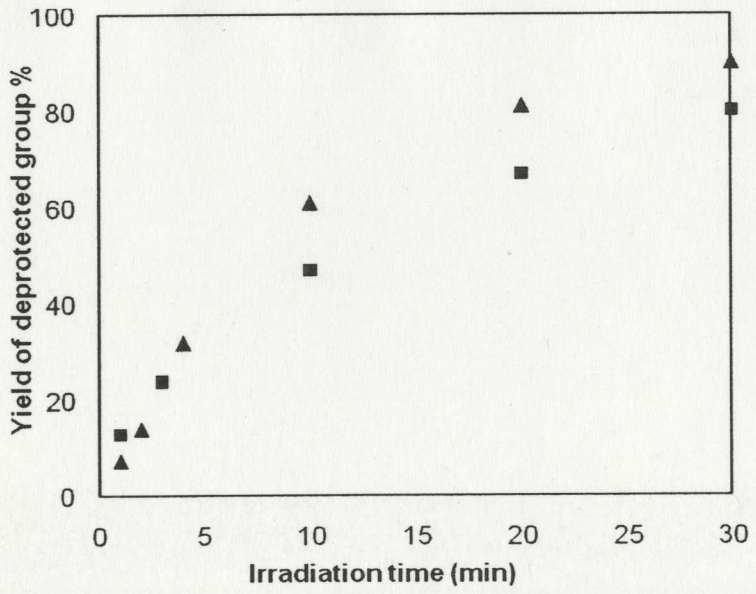

Figure 2.6 Yields of CH_3CH_2OH (▲) and CH_3OH (■) from photolysis of **2.2** and **2.3**, respectively, in 10% D_2O-CD_3CN (λ_{ex} 300 nm), as determined by ^1H NMR (relative to the starting material). Measurement error is ± about 5%.

Acetate ester **2.4** was expected to undergo similar photoredox chemistry as observed for **2.2** and **2.3**, which would offer a method for the photorelease of carboxylic acids. However, to our great surprise, **2.4** proved to be *photoinert* under conditions in which extensive (> 90%) photoredox was observed for **HMAQ** and **2.1-2.3**. In these runs, **2.4** was recovered unchanged after photolysis. Extended photolysis led only to photodecomposition with no evidence of any photoredox reaction. We were puzzled at the complete lack of photoredox chemistry since one would not have anticipated a great deal of difference with respect to electronic character between a CH_3O and a $CH_3(C{=}O)O$ group at the benzylic position of the anthraquinone chromophore. On closer analysis, one would argue that the (ester) oxygen on the acetyl group is less able (via electron withdrawing inductive effects) to stabilize a developing positive charge (which is presented in the proposed mechansim in Section 2.4.7) at the benzylic position compared to an oxygen on a simple alkyl group. Since it is known that a simple methyl group on the anthraquinone leads to an unreactive compound (with respect to photoredox reaction)[62] it would appear that such a small change could lead to lack of reaction. Another possibility is that the carbonyl oxygen of the acetyl group is able to deprotonate (or partially deprotonate) the benzylic proton in the excited state, via a cyclic transition state. If this is completely reversible, only non-productive deactivation of the excited state would result. However, photolysis in D_2O resulted in no observable deuterium incorporation in recovered **2.4** indicating that there is no reversible proton transfer either to solvent water or to the acetyl group. Since **2.4** was completely unreactive, related derivatives were not studied further until a better understanding of the lack of reaction is available.

Recently, Song and coworkers reported a similar anthraquinone system for the photodeprotection of carboxylic acids.[82] In 1:1 H_2O-CH_3CN, 2-(1'-hydroxyethyl)-anthraquinone (**2.22**) was photoinert, which is consistent with our observations with **2.4**. However, photolysis of **2.22** in neat CH_3OH photoreleases the corresponding benzoic acid (Φ = 0.077) (Scheme 2.3). The authors suggested that the proposed mechanism involves a photoreduction via hydrogen abstraction step. Thus, triplet excited **2.22** is reduced by CH_3OH, to give dihydroxyanthracene **2.23**. Subsequently, **2.23** undergoes a photoreaction to release benzoic acid, and give enol **2.24**. Ketonization of **2.24** gives **2.25**. The photodeprotection reaction observed for **2.22** in CH_3OH has significant differences compared to the pathways for **2.2** and **2.3**. Compound **2.22** reacts via initial photoreduction whereas **2.2** and **2.3** react via overall intramolecular photoredox reaction.

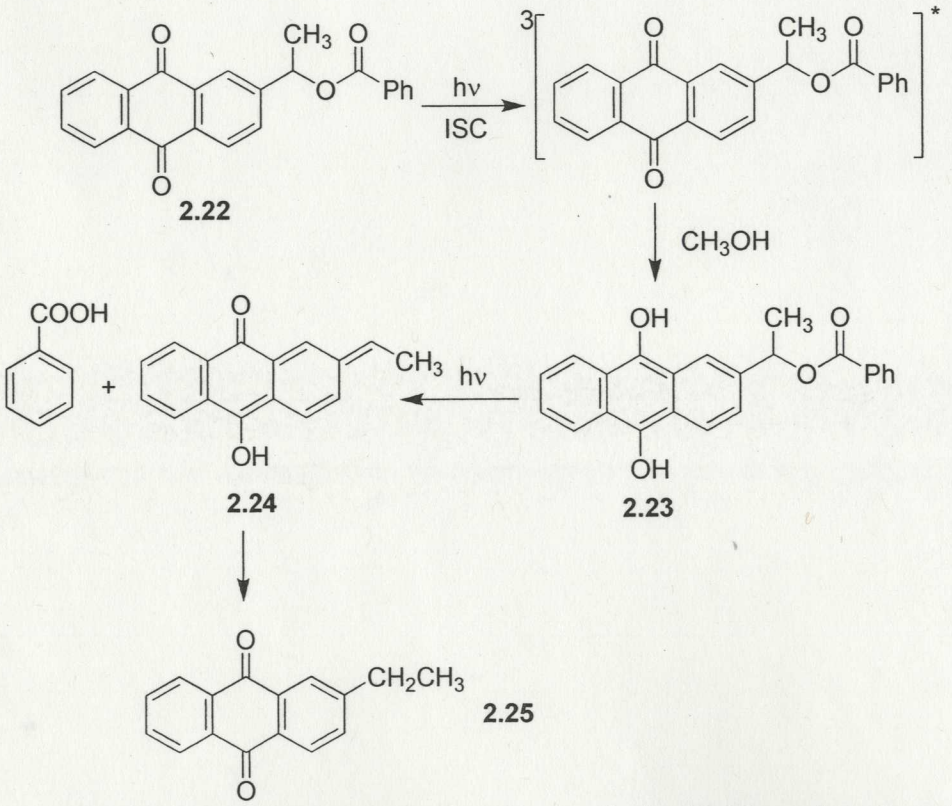

Scheme 2.3 Proposed mechanism for photolysis of **2.22** to release benzoic acid

Based on positive results observed for **2.2** and **2.3**, we anticipated that compounds **2.5** and **2.6** will undergo an analogous photoredox reaction, which would release the corresponding benzaldehyde and acetophonone, respectively as shown in Scheme 2.4. Initial UV-Vis studies of **2.5** showed the requisite formation of a coloured intermediate on photolysis at 300 nm (absorptions at 269, 391 and 450 nm) in 1:3 H_2O-CH_3CN, (bleached on introduction of air), which is assignable to redox product **2.13** (Figure 2.7). The same behaviour was observed for **2.6**.

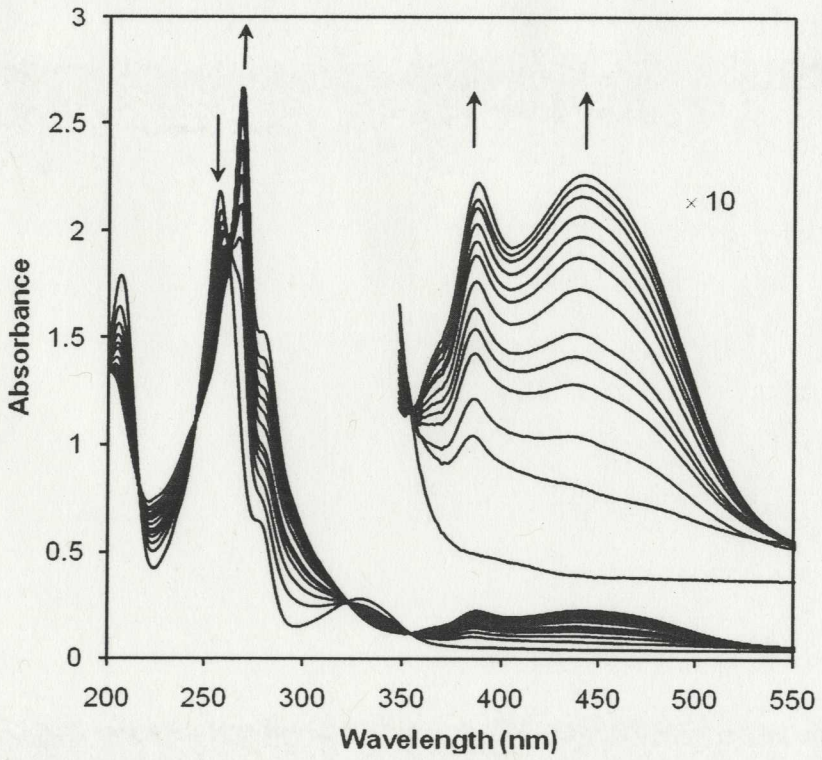

Figure 2.7 UV-Vis traces of photoredox reaction of **2.5** in 1:1 H_2O-CH_3CN (λ_{ex} = 300 nm). Each trace represents 10 s of photolysis. Photolysis resulted in loss of absorption (due to photoreaction of **2.5**) at 258 and 326 nm with formation of **2.13** (269 nm, 391 nm and 450 nm). Insert: ten-fold expansion of the long wavelength region.

The low solubilities of both **2.5** and **2.6** prevented studies in sealed NMR tubes (preventing oxidation of initial photoproducts) which would have been more ideal for the analysis of released benzaldehyde and acetophenone. Instead, semi-preparative photolyses were carried out in 100 mL quartz vessels with work-up in air. In these runs, up to 80% yield of **2.16** was obtainable with formation of the corresponding benzaldehyde (characteristic aldehyde singlet at δ 10.00) and acetophenone (characteristic methyl singlet at δ 2.59). The expected initial redox product **2.13** was not observed. Since the quantum yield for reaction of **2.5** and **2.6** were the lowest observed for this series of compounds ($\Phi \sim 0.02$), long photolysis times were required to achieve significant conversion. One possibility is that initially formed redox product **2.13** was oxidized *in situ* to **2.14** during these long photolysis runs, which on further photolysis (subsequent photoredox reaction) would lead to **2.15** and subsequently **2.16** (Scheme 2.4). This is consistent with the photoredox reaction of **2.14** discussed in Section 2.3.1.

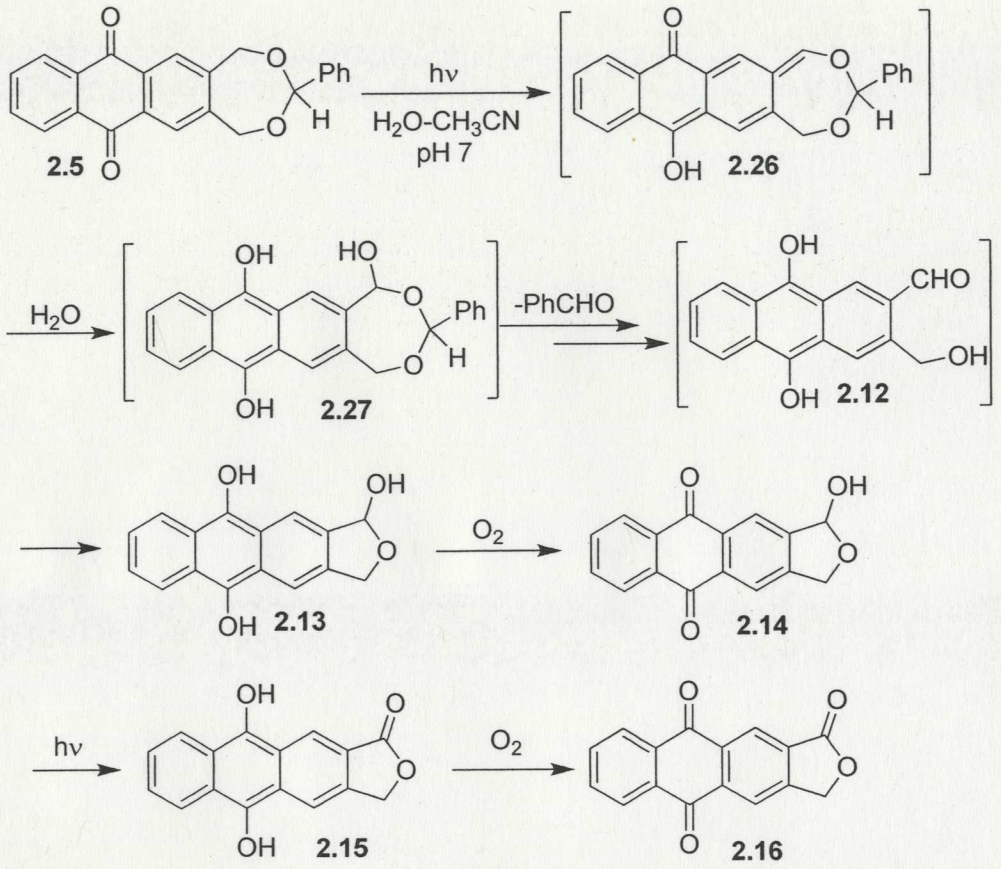

Scheme 2.4 Proposed mechanism for photolysis of **2.5** to release benzaldehyde

2.3.3 Photochemistry of Diketone 2.9

Finally, the potential photoredox chemistry of diketone **2.9** was explored. The compound is related to anthraquinone **HMAQ** except for the lack of "annelation" of the second ring, as well as possessing all of the structural features of benzophenone **1.51**, which is known to undergo efficient photoredox reaction in acid (pH < 3) (eqn. 1.11).[49] We were disappointed initially since no reaction was observed on photolysis of **2.9** in 1:1 H_2O-CH_3CN, pH 1-7 (reported pH is of the aqueous portion). However, at pH ~ 0 (about 5% H_2SO_4), significant changes were observed in the UV-Vis spectrum on photolysis (Figure 2.8), namely, the formation of two distinct bands at 316 and 426 nm which were unchanged on introduction of air to the solution.

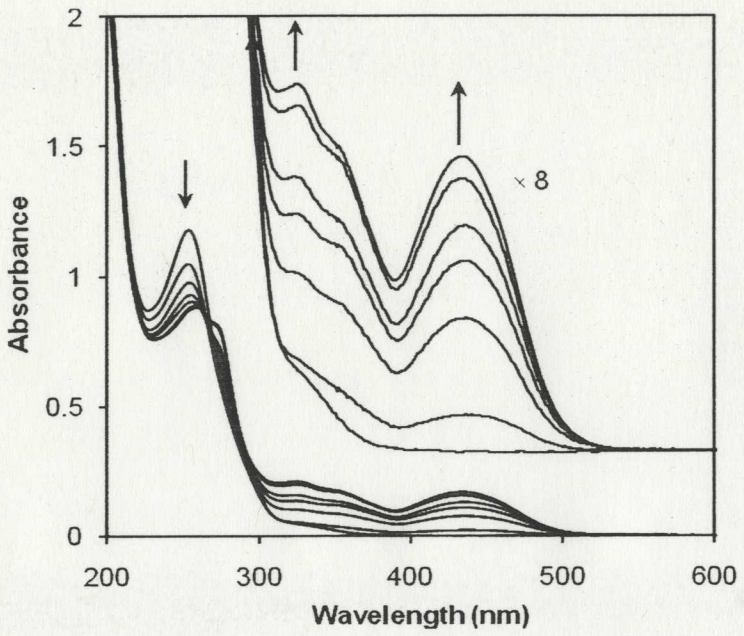

Figure 2.8 UV-Vis traces observed on photolysis of diketone **2.9** in 1:1 H_2O-CH_3CN (λ_{ex} 300 nm; pH 0; argon purged). Each trace represents 10 min of photolysis. Photolysis resulted in loss of absorption (due to photoreaction of **2.9**) at 259 nm with formation of **2.29** (316 nm and 426 nm). Insert: eight-fold expansion of the long wavelength region

Semi-preparative photolysis of **2.9** in 1:1 H_2O-CH_3CN, pH ~ 0 gave diphenylisobenzofuran **2.29** (50%) and diketone aldehyde **2.30** (30%) (combined Φ ~ 0.003) (eqn. 2.9). Consistent with the above UV-Vis traces, isobenzofuran **2.29** has absorption bands at 316 and 426 nm (see Appendix B). Indeed, **2.29** would be the logical acid-catalyzed condensation product of the initially formed intramolecular redox product **2.28** (or an alternate isomer obtained by interchange of the ketone and benzhydrol moieties). Independent photolysis of **2.29** in the presence of oxygen gave **2.30** quantitatively consistent with the literature on the photochemistry of diphenylisobenzofurans.[83]

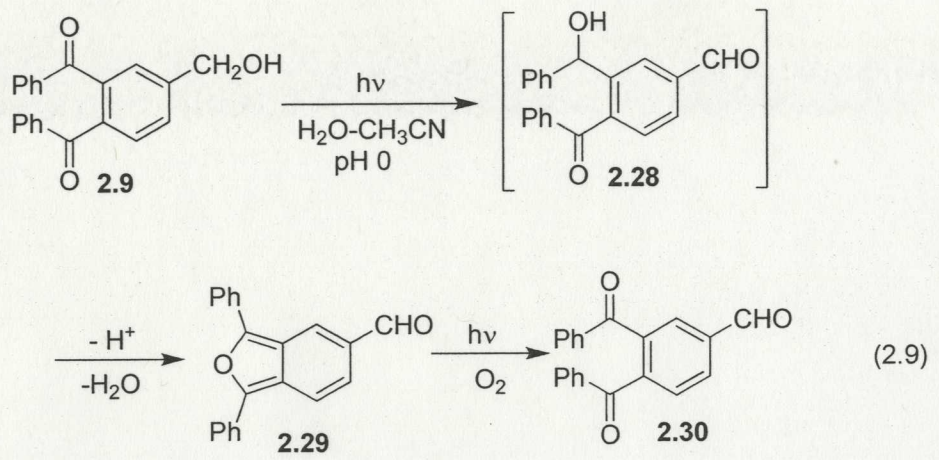

(2.9)

Consistent with its isobenzofuran chromophore, **2.29** in CH_3CN displayed the expected absorption bands from 350 nm to 500 nm (λ_{em} = 550 nm), and long wavelength fluorescence with a broad band between 460 nm and 710 nm (λ_{ex} = 440 nm). Photolysis of **2.29** in the presence of air resulted in the significant decrease of both absorption and fluorescence emision. These observations are rationalized by the photochemical formation of **2.30**, which is not fluorescent, and has very different UV-Vis absorption characteristics compared to **2.29**.

2.4 Mechanistic Studies

2.4.1 Isotope Effects on the Photoredox Reaction

The proposed mechanism[62] of the intramolecular photoredox reaction of anthraquinone **HMAQ** involves two key proton transfer steps. One is protonation of the ketone and the other is deprotonation of the C-H bond of the benzylic CH_2OH moiety. To probe the importance of the C-H bond breaking step, compound **HMAQ-*αD*** was made as this substrate offers the choice between a C-H *vs*. a C-D bond at the CH_2OH moiety. We had also intended to study the α,α–dideutero compound (in direct comparison experiments with **HMAQ**) but were unable to readily synthesize the required

compound. In any event, compound **HMAQ-*αD*** proved to be just as useful as the C-H *vs.* C-D bond breakage occurs from the *same* reactive excited state.

Photolysis of **HMAQ-*αD*** (10^{-5} M, 1:1 H_2O- CH_3CN, pH 7, argon purged, 300 nm) was carried out at 1-4 min intervals and gave oxidized products **FAQ-*D*** and **FAQ** in overall conversions of 25-85% when solutions were worked-up in air, *via* the initially formed redox products **2.31** and **DHA**, respectively (eqn. 2.10). The proportion of **FAQ-D** vs. **FAQ** was calculated based on the integration of the aldehyde proton of **FAQ** *vs.* aromatic proton H_a of **FAQ** and **FAQ-*D***. The product ratio was further confirmed by MS analysis. The ratio of yield for **FAQ-*D***: **FAQ** was 2.1 ± 0.1 which can be equated to an isotope effect for quantum yield of photoredox reaction, $\Phi_H / \Phi_D = 2.1 \pm 0.1$. That is, there is a preference for breaking the C-H bond compared to the C-D bond in this reaction. Indeed, since both C-H and C-D bonds come from the same excited state, this ratio is also equable to a kinetic isotope effect for deprotonation, k_H/k_D.

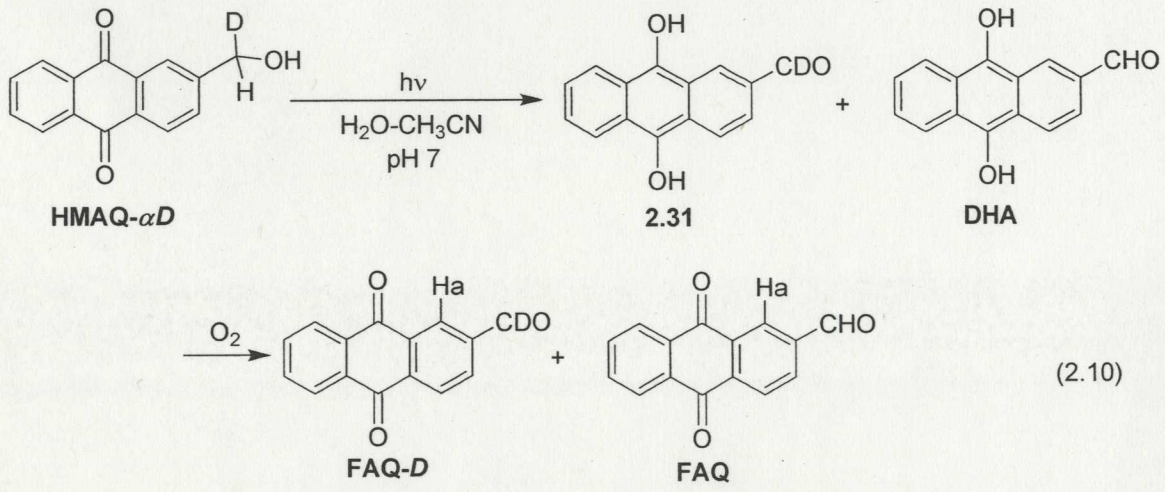

(2.10)

Kinetic isotope effects for the deprotonation of C-H *vs.* C-D are not well reported in organic photochemistry since only a few well-defined excited state carbon acids are known.[18b] We have reported a primary kinetic isotope effect (k_H/k_D) of 2.8 ± 0.4 for the

deprotonation of the benzylic protons of dibenzosuberene,[84] a very strong carbon acid in S_1, and a primary isotope effect for reaction (at the benzylic position) of 1.9 ± 0.2 for a related photoredox reaction of a nitrobiphenyl alcohol.[85] These values are remarkably similar to the value observed for the anthraquinone system under study. This result is consistent with a mechanism in which the rate limiting step probably involves C-H bond breaking (at the CH_2OH moiety) of a prior protonated substrate (at the carbonyl oxygen). This is illustrated in Scheme 2.5 where the excited anthraquinone deprotonation undergoes either loss of the C-H to give **2.32-*αD*** and then **2.31**, or loss of the C-D to give **2.32** and then **DHA**. Remarkably, recovered **HMAQ-*αD*** did not lose deuterium content in exhaustive photolyses carried out in H_2O indicating that the deprotonation step is irreversible.

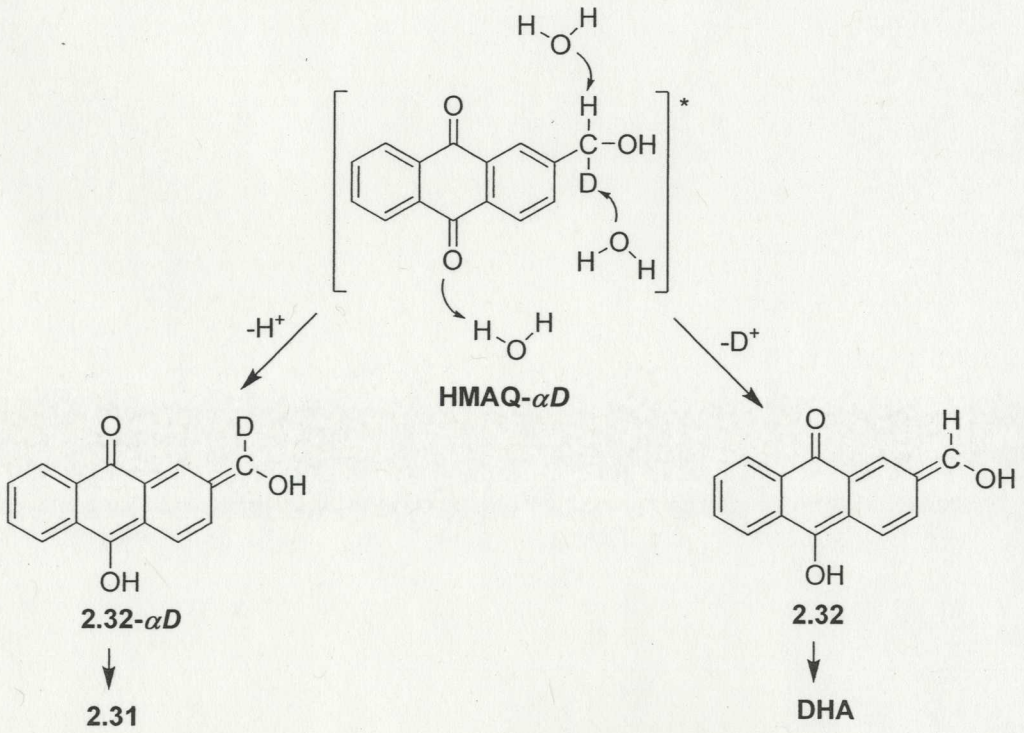

Scheme 2.5 Deprotonation of the excited anthraquinone **HMAQ-*αD***

To explore the effect of H_2O *vs.* D_2O on photoredox reaction of anthraquinone **HMAQ**, photolysis of **HMAQ** was carried out in 3 mL quartz cuvettes (deaerated by argon purge) as a function of H_2O/D_2O content (in CH_3CN). The extent of the photoredox reaction was monitored at 280 nm (formation of **DHA** or dideutero **DHA** in D_2O) and the observed ΔA (which is directly proportional to quantum yield for the reaction) plotted *vs.* water content (Figure 2.9).

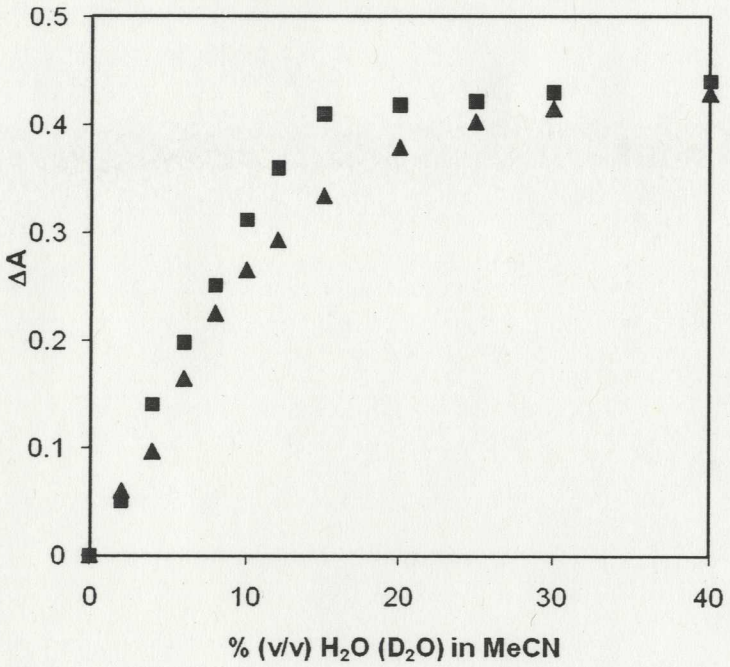

Figure 2.9 Effect of H_2O (■) and D_2O (▲) content (in CH_3CN) on photoredox efficiency of **HMAQ** (λ_{ex} = 300 nm) monitored at 280 nm (formation of **DHA**). Measurement error is about ± 5%.

The photoredox reaction is very sensitive to water content especially at the lower water region noting that no reaction was observed in neat CH_3CN. It reaches a plateau region (in efficiency) at about 20% (v / v) water. Note also that use of D_2O results in a lower quantum yield in most water contents, by as much as 20% at 15% (v/v) $H_2O(D_2O)$. In low and high water regions, we were unable to detect a significant difference in relative

efficiency using the technique employed although in most cases, reaction in the presence of D_2O was always less efficient. It seems reasonable to assume that the details of the photoredox mechanism change with water content since the span of water concentrations convered ranges from mostly CH_3CN to 40% water. An analysis of solvent isotope effects over this range of water content is beyond the scope of this work but it seems clear that proton transfer to the carbonyl oxygen is intimately involved in the reaction mechanism. The generally small solvent isotope effects observed are consistent with fast rates of proton transfer from the solvent to the carbonyl oxygen and this is entirely consistent with excited state proton transfers.

2.4.2 pH Effects on the Photoredox Reaction

Previous studies of benzophenone **1.51** showed that no photoredox reaction was observed for **1.51** in neutral aqueous solution.[49] But when the pH of the solution was lower than 3, an efficient photoredox reaction was observed.[49] This indicates that the photoredox behaviour of benzophenone **2.51** is acid catalyzed. Although **HMAQ** has an efficient photoredox in neutral aqueous solution ($\Phi \sim 0.8$), we wondered whether or not the photoredox of **HMAQ** can be acid catalyzed as was observed for **1.51**.

To explore the effect of pH on the efficiency of the intramolcular photoredox reaction of **HMAQ**, photolyses of **HMAQ** (10^{-4} M, 1:1 H_2O- CH_3CN, argon purged, λ_{ex} = 300 nm, pH 13-1) were carried out in 100 mL quartz vessels. After irradiation, all solutions were worked up in air. Conversion yields (%) of the photoredox product were determined with proton NMR. The results are plotted as a function of pH in Figure 2.10. No acid catalysis for this reaction was observed between pH 9 and pH 1. Instead, the reaction displayed a base inhibition above pH 9. These observations strongly suggest that the

proton (or hydroxide ion) concentration plays an important role in the photoredox reaction. Isotope effect on the photoredox reaction as shown in Section 2.4.1 suggests that the rate limiting step might involve a C-H bond breaking (at the CH_2OH moiety) of a prior protonated substrate (at the carbonyl oxygen). Although basic solution is favourable for the benzylic C-H bond breaking, it is unfavourable for the protonation of the carbonyl oxygen. Alternatively, there may be an unproductive photophysical or a photochemical quenching pathway as hydroxide ion is increased. The details of this quenching pathway were not further investigated.

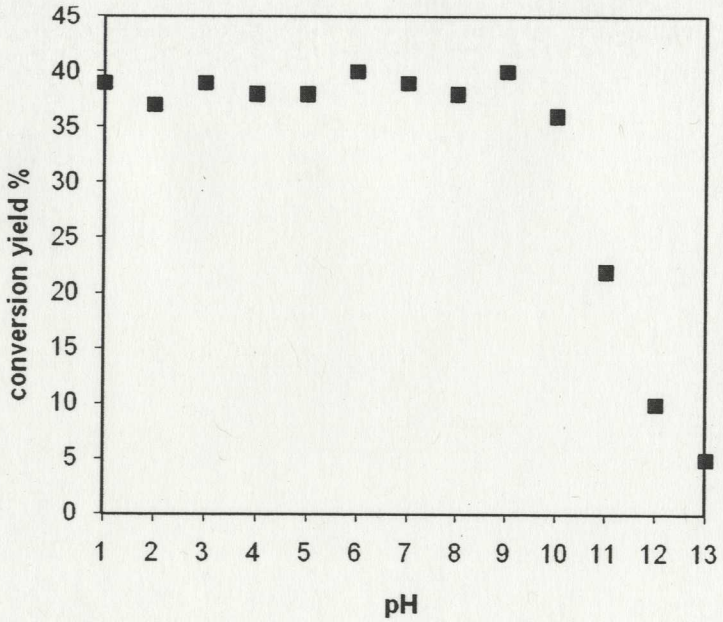

Figure 2.10 pH Dependence of intramolecular photoredox efficiency for **HMAQ** in 1:1 H_2O-CH_3CN, ~ 10^{-4}M, N_2 (pH refers to the aqueous portion). Measurement error is about ± 5%.

2.4.3 Solvent Effects on the Photoredox Reaction

It has been noted[62] that **HMAQ** does not undergo photoredox in neat CH_3CN but upon increasing H_2O content, the photoredox reaction is observed and becomes more efficient. The role of H_2O in the photoredox reaction is believed to be as a mediating solvent and as a catalytic source of protons and weak base, but *not* as a reducing agent. On the other

hand, it is well-known that alcohols function as efficient direct reducing agents (*via* initial hydrogen abstraction from the alcohol) for a variety of photoexcited anthraquinones and related compounds.[59] To explore the effect of an alcoholic solvent on the intramolecular photoredox reaction, photolyses of **HMAQ** were carried out in H_2O-CH_3CH_2OH mixtures.

Initial photolysis of **HMAQ** in neat CH_3CH_2OH (argon saturated, not water-free) followed by work-up in air gave only oxidized aldehyde product **FAQ** up to 25% yield without any photoreduction product. It has been reported[59] that anthraquinones undergo photoreduction in CH_3CH_2OH to give dihydroxyanthracenes which readily react with oxygen to restore the starting materials (anthraquinones). Thus, in principle, photoreduction product **2.33** was probably generated and oxidized quickly to **HMAQ** in the presence of air (Scheme 2.6).

To obtain evidence for the formation of **2.33**, a method of trapping **2.33** was developed to give a stable product that could be isolated and subjected to NMR and MS analyses. Since **2.33** is an aromatic alcohol, a viable trapping method is to convert it to its acetyl ester, by a reaction with Ac_2O using base, which would give diacetoxyanthracene alcohol **2.35**.

The same idea was also used to trap the photoredox product **DHA**, to form diacetoxyanthracene aldehyde **2.34**. Isolation of **2.34** would provide additional evidence that an anthracene moiety is formed in the photoredox reaction. A solution of **HMAQ** (10^{-4} M, 1:1 H_2O-CH_3CN, pH 7, argon purged) was photolyzed in the usual way as described above. After photolysis, sufficient solid NaOH was added to the photolysate to basicify the solution to pH > 10. The solution turned blue upon basification, consistent

with formation of the dianion of a dihydroxyanthracene. Excess Ac_2O were then added, which quenched the blue colour. Upon work-up, diacetoxyanthracene aldehyde **2.34** (up to 85% yield) was isolated (Scheme 2.6). Consistent with its anthracene chromophore, **2.34** exhibits the expected structured five-finger excitation band from 310 to 420 nm and long wavelength fluorescence, with λ_{em} = 461 nm in addition to the standard NMR data.

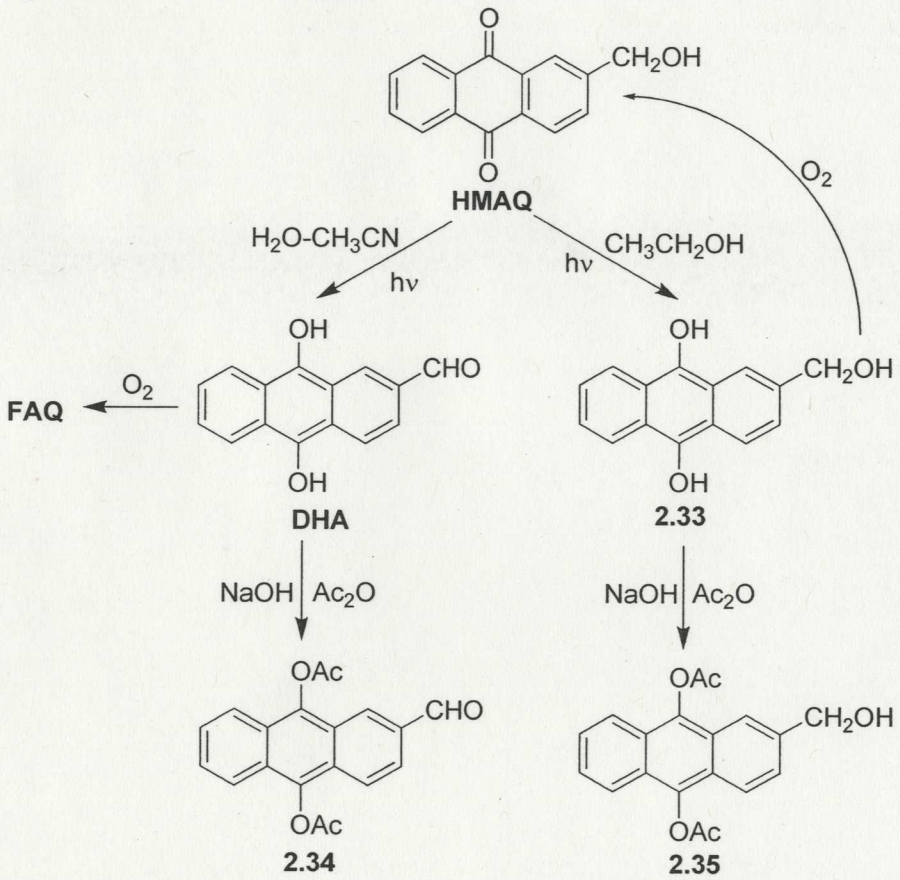

Scheme 2.6 Trapping of photoredox products (**DHA** and **2.33**) of **HMAQ**

Photolysis of **HMAQ** in neat CH_3CH_2OH followed by the above trapping protocol gave a mixture of diacetoxyanthracene alcohol **2.35** (75%) and diacetoxyanthracene aldehyde **2.34** (25%) (Scheme 2.6). Formation of **2.34** is evidence for an intramolecular photoredox pathway which is minor in neat CH_3CH_2OH. The dominant pathway is

simple photoreduction to give **2.33**, which is subsequently trapped by Ac_2O to form **2.35**. Thus in the presence of a weak hydrogen donor such as CH_3CH_2OH, simple photoreduction via initial hydrogen abstraction[59] dominates. However, the fact that the intramolecular photoredox reaction occurred is in direct contrast to the complete lack of reaction observed in neat CH_3CN. This is consistent with the requirement of a hydroxylic solvent to mediate the intramolecular photoredox reaction. When water was added (1:1 (v/v) H_2O- CH_3CH_2OH), photolysis of **HMAQ** resulted in 70% yield of **2.34** and 30% yield of **2.35**. Interestingly, photolysis of **HMAQ** in neat CH_3CH_2OH under oxygen gave only **2.34** suggesting that only intramolecular photoredox reaction occurred. However, the simple photoreduction product **2.33** would be oxidized quickly to **HMAQ** in the presence of oxygen which on further photolysis would eventually give rise to the intramolecular photoredox product **DHA**, which is sufficiently long-lived in oxygen (due to the electron withdrawing aldehyde substituent on the anthracene ring) to be trapped by Ac_2O to give **2.34**.

We have found that it is also possible to follow the competition between simple photoreduction *vs*. intramolecular photoredox using UV-Vis spectrophotometry. UV-Vis studies of **HMAQ** on photolysis in 1:1 H_2O-CH_3CN (only intramolecular redox) showed the formation of dihydroxyanthracene **DHA** with λ_{max} 280, 380 and 450 nm. Photolysis in neat 2-propanol (only photoreduction) resulted in dihydroxyanthracene **2.33** with λ_{max} 267 and 440 nm. By following the OD of the sharper 280 and 267 nm bands, it is possible to qualitatively monitor the competition between simple photoreduction vs intramolecular photoredox of **HMAQ** in H_2O-2-propanol mixtures (Figure 2.11). In 50% H_2O-2-propanol, the major pathway is simple photoreduction. When 2-propanol was replaced

with CH_3CH_2OH, the major pathway in 50% H_2O-CH_3CH_2OH was intramolecular photoredox. These observations are consistent with the better hydrogen donating ability of 2-propanol compared to CH_3CH_2OH.

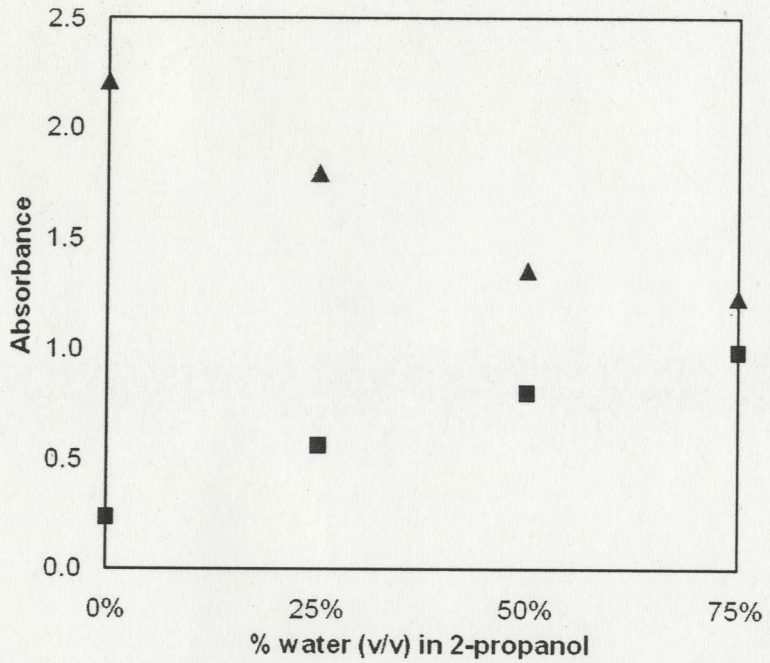

Figure 2.11 Solvent effect on the competition between intramolecular photoredox (formation of **DHA**) and simple photoreduction (formation of **2.33**) on photolysis of **HMAQ** in H_2O-2-propanol mixtures; ■ absorption due to **DHA** at 280 nm; ▲ absorption due to **2.33** at 267 nm. Measurement error is about ± 5%.

2.4.4 Nanosecond Laser Flash Photolysis (LFP) of HMAQ

LFP was employed to gain a better understanding of reaction mechanism, in particular to confirm triplet state reactivity and the possibility of observing critical intermediates which would be expected to be formed by the formal photoredox reaction.

The triplet-triplet absorption spectrum of **HMAQ** (10^{-5} M in neat CH_3CN, flow cell, nitrogen purged) showed an intense absorption band centered at 380 nm (Figure 2.12). The signal decayed with first order kinetics ($1.7 \pm 0.1 \times 10^5$; $\tau \sim 6$ μs). The intensity and lifetime of this transient was significantly reduced in the presence of oxygen ($\tau \sim 0.39$

μs). Similar observations were made for 9,10-anthraquinone, namely, an intense absorption band centered at 380 nm in neat CH_3CN ($\tau \sim 7$ μs in nitrogen saturated solution) that is quenched by oxygen ($\tau \sim 0.6$ μs). All of these observations are consistent with an excited triplet 9,10-anthraquinone (an intense 380 nm absorption, $\tau \sim 6$ μs in nitrogen saturated solution, $\tau \sim 10$ ns in oxygen saturated solution) as reported by Görner.[59a] Based on the above, we assign the 380 nm transient observed for **HMAQ** to the triplet state.

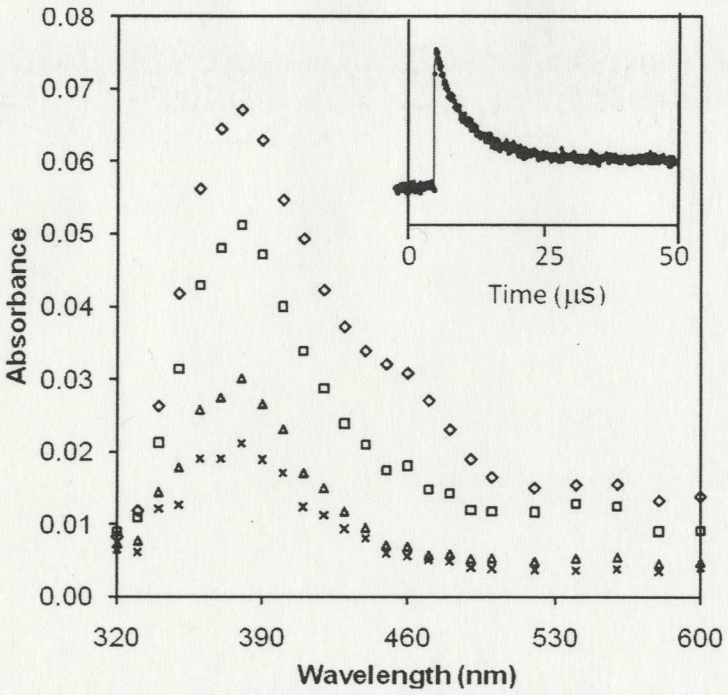

Figure 2.12 Triplet-triplet absorption spectra of **HMAQ** in neat CH_3CN (nitrogen-saturated) after the 266 nm pulse, 1.44 μs (◊), 4.26 μs (□), 16.3 μs (Δ), 38.8 μs (×). Insets: triplet decay ($\tau \sim$ 5.9 μs, at 380 nm). Measurement error is about ±10%.

In the presence of water, LFP of **HMAQ** (10^{-5} M, 1:1 H_2O-CH_3CN, pH 7, nitrogen purged) showed an intense band at 390 nm and a shoulder band at 440 nm. The two signals gradually decayed to give a steady transient with two absorption bands at 390 and

460 nm (the absorption spectrum at 78 μs in Figure 2.13), which is almost identical to the UV-Vis spectrum of **DHA**.[62] Since the photoredox product could be observed in general UV-Vis spectroscopy, it can also be observed by LFP. Thus, the steady transient must be the photoredox product **DHA**. The decay of the signal could not be fitted to a single exponential function, suggesting a presence of more than one species ($\tau \sim < 0.1$ μs and 11 μs). In the presence of oxygen, both absorption bands at 390 and 440 nm also gradually decayed ($\tau \sim < 0.1$ μs and $\tau \sim 9$ μs) to give **DHA** in almost same yield as that in nitrogen saturated solution. Photolysis of 9,10-anthraquinone under the same experimental condition showed only a triplet transient ($\tau \sim 0.6$ μs) with a broad absorption band ranging from 340 nm to 500 nm ($\lambda_{max} = 400$ nm). Thus, the two absorption bands at 390 and 440 nm are assigned to be a combination of a short-lived triplet excited state ($\tau < 0.1$ μs), and a long-lived intermediate state ($\tau \sim 10$ μs). The latter is not quenched by oxygen.

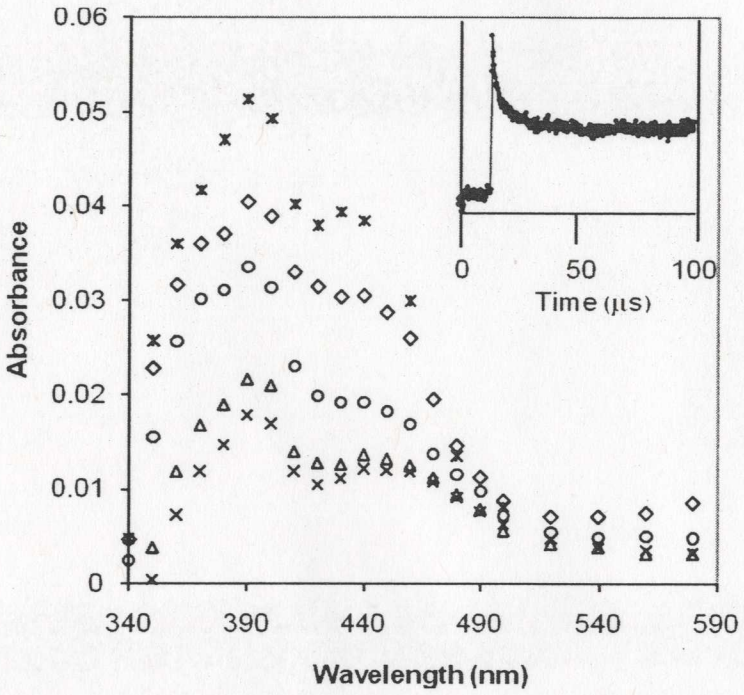

Figure 2.13 Triplet-triplet absorption spectra of **HMAQ** in 1:1 H_2O-CH_3CN (nitrogen-saturated) after the 266 nm pulse, 0.1 us (*), 2 μs (◊), 8 μs (o), 33 μs (Δ), 78 μs (×).Inset: triplet and intermediate decay at 450 nm. Measurement error is about ±10%.

2.4.5 Quenching of Triplet HMAQ

The above LFP studies gave evidence that photolysis of **HMAQ** generates a triplet excited state but not conclusive evidence that triplet **HMAQ** is photoreactive in the photoredox reaction. If the triplet **HMAQ** is reactive, we expect it may be quenched using a triplet quencher, which would result in a significantly lower overall yield of the photoredox product.

An efficient quencher should have a lower triplet energy than the triplet state energy of the substrate (the triplet energy of 9,10-anthraquinone: $^3\Delta E \sim 62$ kcal/mol)[86]. Sorbic acid (a conjugated diene) has $^3\Delta E \sim 60$ kcal/mol and is an excellent quencher of triplet excited states,[44,87] and is water soluble. Thus, sorbic acid was employed to study the reactivity of triplet **HMAQ**.

Photolyses of **HMAQ** (10^{-4} M, 1:1 H_2O- CH_3CN, pH 7, argon purged, λ_{ex} 350 nm) were carried out in 100 mL quartz vessels in the presence of sorbic acid (0 ~ 0.02 M). After work-up in air, the yields (the formation of **FAQ**, 8 ~ 35%) were determined with NMR. A Stern-Volmer plot ($\Phi_0 / \Phi = 1 + k_q\tau$ [Q]) for the photolysis of **HMAQ** was made (Φ_0 / Φ *vs.* the concentration of sorbic acid, where Φ_0 / Φ refers to the ratio of the conversion yields in the absence and presence of sorbic acid, k_q refers to the triplet quenching rate constant, τ refers to the lifetime of the triplet excited state, [Q] refers to the concentration of the quencher). The biphasic plot (Figure 2.14) showed initial linear quenching at low concentrations of sorbic acid (< 0.08 M) and a plateau region with Φ_0 / Φ ~ 4 at the high concentrations of sorbic acid (0.01-0.02 M). These values can be interpreted to mean that with respect of the photoredox reaction, about 25% of **HMAQ** of the reaction cannot be quenched by sorbic acid. This means that about 75% of the photoredox reaction of **HMAQ** proceeds via the triplet excited state. The remaining "unquenchable" fraction (the flat region) is most likely due to the singlet excited state reaction although one cannot rule out the possibility of reaction via another short-lived triplet state. From the initial linear region of the plot, the slope ($k_q\tau$) was 295 M^{-1}. Assuming that the bimolecular triplet quenching rate constant is diffusion-controlled in water (5×10^{-9} $M^{-1}s^{-1}$),[88] it was estimated that the reactive triplet lifetime of **HMAQ** was 60 ns. This result is consistent with the observations for LFP studies that indicates that the reactive triplet **HMAQ** is short-lived ($\tau < 0.1$ μs) in the presence of water.

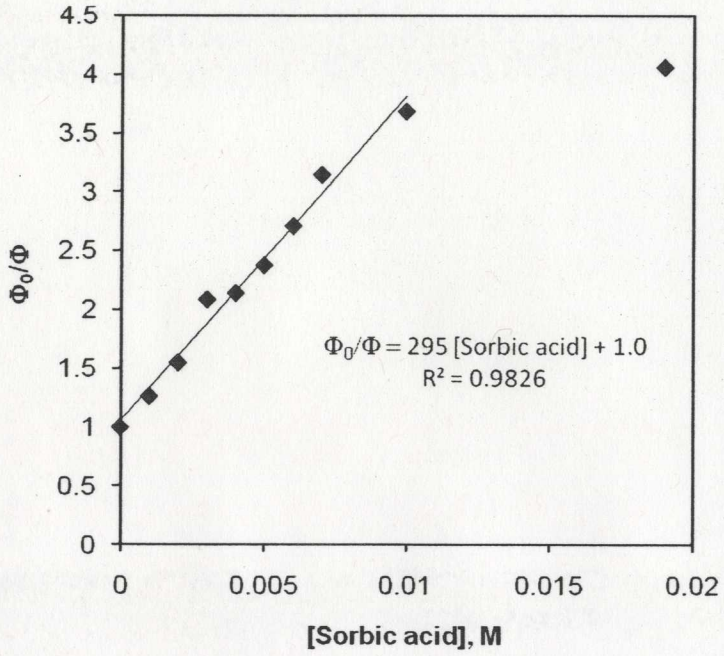

Figure 2.14 Stern-Volmer plot of quenching of the photoredox reaction for **HMAQ** in the presence of sorbic acid. Measurement error is about ± 5%.

Oxygen is also a very efficient quencher ($^3\Delta E \sim 30$ kcal/mol) of triplet excited states. We expected oxygen could quench the triplet **HMAQ** as well. Photolysis of **HMAQ** (10^{-4} M) was carried out in oxygen saturated solution (1:1 H_2O-CH_3CN, pH 7). After work-up in air, the conversion yield of **FAQ** in the absence and presence of oxygen was $\Phi_0/\Phi \sim 1.05$. Since the bimolecular triplet quenching rate constant of oxygen for anthraquinone in benzene is 1.4×10^9 $M^{-1}s^{-1}$, [86] one can estimate that the reactive triplet lifetime of **HMAQ** is 50 ns. The result is consistent with the triplet quenching studies using sorbic acid.

2.4.6 HOMO/LUMO Calculations

As Section 1.3 noted, an excited state may be thought of as originating when an electron is promoted from the HOMO to the LUMO. To gain additional insights into the

possible underlying reasons for the photochemical behaviour of **HMAQ**, the HOMO and LUMO of **HMAQ** were calculated at the AM1 level using Chem 3D.

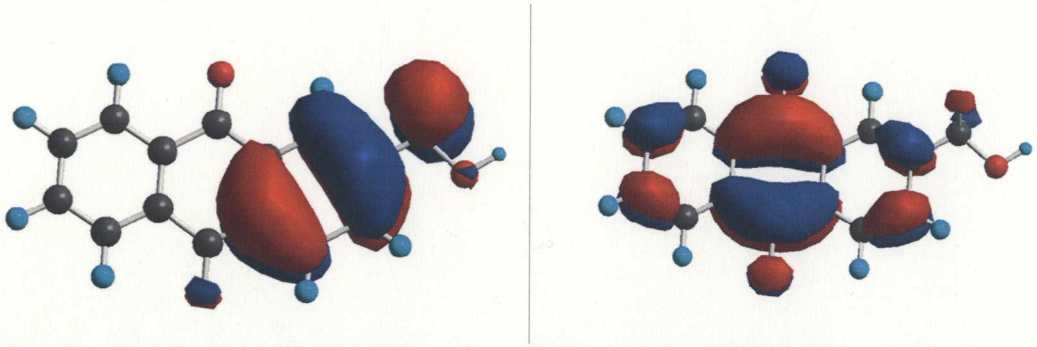

Figure 2.15 Calculated HOMO (left) and LUMO (right) for **HMAQ** (Chem 3D, AM1)

Shown in Figure 2.15 are the results for the HOMO and LUMO of **HMAQ**, which is typical for most of the anthraquinones studied in this work. If one assumes that the electronic distribution of the excited singlet or triplet state can be approximated by the change in MO coefficients on promotion of an electron from the HOMO to the LUMO, then it is clear that the excited state will gain electron density at the central ring and in particular at the carbonyl carbon and oxygen atoms, and lose electron density from the ring with the attached substituent. Note in particular the loss of electron density from the $ArCH_2$ protons. These predictions in change in electron density corroborates the proposed mechanism in which protonation of the carbonyl oxygen is required along with deprotonation of one of the $ArCH_2$ protons (details are presented in Section 2.4.7). Interestingly, the same calculations showed that the loss of electron density from the benzene ring containing the CH_2OH group in **2.9** would be minor, and this correlates with the low photoredox reactivity observed for this compound.

2.4.7 Proposed Reaction Mechanisms

LFP and triplet quenching studies (Section 2.4.4 and 2.4.5) gave evidence that the triplet excited state is reactive. Although we can not rule out reaction via a short-lived singlet excited state, that the triple state is reactive is consistent with much of the known photochemistry of anthraquinones.[59,89] Isotope effect studies of **HMAQ-*αD*** (Section 2.4.1) are consistent with a reaction limiting step involving deprotonation of the benzylic C-H. Based on the above mechanistic studies, a postulated mechanism is shown in Scheme 2.7.

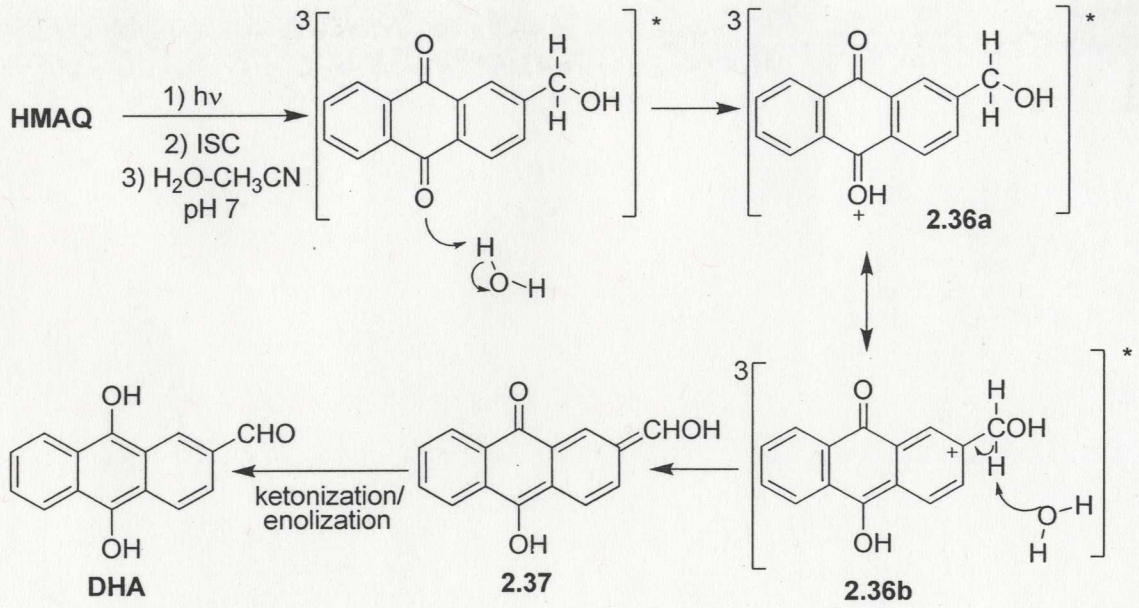

Scheme 2.7 Proposed mechanism for the intramolecular photoredox reaction of **HMAQ**

The photoredox reaction requires water. Not only does water act as the proton source and base for deprotonation necessary for the photoredox reaction, but it provides a polar environment for the reaction. Increasing the percent of water in the solvent mixture (H_2O-CH_3CN) increases the polarity of the solvent mixture. Change of solvent polarity has a

significant effect on the efficiency of the photoredox reaction. Just as Section 2.4.2 noted, when the percent of water was lower than 15%, the yield of redox product dropped dramatically with the decrease of the amount of water. However, note that even at the lowest percent of 1%, there is still 1.7 mM water. Compared with the concentration (10^{-5} M) of anthraquinone **HMAQ**, there is still a large excess of water for the photoredox reaction. Thus, we suggest that the photoredox reaction proceeds via the π–π^* lowest triplet state because polar solvents stabilize the π–π^* triplet state.[90] Lack of water may result in a switch between the π–π^* triplet state and n–π^* triplet state. This is favourable for hydrogen abstraction which leads to photoreduction. This is consistent with the observation of photoreduction products when a hydrogen donor solvent is used as shown in Section 2.4.3.

Simple HOMO/LUMO calculations (Section 2.4.6) shows that the LUMO has a high electron density on the center ring of the anthraquinone moiety and low electron density on the benzylic carbon. Thus, anthraquinone ketone should exhibit enhanced basicity. Upon protonation (**2.36a**), assuming the compound is still in the excited state and the charge distribution does not change, the benzene ring with the attached hydroxymethyl group is still electron deficient since its previous charge has been transferred to the central ring on the anthraquinone moiety. This results in a net positive charge localized at the 2-position of benzene ring. Deprotonation by water at the benzylic position gives the dienol **2.37**, which upon ketonization/enolization gives **DHA** (Scheme 2.7).

One may postulate that the first protonation of carbonyl oxgen might occur at the 9 position instead of the 10 position as shown in the alternative mechanistic pathway of the Scheme 2.8. Indeed, simple HOMO/LUMO calculations do not show any difference of

electron density between these two positions. Thus, the proton transfer from water to carbonyl oxygen may occur at the 9-position. The possible mechanism is very similar to that of the photoredox reaction observed for benzophenone **1.51**,[49] which generates a biradical dienol **1.54** (Scheme 1.9). Note that in this case, **2.38** is the anologue of **1.54**. Thus, **2.38** will transfer to **2.39**, which ultimately will give **DHA**.

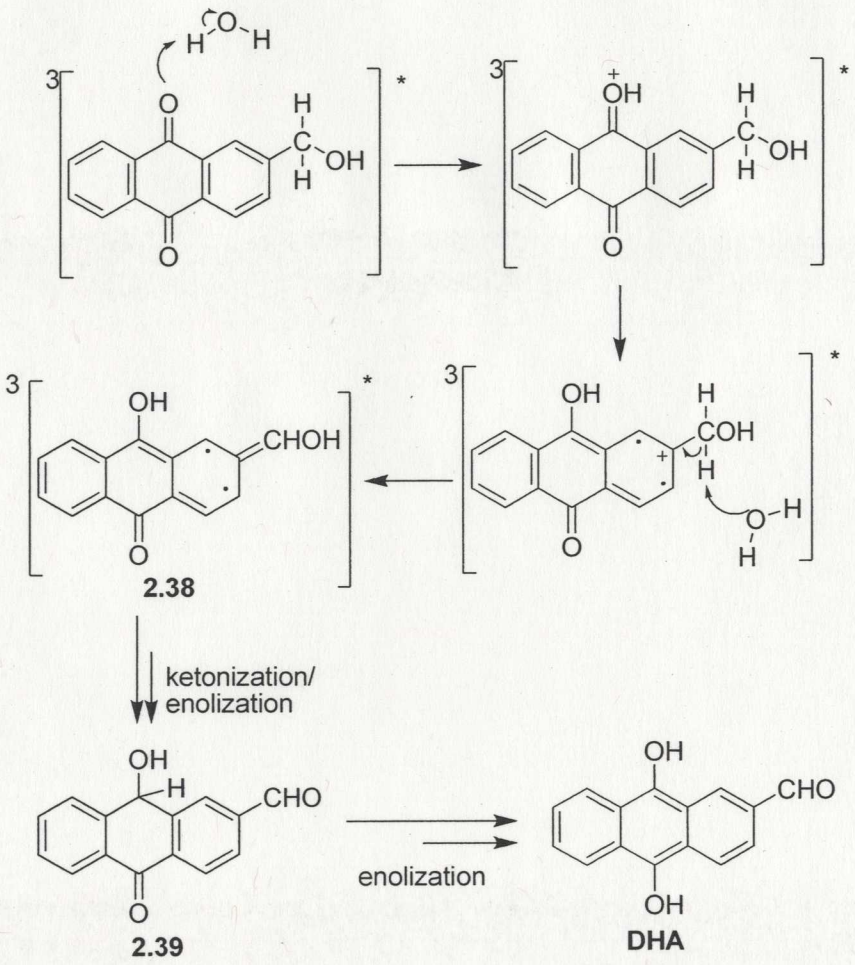

Scheme 2.8 Alternative mechanistic pathway for the photoredox reaction of **HMAQ**

As noted before, the photoexcited compound is highly polarized with enhanced electron density on the central ring of the anthraquinone moiety and low electron density on the benzene ring with the attached hydroxymethy group. Thus, one may also postulate

that the deprotonation of the benzylic C-H might occur first (eqn. 2.11), to form benzylic carbanion **2.40** and eventually **2.41**, which has a net negative charge on the carbonyl oxygen. This would undergo protonation by water and follow the same steps as shown in Scheme 2.7, to give photoredox product **DHA**.

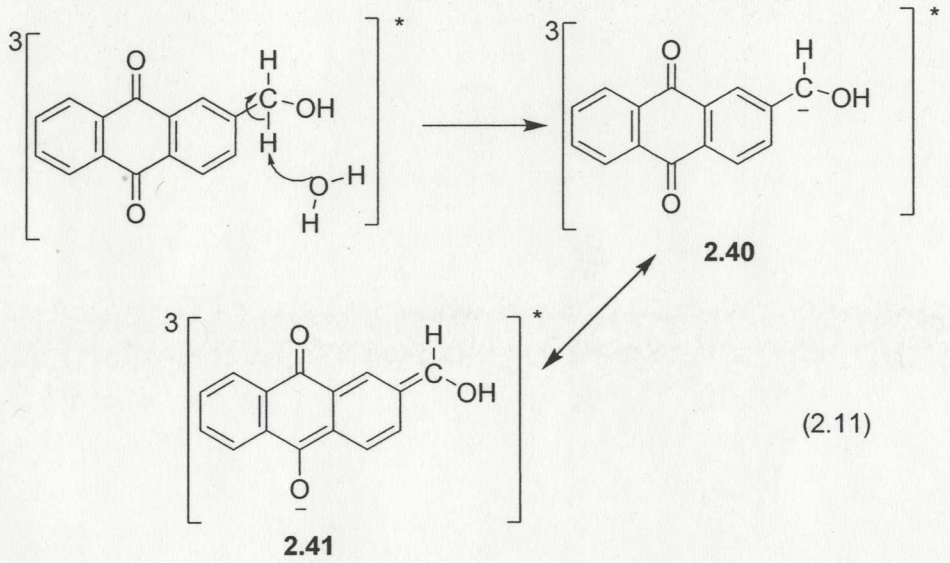

(2.11)

However, the effect of pH on the efficiency of the photoredox reaction of **HMAQ** (Section 2.4.2) shows that at pH > 9, the yield of photoredox product **DHA** dropped dramatically. These observations suggest that the protonation of carbonyl oxygen is most likely the first step. At pH > 9, protonation of carbonyl oxygen by water or hydronium is highly unlikely. This would inhibit the subsequent deprotonation of the benzylic C-H, resulting in a low overall yield of the photoredox reaction.

2.5 Summary

Results presented in this chapter showed that the intramolecular photoredox reaction observed for **HMAQ** is a reasonably general reaction for a variety of anthraquinones **2.1-2.9** (except **2.4**) in aqueous solution (Table 2.1). Some of these derivatives have potential as photoprotecting agents, releasing their protected moieties *via* intramolecular

photoredox reaction. Diketone **2.9** also undergoes an analogous photoredox reaction in acidic aqueous solution ($\Phi = 0.003$, pH 0), demonstrating that other aromatic diketones can react in an analogous fashion.

Table 2.1 Quantum yields for the formation of photoredox products of anthraquinone derivatives

Anthaquinone derivatives	Photoredox products	Photoreleased products	Quantum yield (Φ)
2.1	**2.11**	/	0.7[a]
2.2	**FAQ**	Ethanol	0.4[a]
2.3	**2.11**	Methanol	0.4[a]
2.5	**2.16**	benzaldehyde	0.02[b]
2.6	**2.13**	acetophenone	0.02[b]
2.7	**2.13**	/	0.5[b]
2.8	**2.18**	/	0.3[a]

[a] Solvent is 1:1 H_2O-CH_3CN, pH 7. [b] Solvent is 1:3 H_2O-CH_3CN, pH 7.

The intramolecular photoredox reaction is different from simple photoreduction, which is a well-known primary reaction for aromatic ketones. The photoredox reaction requires water, a solvent in which simple photoreduction cannot occur. It is known that photoreduction of aromatic ketones goes via the n,π^* triplet state, whereas the photoredox reaction most likely proceeds via the π,π^* triplet state. The photoredox reaction is unimolecular with respect to the anthraquinone moiety whereas photoreduction must be bimolecular involving substrates and reducing agents. The essential steps in the photoredox mechanism include (a) protonation of the carbonyl oxygen of the triplet excited state; (b) deprotonation of the benzylic carbon; (c) thermal ketonization and enolization of a dienol to form the photoredox product. In the following chapters of this Thesis, the photoredox reaction will be extended to substrates in which

the reduced and oxidized moieties are separated by greater molecular distances (further apart), demonstrating further generality and applicability of the photoredox reaction.

2.6 Experimental

2.6.1 General

NMR spectra were recorded on Bruker instruments, 300 or 500 MHz for ^{1}H, and 75 or 125 MHz for ^{13}C. IR spectra were recorded on a Perkin-Elmer 283 instrument. UV-Vis spectra were taken on a Cary 1 spectrophotometer. Mass spectra were obtained on a Kratos Concept H spectrometer. All solvents for synthesis (ACS grade) were purchased from Aldrich and used as received. CH_3CN (HPLC grade) and distilled water were used in photolyses. $CDCl_3$, D_2O and acetone-d_6 were purchased from Cambridge Isotope laboratory and D_2SO_4 was obtained from Aldrich. Preparative TLC was carried out on 20 cm × 20 cm silica gel GF Uniplates (Analtech). All readily available organic and inorganic reagents required in the synthesis and photolyses were purchased from Aldrich and used as received.

2.6.2 UV-Vis Studies

UV-Vis studies (~10^{-5} M in H_2O-CH_3CN, pH 7) were carried out in 3.0 mL quartz cuvette (1 cm). Solutions were bubbled using a fine needle with argon for 5 min to remove any dissolved oxygen. Parafilm was then used to seal the open side of the cuvette. Solutions were then irradiated at 300 nm or 350 nm in a Rayonet photochemical reactor. UV-vis spectra were recorded before and after each photolysis.

2.6.3 Product Studies

Compounds were photolyzed in 100 mL quartz tubes using a Rayonet RPR 100 photochemical reactor equipped with 300 nm or 350 nm lamps. Typically, a solution of

the compound (10^{-4}-10^{-5} M, H_2O-CH_3CN (1:1 or 1:3), pH7 or 0) was bubbled with argon for 15 min and then irradiated under argon purge. The irradiated solution was extracted by 3 × 50 mL CH_2Cl_2 in air and the collected organic extracts was dried over anhydrous $MgSO_4$. The solvent was removed under reduced pressure and the photolysate analyzed by NMR, MS and IR.

In order to monitor the initially formed redox product, photolyses were carried out in NMR tubes which allowed characterization of the first formed redox products. NMR tubes were filled with 1 mL of the appropriate solution (10^{-3} M, 10% D_2O-CD_3CN). Solutions were bubbled using a fine needle through rubber stoppers with argon for 15 min before irradiation then irradiated with 300 nm or 350 nm lamps.

2.6.4 Quantum Yield Measurements

Quantum yields were measured using NMR and the reaction of 2-(hydroxymethyl)anthraquinone (**HMAQ**) as a secondary actinometer ($\Phi = 0.8$).[62] A solution of the compound (**2.1**-**2.9**, 10^{-4} M, in H_2O-CH_3CN (1:1 or 1:3), pH 7 or 0) was purged with argon for 15 min and irradiated for 1 min at 300 nm (2 lamps) under argon purge. After irradiation, the conversion to product was determined by ^1H NMR and compared to an identical run using **HMAQ**. All converions were kept below 30% and repeated twice.

2.6.5 Nanosecond Laser Flash Photolysis Studies of HMAQ

LFP studies were conducted at the University of Victoria LFP facility employing a Spectra Physics Quanta-Ray YAG laser, model GSR-11, with a pulse width of ~ 10 ns and excitation wavelength 266 nm. The energy of the laser puse was less than 20 mJ / Pulse, with a repetition rate of 1 Hz. Quartz flow cells were used and solutions were

purged with nitrogen or oxygen for 20 min prior to measurement. Optical densities at 266 nm were ~ 0.6.

2.6.6 Synthesis of Anthraquinone Derivatives HMAQ-αD, 2.1-2.9

α–*D*-2-(Hydroxymethyl)-9,10-anthraquinone (**HMAQ-*αD***)

$NaBD_4$ (0.023g, 2.4 mmol) in 20 mL of anhydrous CH_3OH was added dropwise to 2-formylanthraquinone (**FAQ**, 0.14 g, 0.6 mmol) in 20 mL of anhydrous CH_3OH under N_2. The mixture was stirred in an ice water bath for 2 h. After reaction, 20 ml of saturated NH_4Cl was added and the resulting solution extracted by 2 × 25 mL of CH_2Cl_2. The collected extractions were dried over anhydrous $MgSO_4$ and the solvent was removed. The residue was purified by column chromatography with silica gel using 5% EtOAc in CH_2Cl_2 as a eluent, to give **HMAQ-*αD*** (white powder, 0.13 g, m.p 183-185°C) in 90% yield. ^{1}H NMR ($CDCl_3$, 300 MHz) δ 8.31-8.20 (m, 4H), 7.82-7.20 (m, 3H), 4.86 (s, 1H), 2.0 (s, broad OH peak); MS (EI), m/z 239 (M^+, 100), 238 (20), 237 (32), 235 (42).

The 2-formylanthraquinone (**FAQ**) was prepared by photolysis of 2-(hydroxymethyl)anthraquinone (**HMAQ**) which was purchased from Aldrich. A solution (100 mg of **HMAQ** in 1:1 H_2O-CH_3CN, argon purged, in 300 mL of photolysis quartz tube) was irradiated for 10 min and extracted with 3 × 50 mL CH_2Cl_2. The combined extractions were dried over anhydrous $MgSO_4$ and solvent was removed. The same procedure was repeated three times. The combined material was purified by column chromotography with silica gel using CH_2Cl_2 as an eluent, to give **FAQ** (pale yellow powder, 0.24 g) in 80% yield. ^{1}H NMR ($CDCl_3$, 300 MHz) δ 10.20 (s, 1H), 8.74 (s, 1H), 8.41 (d, 1H, J = 8.1 Hz), 8.37-8.25 (m, 2H), 8.26 (d, 1H, J = 8.1 Hz), 7.90-7.77 (m, 2H); ^{13}C NMR ($CDCl_3$, 75 MHz) 191.0, 182.6, 182.3, 140.1, 137.1, 134.9, 134.8, 134.3, 133.5

(2C), 133.3, 129.7, 128.4, 127.7 (2C); MS (EI), m/z 236 (M^+, 100), 237 (75), 235 (90), 207 (38).

Benzylic bromides **HMAQ-b** and **2.1b**

A mixture of **HMAQ-a** (2 g, 8 mmol), NBS (1.8 g, 10 mmol) and benzoyl peroxide (0.2 g, 0.8 mmol) in 100 mL of benzene was refluxed overnight. After reaction, the mixture was washed with distilled water (2 × 50 mL) and the collected organic solution was dried over anhydrous $MgSO_4$. After the solvent was removed, the brown crude product was purified by column chromatography with silica gel using CH_2Cl_2 as an eluent, to give **HMAQ-b** (yellow powder, 2.3 g) in 92% yield. ^{1}H NMR ($CDCl_3$, 300 MHz) δ 8.33-8.22 (m, 4H), 7.84-7.71 (m, 3H), 4.57 (s, 1H).

Compound **2.1b** (yellow powder, 2.1 g, 90% yield) was prepared by bromination of **2.1a** following the same procedure as that described for **HMAQ-b**. ^{1}H NMR ($CDCl_3$, 300 MHz) δ 8.32-8.13 (m, 3H), 8.03 (d, 1H, J = 8.1 Hz), 7.78 (d, 1H, J = 8.1 Hz), 7.75-7.67 (m, 2H), 5.20 (q, 1H, J = 6.6 Hz), 2.03 (d, 3H, J = 6.6 Hz).

2-(1-Hydroxyethyl)-9,10-anthraquinone (**2.1**)*

A mixture of **2.1b** (2.0 g, 6.3 mmol) and $CaCO_3$ (4.5 g, 4.5 mmol) in 50 mL of 1:1 water and dioxane was refluxed for 2 days. After the reaction, 5 mL of H_2SO_4 (0.5 M) was added to the mixture to neutralize the excess $CaCO_3$ and extracted with 2 × 50 mL CH_2Cl_2. The collected extractions were dried over anhydrous $MgSO_4$ and solvent was removed. The crude material was purified by column chromatography with silica gel using a mixture of hexane and EtOAc as eluent, to give **2.1** (yellow powder, 1.2 g, m.p. 101-103°C) in 75% yield, ^{1}H NMR (300MHz, $CDCl_3$) δ 8.35-8.24 (m, 4H), 7.87-7.74 (m,

* The compound has been previously synthesized. (G. Manecke, and W. Storck, The Vinyl-9,10-anthraquinone, *Chemische Berichte*, 1961, 94, 3239-3250)

3H), 5.08 (q, 1H, J = 6.6 Hz), 2.0 (s, broad OH peak), 1.56 (d, 3H, J = 6.6 Hz); ^{13}C NMR ($CDCl_3$, 75 MHz) 183.3, 183.1, 152.9 (2C), 134.4, 134.3, 133.7, 133.6, 132.7, 131.3, 127.9, 127.4, 127.3, 124.2; MS (EI), m/z 252 (M^+, 3), 237 (75), 210 (100); HRMS calculated for $C_{16}H_{12}O_3$ 252.0786; observed 252.0776; IR (KBr, cm^{-1}) 3418, 3069, 2973, 1675, 1591.

2-(Ethoxymethyl)-9,10-anthraquinone (**2.2**)*

A mixture of **HMAQ-b** (0.37 g, 1.2 mmol) and $CaCO_3$ (0.31 g, 6 mmol) in 20 mL of CH_3CH_2OH was refluxed overnight. After the reaction, 6 mL of H_2SO_4 (0.5 M) was added to neutralize the excess $CaCO_3$ and extracted by 2 × 50 mL CH_2Cl_2. The collected extracts were dried over anhydrous $MgSO_4$ and solvent was removed to give a brown crude material which was purified by column chromatography with silica gel using CH_2Cl_2 as an eluent, to give **2.2** (pale yellow powder, 0.18g, 115-117°C) in 56% yield. ^{1}H-NMR (300MHz, $CDCl_3$) δ 8.33-8.25 (m, 3H), 8.23 (s, 1H), 7.82-7.74 (m, 2H), 4.65 (s, 2H), 3.61 (q, 2H, J = 7.4 Hz), 1.28 (t, 3H, J = 7.4 Hz); ^{13}C-NMR ($CDCl_3$, 75 MHz) 183.3, 183.1, 152.9 (2C), 134.4, 134.3, 133.7, 133.6, 132.7, 131.3, 127.9, 127.4, 127.3, 124.2; MS (EI), m/z 266 (M^+, 10), 237 (75), 210 (100); HRMS calculated for $C_{17}H_{14}O_3$ 266.0943; observed 266.0945; IR (KBr, cm^{-1}) 3068, 2974, 2867, 1677, 1590.

2-(1-Methoxyethyl)-9,10-anthraquinone (**2.3**)

A mixture of **2.1b** (0.27 g, 0.86 mmol) and $CaCO_3$ (0.43g, 4.3 mmol) in 30 mL of CH_3OH was refluxed for 3 days. After the reaction, 9 mL of H_2SO_4 (0.5 M) was added to neutralize excess $CaCO_3$. This was followed by the addition of 200 mL of water to the mixture to give a yellow precipitate. After suction filtration, the yellow precipitate

---

* The compound has been previously synthesized. (G. Izoret, J. Camier, J. J. Brun, and G. Lonchambon, Some Derivatives of 2-Methylanthraquinone, *Bulletin de la Societe Chimique de France*, 1964, 822-827)

(powder) was recrystallized from CH_3CH_2OH to give **2.3** (yellow crystalline plates, 0.17g, m.p. 95-96°C) in 74% yield. ^1H NMR ($CDCl_3$, 300 MHz) δ 8.34-8.26 (m, 3H), 8.22 (s, 1H), 7.82-7.73 (m, 3H), 4.47(q, 1H, J = 6.6 Hz), 3.28 (s, 3H), 1.47 (d, 3H, J = 6.6 Hz); ^{13}C NMR ($CDCl_3$, 75 MHz) 183.4, 183.1, 150.9 (2C), 134.4, 134.3, 133.9, 133.7, 133.0, 131.8, 128.0, 127.4 (2C), 125.1, 79.3, 57.1, 23.8; MS (EI), m/z 266 (M^+, 10), 251 (100), 235 (20); HRMS calculated for $C_{17}H_{14}O_3$ 266.0943; observed 266.0941; IR (KBr, cm^{-1}) 3064, 2974, 2823, 1677, 1590.

2-(Acetoxymethyl)-9,10-anthraquinone (**2.4**)*

A mixture of **HMAQ** (0.20 g, 0.8 mmol) and CH_3COCl (0.12 g, 1.6 mmol) was refluxed in 10 mL of THF for 12 h in the presence of pyridine (0.3 mL). After the reaction, the solution was poured into 50 mL of ice-cold water and stirred to give a yellow precipitate. The precipitate was isolated by suction filtration and purified by column chromatography with silica gel using 20% EtOAc-CH_2Cl_2 as an eluent, to give **2.4** in 70% yield (pale yellow powder, 0.14 g, m.p. 149-150°C); ^1H NMR ($CDCl_3$, 300 MHz) δ 8.35-8.25 (m, 4H), 7.85-7.72 (m, 3H), 5.25 (s, 2H), 2.16 (s, 3H); ^{13}C NMR ($CDCl_3$, 75 MHz) 183.1, 182.9, 170.8, 142.9 (2C), 134.5, 134.4, 133.9, 133.7, 133.3, 133.1, 127.9, 127.5 (2C), 126.3, 65.3, 21.1; MS (EI), m/z 280 (M^+, 3), 238 (100), 221 (10), 209 (25); HRMS calculated for $C_{17}H_{12}O_4$ 280.0736; observed 280.0740; IR (KBr, cm^{-1}) 3068, 2945, 1741, 1677, 1590.

9-Phenyl-7,11-dihydro-8,10-dioxa-cyclohepta [b]anthracene-5,13-dione (**2.5**)

A solution of **2.7** (0.2 g, 0.74 mmol) and benzaldehyde (0.4 mL, 3.0 mmol) in 10 mL of toluene along with one drop of conc. H_2SO_4 was refluxed for 0.5 h in a Dean-Stark

---

* The compound has been previously synthesized. (G. Izoret, J. Camier, J. J. Brun, and G. Lonchambon, Some Derivatives of 2-Methylanthraquinone, *Bulletin de la Societe Chimique de France*, 1964, 822-827)

apparatus, to give a brown solution. After the reaction, the solution was neutralized with 5% $NaHSO_3$ to give a brown precipitate. The brown precipitate was isolated by suction filtration and purified by column chromatography with silica gel using CH_2Cl_2 as eluent, to give **2.5** (pale yellow powder, 0.13 g, m.p. 223-225°C) in 49% yield. ^1H NMR ($CDCl_3$, 300 MHz) δ 8.35-8.24 (m, 2H), 8.06 (s, 2H), 7.84-7.75 (m, 2H), 7.60-7.52 (m, 2H), 7.44-7.33 (m, 3H), 6.00 (s, 1H), 5.12 (d, 2H, J = 14.7 Hz), 5.02 (d, 2H, J = 14.7 Hz); ^{13}C NMR ($CDCl_3$, 75 MHz) 183.0 (2C), 145.6 (2C), 138.0, 134.4 (2C), 133.7 (2C), 132.5 (2C), 129.1, 128.6 (2C), 127.5 (2C), 126.7 (2C), 125.8 (2C), 103.6, 68.4 (2C); MS (EI)), m/z 356 (M^+, 2), 250 (80), 234 (100); IR (KBr, cm^{-1}) 3057, 2958, 2885, 1671, 1590.

9-Methyl-9-phenyl-7,11-dihydro-8,10-dioxa-cyclohepta [b]anthracene-5,13-dione (**2.6**)

Compound **2.6** was prepared from **2.7** (0.1g, 0.37 mmol) and acetophenone (0.18 mL, 1.5 mmol) following the synthetic procedure described for **2.5** in 30% overall yield (**2.6**, white powder, 0.041 g, m.p. 209-210°C). ^1H NMR ($CDCl_3$, 300 MHz) δ 8.26-8.18 (m, 2H), 7.92 (s, 2H), 7.76-7.68 (m, 2H), 7.58-7.51 (m, 2H), 7.38-7.24 (m, 3H), 5.02 (d, 2H, J = 15.5 Hz), 4.82 (d, 2H, J = 15.5 Hz), 1.64 (s, 3H); ^{13}C NMR ($CDCl_3$, 75 MHz) 183.0 (2C), 145.4 (2C), 142.4, 134.3 (2C), 133.8 (2C), 132.3 (2C), 128.6, 128.4 (2C), 127.4 (2C), 126.2 (2C), 125.3 (2C), 104.7, 65.7 (2C), 26.1; MS (EI), m/z 370 (M^+, 2), 355 (20), 250 (40), 105 (100); HRMS calculated for $C_{24}H_{18}O_4$ 370.1205; observed 370.1209; IR (KBr, cm^{-1}) 3050, 2934, 2867, 1675, 1591.

2,3-Di(hydroxymethyl)-9,10-anthraquinone (**2.7**)

A mixture of **2.7a** (Aldrich, 1.0 g, 4.5 mmol), NBS (1.8 g, 10.4 mmol) and benzoyl peroxide (0.10 g, 0.04 mmol) in 50 mL of benzene was refluxed overnight. After the reaction, the mixture was washed with distilled water (2 × 50 mL) and the collected

organic solution was dried over anhydrous $MgSO_4$. After solvent was removed, a brown residue (**2.7b**, 1.8g, 90% yield) was obtained. A mixture of **2.7b** (1.8 g, 4.6 mmol) and $CaCO_3$ (4.6g, 46 mmol) was refluxed in 1:1 water and dioxane for 2 days to give a brown solution. After the reaction, 75 mL of H_2SO_4 (0.5 M) was added to neutralized excess $CaCO_3$. Upon addition of 200 mL water, a brown precipitate was formed which was collected by suction filtration. This crude material was recrystallized from toluene to give **2.7** (yellow brown needles, 0.34 g, m.p. 214-216°C) in 30% yield. ^{1}H NMR (acetone-d_6, 500 MHz) δ 8.42 (s, 1H), 8.30-8.26 (m, 2H), 7.94-7.90 (m, 2H), 4.88 (d, 2H, J = 5.5 Hz), 4.65 (t, OH, J = 5.5 Hz); ^{13}C NMR (acetone-d_6, 125 MHz) 183.6 (2C), 147.3 (2C), 135.1 (2C), 134.7 (2C), 133.2 (2C), 127.7 (2C), 125.8 (2C), 61.7 (2C); MS (EI), m/z 267 (M^+-1, 3), 264 (70), 248 (65), 235 (100); IR (KBr, cm^{-1}) 3205, 3069, 2932, 1672, 1587.

2-[1,3]Dioxolan-2-yl-9,10-anthraquinone (**2.8**)

Compound **2.8** was prepared from **FAQ** (0.3 g, 1.3 mmol) and ethylene glycol (0.08 g, 1.3 mmol) followed the procedure described for **2.5** with 74% overall yield (**2.8**, pale yellow powder, 0.27 g, m.p. 129-131°C). ^{1}H NMR ($CDCl_3$, 300 MHz) δ 8.34 (s, 1H), 8.28-8.19 (m, 3H), 7.84 (d, 1H, J = 8.1 Hz), 7.78-7.70 (m, 2H), 5.89 (s, 1H), 4.16-4.00 (m, 4H); ^{13}C NMR ($CDCl_3$, 75 MHz) 183.1 (2C), 144.7 (2C), 134.4, 134.1, 133.8, 133.7, 133.6, 132.2, 127.8, 127.5, 127.4, 125.7, 102.8, 65.8 (2C); MS (EI), m/z 280 (M^+, 75), 279 (100); HRMS calculated for $C_{17}H_{12}O_4$ 280.0736; observed 280.0728; IR (KBr, cm^{-1}) 3069, 2956, 2889, 1724, 1676, 1592.

1,2-Dibenzoyl-4-methylbenzene (**2.9**)

Compound **2.9** was prepared from **2.9a** (0.8 g, 2.7 mmol) following the synthetic procedure described for **2.7**. Colum chromatography with silica gel by using CH_2Cl_2 was employed to give pure **2.9** in an overall yield of 65% (**2.9**, pale yellow oil, 0.55 g). ^1H NMR ($CDCl_3$, 300 MHz) δ 7.70-7.61 (m, 4H), 7.57 (s, 1H), 7.56 (d, 2H, J = 5.9 Hz), 7.53-7.44 (tt, 2H, J = 8.1 Hz), 7.53-7.43 (tt, 4H, J = 8.1 Hz), 4.79 (s, 2H), 2.0 (s, broad OH peak); ^{13}C NMR ($CDCl_3$, 75 MHz) 197.1, 196.6, 144.3, 140.7, 138.9, 137.4, 137.3, 133.3, 133.2, 130.4, 130.0 (2C), 129.9 (2C), 128.6 (2C), 128.5 (2C), 128.4, 127.7, 64.4; IR (KBr, cm^{-1}) 3448, 3059, 2870, 1655, 1596; MS (EI), m/z 316 (M^+, 10), 314 (M^+-2, 60), 237 (55), 105 (100).

Compound **2.9a** was in turn prepared following a literature procedure[79] with 30% overall yield (**2.9a**, pale yellow oil, 1.2 g). ^1H NMR ($CDCl_3$, 300 MHz) δ 7.65-7.54 (m, 4H), 7.49-7.35 (m, 3H), 7.35-7.22 (m, 6H), 2.38 (s, 3H); ^{13}C NMR ($CDCl_3$, 75 MHz) 197.2, 196.5, 141.7, 140.8, 137.7, 137.6, 137.0, 133.2, 133.0, 131.0, 130.4, 130.3, 130.0 (2C), 129.9 (2C), 128.6 (2C), 128.5 (2C), 21.7; MS (EI), m/z 300 (M^+, 60), 223 (100).

2.6.7 Photolysis Procedures for HMAQ-αD, 2.1-2.9 and Characterization of Products

Photolysis of **HMAQ-*αD***

Compound **HMAQ-*αD*** (6 mg in 50 mL CH_3CN and 50 mL H_2O, pH 7) was irradiated for 1 min, 2 min and 4 min at 300 nm (2 lamps) under argon, to give a yellow brown solution. After work-up in air, the brown residue was characterized by ^1H NMR to give a mixture of **FAQ** (8-28%) and **FAQ-*D*** (17-57%). Further purification was obtained by prep. TLC (silica gel, CH_2Cl_2) to give a mixture of **FAQ** and **FAQ-*D*** (yellow powder, 5 mg), ^1H NMR ($CDCl_3$, 300 MHz) δ 10.2 (s, 1H), 8.77 (s, 3.1 H), 8.45 (d, 3.1 H, J = 8.1

Hz), 8.40-8.23 (m, 8.8 H), 7.91-7.76 (m, 6.2 H); MS (EI), m/z 237 (M^+, 80), 236 (60), 235 (100).

Photolysis of **2.1 and 2.3**

Photolysis of compound **2.1** (10 mg, 1:1 H_2O-CH_3CN, 350 nm, 16 lamps, 1 min, argon purged) gave a yellow brown solution. After work-up in air, the brown residue was characterized by ^1H NMR to give **2.11** (70% conversion). Further purification was obtained by prep. TLC (silica gel, CH_2Cl_2), to give **2.11** (yellowish powder, 6 mg, 60% yield). Following the same photolysis procedure of **2.1**, photolysis of **2.3** also gave product **2.11** (60% yield). ^1H NMR ($CDCl_3$, 300 MHz) δ 8.79 (s, 1H), 8.41-8.23 (m, 4H), 7.86-7.75 (m, 2H), 2.73 (s, 3H); ^{13}C NMR ($CDCl_3$, 125 MHz) 196.97, 182.7, 182.6, 141.3, 136.3, 134.7 (2C), 134.0, 133.7, 133.6, 133.1, 128.1, 127.69, 127.67, 127.6, 22.3; MS (EI), m/z 322 (M^+, 3), 280 (10), 238 (100); HRMS calculated for $C_{19}H_{14}O_5$ 250.0630; observed 250.0630; IR (KBr, cm^{-1}) 3065, 1693, 1673, 1589.

Photolysis of **2.2**

Following the same photolysis procedure as for **2.1**, photolysis of **2.2** gave product **FAQ** (yellow powder, 60% yield).

Photolysis of **2.5** and **2.6**

Photolysis of **2.5** (5 mg, 1:3 H_2O-CH_3CN, pH 7, 300 nm, 16 lamps, 5 min, argon purged) gave a yellow brown solution. After work-up in air, the brown residue was characterized by ^1H NMR to give **2.16** (30% conversion). Further purification was obtained by TLC (silica gel, CH_2Cl_2) to give **2.16** (white powder, 1 mg, 25% yield). Photolysis of **2.6** also gave **2.16** by following the same photolysis procedure of **2.5**. ^1H NMR (Acetone-d_6, 500 MHz) δ 8.66 (s, 1H), 8.59 (s, 1H), 8.37-8.33 (m, 2H), 8.03-7.98

(m, 2H), 5.67 (s, 2H); MS (EI), m/z 264 (M^+, 60), 248(5), 235 (100); HRMS calculated for $C_{16}H_8O_4$ 264.0432; observed 2264.0420; IR (KBr, cm^{-1}) 3076, 2932, 1764, 1673, 1586, 1332, 1303.

Photolysis of **2.7**

Photolysis of **2.7** (5 mg, 1:3 H_2O-CH_3CN, pH 7, 300 nm, 16 lamps, 1 min, argon purged) gave a brown solution. After work-up in air, the brown residue was characterized by ^1H NMR to give **2.14** (50% conversion). Further purification was obtained by prep. TLC (silica gel, 20% EtOAc-CH_2Cl_2) to give **2.14** (brown yellow powder, 2 mg, 40%). ^1H NMR (Acetone-d_6, 300 MHz) δ 8.40 (s, 1H), 8.36-8.28 (m, 2H), 8.23 (s, 1H), 7.85-7.77 (m, 2H), 6.63 (d, 1H, J = 7.3 Hz), 5.38 (d, 1H, J = 14.0 Hz), 5.17 (d, 1H, J = 14.0 Hz), 3.08 (d, OH, J = 7.3 Hz); MS (EI), m/z 266 (M^+, 60), 248(100), 235 (45); HRMS calculated for $C_{16}H_{10}O_4$ 266.0579; observed 266.0572; IR (KBr, cm^{-1}) 3368, 3067, 2916, 2866, 1675 1590, 1327, 1300.

Photolysis of **2.8**

Photolysis of **2.8** (10 mg, 1:1 H_2O-CH_3CN, pH 7, 300 nm, 16 lamps, 1 min, argon purged) gave a yellow solution. After work-up in air, the yellow residue was characterized by ^1H NMR to give **2.18** in 40% yield. Separation and purification was achieved by prep. TLC (silica gel, CH_2Cl_2) to give **2.18** (yellow powder, 3.5 mg, 30%). ^1H NMR (CD_3Cl, 500 MHz) δ 8.94 (d, 1H, J = 1.8), 8.44 (dd, 1H, J = 1.8, J = 8.1,), 8.38 (d, 1H, J = 8.1), 8.35-8.30 (m, 2H), 7.85-7.80 (m, 2H), 4.54 (t, 2H, J = 4.6 Hz), 4.02 (t, 2H, J = 4.6 Hz); ^{13}C NMR (CD_3Cl, 500 MHz) 182.4, 182.2, 165.2, 136.1, 134.8, 134.6, 134.44, 134.38, 133.5, 133.33, 133.3, 128.6, 127.5 127.4, 127.3, 67.3, 61.1; MS (EI), m/z

295 (M^+-1, 1), 253 (M^+-C_2H_3O, 70), 235(100), 207 (25); IR (KBr, cm^{-1}) 3358, 3056, 2956, 2884, 1726, 1680, 1591, 1273, 1247.

Photolysis of **2.9**

Photolysis of **2.9** (20 mg, 1:1 H_2O-CH_3CN, pH ~ 0 (5% H_2SO_4), 300 nm, 16 lamps, 1.5 h, argon purged) gave a yellow solution. After work-up in air, the yellow powder was characterized by ^1H NMR and assigned to be a mixture of product **2.29** (30% conversion) and **2.30** (14% conversion). The mixture was separated by prep. TLC (silica gel, 20% EtOAc-CH_2Cl_2) to give pure **2.30** (colourless oil, 2 mg, 10% yield) and **2.29** (yellow-orange powder, 5 mg) contaminated with 10% of **2.30** since **2.29** was found to be sensitive to oxygen and light, being readily converted to **2.30** under such conditions. Characterization of **2.29**: ^1H NMR (CD_3Cl, 300 MHz) δ 9.95 (s, 1H), 8.35 (s, 1H), 8.03-7.83 (m, 5H), 7.59-7.44 (m, 5H), 7.44-7.29 (m, 2H); MS (EI), m/z 298 (M^+, 100), 269(15); HRMS calculated for $C_{21}H_{14}O_2$ 298.0994; observed 298.0995. Characterization of **2.30**: ^1H NMR (CD_3Cl, 300 MHz) δ 10.12 (s, 1H), 8.12 (d, 1H, J = 8.8 Hz), 8.10 (s, 1H), 7.75 (d, 1H, J = 8.8 Hz), 7.70 (d, 4H, J = 7.3 Hz), 7.59-7.50 (m, 2H), 7.45-7.35 (tt, 4H, 1H, J = 7.3 Hz); ^{13}C NMR ($CDCl_3$, 75 MHz) 196.0, 195.5, 190.9, 145.7, 140.8, 137.1, 136.7 (2C), 133.8, 133.7, 131.5, 130.7, 130.2 (2C), 130.0 (2C), 128.8 (4C); MS (EI), m/z 314 (M^+, 80), 237 (70), 105 (100); HRMS calculated for $C_{21}H_{14}O_3$ 314.0943; observed 314.0937; IR (neat film, cm^{-1}) 3061, 1703, 1664, 1597.

2.6.8 Trapping of Photolysis Product of HMAQ

Compound **HMAQ** (20 mg in 50mL of CH_3CN and 50 mL of H_2O, pH 7) was irradiated for 1 min at 300 nm (16 lamps) under argon to give a yellow brown solution. Sufficient solid NaOH was added to change the solution colour to blue. This was

followed by the addition of 1 mL of Ac_2O, which turned the solution to a bright yellow. After work-up in air, the material was characterized by ^1H NMR showing formation of **2.34** (50 % conversion). Separation and purification was achieved by prep. TLC (silica gel, CH_2Cl_2) to give **2.34** in 40% yield (yellow powder, 11 mg, m.p. 175-177°C). ^1H NMR ($CDCl_3$, 300 MHz) δ 10.16 (s, 1H), 8.43 (s, 1H), 8.05-7.91 (m, 4H), 7.66-7.05 (m, 2H), 2.69 (s, 3H), 2.65 (s, 3H); ^{13}C NMR ($CDCl_3$, 75 MHz) 191.8, 169.5 (2C), 142.6, 140.8, 134.5 (2C), 130.4, 128.2, 127.5, 126.7, 125.7, 125.1, 123.5, 122.4 (2C), 122.2, 21.0, 20.9; MS (EI), m/z 322 (M^+, 3), 280 (10), 238 (100); HRMS calculated for $C_{19}H_{14}O_5$ 322.0841; observed 322.0845; IR (KBr, cm^{-1}) 3067, 2918, 2849, 1757, 1689, 1626.

Following with the above procedure, photolysis of compound **HMAQ** (20 mg, 350 nm, 16 lamps, 20 min) in neat CH_3CH_2OH gave **2.35** (75% conversion). Further purification was obtained by prep. TLC (silica gel, CH_2Cl_2) to give **2.35** in 60% yield (pale yellow powder, 16 mg, m.p. 194-196°C). ^1H NMR ($CDCl_3$, 300 MHz) δ 7.97-7.89 (m, 3H), 7.87 (s, 1H), 7.56-7.45 (m, 3H), 4.87 (s, 2H), 2.63 (s, 3H), 2.62 (s, 3H); MS (EI), m/z 324 (M^+, 10), 282 (15), 240 (100); HRMS calculated for $C_{19}H_{16}O_5$ 324.0998; observed 324.1000; IR (KBr, cm^{-1}) 3449, 1751.

2.6.9 pH Effects on Photolysis Efficiency of HMAQ

Solutions of **HMAQ** (10^{-4} M, 1:1 H_2O-CH_3CN, pH from 1 to 13) in 100 mL quartz vessels were purged with Ar for 15 minutes prior to photolysis and were irradiated (300 nm, 2 lamps for 1 min. Irradiated solutions were neutralized by 5% $NaHCO_3$ solution and were extracted by 3 × 50 mL CH_2Cl_2 in air. Collected organic extracts was dried over anhydrous $MgSO_4$. Removal of solvent was carried out under reduced pressure.

Photolysis yields (%) were determined with proton NMR. Conversion yields (%) were calculated based on the integration of the aldehyde proton of **FAQ** *vs.* the total integration of the aldehyde proton of **FAQ** and one methylene proton of **HMAQ**.

2.6.10 Quenching of Triplet HMAQ

A mixture of **HMAQ** (10^{-4} M) and sorbic acid (0.001 M) in 1:1 H_2O-CH_3CN (pH 7) in a 100 mL large quartz tube was purged with Ar for 15 minutes prior to photolysis and were irradiated (300 nm, 2 lamps) for 1 min. After work-up in air (followed the same procedure as shown in Section 2.6.3), a brown residue was characterized by ^{1}H NMR to give **FAQ** in 24 % conversion yield. Following the above procedure, photolysis of **HMAQ** (10^{-4} M) and sorbic acid (0-0.02 M) in 1:1 H_2O-CH_3CN (pH 7) were carried out to give **FAQ** in 5-34% yield.

Following the above irradiation procedure and the work-up procedure as shown in Section 2.6.3, photolysis of **HMAQ** in oxygen saturated solution (1:1 H_2O-CH_3CN, pH 7) gave **FAQ** in 28% yield.

3. Long-Range Intramolecular Photoredox Reaction of Biphenyl Anthraquinones Mediated by Water*

3.1 Introduction

Previous studies of **HMAQ** (Chapter 2) supported a mechanism involving a highly polarized triplet excited state in which electron density of the "distal" phenyl moiety is transferred to the central anthraquinone ring via a conjugated π system (Sections 2.4.6 and 2.4.7), which is subsequently trapped adiabatically by protonation at the anthraquinone carbonyl oxygen and deprotonation at the benzyl C–H. This eventually results in an overall photoredox reaction. We wondered whether or not the photoredox reaction observed for **HMAQ** could occur for substrates in which the benzyl alcohol moiety is much further away from the anthraquinone ketone.

Since the electronic communication for the above reaction relies on π system conjugation, a good way of separating the above reactive moieties (CH_2OH and carbonyl group) is to insert phenyl ring "spacers" that will still allow for potential electronic communication through the π system (in the excited state) but clearly lack substantial ground state electronic communication (due to the twisted nature of biphenyls and biaryls in general). Wan and coworkers have reported the photochemistry of twisted ground state biaryls,[92] that it is possible to induce photochemistry (e.g., photosolvolysis) at one end, by a "reactive" chromophore at the other end in a number of biphenyl and terphenyl systems. Exploring the photoredox chemistry of the proposed new types of anthraquinones could give new insights into the photoactivation of distal functional groups mediated by

---

* [Y. Hou, L. A. Huck, and P. Wan, Long-Range Intramolecular Photoredox Reaction via Coupled Charge and Proton Transfer of Triplet Excited Anthraquinones Mediated by Water, *Photochem. Photobiolo. Sci.*, **2009**, 8, 1408-1415.]-Reproduced by permission of The Royal Society of Chemistry (RSC) on behalf of the European Society for Photobiology, the European Photochemistry Association, and RSC.

phenylene (aromatic) spacers. Thus, we synthesized new anthraquinones **3.1-3.4** with phenyl and biphenyl "spacers" between two potentially reactive functional groups (Chart 3.1).

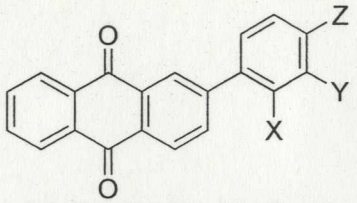

3.1 X = CH_2OH; Y = Z = H
3.2 X = Z = H; Y = CH_2OH
3.3 X = Y = H; Z = CH_2OH

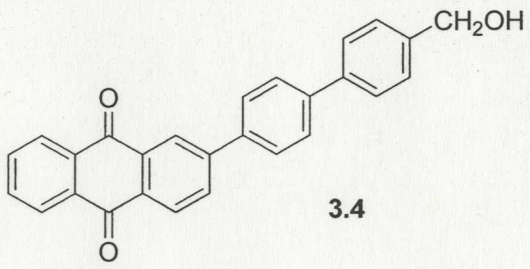

3.4

Chart 3.1

3.2 Syntheses

3.2.1 Synthesis of 3.1-3.3

Phenyl-substitited anthraquinones are relatively rare compounds. Additionally, we were unable to locate general procedures for Suzuki-type couplings in which one of the coupling partners was an anthraquinone. However, we were eventually successful in using a general Suzuki-type coupling for the synthesis for all of **3.1-3.3**. Thus, the synthesis of **3.1-3.3** employed the palladium-catalyzed Suzuki coupling reaction which in this case involved the required phenylboronic acids and the key anthraquinone triflate **3.5** (Scheme 3.1). Initial $Pd(PPh_3)_4$ catalyzed coupling gave the corresponding methylphenyl compounds (**3.1a-3.3a**) which were readily transformed to **3.1-3.3** via **3.1b-3.3b** using standard functional group manipulation. The overall yields of **3.1-3.3** are 50-60%.

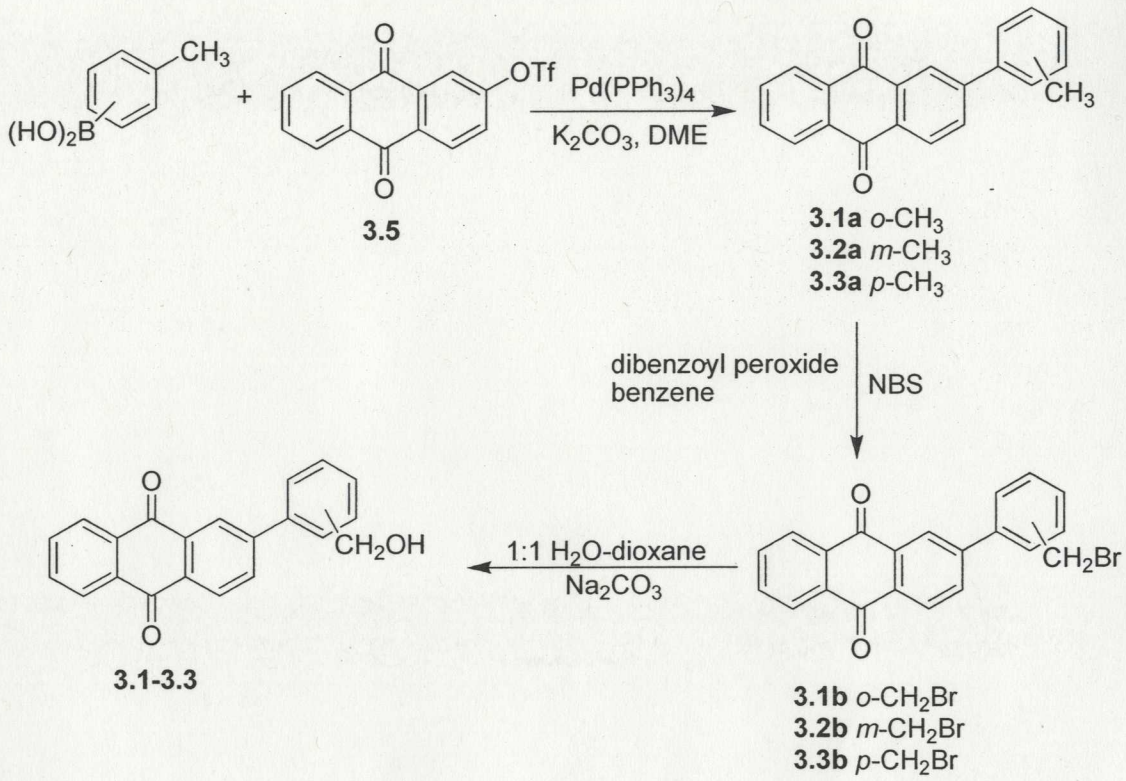

Scheme 3.1 Syntheses of phenyl-substitited anthraquinones **3.1-3.3**

3.2.1 Synthesis of 3.4

The synthesis of **3.4** also utilized the key anthraquinone triflate **3.5** (Scheme 3.2). The required bromobiphenyl **3.6** was synthesized from an initial Suzuki coupling of *p*-methylphenylboronic acid with *p*-iodobromobenzene. Transformation of **3.6** to the corresponding boronic acid **3.7** was followed by Suzuki coupling with **3.5**, to give initially **3.4a**, which was transformed to **3.4b**, and then ultimately to the required **3.4** in 20% overall yield.

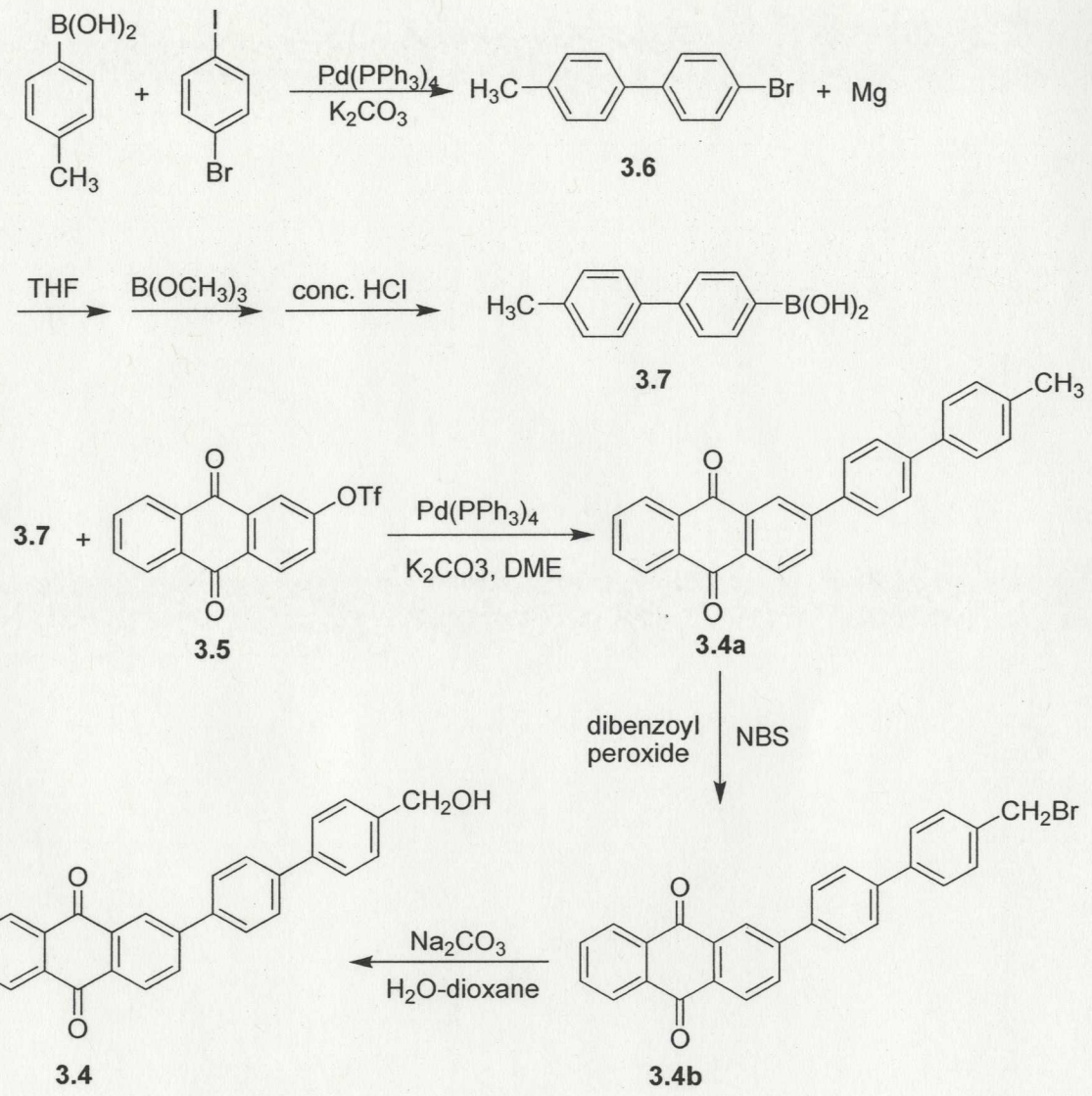

Scheme 3.2 Synthesis of biphenyl anthraquinone **3.4**

3.3 Product Studies

3.3.1 Photoredox Chemistry of 3.1-3.3

We anticipated that the **3.1-3.3** could undergo intramolecular photoredox reaction in the manner observed for the parent compound **HMAQ**. Thus, initial studies of the photochemistry of **3.1-3.3** were carried out using semi-preparartive scales in 1:1 H_2O-CH_3CN in 100 mL quartz vessels (10^{-4} M, pH 7, λ_{ex} = 300 nm, argon purged) and worked up in air. After irradiation in argon saturated solution, all compounds gave rise to a light

yellow color. When the solutions were exposed to air, the color was bleached quickly. On work-up, these runs gave *cleanly* the fully oxidized anthraquinone-aldehyde products **3.8-3.10** but in low yield (<10%) (eqn. 3.1). However, photolyses at pH 1 resulted in much higher yields, up to almost quantitative conversion. This is the *first observation* of acid catalysis of the photoredox reaction of anthraquinones. For these compounds, the catalytic effect is observable below *ca.* pH 3. No reaction was observed on photolysis in neat CH_3CN or when the above solutions were left in the dark. Moreover, photolysis of the corresponding methylphenyl compounds **3.1a-3.3a** did not give any reaction under similar photolysis times and solvent conditions, showing the need for the readily oxidizable benzyl alcohol moiety.

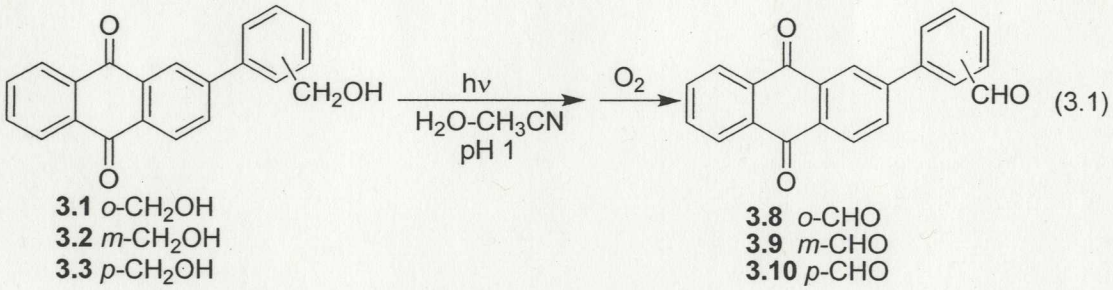

3.1 *o*-CH_2OH
3.2 *m*-CH_2OH
3.3 *p*-CH_2OH

3.8 *o*-CHO
3.9 *m*-CHO
3.10 *p*-CHO

(3.1)

To further explore the nature of the coloured species formed initially in the photolysis (before the addition of oxygen on work-up), the photochemical reactions of **3.1-3.3** were studied by UV-Vis spectroscopy. UV-Vis traces of photolysis of **3.1** (10^{-5} M, 1:1 H_2O-CH_3CN, pH 1, argon purged, λ_{ex} = 300 nm) showed formation of two new bands at 270 and 395 nm, the latter being a completely new long wavelength band (Figure 3.1). The presence of several isosbestic points indicate all these new bands belong to the same product(s) and no secondary reactions occur. These new bands are bleached within 40 min after aeration, to give rise to a spectrum identical to that of anthraquinone aldehyde

3.8. Visually, the almost colorless solution turned to medium yellow on exposure to light, and then back to colorless on aeration.

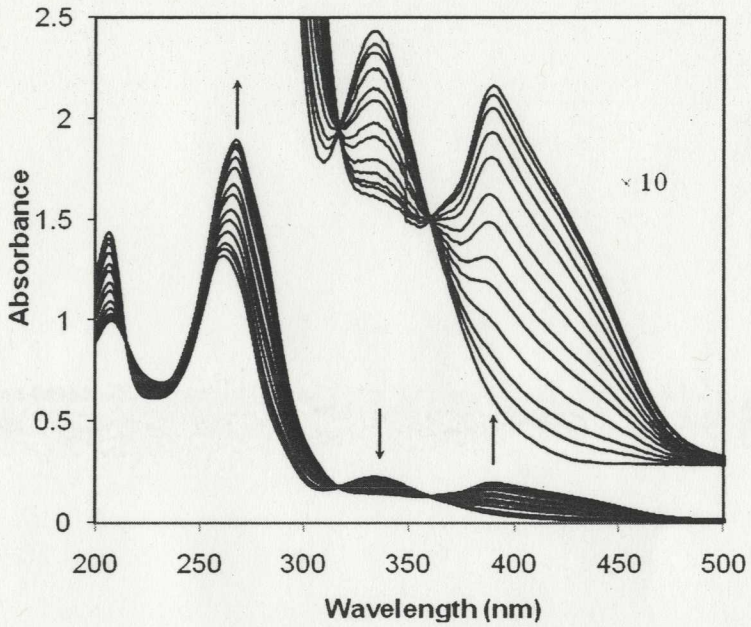

Figure 3.1 UV-Vis traces for photolysis of **3.1** in 1:1 H_2O-CH_3CN, pH 1 (λ_{ex} = 300 nm; argon purged). Each trace represents 5 s of photolysis. Photolysis resulted in loss of absorption (due to photoreaction of **3.1**) at 266 and 338 nm and formation of new absorption bands at 270 and 395 nm. Inset: ten-fold expansion of the long wavelength region.

To further exemplify the observed clean photochemical reaction of **3.1**, NMR studies of **3.1** were carried out in NMR tubes (10^{-3} M, 10% D_2O-CD_3CN, pD 1, argon purged). Photolysis (5 min) of **3.1** gave a yellow species that is consistent with **3.11-*OD*** (100% conversion since the benzylic proton (δ 4.49) of **3.1** was fully consumed, and all of the aromatic protons assignable to **3.11-*OD***), with a distinctive aldehyde peak at δ 10.05. After aeration, the yellow color disappeared. The NMR spectrum is now entirely consistent with the quantitative formation of **3.8**, with an aldehyde peak shifted upfield to δ 9.95 (Figure 3.2) (Scheme 3.3). All of these observations indicate that **3.1** undergoes a

clean photoredox reaction in aqueous solution catalyzed by acid. The need for water was further illustrated by a photolysis in neat CD_3OD (NMR tube) which resulted in only photodecomposition with little if any photoredox reaction.

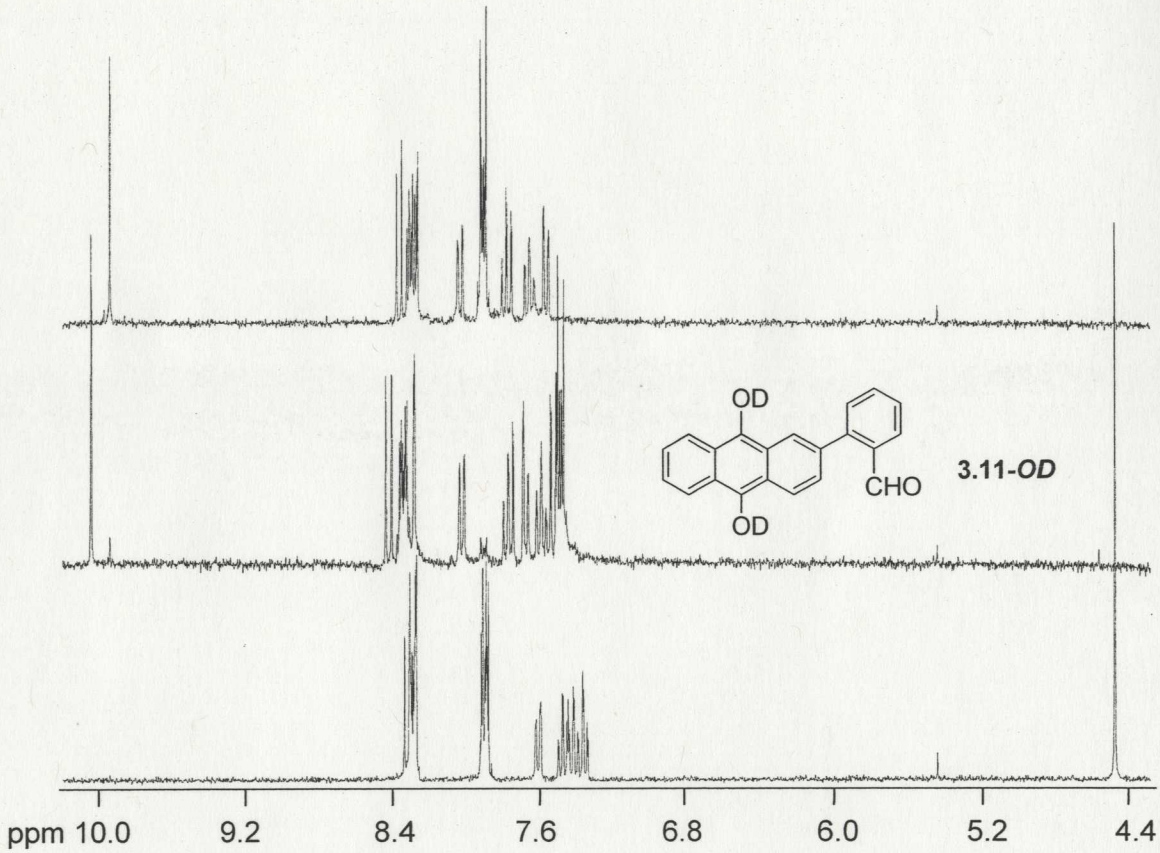

Figure 3.2 Proton NMR studies of photolysis of **3.1** in 10% D_2O-CD_3CN (pD 1, argon saturated). Bottom spectrum for **3.1** prior to photolysis, middle spectrum shows formation of **3.11-*OD***, and the top spectrum is that of **3.8** (formed upon aeration of **3.11-*OD***).

Although the initially formed photoredox product **3.11** could be observed by proton NMR on photolysis *in situ* in an NMR tube (the direct product is **3.11-*OD***), it could not be isolated in preparatory runs; only the oxidized product **3.8** could be characterized in these experiments (eqn. 3.1). However, we have successfully trapped **3.11** as follows. Photolysis of **3.1** (10^{-4} M, argon saturated 1:1 H_2O-CH_3CN) was carried out in a large 100

mL quartz tube to give a yellow species assignable to **3.11**. This was deprotonated by addition of excess NaOH pellets, to give a dark red solution (assigned to the dianion of the dihydroxyanthracene **3.11**). The red solution was bleached by the addition of excess Ac_2O. Upon work-up, diacetate **3.11-OAc** was isolated in 90% yield (Scheme 3.3), thus confirming the formation of **3.11**. In the absence of Ac_2O and NaOH, only the oxidized product **3.8** (90% conversion) was isolated.

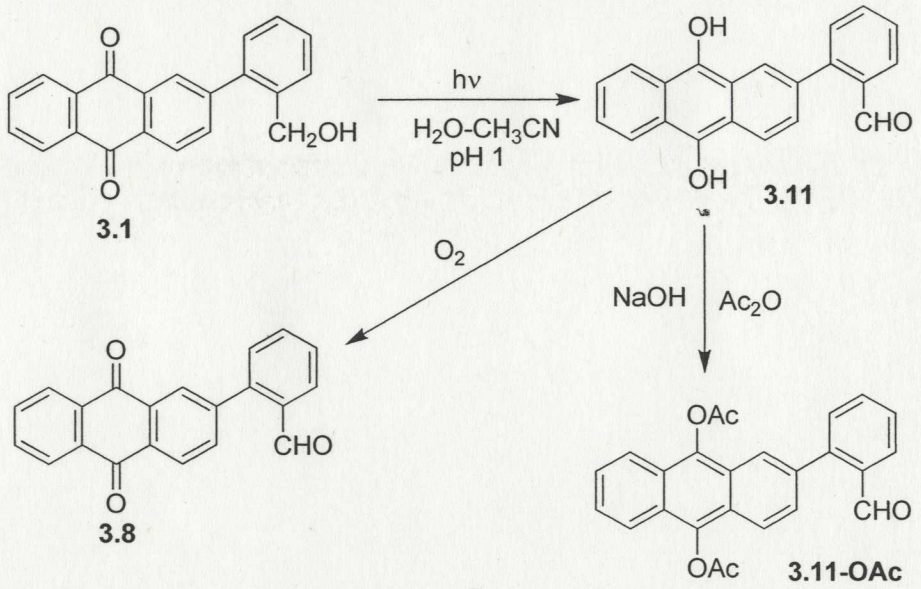

Scheme 3.3 Photolysis of **3.1** and trapping of the photoredox product **3.11** of **3.1**

UV-Vis studies of **3.2** also showed the clean photoredox reaction, to generate an initial photoredox product which has absorption bands at 288 nm and 399 nm. These two absorption bands were bleached to give the spectrum identical to that of anthraquinone aldehyde **3.9** within 20 min after aeration (Figure 3.3). Similar results were observed for **3.3**.

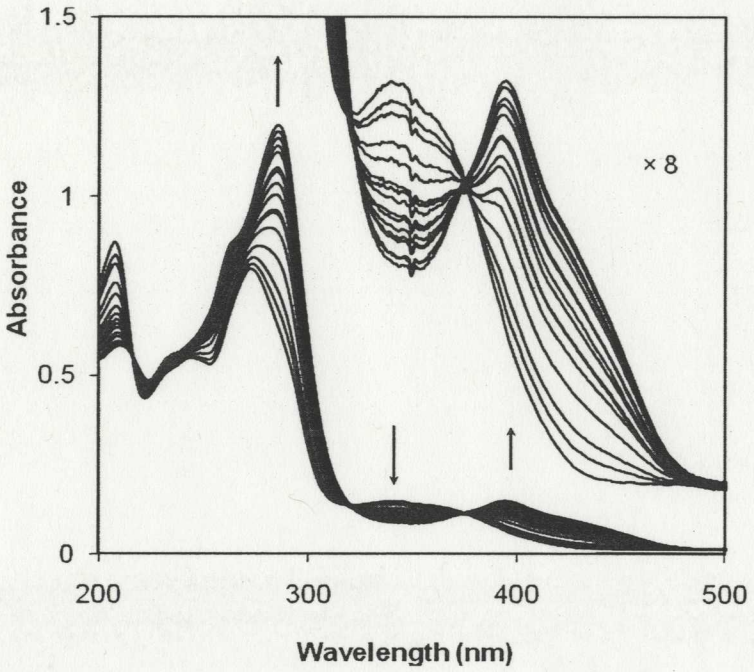

Figure 3.3 UV-Vis traces of photolysis of **3.2** in 1:1 H_2O- CH_3CN, pH 1 (λ_{ex} = 300 nm; argon purged). Each trace represents 5 s of photolysis. Photolysis resulted in loss of absorption (due to photoreaction of **3.2**) at 267 and 341 nm with formation of **3.12** (288 and 399 nm). Inset: eight-fold expansion of the long wavelength region.

Product studies of **3.2** in NMR tubes also comfirmed the formation of an initial photoredox product. Photolysis (5 min) of **3.2** (10% D_2O-CD_3CN, pD 1, argon purged) gave a yellow species that is consistent with **3.12-*OD*** (100% conversion since the benzylic proton (δ 4.68) of **3.2** is fully consumed, and all the aromatic protons assignable to **3.12-*OD***) with a distinctive aldehyde peak at δ 10.13 (Figure 3.4) (eqn. 3.2). After aeration, the yellow color disappeared. The NMR spectrum is now entirely consistent with quantitative formation of **3.9**, with an aldehyde peak shifted upfield to δ 10.12. Anthraquinone **3.3** also underwent clean photoreaction to generate the corresponding initial photoredox product **3.13-*OD*** which were observed by proton NMR.

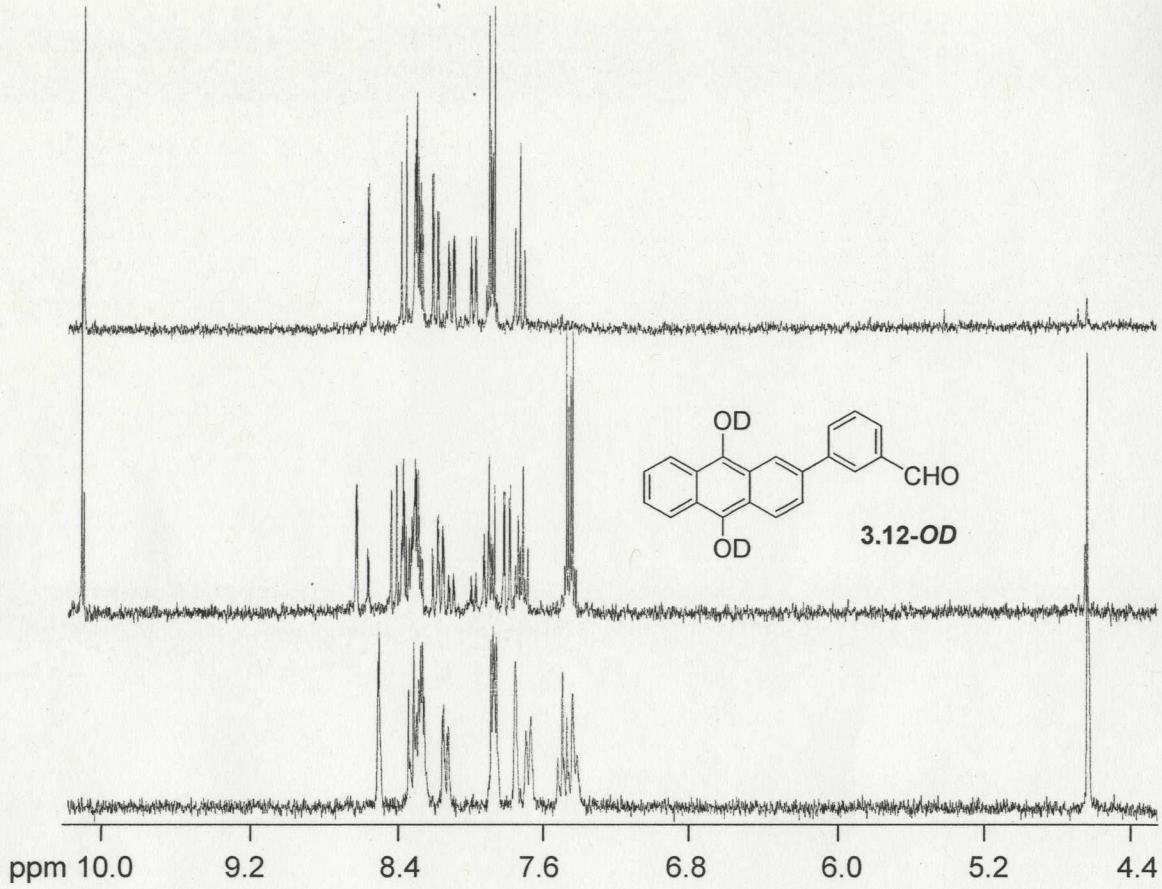

Figure 3.4 Proton NMR studies of photolysis of **3.2** in 10% D_2O-CD_3CN (pD 1, argon saturated). Bottom spectrum is **3.2** prior to photolysis, middle spectrum is **3.12-*OD***, and top spectrum is that of **3.9** (formed upon aeration of **3.12-*OD***).

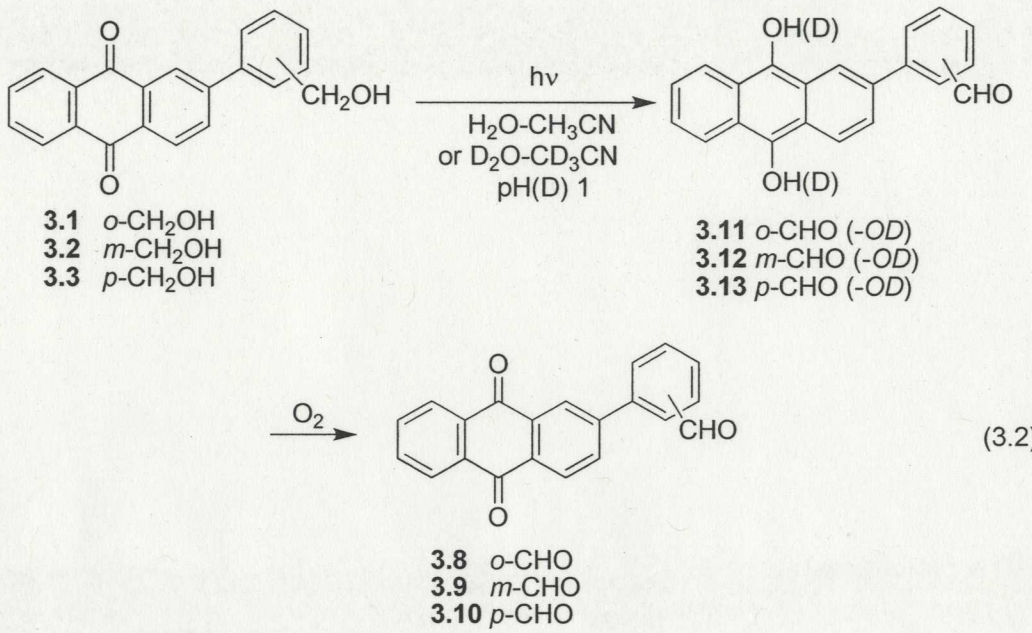

(3.2)

As noted above, the efficiency of the photoredox reaction of **3.1-3.3** was rather low at pH 7. This was confirmed by quantum yield measurements which were measured by the formation of oxidized products (**3.8-3.10**) with ^{1}H NMR (Table 3.1). Indeed, when compared to the parent compound **HMAQ** ($\Phi \sim 0.8$; pH 7), this was rather disappointing. However, they have substantially high quantum yields at pH 1, which is a redeeming feature (eqn. 3.2). The parent compound **HMAQ** does not exhibit acid catalysis of reaction in the pH range of 7-1 (Section 2.4.2 in Chapter 2), which is not surprising since its quantum yield of reaction is already quite high in neutral solution.

Table 3.1 Quantum yields for the formation of photoredox products of biphenyl anthraquinones 3.1-3.3 in 1:1 H_2O-CH_3CN

Biphenyl anthaquinones	Photoredox products	pH	Quantum yield (Φ)
3.1	**3.11**	7	0.08
		1	0.6
3.2	**3.12**	7	0.05
		1	0.3

3.3	**3.13**	7	0.07
		1	0.5

3.3.2 Photoredox Chemistry of 3.4

We finally turned our attention to terphenyl system **3.4**, which has the longest separation of the two reactive functional groups in our studied anthraquinones. Photolysis of **3.4** (10^{-4} M, 1:3 H_2O-CH_3CN, pH 7) in 100 mL quartz vessels gave only a trace yield of **3.14** after work-up in air. However, when the photolysis was carried out in acidic solution (pH 1), a much more intense yellow solution was generated, which was oxygen sensitive. Work-up gave the expected oxidized product **3.14** in good yields (up to 80%; $\Phi \sim 0.1$) (eqn. 3.3).

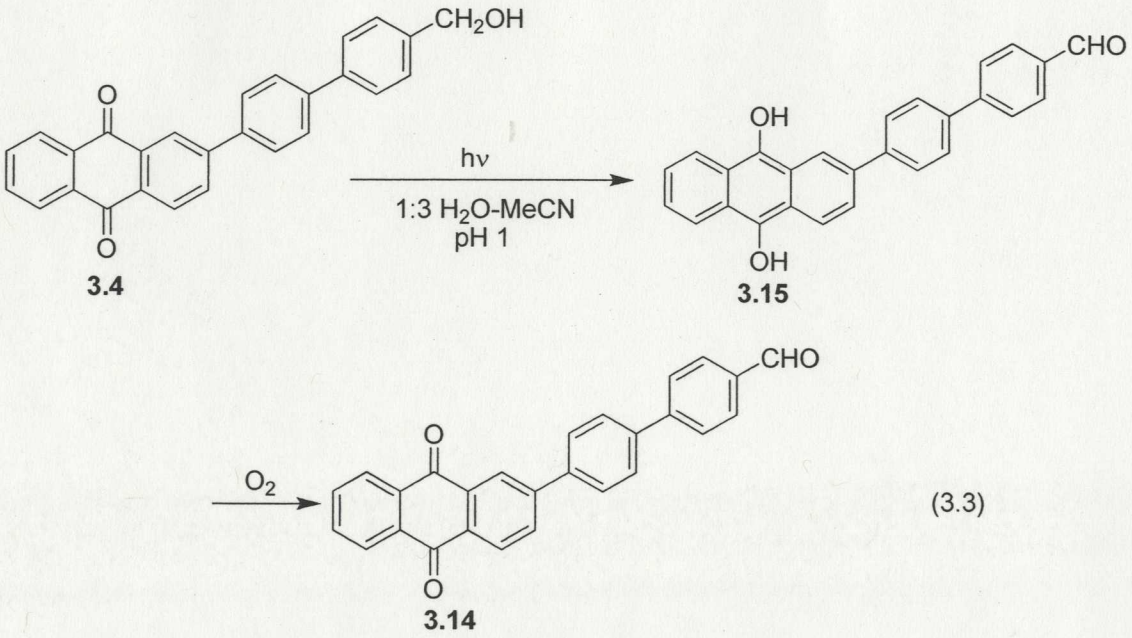

(3.3)

UV-Vis studies were carried out for **3.4** (10^{-5} M) in 1:3 H_2O-CH_3CN (pH 1). Exposure to 300 nm resulted in the formation of an intense band at 312 nm and a less intense band at 399 nm. These two bands are bleached within 20 min after aeration, to give rise to a spectrum identical to that of anthraquinone aldehyde **3.14** (Figure 3.5) (eqn. 3.3).

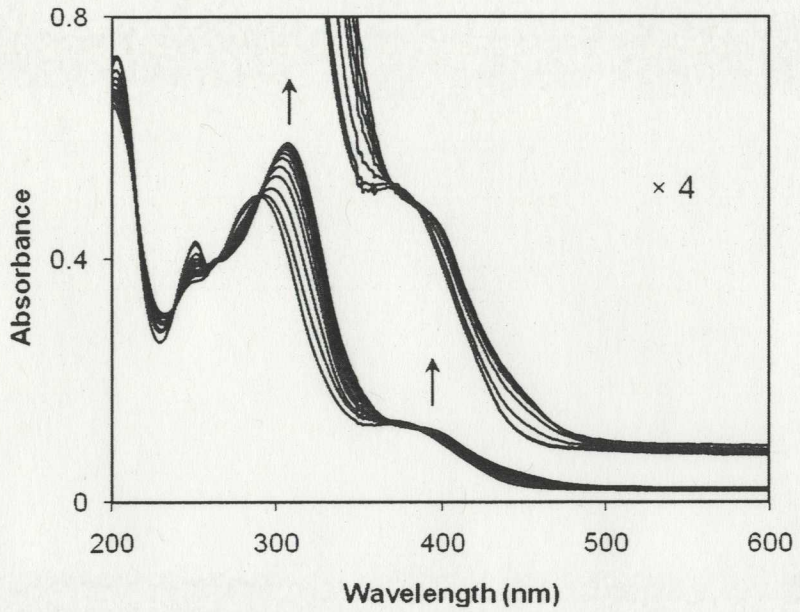

Figure 3.5 UV-Vis traces of photolysis of **3.4** (10^{-5} M, 1:1 H_2O-CH_3CN, pH 1, argon purged, λ_{ex} = 300 nm). Each trace represents 1 min of photolysis. Photolysis resulted in loss of absorption (due to photoreaction of **3.4**) at 292 and 381 nm with formation of **3.15** (312 and 399 nm). Inset: four-fold expansion of the long wavelength region.

Proton NMR studies of **3.4** also confirmed formation of **3.15** (characteristic aromatic and aldehyde peaks). Finally, semi-preparative photolysis of **3.4** (10^{-4} M, 1:3 H_2O-CH_3CN, pH 1, argon saturated) was carried out in 100 mL quartz vessels and worked up in air, to give the oxidized product **3.14** (eqn. 3.4). Although the insertion of an additional phenyl group spacer in **3.4** has modulated the reaction efficiency, the clean photoredox reaction that was still observed indicates that the inherent driving force of this reaction is still apparent and substantial.

3.4 Mechanistic Studies

3.4.1 pH Effects on Photolysis Efficiency of 3.1-3.4

As noted above, the photoredox reactions of **3.1-3.3** exhibited acid catalysis. To explore the effect of pH on the efficiency of the intramolcular photoredox reaction of **3.1-3.3**, photolyses of **3.1-3.3** (10^{-4} M, 1:3 H_2O-CH_3CN, argon purged, λ_{ex} = 300 nm, pH 7-0) were carried out in 100 mL quartz vessels. After irradiation, all solutions were worked up in air. Conversion yields (%) of the photoredox product were determined with proton NMR. The results are plotted as a function of pH as shown in Figure 3.6. The photoredox reaction of **3.1-3.3** displayed acid catalysis above pH 3. These observations strongly suggest that the possible mechanistic step of the photoredox reaction of **3.1-3.3** involves protonation of carbonyl oxygen on the anthraquinone moiety. A similar result was observed for **3.4**.

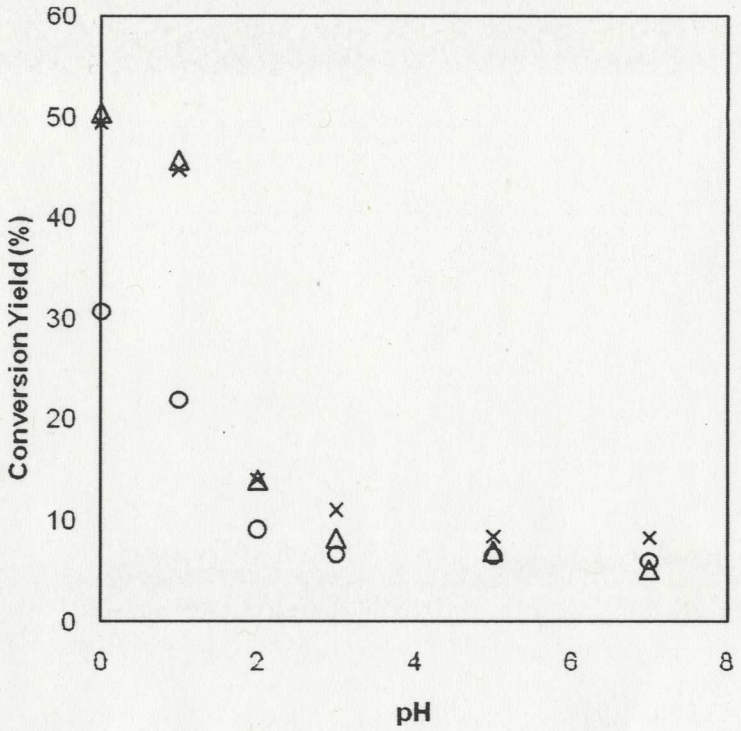

Figure 3.6 pH Dependence of intramolecular photoredox efficiency for **3.1** (Δ), **3.2** (o) and **3.3** (×) (~ 10^{-4}M, 1:3 H_2O-CH_3CN, argon saturated) (pH refers to the aqueous portion). Measurement error is about ± 5%.

3.4.2 Evidence for Unimolecular Reaction in Anthraquinone

Prior studies[62] provided evidence that the photoredox reaction of **HMAQ** is unimolecular in anthraquinone molecule. In this work, additional supporting kinetic evidence is provided. In a reaction mechanism that is unimolecular in anthraquinone molecule, due to the large excess of water, the reaction rate will be directly proportional to the concentration of anthraquinone (pseudo first order reaction). The kinetics for photoredox reaction of **3.1** (10^{-7}~10^{-5} M, 1:1 H_2O-CH_3CN, pH 1, argon saturated) were studied by monitoring the absorption intensity of product **3.11** at 387 nm with UV-Vis spectroscopy, to generate observed reaction rates at different substrate concentrations. The plot of observed rate vs. concentration of **3.1** clearly showed a linear relationship

with respect to **3.1** in the 10^{-7}-10^{-5} M range, with an apparent rate constant of 1.6×10^{-3} $L \cdot mol^{-1} \cdot s^{-1}$ (Figure 3.7).

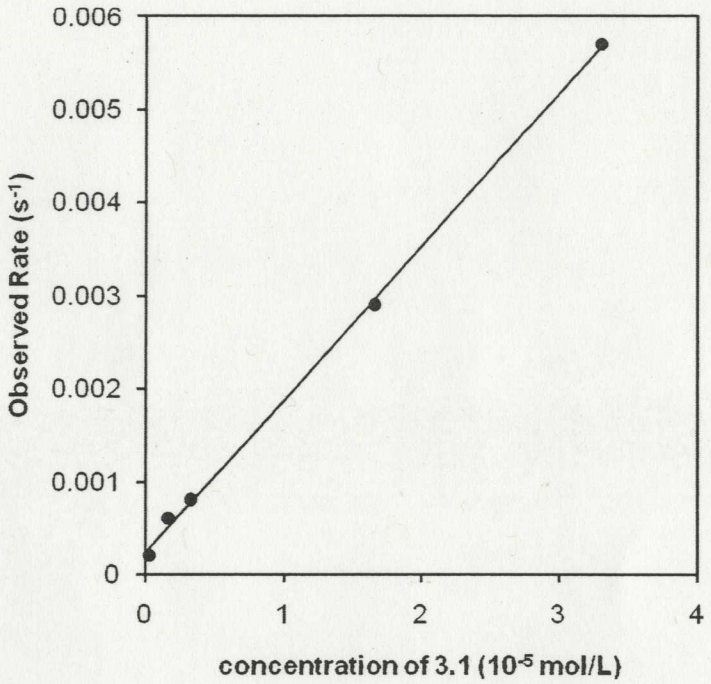

Figure 3.7 Effect of concentration of **3.1** (1:1 H_2O-CH_3CN, pH 1, argon purged) on the observed reaction rate of photoredox reaction. Measurement error is about ± 5%.

Additionally, if the mechanism of reaction proceeded via a bimolecular interaction of an excited anthraquinone with a ground state partner, one would expect the initial formation of equal amounts of "half-oxidized" (e.g., **3.8**) and "half-reduced" (i.e., **3.11** but with the aldehyde replaced by CH_2OH) products. Such types of mixtures were never observed at any conversion. Moreover, bimolecular-type coupling products that might be anticipated on bimolecular reaction were never observed. All of these observations are consistent with an intramolecular redox reaction that is unimolecular in substrate and may be regarded as "single molecule" reaction catalyzed by water or acid.

3.4.3 Solvent istope Effect on Photoredox Reaction

The proposed mechanism (Scheme 2.8) of the intramolecular photoredox reaction of anthraquinone **HMAQ** involves two key proton transfer steps. One is protonation of the carbonyl oxygen on the anthraquinone moiety and the other is deprotonation of the C-H bond on the benzyl CH_2OH moiety. A kinetic isotope effect of 2.1 ± 0.1 for C-H bond breaking was also presented in Section 2.4.1. In addition, the effect of H_2O vs. D_2O on photoredox reaction of **HMAQ** was also explored in which lower quantum yields (ca. 20%) were observed in D_2O compared to H_2O. All these results are consistent with the required proton transfers in the proposed mechanism (Scheme 2.8).

To explore the effect of H_2O vs. D_2O in the present study, photolysis of **3.1** was carried out in a 50 mL quartz tube (deaerated by argon purge) as a function of water (H_2O or D_2O) content in CH_3CN (pH or pD 1) and worked up in air. The yield of the photoredox product **3.8** were determined by proton NMR and plotted as a function of H_2O/D_2O content (Figure 3.8). The results show a reaction that is highly sensitive to water content in CH_3CN but no reaction in neat CH_3CN. The efficiency of reaction is always lower in D_2O compared to H_2O, by as much as 10% at 10% (v/v) $H_2O(D_2O)$. These results are consistent with a mechanism that requires protonation of the carbonyl oxygen (by H_2O or H_3O^+) in the rate limiting step.

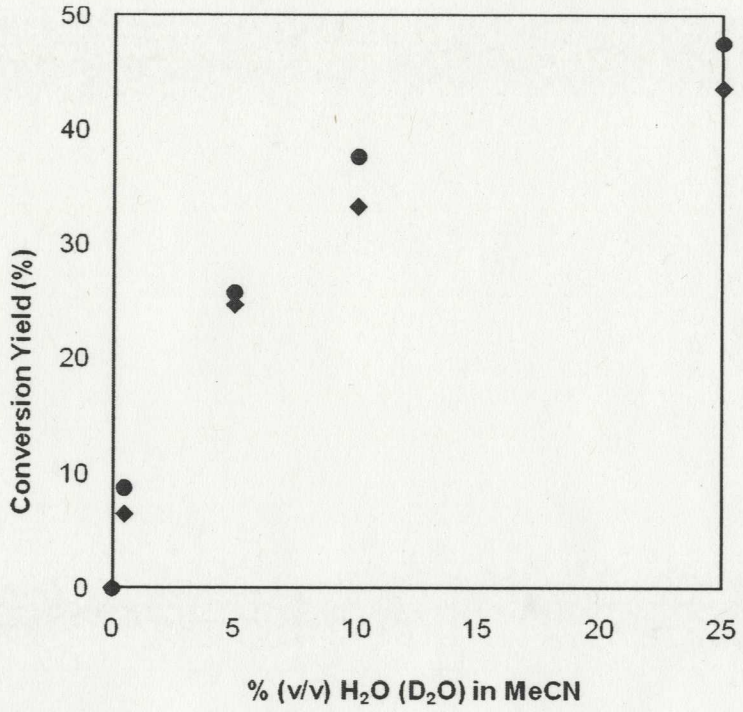

Figure 3.8 Solvent isotope effect (H_2O (•) and D_2O (♦) (pH or pD = 1, 50% CH_3CN as co-solvent) on the photoredox efficiency of **3.1** as determined by ^1H NMR (% yield is for the formation of **3.8**). Measurement error is about ± 5%.

3.4.4 Nanosecond Laser Flash Photolysis (LFP) of 3.1

LFP of **HMAQ** in Section 2.4.4 showed a triplet excited state transient at 390 nm. We expect compounds **3.1-3.4** would have a triplet excited transient state due to the same anthraquinone chromophore, which could be observed on LFP. Compound **3.1** was chosen for study since it has the highest quantum yield of reaction of all the compounds. LFP of **3.1** (10^{-5} M, in neat CH_3CN, argon saturated) showed a weak absorption band at 380 nm and an intense broad band at 600 nm (within the laser pulse) (Figure 3.9). Both signals decayed with the first order kinetics ($1.4 \pm 0.1 \times 10^5$ s^{-1}; $\tau \sim 7.0$ μs). The intensity and lifetime of this transient was significantly reduced in the presence of oxygen ($\tau \sim$ 0.14 μs).

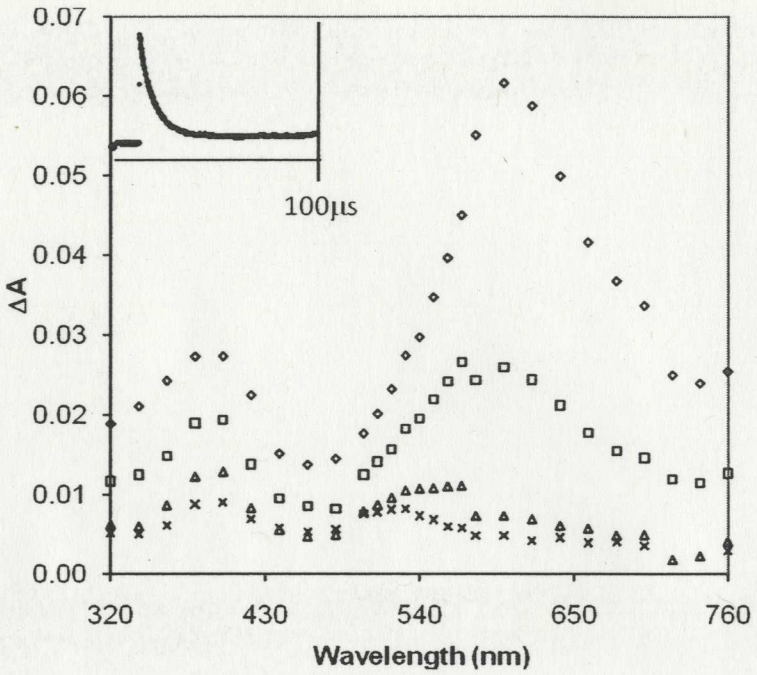

Figure 3.9 Triplet-triplet absorption spectra of **3.1** in neat CH_3CN (nitrogen-saturated) after the 266 nm pulse, 1.8 μs(◊), 7.9 μs (□), 21 μs (Δ), 78 μs (×). Inset: triplet decay at 600 nm. Measurement error is about ±10%.

It is not possible to assign the above bands from previous literature since no prior articles about photochemical and photophysical studies of **3.1** have been reported. A suvey of the literature shows that photochemical and photophysical studies of **3.16** were reported only by Shigorin *et al.*[93] Compound **3.16** undergoes a photoreduction reaction in CH_3CH_2OH as for 9,10-anthraquinone. The authors suggested that the reaction proceeds via a lowest π,π* triplet. However, no details of the excited transients such as a triplet-triplet absorption spectrum were reported.

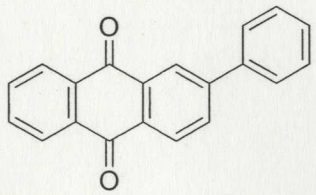

3.16

Photochemical and photophysical studies of 9,10-anthraquinone are well-known. Triplet 9,10-anthraquinone has an intense 380 nm absorption ($\tau \sim 6$ μs in argon saturated solution), and is quenched by oxygen ($\tau \sim 10$ ns),[59a] Similar observations were obtained for **HMAQ** in neat CH_3CN or aqueous solution (Chapter 2). Triplet excited **HMAQ** has an intense 380 nm absorption ($\tau \sim 6$ μs) in argon saturated CH_3CN and has an intense 390 nm absorption ($\tau < 0.1$ μs) in argon saturated H_2O-CH_3CN. Although there is a big difference between absorption bands of **3.1** (380/600 nm) and 9,10-anthraquinone or **HMAQ** (380 nm), it can be rationalized by the differences of their chromophores. Since **3.1** with an attached phenyl ring is more planar on the electronically excited state than on the ground state, electronically excited **3.1** has a longer conjugated system (details are presented in Section 3.4.6) and is expected to have a longer wavelength absorption band than excited **HMAQ**. Based on these facts, we tentatively assigned the 380/600 nm transient observed for **3.1** to the triplet state. The assignment was also confirmed by LFP studies of methyl compound **3.1a** in neat CH_3CN, which showed only formation of the triplet excited state (380/600 nm, $\tau \sim 15$ μs, quenched by oxgen, $\tau_{ox} \sim 0.18$ μs).

In the presence of water, LFP of **3.1** (1:1 H_2O-CH_3CN, pH 7, N_2 purged) also showed the formation of the triplet state but at 620 nm (red shifted) with significantly shorter lifetime ($\tau \sim 0.74$ μs) compared to neat CH_3CN, consistent with photochemical reactivity in aqueous solution. With decaying of the triplet excited transient, a new long lived transient ($\tau \sim 2.4$ ms) was observed at 520 nm (Figure 3.10). Its yield was reduced greatly by the presence of oxygen, but its decay rate was not affected. These observations are consistent with the 520 nm being a ground state species and generated from the triplet excited state. This assignment is also consistent with the observation that LFP studies of

the methyl compound **3.1a** in 1:1 H_2O-CH_3CN (pH7) showed only formation of the triplet excited state (620 nm, τ ~2.5 μs, quenched by oxgen, τ_{ox} ~ 0.27 μs) *without* the formation of the 520 nm species.

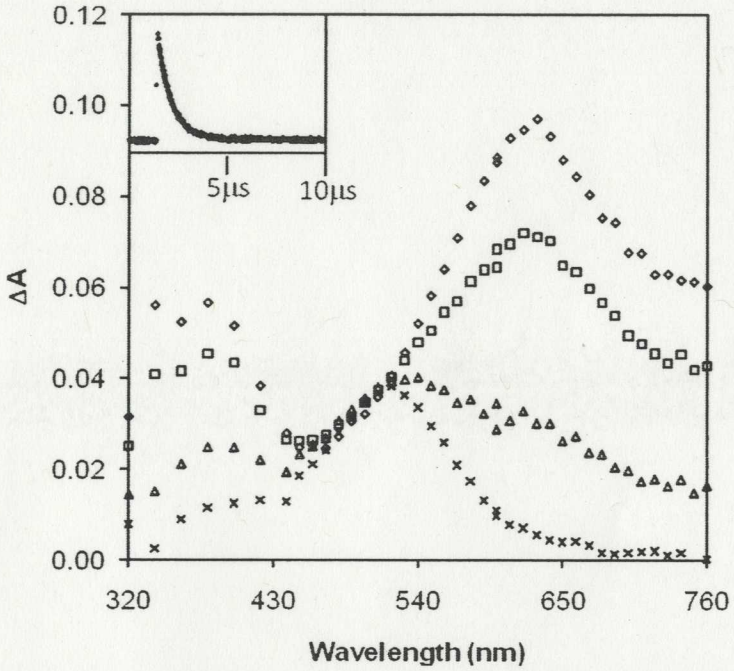

Figure 3.10 Triplet-triplet absorption spectra of **3.1** in 1:1 H_2O-CH_3CN (pH 7, nitrogen-saturated) after the 266 nm pulse, 0.23 μs(◊), 0.60 μs (□), 1.7 μs (Δ), 6.3 μs (×). Inset: triplet decay at 620 nm. Measurement error is about ±10%.

The effect of pH on the decays of the above transients offered a critical clue for assigning the 520 nm transient to an intermediate. In pH 1 the triplet signal at 620 nm was shorter lived (τ ~ 0.39 μs, compared to 0.74 μs at pH 7), consistent with acid catalysis of the reaction. In addition, the observed decay rate of the 520 nm transient was strongly dependent on pH (k_{pH7}:k_{pH1} ~ 40:1), consistent with ketonation of the enol generated from p-benzoylphenylacetic acid (k_{pH7}:k_{pH1} ~ 100:1).[94] The faster decay at pH 7 is associated with base catalysis of ketonization.[94] Thus, we tentatively assign the 520 nm

transient to an enol intermediate. Indeed, the decay of this species ultimately leads to a weak broad absorption in the 400 nm region that is assignable to the photoredox product **3.11** which was observed by LFP (100 ms time scale) (Figure 3.11). LFP studies of the methyl compound **3.1a** at pH 1 also supported the assignment.

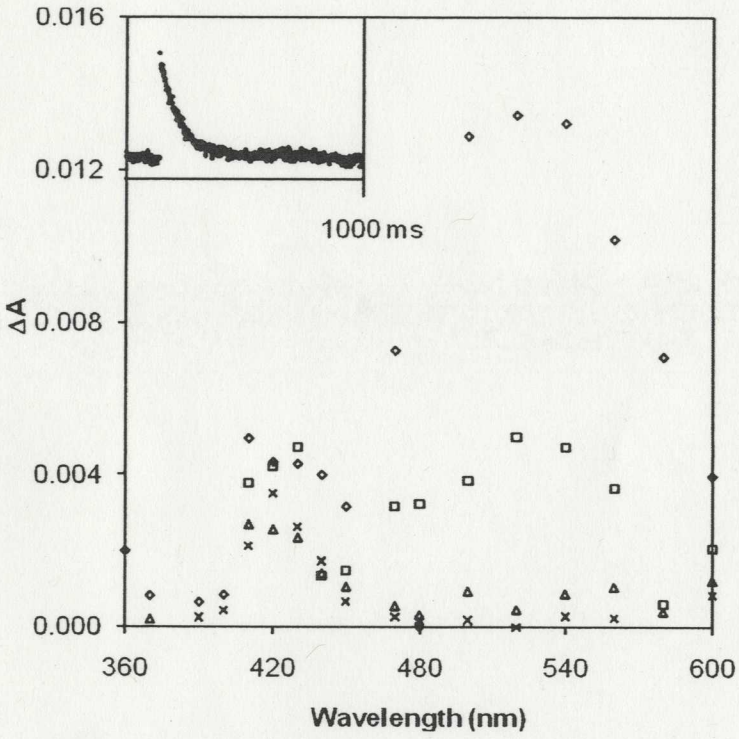

Figure 3.11 Triplet-triplet absorption spectra of **3.1** in 1:1 H_2O-CH_3CN (pH 1, nitrogen-saturated) after the 266 nm pulse, 31 ms(◊), 122 ms (□), 405 ms (Δ), 686 ms (×). Inset: intermediate decay at 520 nm. Measurement error is about ±10%.

3.4.5 Quenching of Triplet 3.1

To explore the reactivity of the triplet **3.1**, photolyses of **3.1** (10^{-4} M, 1:1 H_2O-CH_3CN, pH 1, argon purged, λ_{ex} 350 nm) were carried out in 100 mL solution in a quartz tube with a triplet quencher, sorbic acid (0 ~ 0.01 M). After work-up in air, the photolysis conversion yields (the formation of **3.8**, 10%~ 40%) were determined with NMR. A Stern-Volmer plot for the photolysis of **3.1** was made (Φ_0/Φ *vs.* the concentration of

sorbic acid). The biphasic plot (Figure 3.12) showed initial linear quenching at low concentrations of sorbic acid (< 0.004 M) and a plateau region with $\Phi_0/\Phi \sim 3$ at the high concentrations of sorbic acid (0.004-0.01 M).

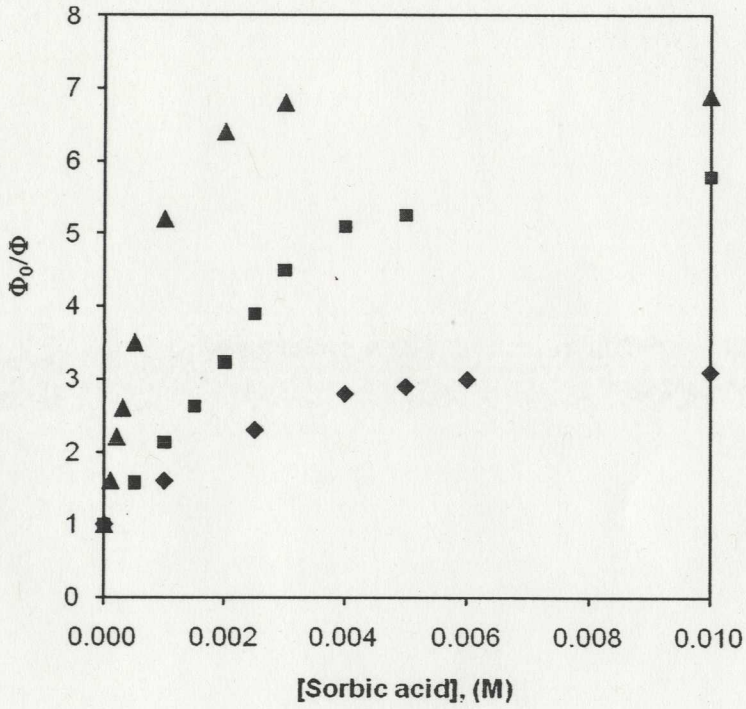

Figure 3.12 Stern-Volmer plots of quenching of photoredox reactions for **3.1** (♦), **3.2**(▲) and **3.3** (■) in the presence of sorbic acid. Φ_0 / Φ refer to the yields in the absence and presence of quencher. Measurement error is about ± 5%.

These values can be interpreted to mean that with the respect of the photoredox reaction, about 33% of the photoredox reaction of **3.1** cannot be quenched by sorbic acid. This means that about 67% of the photoredox reaction of **3.1** is via the triplet excited state. The remaining "unquenchable" fraction (the flat region) is most likely due to the singlet excited state reaction although one cannot rule out the possibility of reaction via another short-lived triplet state. From the initial linear region of the plot, the slope ($k_q\tau$) was determined to be 458 M^{-1}. Assuming that the bimolecular triplet quenching rate

constant is diffusion-controlled in water (5×10^9 $M^{-1}s^{-1}$),[88] it was estimated that the reactive triplet lifetime of **3.1** was 90 ns. This result is consistent with the observations from LFP studies that indicates that the reactive triplet **3.1** was short-lived in acidic aqueous solution. Similar results were observed for **3.2** and **3.3**. About 85% and 80% of the photoredox reaction for **3.2** and **3.3** are via the triplet excited state. Estimated reactive triplet lifetimes of **3.2** and **3.3** are 1.0 μs and 0.23 μs, respectively.

Oxygen quenching for the triplet **3.1-3.3** were also carried out in large quartz vessels with oxygen saturated solution (1:1 H_2O-CH_3CN, pH 1). After work-up in air, conversion yield of **3.8-3.10** in the absence and presence of oxygen was $\Phi_0/\Phi \sim 1.38$, 5.0 and 4.7. Thus, it was concluded that the triplet state is reactive, which is consistent with much of the known photochemistry of anthraquinones.[56,59]

3.4.6 HOMO/LUMO Calculations

We have shown that a variety of "extended" anthraquinones **3.1-3.4** undergo a clean intramolecular photoredox reaction, to generate the corresponding initially formed dihydroxyanthracenes **3.11-3.13** with high quantum yields in acid. Based on examinations of calculated HOMOs and LUMOs (AM1, Chem 3D, MOPAC) (Figure. 3.13 and 3.14), one can readily see that electronic excitation would give rise to excited states that would be highly polarized. For example, in the case of **3.2** (Fig. 3.13), electron density would be transferred from the benzene ring with the CH_2OH substituent (and the anthraquinone carbons closest to this ring) to the central anthraquinone ring including the carbonyl oxygens. For **3.4** (Figure 3.14), electron density would be transferred from *both* of the attached biphenyl rings to the central anthraquinone ring system. Such excited states would exhibit high basicity at the

anthraquinone carbonyl oxygen. Note also that the AM1 calculations show the biphenyl and terphenyl rings to be twisted (dihedral angle ~ 30-40°). There is tendency for these rings to be more planar on electronic excitation that would facilitate the charge transfer.[92a]

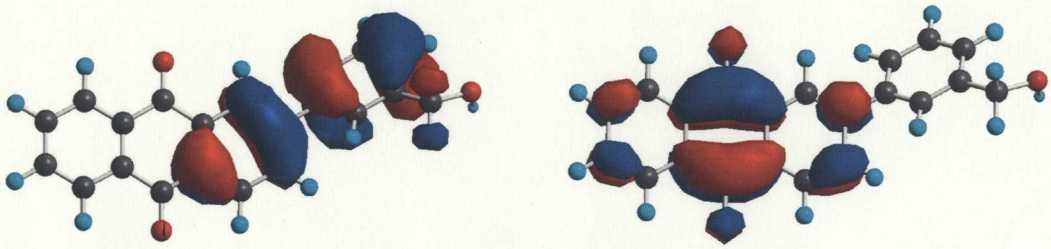

Figure 3.13 Calculated (AM1) HOMO (left) and LUMO (right) for **3.2**

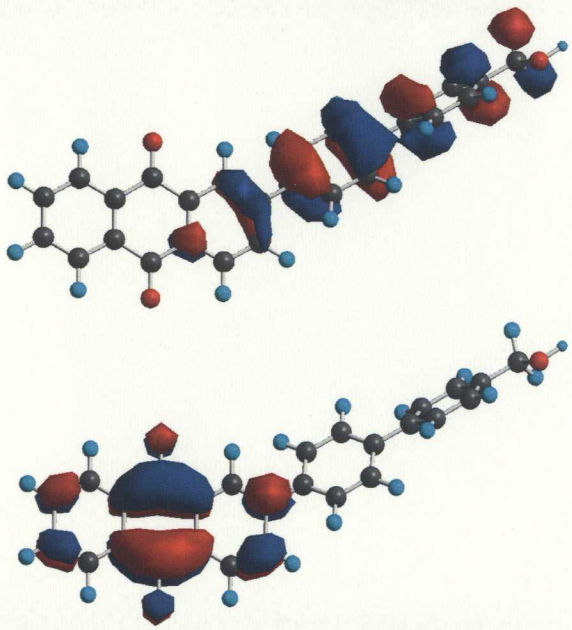

Figure 3.14 Calculated (AM1) HOMO (top) and LUMO (bottom) for **3.4**

3.4.7 Proposed Mechanism

The intramolecular photoredox reactions of phenyl and biphenyl anthraquinones are proposed to proceed via a mechanism similar to that of **HMAQ** presented in Section 2.4.7. Like **HMAQ** in Chapter 2 and phenyl anthraquinone **3.16**,[93] the lowest triplet states for **3.1-3.3** should also be π,π^* states since these photoredox reactions occur in the

presence of a highly polar solvent such as water (even acidic solution), which is essential to stabilize the initial excited states (the lowest triplet).

In the proposed mechanism (Scheme 3.4), the carbonyl oxygen of the highly polarized triplet **3.1** is protonated by solvent water (or proton, depending on pH), to give **3.17a**. This results in a net positive charge on the benzene ring with the attached hydroxymethyl group (**3.17b**). Deprotonation of **3.17b** gives (after ISC) a double enol intermediate **3.18**. This is followed by ketonization/enolization to give the final product **3.11**.

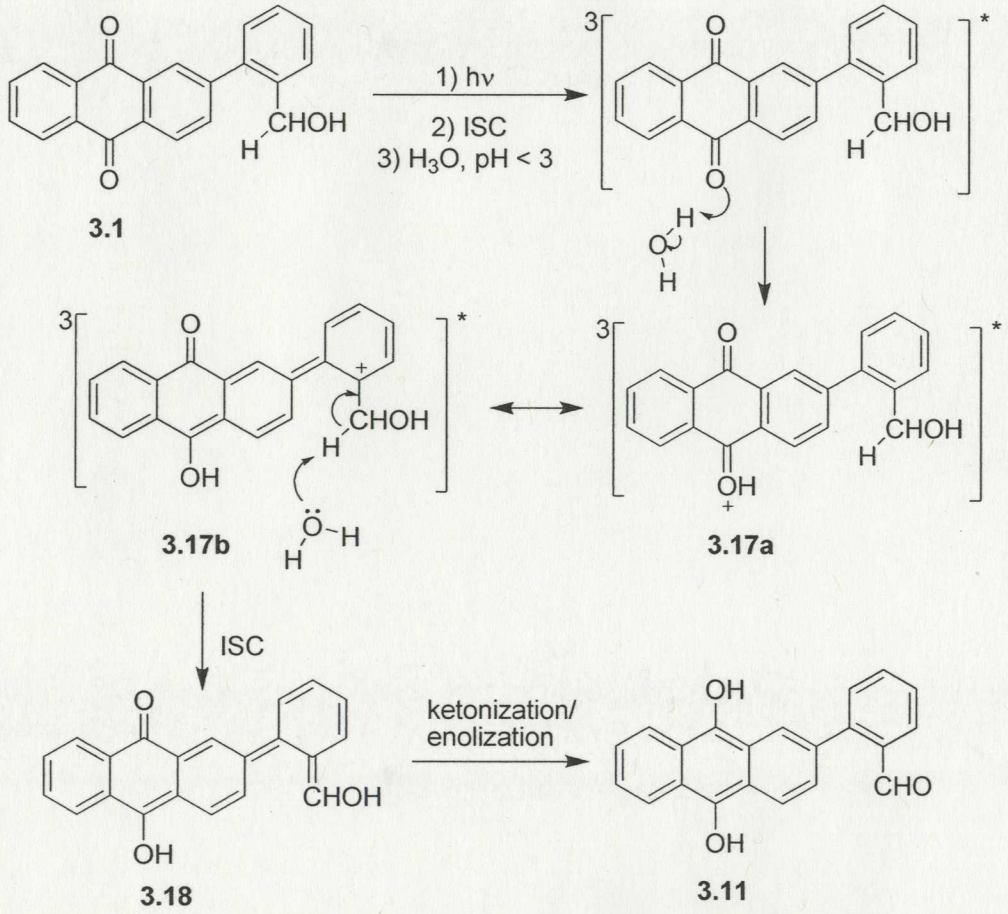

Scheme 3.4 Proposed mechanism for the intramolecular photoredox reaction of **3.1**

3.5 Summary

The photoredox reaction of **HMAQ** has been successfully extended to phenyl anthraquinone derivatives. We have shown that suitably designed triplet excited anthraquinones with distal benzyl alcohol moieties possess high degrees of electronic communication through the aromatic π system that can lead to clean intramolecular photoredox electron in aqueous solution. Electronic communication in the excited state is apparently a key step for the reaction. Just as noted in the introduction, since excited phenyl and biphenyl anthraquinones tend to a planar structure, electronic communication between the anthraquinone carbonyl and the benzylic alcohol occurs through the extended π system, and result in formation of the highly polarized excited state. This leads to protonation of the ketone on the anthraquinone moiety and deprotonation of the benzylic C-H to give photoredox products. Different quantum yields of studied compounds also suggest the different efficiency of electronic communication in these molecules. The longer the distance between the carbonyl group and the benzylic alcohol, the lower the efficiency of reaction.

3.6 Experimental

3.6.1 General

EI mass spectra were obtained using a double focusing mass spectrometer (Kratos MS-50) coupled with a MASPEC data system. All of these data were taken at the University of British Columbia. The other details are reported in 2.6.1.

3.6.2 UV-Vis Studies

UV-Vis studies (~10^{-5} M in H_2O-CH_3CN, pH 7 and pH1) were carried out in 3.0 mL quartz cuvette. Details are reported in Section 2.6.2.

3.6.3 Product Studies

Compounds were photolyzed in 100 mL quartz tubes using a Rayonet RPR 100 photochemical reactor equipped with 300 nm or 350 nm lamps. Typically, a solution of the compound (10^{-4}-10^{-5} M, H_2O-CH_3CN (1:1 or 1:3), pH7 or 1) was bubbled with argon for 15 min and then irradiated under argon purge. The irradiated solution was extracted by 3 × 50 mL CH_2Cl_2 in air and the collected organic extracts was dried over anhydrous $MgSO_4$. The solvent was removed under reduced pressure and the photolysate analyzed by NMR, MS and IR.

In order to monitor the initially formed redox product, photolyses were carried out in NMR tubes which allowed characterization of the first formed redox products. NMR tubes were filled with 1 mL of the appropriate solution (10^{-3} M, 10% D_2O-CD_3CN). Solutions were bubbled using a fine needle through rubber stoppers with argon for 15 min before irradiation then irradiated with 300 nm or 350 nm lamps.

3.6.4 Quantum Yield Measurements

Quantum yields were measured using NMR and the reaction of 2-(hydroxymethyl)anthraquinone (**HMAQ**) as a secondary actinometer ($\Phi = 0.8$).[62] A solution of the compound (**3.1-3.4**, 10^{-4} M, in H_2O-CH_3CN (1:1 or 1:3), pH 7 or 1) was purged with argon for 15 min and irradiated for 1 min at 300 nm (2 lamps) under argon purge. After irradiation, the conversion to product was determined by ^{1}H NMR and compared to an identical run using **HMAQ**. All conversions were kept below 30% and repeated twice.

3.6.5 Nanosecond Laser Flash Photolysis Studies of HMAQ

LFP studies were conducted at the University of Victoria LFP facility employing a Spectra Physics Quanta-Ray YAG laser, model GSR-11, with a pulse width of ~ 10 ns

and excitation wavelength 266 nm. Quartz flow cells were used and solutions were purged with nitrogen or oxygen for 20 min prior to measurement. Optical densities at 266 nm were ~ 0.6.

3.6.6 Syntheses of 3.1-3.4

Methylphenyl boronic acids

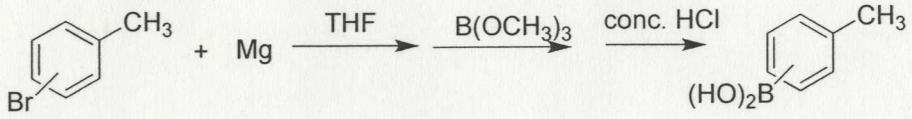

Bromotoluene (ortho, meta and para) (0.3, 1.8mmol) in 20 mL of THF was added dropwise into THF solution with Mg under N_2 at room temperature and the mixture was stirred for 2 hours. After the reaction, the Grignard solution under N_2 was transferred into a solution of $B(OCH_3)_3$ at -30°C in 0.5 hour. After the addition, the solution was warmed up and stirred overnight at room temperature to give a white paste. The solution was washed with conc. HCl to give white precipitates. The precipitates were recrystallized by water to give methyl phenyl boronic acid (white needle crystals, 70-80% yield). ^{1}H NMR ($CDCl_3$, 300 MHz) (*o*-methylphenyl)boronic acid: δ 8.20 (d, H, J = 8.1 Hz), 7.42-7.30 (m, H),7.35-7.25 (m, 2H), 2.81 (s, 3H); (*m*-methylphenyl)boronic acid: δ 8.06-8.01 (m, 2H), 7.42-7.38 (m, 2H), 2.47 (s, 3H); (*p*-methylphenyl)boronic acid: δ 8.11 (d, 2H, J = 8.1 Hz), 7.30 (d, 2H, J = 8.1 Hz), 2.43 (s, 3H).

Preparation of **3.5**

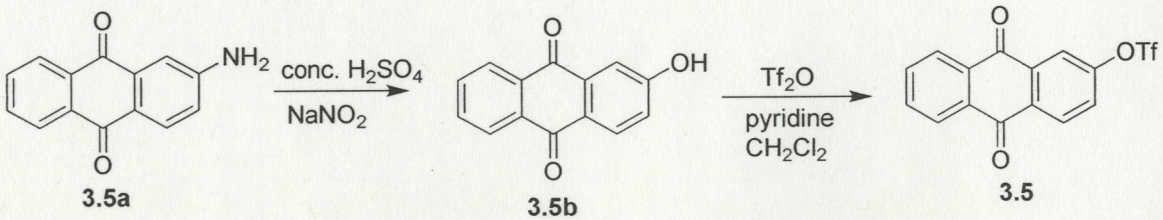

3.5a **3.5b** **3.5**

$NaNO_2$ (0.56 g, 8.1 mmol) was added in three portions into a solution of **3.5a** (1.5g, 6.8 mmol) in conc. H_2SO_4 (15 mL) cooled in an ice bath. After the addition, the mixture was stirred in the ice bath for 10 min and warmed up to room temperature and stirred for 4 hours. The mixture was poured onto 100 mL of ice and transferred to 500 mL flask and refluxed for 45 min. After cooling, the brown solid was filtered, washed with water and dissolved in 10 mL of 1 M NaOH. The dark red solution was washed 3 × 25mL CH_2Cl_2. The combined aqueous layers was acidified with conc. HCl and extracted with 5 × 25 mL EtOAc, dried over anhydrous $MgSO_4$. A yellow brown powder **3.5b** (1.1 g, 70% yield) was obtained after removal of solvent. ^{1}H NMR ($CDCl_3$, 300 MHz) δ 8.30-8.24 (m, 2H), 8.21 (d, 1H, J = 8.5 Hz), 7.94-7.88 (m, 2 H), 7.67 (d, 1H, J = 2.6 Hz), 7.34 (dd, 1H, J = 2.6 Hz, 8.5 Hz).

A solution of **3.5b** (0.90, 4.0 mmol) in 50 mL of CH_2Cl_2 in a cold water bath was flushed with N_2. Pyridine (1.95 mL, 24.1 mmol) was added dropwise into the above solution, then Tf_2O (2.0 mL, 12 mmol) was added. After the addition, the mixture was warmed up to room temperature and stirred for overnight. After the reaction, the solvent was removed and the residue was washed with 2 × 25 mL water. The combined aqueous solutions were extracted with 2 × 25 mL EtOAc. The collected organic layers were dried over anhydrous $MgSO_4$. After removal of solvent, a brown powder was purified by column chromatography with silica gel using CH_2Cl_2 as an eluent, to give **3.5** (white powder, 1.4 g) in 98% yield. ^{1}H NMR ($CDCl_3$, 300 MHz) δ 8.44 (d, 1H, J = 8.8 Hz), 8.36-8.29 (m, 2H), 8.18 (d, 1H, J = 2.2 Hz), 7.87-7.80 (m, 2H), 7.67 (dd, 1H, J = 8.8, 2.2 Hz).

2-(*o*-Hydroxymethylphenyl)-9,10-anthraquinone (**3.1**)

A mixture of (*o*-methylphenyl)boronic acid (0.50 g, 2.4 mmol), **3.5** (0.27 g, 2 mmol), anhydrous K_2CO_3 (1.93g, 14 mmol) and $Pd(PPh_3)_4$ (100 mg) was added into a 100 mL flask contained 60 mL of DME saturated with N_2. The mixture was refluxed for 3 days under N_2. After the reaction, solvent was removed and the residue was dissolved in 100 mL CH_2Cl_2 and washed with 2 × 25 mL of 1 M NaOH. The solution was dried over anhydrous $MgSO_4$. After removal of solvent, a brown powder was purified by column chromatography with silica gel using CH_2Cl_2 as an eluent, to give 2-(*o*-methylphenyl)-9,10-anthraquinone (**3.1a**) (yellow powder, 0.41 g, mp. 160-161°C) in 70% yield. ^1H NMR ($CDCl_3$, 300 MHz) δ 8.39-8.24 (m, 4H), 7.84-7.71 (m, 3H), 7.34-7.25 (m, 4H), 2.31 (s, 3H); ^{13}C ($CDCl_3$, 75 MHz) 183.44, 183.20, 148.41, 140.11, 135.38, 135.12, 134.38, 134.31, 133.84 (2C), 133.55, 132.19, 130.96, 129.73, 128.64, 128.08, 127.52, 127.46, 127.44, 126.38, 20.64; IR (neat from CH_2Cl_2 solution, NaCl plates) *v* 3054, 1673, 1588, 1327, 1289, 930, 707 cm^{-1}.

A mixture of **3.1a** (0.30 g, 1.0 mmol) and NBS (0.21 g, 1.2 mmol) in benzene (30 mL) was refluxed for overnight under N_2. After the reaction, the solution was washed with 2 × 25 mL water and the collected organic layer was dried over anhydrous $MgSO_4$. After the removal of solvent, a brown residue (**3.1b**) was obtained. The brown residue and Na_2CO_3 (0.42 g, 5.0 mmol) in 1:1 H_2O-dioxane were refluxed for overnight under N_2. After the reaction, the mixture was acidized by 10 mL of 1 M HCl and extracted with 2 × 25 mL CH_2Cl_2. The collected extracts were dried over anhydrous $MgSO_4$ and evaporated to give brown powders. The crude product was purified by column chromatography with silica gel using 20% EtOAc-CH_2Cl_2 as an eluent to give yellow powder. The yellow powder was further purified with recrystallization from CH_3CH_2OH to give 2-(*o*-

hydroxymethylphenyl)-9,10-anthraquinone (**3.1**) (yellow needle crystals, 0.22 g, mp.184-185°C) in 70% yield. ^{1}H NMR ($CDCl_3$, 500 MHz) δ 8.36 (d, 1H, J = 7.7 Hz), 8.34-8.30 (m, 3H), 7.85 (dd, 1H, J = 7.7, 1.8 Hz), 7.83-7.78 (m, 2H), 7.60 (d, 1H, J = 7.0 Hz), 7.46 (td, 1H, J = 7.5, 1.5 Hz), 7.41 (td, 1H, J = 7.5, 1.5 Hz), 7.34 (dd, 1H, J = 7.5, 1.5 Hz), 4.63 (s, 2H), 1.63 (s, broad OH peak); ^{13}C NMR ($CDCl_3$, 125 MHz) 183.39, 183.16, 147.16, 139.74, 138.08, 135.12, 134.45, 134.38, 133.84 (2C), 133.63, 132.53, 130.11, 129.22, 129.10, 128.35, 128.05, 127.63, 127.52, 127.50, 63.24; IR (neat from CH_2Cl_2 solution, NaCl plates) v 3384, 3060, 2884, 1673, 1588, 1330, 1294, 707 cm^{-1}; MS (EI) m/z 314 (M^+, 100), 297 (28), 283 (19); HRMS, calculated for $C_{21}H_{14}O_3$ 314.09429; observed 314.09436.

2-(*m*-Hydroxymethylphenyl)-9,10-anthraquinone (**3.2**)

By following the same synthetic procedure of **3.1**, 2-(*m*-methylphenyl)-9,10-anthraquinone (**3.2a**) (yellow powder, 0.30g, m.p. 137-138°C) in 70% yield was obtained. ^{1}H NMR ($CDCl_3$, 300 MHz) δ 8.47 (d, 1H, J = 1.5 Hz), 8.34-8.25 (m, 3H), 7.97 (dd, 1H, J = 8.1, 1.5 Hz), 7.81-7.73 (m, 2H), 7.49 (d, 2H, J = 8.1 Hz), 7.36 (t, 1H, J = 8.1 Hz), 7.22 (d, 1H, J = 8.1 Hz), 2.43 (s, 3H); ^{13}C NMR ($CDCl_3$, 75 MHz) 183.43, 183.06, 147.15, 139.05 (2C), 134.35, 134.22, 134.02, 133.84, 133.80, 132.54, 132.25, 129.84, 129.24, 128.25, 128.18, 127.47, 127.40, 125.72, 124.62, 21.74; IR (neat from CH_2Cl_2 solution, NaCl plates) v 3060, 3027, 2912, 1670, 1588, 1330, 1278, 932, 770, 707 cm^{-1}.

2-(*m*-Hydroxymethylphenyl)-9,10-anthraquinone (**3.2**) (yellow plate, 0.20 g, mp.158-161°C) in 80% yield was obtained via bromination of **3.2a** followed with hydrolysis of **3.2b**. ^{1}H NMR ($CDCl_3$, 500 MHz) δ 8.53 (d, 1H, J = 2.0 Hz), 8.37 (d, 1H, J = 8.1 Hz), 8.34-8.31 (m, 2H), 8.01 (dd, 1H, J = 8.1, 2.0 Hz), 7.83-7.79 (m, 2H), 7.73 (t, 1H, J = 1.8

Hz), 7.65 (dt, 1H, J = 7.7, 1.8 Hz), 7.50 (t, 1H, J = 7.7 Hz), 7.44 (d, 1H, J = 7.7 Hz), 4.81(s, 1H), 1.59 (s, broad OH peak); ^{13}C NMR ($CDCl_3$, 125 MHz) 183.46, 183.12, 146.90, 142.12, 139.53, 134.44, 134.31, 134.16, 133.90, 133.86, 132.64, 132.49, 129.62, 128.31, 127.59, 127.54, 127.47, 126.83, 126.07, 125.84, 65.37; IR (neat from CH_2Cl_2 solution, NaCl plates) v 3307, 3017, 2912, 2862, 1670, 1588, 1333, 1281, 707 cm^{-1}; MS (EI) m/z 314 (M^+, 100), 285 (67), 283 (18), 208 (11); HRMS, calculated for $C_{21}H_{14}O_3$ 314.09429; observed 314.09421.

2-(p-Hydroxymethylphenyl)anthraquinone (**3.3**)

By following the same synthetic procedure of **3.1**, 2-(p-methylphenyl)-9,10-anthraquinone (**3.3a**) (yellow powder, 0.50g, m.p. 166-167°C) in 75% yield was obtained. ^{1}H NMR ($CDCl_3$, 300 MHz) δ 8.47 (d, 1H, J = 1.5 Hz), 8.34-8.25 (m, 3H), 7.97 (dd, 1H, J = 8.1, 1.5 Hz), 7.81-7.73 (m, 2H), 7.59 (d, 2H, J = 8.1 Hz), 7.28 (d, 1H, J = 8.1 Hz), 2.40 (s, 3H); ^{13}C NMR ($CDCl_3$, 125 MHz) 183.47, 183.06, 146.95, 139.21, 136.18, 134.34, 134.20, 133.85, 133.82, 132.26, 132.08, 130.07 (2C), 128.22, 127.46, 127.39, 127.35 (2C), 125.42, 21.45; IR (neat from CH_2Cl_2 solution, NaCl plates) v 3021, 2917, 1673, 1588, 1330, 1275, 812, 707 cm^{-1}.

2-(p-hydroxymethylphenyl)-9,10-anthraquinone (**3.3**) (yellow needle, 0.30 g, mp.199-201°C) in 70% yield was obtained via bromination of **3.3a** followed with hydrolysis of **3.3b**. ^{1}H NMR (300MHz, $CDCl_3$) δ 8.54 (d, 1H, J = 2.0 Hz), 8.37 (d, 1H, J = 8.1 Hz), 8.35-8.31 (m, 2H), 8.01 (dd, 1H, J = 8.1, 2.0 Hz), 7.83-7.79 (m, 2H), 7.73 (d, 2H, J = 8.1 Hz), 7.51 (d, 2H, J = 8.1 Hz), 4.78 (s, 1H), 1.72 (s, broad OH peak); ^{13}C NMR ($CDCl_3$, 125 MHz) 183.48, 183.12, 146.74, 141.90, 138.52, 134.44, 134.31, 134.18, 133.91, 133.87, 132.53, 132.43, 128.33, 127.86 (2C), 127.76 (2C), 127.54, 127.48, 125.73, 65.13; IR (neat from CH_2Cl_2 solution, NaCl plates) v 3247, 3057, 2906, 2846, 1673, 1591, 1330,

1303, 820, 707 cm^{-1}; MS (EI) *m/z* 314 (M^+, 100), 318 (M^+, 60), 298 (16), 285 (79), 283 (16); HRMS, calculated for 314.09429; observed 314.09441.

Bromobiphenyl **3.6**

A mixture of (*p*-methylphenyl)boronic acid (0.80 g, 5.9 mmol), *p*-bromoiodobenzene (8.4 g, 30 mmol), anhydrous K_2CO_3 (1.64g, 11.9 mmol) and $Pd(PPh_3)_4$ (0.69 g, 0.59 mmol) in 50 mL of DME was refluxed for 20 h under N_2. After the reaction, black solids were removed by filtration through Celite and rinsed by CH_2Cl_2. After removal of solvent, white plate crystals were obtained and purified by column chromatography with silica gel using neat hexane as an eluent to give **3.6** (white powder, 0.62 g) in 42 % yield. ^{1}H-NMR (300MHz, $CDCl_3$) δ 7.53 (d, 2H, J = 8.5 Hz), 48-7.38 (m, 4H), 7.24 (d, 2H, J = 8.0 Hz).

Boronic acid **3.7**

A solution of **3.6** (0.50 g, 2.0 mmol) in 10 mL of THF (water and oxygen free) was added dropwise into the solution of THF with Mg under N_2. The mixture was refluxed for 1 h. After cooling, the Gringard reagent under N_2 was transferred into the solution of trimethyl borate in 10 mL of THF at -78°C. After the addition, the mixture was warmed up to room temperature and stirred for overnight to give a white paste. The white paste was poured into 20 mL of cold water and acidified to pH 2 with 0.1 M H_2SO_4. The solution was extracted by 2 × 30 mL of ethyl ether and collected organic solution was dried over $MgSO_4$. After the removal of solvent, a white powder was obtained. Further purification was operated with column chromotagraphy on silica gel using 20% EtOAc-CH_2Cl_2 to give a white powder (**3.7**, 0.20 g, 47% yield). ^{1}H-NMR (250 MHz, $CDCl_3$) δ

8.31 (d, 2H, J = 8.0 Hz), 7.73 (d, 2H, J = 8.0 Hz), 7.58 (d, 2H, J = 8.0 Hz), 7.29 (d, 2H, J = 8.0 Hz).

2-(*p*-Methylbiphenyl)-9,10-anthraquinone (**3.4a**)

By following the same synthetic procedure of **3.1a**, 2-(*p*-methylbiphenyl)-9,10-anthraquinone (**3.4a**) (0.12 g, 83%, yellow powder, mp. 235~236°C) was obtained. ^{1}H-NMR (500 MHz, $CDCl_3$) δ 8.58 (d, 1H, J = 1.8 Hz), 8.38 (d, 1H, J = 8.0 Hz), 8.35-8.31 (m, 2H), 8.05 (dd, 1H, J = 1.8, 8.0 Hz), 7.82-7.78 (m, 4H), 7.72 (td, 2H, J = 1.8, 8.5 Hz), 7.50 (td, 2H, J = 1.8, 8.0 Hz), 7.27 (d, 2H, J = 8.0 Hz), 2.40 (s, 3H); ^{13}C-NMR ($CDCl_3$, 125 MHz) 183.49, 183.10, 146.65, 141.94, 137.86, 137.65, 137.54, 134.41, 134.27, 134.19, 133.92, 133.87, 132.36 (2C), 129.87 (2C), 128.33, 127.90 (2C), 127.83 (2C), 127.52, 127.46, 127.15 (2C), 125.58, 21.37; IR (neat from CH_2Cl_2 solution, NaCl plates) v 3025, 2915, 1668, 1588, 806, 705 cm^{-1}.

2- (*p*-Hydroxymethylbiphenyl)-9,10-anthraquinone (**3.4**)

2- (*p*-Hydroxymethylbiphenyl)-9,10-anthraquinone (**3.4**) was obtained by bromonation of **3.4a** followed by the hydrolysis of **3.4b** in 74% yield (**3.4**, 0.10 g, yellow powder, decomposed at 224°C) ^{1}H-NMR (300 MHz, $CDCl_3$) δ 8.54 (d, 1H, J = 1.8 Hz), 8.34 (d, 1H, J = 8.1 Hz), 8.32-8.26 (m, 2H), 8.01 (dd, 1H, J = 1.8, 8.1 Hz), 7.80-7.73 (m, 4H), 7.68 (td, 2H, J = 1.8, 8.5 Hz), 7.61 (td, 2H, J = 1.8, 8.2 Hz), 7.42 (d, 2H, J = 8.2 Hz), 4.71 (s, 2H); ^{13}C-NMR ($CDCl_3$, 125 MHz) 183.50, 183.11, 146.56, 141.60, 140.66, 139.86, 138.06, 134.45, 134.31, 134.22, 133.93, 133.87, 132.44, 132.41, 128.37, 128.00 (2C), 128.99 (2C), 127.80 (2C), 127.54, 127.52, 127.48 (2C), 125.64, 65.31; IR (neat from CH_2Cl_2 solution, NaCl plates) v 3164, 2917, 2851, 1670, 1588, 1327, 1303, 803,

707 cm^{-1}; MS (EI) *m/z* 390 (M^+, 100), 374 (M^+, 25), 273 (12), 361 (25); HRMS, calculated for 390.12339; observed 390.12528.

3.6.7 Photolysis Procedures for 3.1-3.4 and Characterization of Products

All photolyses were carried out in H_2O-CH_3CN (pH 1) under argon purged. After the photolysis, solutions were neutralized by 5% $NaHCO_3$ solution and were extracted by 3 × 25 mL CH_2Cl_2 in air. The combined organic solutions were dried over anhydrous $MgSO_4$ and solvent was removed by reduced evaporation. Crude products were purified by prep. TLC (silica gel).

Photolysis of **3.1**

Compound **3.1** (5 mg in 50 mL CH_3CN and 50 mL H_2O, pH 1) was irradiated for 1 min at 300 nm (2 lamps) under argon, to give a yellow solution. After work-up in air, the brown residue was characterized by ^1H NMR to give **3.8** (45% yield). Further purification was obtained by prep. TLC (silica gel, CH_2Cl_2) to give **3.8** (yellow powder, 2 mg), ^1H NMR ($CDCl_3$, 300 MHz) δ 9.94 (s, 1H), 8.36 (d, 1H, J = 7.9 Hz), 8.32-8.26 (m, 3H), 8.02 (dd, 1H, J = 1.5, 7.6 Hz), 7.80-7.71 (m, 3H), 7.66 (dt, 1H, J = 1.5, 7.6 Hz), 7.54 (mt, 1H, J = 7.6 Hz), 7.44 (dd, 1H, J = 1.1, 7.6 Hz); ^{13}C-NMR ($CDCl_3$, 125 MHz) 191.14, 182.76, 182.61, 144.08, 143.28, 135.32, 134.36, 133.37, 133.36, 133.27, 132.65, 130.68, 128.94, 128.68, 128.19, 127.34, 127.17, 127.15, 116.55; IR (neat from CH_2Cl_2 solution, NaCl plates) *v* 3053, 1690, 1676, 1591, 1330, 1292, 705 cm^{-1}; MS (EI) *m/z* 312 (M^+, 100), 283 (23); HRMS, calculated for $C_{21}H_{12}O_3$ 312.07864; observed 312.07874.

Photolysis of **3.2**

Compound **3.2** (6 mg in 50 mL of CH_3CN and 50 mL of H_2O, pH 1) was irradiated for 1 min at 300 nm (2 lamps) under argon, to give a yellow solution. After work-up in air,

the brown residue was characterized by ^{1}H NMR to give **3.9** (22% yield). Further purification was obtained by prep. TLC (silica gel, CH_2Cl_2) to give **3.9** (yellow powder, 1 mg), ^{1}H NMR ($CDCl_3$, 300 MHz) δ 10.07 (s, 1H), 8.52 (d, 1H, J = 1.8 Hz), 8.37 (d, 1H, J = 8.2 Hz), 8.33-8.25 (m, 2H), 8.18 (t, 1H, J = 1.8 Hz), 8.00 (dd, 1H, J = 2.0, 8.2 Hz), 7.97-7.88 (m, 2H), 7.81-7.73 (m, 2H), 7.64 (t, 1H, J = 7.6 Hz); ^{13}C-NMR ($CDCl_3$, 75 MHz) 191.79, 182.88, 182.71, 145.25, 139.98, 137.17, 134.30, 134.18, 134.04, 133.57, 133.52, 133.06, 132.69, 132.36, 130.02, 129.92, 128.26 (2C), 127.35, 127.29, 125.65; IR (neat from CH_2Cl_2 solution, NaCl plates) v 3060, 1700, 1673, 1591, 1327, 705 cm^{-1}; MS (EI) m/z 312 (M^+, 100), 283 (18); HRMS, calculated for $C_{21}H_{12}O_3$ 312.07864; observed 312.07866.

Photolysis of **3.3**

Compound **3.3** (5 mg in 50 mL CH_3CN and 50 mL H_2O, pH 1) was irradiated for 1 min at 300 nm (2 lamps) under argon, to give a yellow solution. After work-up in air, the brown residue was characterized by ^{1}H NMR to give **3.10** (45% yield). Further purification was obtained by prep. TLC (silica gel, CH_2Cl_2) to give **3.10** (yellow powder, 2 mg), ^{1}H NMR ($CDCl_3$, 300 MHz) δ 10.04 (s, 1H), 8.52 (d, 1H, J = 1.8 Hz), 8.37 (d, 1H, J = 8.2 Hz), 8.32-8.25 (m, 2H), 8.03-7.94 (m, 3H), 7.83 (td, 2H, J = 1.8, 8.2 Hz), 7.80-7.73 (m, 2H); ^{13}C-NMR ($CDCl_3$, 75 MHz) 191.60, 182.92, 182.68, 145.24, 144.70, 136.26, 134.34, 134.23, 134.00, 133.55, 133.50, 132.92, 132.55, 130.43 (2C), 128.22, 128.00 (2C), 127.35, 127.30, 125.96; IR (neat from CH_2Cl_2 solution, NaCl plates) v 3049, 1700, 1673, 1591, 1333, 1278, 707 cm^{-1}; MS (EI) m/z 312 (M^+, 100), 283 (28); HRMS, calculated for $C_{21}H_{12}O_3$ 312.07864; observed 312.07854.

Photolysis of **3.4**

Compound **3.4** (6 mg in 50 mL CH_3CN and 50 mL H_2O, pH 1) was irradiated for 1 min at 300 nm (16 lamps) under argon, to give a yellow solution. After work-up in air, the brown residue was characterized by ^1H NMR to give **3.14** (23% yield). Further purification was obtained by prep. TLC (silica gel, CH_2Cl_2) to give **3.14** (yellow powder, 1 mg), ^1H NMR ($CDCl_3$, 500 MHz) δ 10.06 (s, 1H), 8.59 (d, 1H, J = 1.8 Hz), 8.40 (d, 1H, J = 8.1 Hz), 8.36-8.32 (m, 2H), 8.07 (dd, 1H, J = 1.8, 8.1 Hz), 7.98 (td, 2H, J = 1.8, 8.4 Hz), 7.85 (td, 2H, J = 1.8, 8.4 Hz), 7.83-7.80 (m, 4H), 7.79 (td, 2H, J = 1.8, 8.4 Hz); ^{13}C-NMR ($CDCl_3$, 125 MHz) 192.05, 183.44, 183.06, 146.39, 146.18, 140.39, 139.22, 135.75, 134.51, 134.37, 134.24, 133.88, 133.83, 132.64, 132.47, 130.61, 128.42, 128.33, 128.19, 127.90, 127.56, 127.51, 125.75; IR (neat from CH_2Cl_2 solution, NaCl plates) v 3023, 1673, 1591, 1330, 809, 705 cm^{-1}; MS (EI) *m/z* 388 (M^+, 100), 359 (9); HRMS, calculated for $C_{27}H_{16}O_3$ 388.10994; observed 388.11046.

3.6.8 Trapping of Photolysis Product of 3.1

Photolysis of **3.1** (20 mg, 1:1 H_2O-CH_3CN, pH 1) was carried out in a 100 mL quartz tube under argon to give a yellow photoredox product **3.11**. Under Ar, NaOH (solid, 2 g) were added into the above solution to give a dark red solution which was converted to yellow solution with the addition of Ac_2O (2 mL). After the addition, the solution was extracted with 2 × 25 mL CH_2Cl_2 and the collected organic layer was dried over anhydrous $MgSO_4$. After the removal of solvent, a brown residue was obtained. The brown residue was purified by prep. TLC by neat CH_2Cl_2 as an eluent to give **3.11-OAc** (10 mg, light red) ^1H NMR ($CDCl_3$, 300 MHz) δ 9.98 (s, 1H), 8.02 (dd, 1H, J = 1.5, 8.0Hz), 7.99 (d, 1H, J = 0.5, 9.0 Hz), 7.96-7.87 (m, 2H), 7.80 (s, 1H), 7.93 (td, 1H, J = 1.5, 8.0 Hz), 7.55-7.46 (m, 5H), 2.60 (s, 3H), 2.53 (s, 3H); ^{13}C-NMR ($CDCl_3$, 125 MHz)

192.31, 169.65 (2C), 145.35, 140.97, 140.69, 135.88, 134.35, 133.89, 131.19, 128.55, 128.50, 128.18, 127.09 (2C), 125.06, 124.89, 123.87, 123.53, 123.43, 122.60, 122.05 (2C), 21.00, 20.95; MS (EI) *m/z* 398 (M^+, 7), 356 (27), 314 (100); HRMS, calculated for $C_{25}H_{18}O_5$ 398.11542; observed 398.11570.

3.6.9 Concentration Effects on Photolysis Conversions of 3.1

Photolysis of **3.1** (10^{-7}~10^{-5} M, 1:1 H_2O-CH_3CN, pH 1, argon saturated) was carried out in a 3 mL quartz cuvette and the absorption intensity of product **3.11** at 387 nm was determined with UV-Vis spectroscopy. The rates at different concentrations were determined by taking the slope of the plot of absorbance *vs* time (0~20s). The rate constant was obtained by taking the slope of the plot of rates *vs* concentration. The experimental results showed the rates were reasonably linear with respect to concentrations of **3.1** and the rate constant 1.6×10^{-3} $L \cdot mol^{-1} \cdot s^{-1}$.

3.6.10 pH Effects on Photolysis Efficiency of 3.1-3.4

Solutions of **3.1-3.4** (1 mg 1:1 H_2O-CH_3CN, pH from 0 to 7) in a 100 mL large quartz tube were purged with Ar for 15 minutes prior to photolysis and were irradiated (300 nm, 2 lamps for 1 min (**3.1-3.3**) and 8 lampls for 1 min (**3.4**). After work-up (followed the same procedure as shown in Section 3.6.7), the photolysis yields (%) were determined with proton NMR.

3.6.11 Quenching of Triplet 3.1-3.3

A mixture of **3.1** (10^{-4} M) and sorbic acid (0.001 M) in 1:1 H_2O-CH_3CN (pH 1) in a 100 mL large quartz tube was purged with Ar for 15 minutes prior to photolysis and were irradiated (300 nm, 2 lamps) for 1 min. After work-up in air (followed the same procedure as shown in Section 3.6.7), a brown residue was characterized by ^1H NMR to

give **3.8** in 22 % conversion yield. Following the above procedure, photolysis of **3.1** (10^{-4} M) and sorbic acid (0-0.01 M) in 1:1 H_2O-CH_3CN (pH 1) were carried out to give **3.8** in 12-36% yield. The same procedure was employed for **3.2** and **3.3**.

Following the above irradiation procedure and the work-up procedure as shown in Section 3.6.7, photolysis of **3.1** in oxygen saturated solution (1:1 H_2O-CH_3CN, pH 1) gave **3.8** in 26% yield. The same procedure was employed for **3.2** and **3.3**.

4. A Pentacene Intermediate via Intramolecular Photoredox of a 6,13-Pentacenequinone in Aqueous Solution*

4.1 Introduction

Pentacene is a promising candidate for application as a novel organic semiconductor.[95] However, it is highly sensitive to both oxygen and light, and has low solubility. To overcome these disadvantages, considerable efforts have been directed at synthesizing new pentacene derivatives.[96] Among them, pentacenequinone derivatives have been employed as synthetic precusors due to their stability and ready accessibility. Recently, photochemical methods based on extrusion of molecular fragments for the synthesis of pentacenes have also been reported.[97,98]

Chapter 2 has shown that anthraquinone derivatives undergo a very efficient intramolcular photoredox in neutral aqueous solution to give the corresponding photoredox products with high quantum yields. Chapter 3 showed that phenyl or biphenyl anthraquinones in which the benzyl alcohol moiety is much further away from the carbonyl group also undergo the same photoredox reaction, but require pH < 3. We anticipated that 2-(hydroxymethyl)-6,13-pentacenequinone (**4.1**) might undergo the photoredox reaction as well, which would give rise to the corresponding dihydroxypentacene aldehyde. Thus, we might have a new photochemical method involving an intramolecular redox process to prepare a pentacene intermediate from **4.1**.

In addition, both Chapter 2 and Chapter 3 presented photoredox reactions that involve electronic communication between the benzyl alcohol moiety and the anthraquione carbonyl group in the excited state via the π conjugated system. In particular, the

---

* Y. Hou and P. Wan, A Pentancene Intermediate via Formal Intramolecular Photoredox of a 6,13-Pentacenequinone in Aqueous Solution, *Can. J. Chem.*, **2007**, 85, 1023-1032.

tendency for electronically excited phenyl and biphenyl anthraquinones (Chapter 3) to be more planar results in strong electronic communication. The same reaction would not occur in the corresponding ground state. Note that the anthraquinone moiety of **HMAQ** has one benzene ring on each side of the central quinone. The structure is symmetric. Thus, we would not know whether or not the benzene ring on the side without the attached hydroxymethyl group would have any effect on the electronic communication. In order to further study the electronic communication via π conjugation, a good way of increasing or decreasing π system conjugation is to add or remove benzene rings to the anthraquinone moiety. Thus, pentacenequinone **4.1** and associated acenequinones **4.2-4.4** were synthesized (Chart 4.1) and their potential photoredox chemistry explored in this chapter.

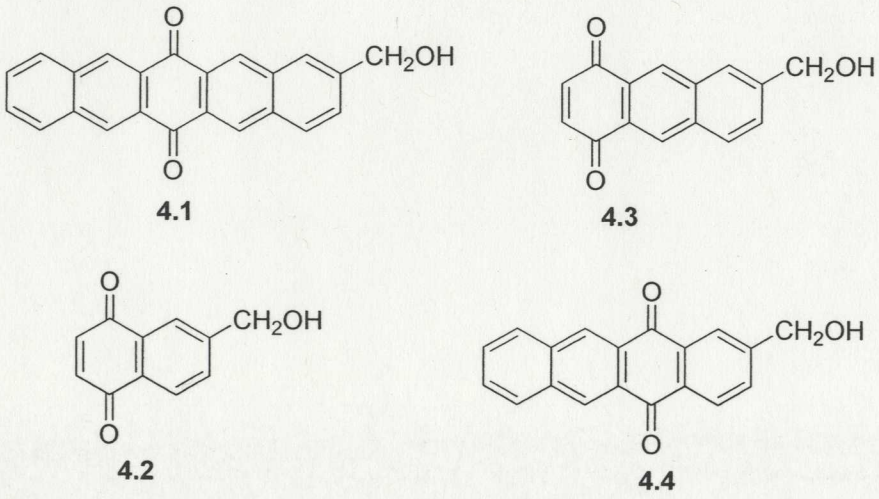

Chart 4.1

4.2 Synthesis

Acenequinones **4.1** and **4.4** were readily prepared via the condensation (*in situ* Diels-Alder reaction) of the corresponding acenequinones **4.3** and **4.2**, respectively, with α,α,α',α'-tetrabromo-*o*-xylene (Scheme 4.1). The reaction proceeds via initial

debromination of the tetrabromide, to generate the diene, which reacts with **4.2** and **4.3** via Diels-Alder reaction. This is subsequently followed by another debromination step to regenerate the aromatic system, and hence **4.1** or **4.4**. Acenequinones **4.2** and **4.3** are known compounds and were prepared by following or adapting the corresponding literature methods.[99,100] Methylpentacenequinone **4.1a** was also studied to test the requirement of a hydroxymethyl (alcohol) moiety in the anticipated photoredox chemistry. It was made using the same reaction shown in Scheme 4.1, starting with methylnaphthoquinone **4.3a**.

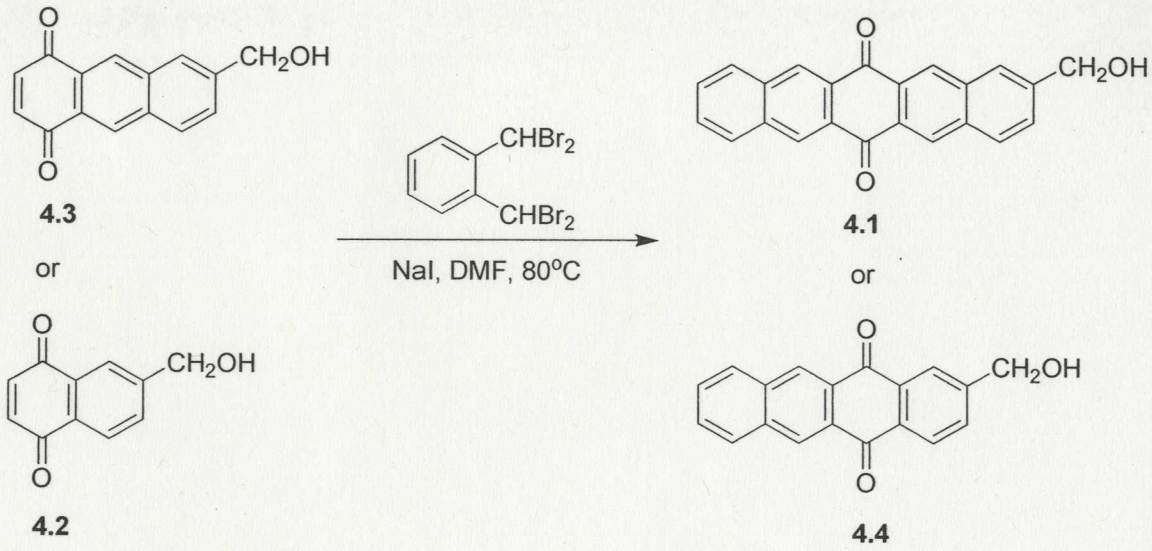

Scheme 4.1 Syntheses of acenequinones **4.1** and **4.4**

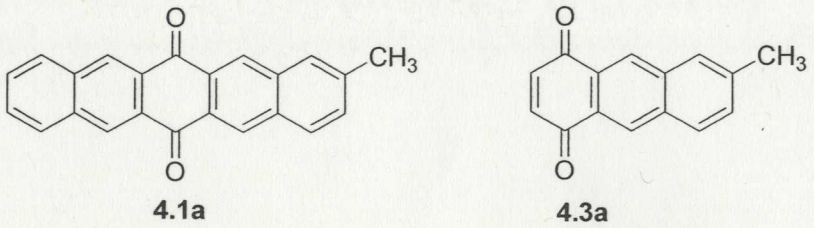

4.3 Product Studies

4.3.1 Photoredox Chemistry of 4.1

Pentacenequinone **4.1** was the first compound studied in this chapter not only because it is the synthetic precursor of pentacene introduced in Section 4.1, but also because it has a unique structure. Pentacenequinone **4.1** has one more benzene ring on the each side of the central quinone than **HMAQ**. This keeps the same symmetric structure on the acenequinone moiety as for **HMAQ**. However, this increases the distance between the benzyl alcohol moiety and the quinone carbonyl group. This might have an effect on electronic communication on the excited state of **4.1** and hence photoredox efficiency.

As already shown for reactions of many anthraquinone derivatives (Chapters 2 and 3), UV-Vis studies were particular informative of reaction since the photochemical transformation involves a substantial change in chromophore, going from an aromatic ketone/quinone to a dihydroxy-substituted polycyclic aromatic compound (anthracene). In the case of **HMAQ**, the initial photochemical product **DHA** is coloured orange. We anticipated that similar UV-Vis changes will take place on photoredox reaction of **4.1**. UV-Vis studies of **4.1** (10^{-6} to 10^{-5} M, 25% H_2O-CH_3CN, pH 1 and 7 (water portion), argon purged, 300 or 350 nm lamps, 3.0 mL quartz cuvette) were initially carried out. No changes were observed in neat CH_3CN or in pH 7, but dramatic changes were observed at pH 1 (Figure 4.1). Photolysis at this pH resulted in formation of an intense new absorption band at 318 nm and two additional (less intense) visible bands at 470 and 660 nm, the latter a very broad band covering 550-780 nm.

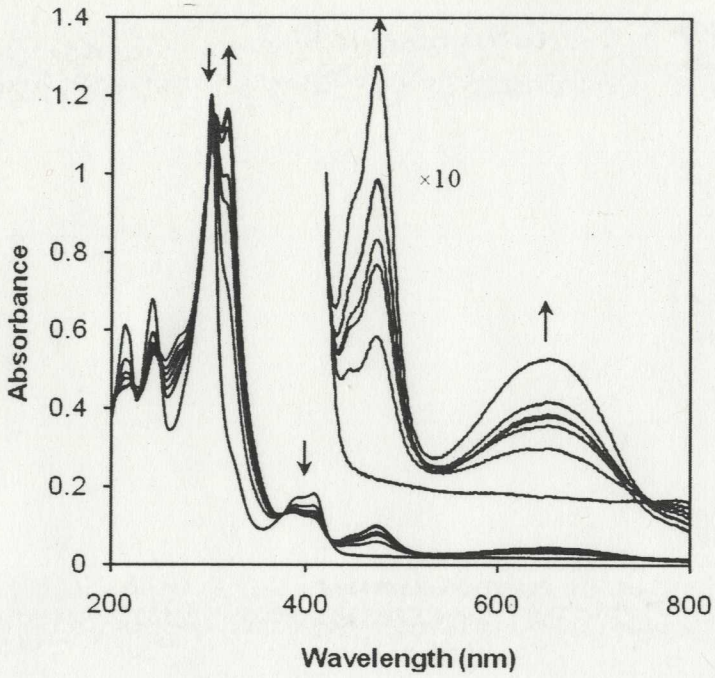

Figure 4.1 UV-Vis traces observed on photolysis of pentacenequinone **4.1** (25% H_2O-CH_3CN, pH 1, λ_{ex} 350 nm, argon purged). Each trace represents 10-20 s of photolysis except for the final trace (2 min). Photolysis resulted in the loss of absorption (due to photoreaction of **4.1**) at 302 and 407 nm with the formation of **4.5** (318, 473 and 657 nm).Inset: ten-fold expansion of the long wavelength region

Based on what is known for **HMAQ**, the same reaction for **4.1** would give rise to 6,13-dihydroxypentacene **4.5** (eqn. 4.1). Pentacenes are known to absorb strongly in the visible region, with longest wavelength band in the 500-700 nm, depending on substituents.[98a,100] The broad absorption at 660 nm is consistent with formation of a pentacene. These new absorption bands disappeared within 1 min of opening the cuvette to air or oxygen (Figure 4.2), and within 1 h when the cuvette was unopened. The resulting UV-Vis spectrum was identical to an authentic sample of pentacenequinone aldehyde **4.6**, which has a UV-Vis spectrum similar to that of **4.1**. This is consistent with a highly reactive dihydroxypentacene derivative that is readily air-oxidized to give **4.6**. 2-

Methyl-6,13-pentacenequinone (**4.1a**) was also studied, to test the requirement of a hydroxymethyl (alcohol) moiety in the anticipated photoredox chemistry. Notably, **4.1a**, although structurally very similar to **4.1**, did not show a reaction under the above conditions.

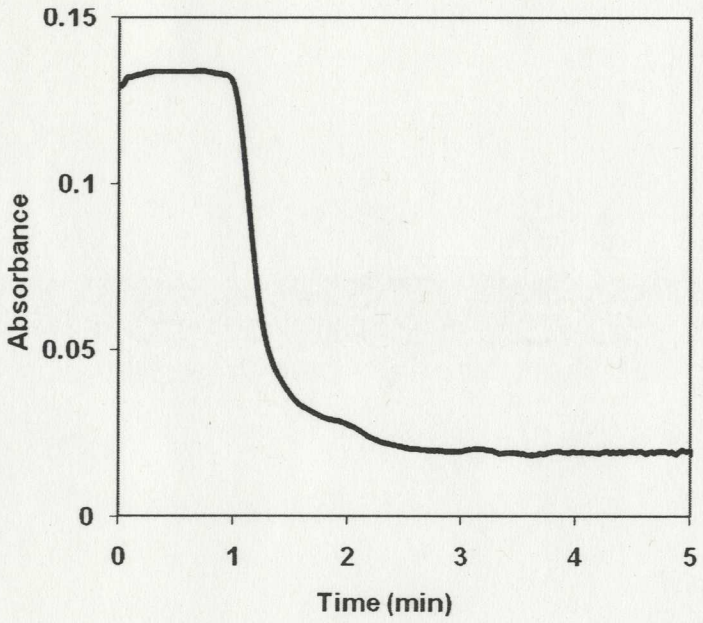

Figure 4.2 Decay of photogenerated dihydroxypentacene **4.5** (from pentacenequinone **4.1** in 25% H_2O-CH_3CN, pH 1) on exposure to air upon opening cuvette (time "0") monitored at 473 nm.

Semi-preparative photolysis of **4.1** (pale yellow) in 25% H_2O-CH_3CN (pH 1) gave a green to dark green solution depending on irradiation time indicative of photoredox chemistry. When left standing in the photolysis tube after irradiation with no precautions to prevent entry of air, the colour changed to a pale yellow within one hour, indicative of a reactive initial photoproduct. When the photolyzed solution was exposed to air after photolysis (pouring the solution into a flask exposed to air), the green colour disappeared immediately. In view of the reactive nature of the initially formed photoproduct no

attempts were made to isolate it in these runs. Instead, the solutions were exposed to air after photolysis and extracted with CH_2Cl_2. Work-up using this method gave exclusively 2-formyl-6,13-pentacenequinone (**4.6**) (yields 20-70 % by NMR, depending on photolysis time) (eqn. 4.1). No reaction was observed when photoyzed in pH 7 or in neat CH_3CN, consistent with the UV-Vis studies reported above. In addition, no reactions were observed without photolysis (in the presence or absence of oxygen). Using the photoredox reaction reported for **HMAQ** as a secondary actinometer (Φ = 0.8, pH 1), we estimated a quantum yield of photoredox for **4.1** (25% H_2O-CH_3CN, pH 1) to be about 0.2. Although pentacenequinone **4.1** is not as reactive as the parent anthraquinone system **HMAQ**, it nevertheless has substantial quantum yields of reaction at a suitable pH.

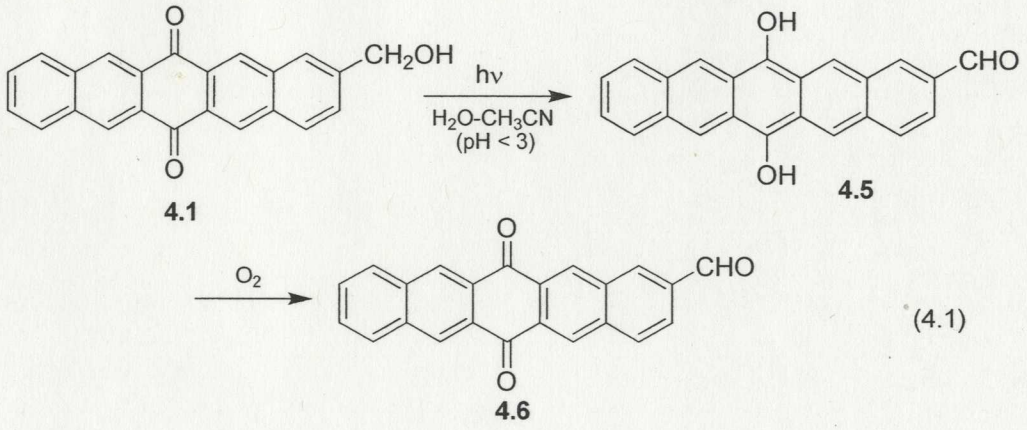

(4.1)

Photolysis of the closely related methylpentacenequinone **4.1a** under similar conditions as for **4.1** or even on extended photolysis did not give any reaction. The photolyzed solution did not develop any colour and upon work-up, the starting material was recovered unchanged. Thus, the photoredox reaction requires an α-hydroxy moiety at the carbon directly attached to the aromatic ring for the reaction to proceed.

Attempts were made to characterize the initially formed (green) dihydroxyanthracene intermediate **4.5**. Initial experiments were carried out by photolyzing samples of **4.1** in

an NMR tube so the formation of **4.5** could be observed directly by NMR without work-up or exposure to air. However, due to the very low solubility of **4.1** in aqueous CH_3CN these photolyses proved to be impractical. Attempts were also made to trap **4.5** using acetic anhydride (as the ester) and methyl iodide (as the methyl ether) *in situ* (Scheme 4.2) but in all experiments attempted, only **4.6** was isolated, consistent with the highly reactive nature of the initially formed product **4.5**.

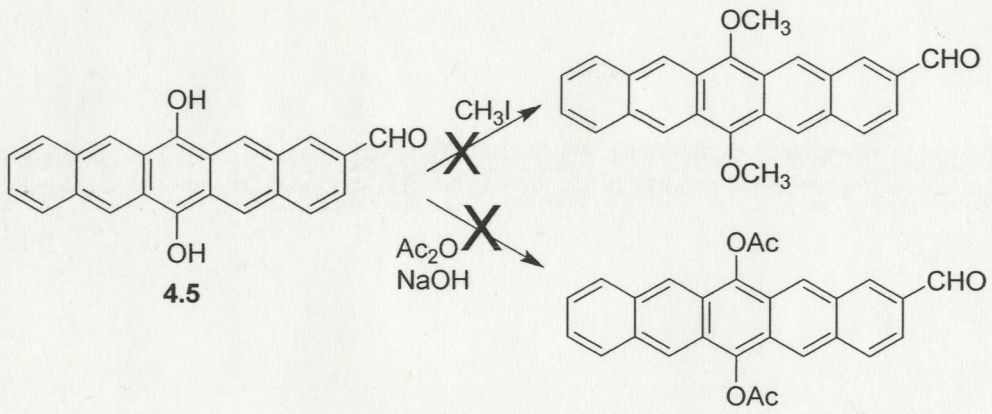

Scheme 4.2 Attempts to trap the photoredox product **4.5**

4.3.2 Photoredox Chemistry of 4.2

Naphthoquinone **4.2** has one less benzene ring on the side of the central quinone without the attached hydroxymethyl group than **HMAQ**. UV-Vis studies of **4.2** (pH 7) gave rise to two new strongly absorbing bands at 268 and 392 nm which were assignable to dihydroxynaphthalene **4.7** (Figure 4.3, Scheme 4.3). For this compound, acid was not required for the photoredox reaction, contrary to what was observed for **4.1**. Indeed, use of acid did not result in any enhancement of the photoredox reaction. Photolysis in neat CH_3CN gave no observable changes. The photoredox product in this case (dihydroxynaphthalene **4.7**) was more stable to air or oxygen as the coloured intermediate remained for at least 1 day in the sealed cuvette.

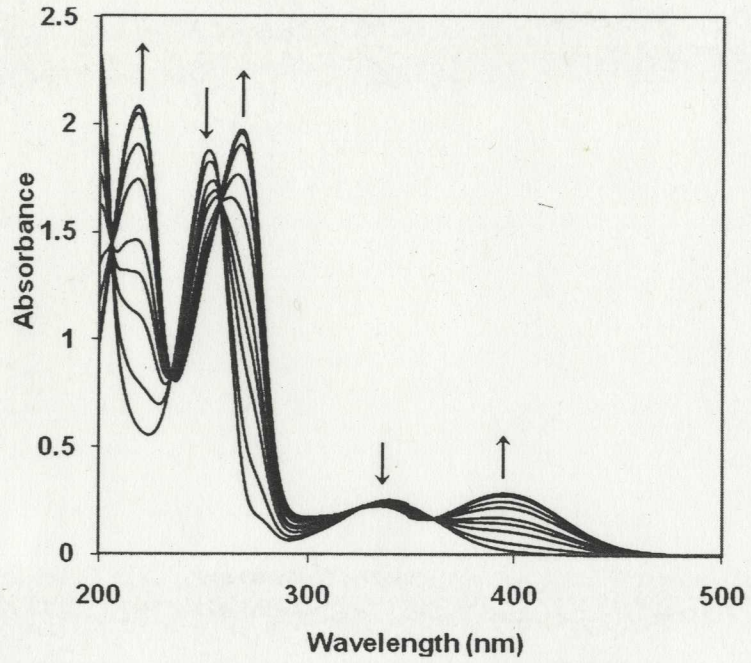

Figure 4.3 UV-Vis traces observed on photolysis of naphthoquinone **4.2** (50% H_2O-CH_3CN, pH 7, λ_{ex} 350 nm, argon purged). Photolysis times were 2-20 s. Growth of absorption bands at 268 and 392 nm is consistent with formation of dihydroxynaphthalene **4.7**.

Shown in Figure 4.4 are solutions of photolyzed acenequinones **HMAQ**, **4.1** and **4.2** illustrating the varied colours observable in this family of photoredox reactions in aqueous solution.

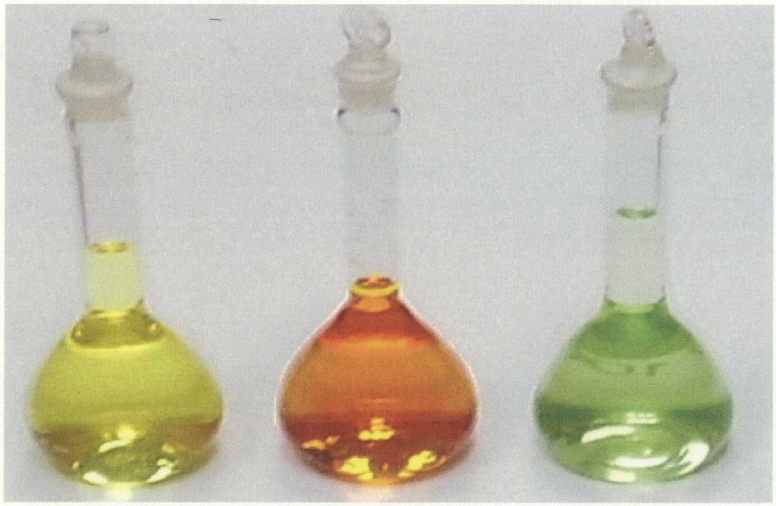

Figure 4.4 Dramatic differences in observed colors in the photolysis of **4.2** (pH 7), **HMAQ** (pH 7), and **4.1** (pH 1) (L to R) in 1:1 H_2O-CH_3CN (λ_{ex} 350 nm; 15 min; argon purged). The color remained unchanged for at least a day for **4.2** and **HMAQ** and a few hours for **4.1**.

Photolysis of **4.2** (50% H_2O-CH_3CN, pH 7) resulted in a yellow solution which slowly (several days) faded when left in the vessel and which turned to pale yellow within a few hours when exposed to air. On work-up in air, naphthoquinone aldehyde **4.8** was formed exclusively (> 60 %; $\Phi \sim 0.4$). In order to provide further evidence for the reaction scheme shown in Scheme 4.3, trapping of **4.7** was attempted. Thus, after photolysis under an argon purge, sufficient solid NaOH was added to the photolysate to basicify the solution. This resulted in the solution turning from yellow to red consistent with formation of a naphtholate chromophore (via deprotonation of **4.7**). Excess Ac_2O was then added under argon, which quenched the red colour. Upon work-up, the only product isolable was diacetoxyanthracene aldehyde **4.7-OAc** thus confirming the reaction sequence shown in Scheme 4.3.

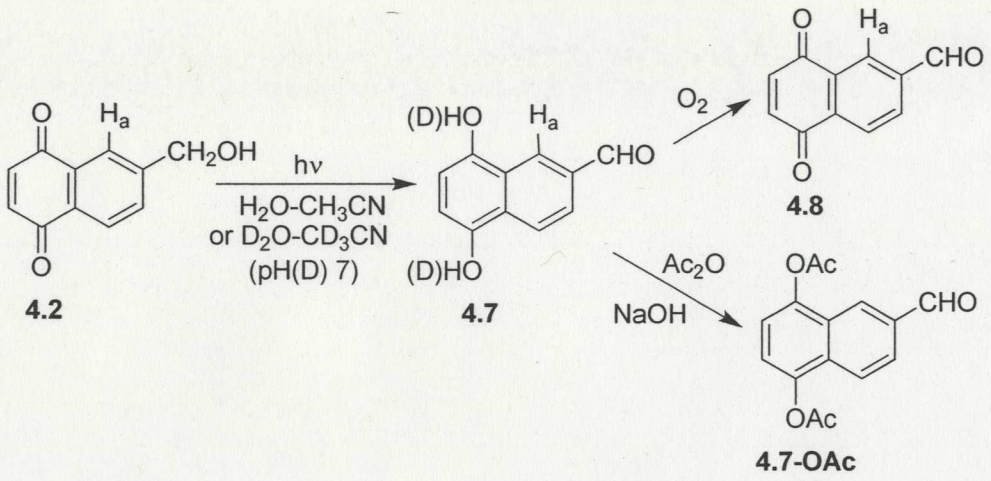

Scheme 4.3 Photolysis of **4.2** and trapping of the photoredox product **4.7** of **4.2**

As further evidence for formation of **4.7** as the primary photochemical product from **4.2**, photolyses were also carried out in NMR tubes (10^{-3} **M**, 10 % D_2O-CD_3CN, pD 7, λ_{ex} 350 nm, argon purged, 10 min). Photolysis gave a dark yellow solution with reduction of the signals at δ 4.80 (s) and 8.07 (s) assigned to the methylene and aromatic H_a protons of **4.2**, respectively (Scheme 4.2), with concomitant growth of the aldehyde (CHO; δ 10.07) and H_a (δ 8.65) protons assignable to the initial photoredox product **4.7**. Based on NMR integration, the yield of **4.7** was estimated to be about 14%. Upon introduction of oxygen via a syringe needle, the dark yellow colour was bleached. In the NMR, the peaks assignable to **4.7** disappeared. In particular, a new aldehyde peak at δ 10.13 and an aromatic singlet (H_a) at δ 8.55 are assignable to oxidized product **4.8**.

4.3.4 Photoredox Chemistry of 4.3 and 4.4

Anthraquinone **4.3** has one more benzene ring between benzyl alcohol and quinone moiety than **4.2**. Based on studies of **4.1** and **4.2**, we expected that **4.3** would also undergo the same photoredox reaction. UV-Vis studies of **4.3** (pH 1 and 7) gave only

small incremental changes even on prolonged photolysis, indicative of a much less reactive chromophore. Semi-preparative studies of **4.3** in 100 mL quartz vessels showed that although acenequinone **4.3** underwent the photoredox reaction, it exhibited low reactivity in neutral or acidic solution ($\Phi \sim 0.01$). This compound required photolysis times that were about an order of magnitude longer for similar conversion. Due to its much lower reactivity, no attempts were made to characterize the initially formed photoredox product and only the final air-oxidized product **4.9** was isolated (eqn. 4.2). No reaction was observed without irradiation (in the presence or absence of oxygen).

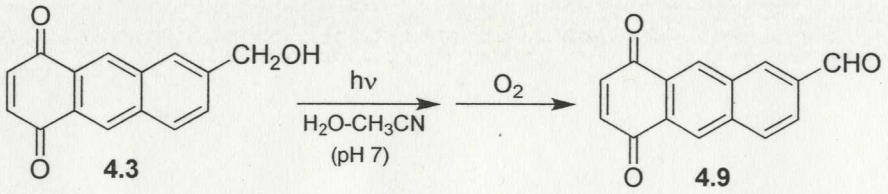

(4.2)

Naphthacenequinone **4.4** has one more benzene rings on the side of the central quinone with the attached hydroxylmethyl group than **HMAQ**. Thus, we also expected that **4.4** would undergo photoredox reaction efficiently. However, UV-Vis studies of **4.4** gave no observable changes in the UV-Vis spectrum (pH 1 or 7) even on prolonged irradiation time indicative of an essentially unreactive acenequinone. Of all the acenequinones studied in this work, compound **4.4** proved to be the only one that was photochemically inert. Semi-preparative photolysis of this compound (pH 1, 7) gave no reaction and the compound could be recovered unchanged. Initially we were puzzled by this result although one could imagine a number of photophysical reasons to explain the lack of reaction. However, the lack of reactivity of this compound as well as the reactivity of the other systems can be partly rationalized by resorting to examination of HOMO/LUMO characteristics (presented in Section 4.4.3).

4.4 Mechanistic Studies of Photoredox Reaction of Pentacenequinone 4.1

4.4.1 pH Effects on the Photoredox Reaction

The effect of pH on the relative quantum efficiency of the photoredox reaction of **4.1** is examined in this chapter. As noted, in pH 7, no reaction was observed. (Section 4.3.1) Using the UV-Vis method, the relative quantum efficiency for formation of **4.5** was followed at different pH's (25% H_2O-CH_3CN, pH of the water portion varied). The results are shown in Figure 4.5 and show a strong dependence of photoredox efficiency on solution pH. The photoredox reaction was not observable above pH 3 and reaches maximum efficiency at about pH ≅ 0, although higher acidities were not employed in this study. The observations strongly suggest that the possible mechanistic step of the photoredox reaction of **4.1** might involve the protonation of the carbonyl oxygen on the anthraquinone moiety.

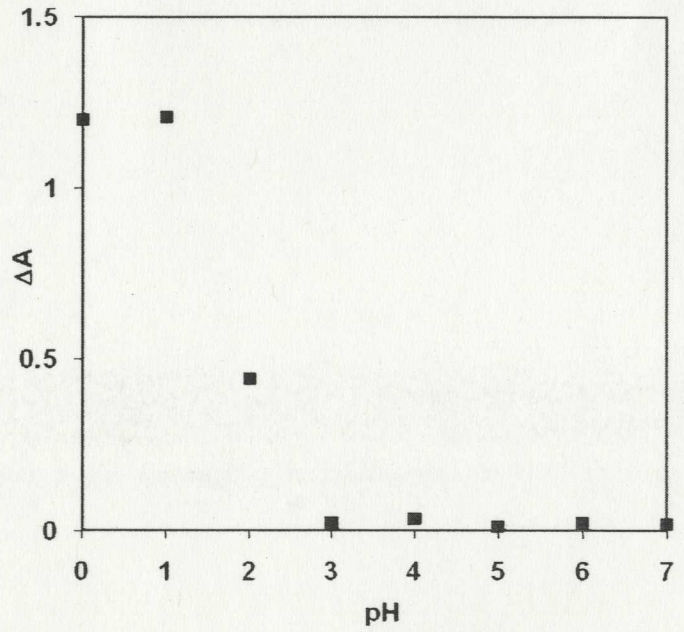

Figure 4.5 Effect of pH on the efficiency of photoredox reaction of pentacenequinone **4.1** monitored at 318 nm (formation of dihydroxypentacene **4.5**; λ_{ex} 350 nm; 25% H_2O-CH_3CN (pH

1), argon purged). ΔA is the difference of the absorbance before and after irradiation. Measurement error is about ± 5%.

4.4.2 Nanosecond laser flash photolysis (LFP) of 4.1

LFP studies of **4.1** (10^{-5} M, in neat CH_3CN, argon saturated) showed a sharp absorption band at 430 nm and an intense broad band at 570 nm (within the laser pulse). Both signals decayed with the first order kinetics ($1.1 \pm 0.1 \times 10^5$ s^{-1}; $\tau \sim 9.0$ μs) (Figure 4.6). The intensity and lifetime of this transient were significantly reduced in the presence of oxygen ($\tau \sim 0.09$ us). Triplet excited 6,13-pentencenquinone has been reported by G $\bar{r}$ner.[61a] It has two absorption band at 430 nm and 590 nm in neat CH_3CN ($\tau \sim 9$ μs in argon saturated solution) and is quenched by oxygen ($\tau \sim 10$ ns). Based on these facts, we assign the 430/580 nm transient observed for **4.1** to the triplet state.

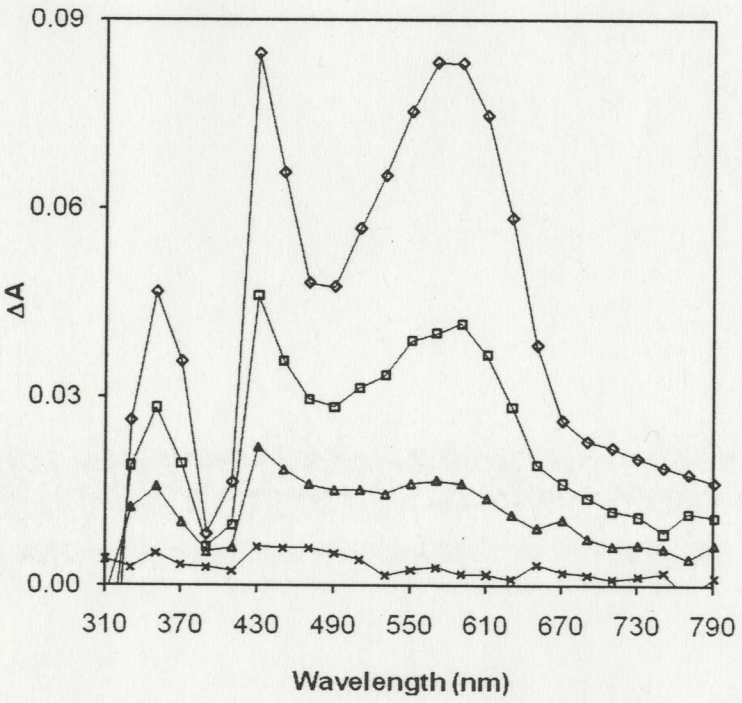

Figure 4.6 Transient absorption spectra of **4.1** in neat CH_3CN ($1.1 \pm 0.1 \times 10^5$ s^{-1}; $\tau \sim 9.0$ μs) (nitrogen-saturated) after the 266 nm pulse, 3.2 μs(◊), 9.6 μs (□), 21 μs (Δ), 66 μs (×). Measurement error is about ± 10%.

In the presence of water, LFP of **4.1** (1:1 H_2O-CH_3CN, pH 7, N_2 purged) also showed formation of the triplet state with a lifetime ($\tau \sim 10$ μs) similar to that in neat CH_3CN. With decaying of the triplet excited transient, a new and weak signal ($\tau \sim 10$ μs) was observed at 450 nm. In the presence of oxygen, with fast decaying of the triplet state ($\tau \sim 0.33$ μs), no new band at 450 nm was observed. These observations suggest that the transient at 450 nm might be an intermediate generated from the triplet excited state. Due to the fast quenching of the triplet state to the ground state, no transient at 450 nm could be observed, consistent with very low photochemical reactivity in neutral aqueous solution. This assignment is also supported by with the observation that LFP studies of the methyl compound **4.1a** (does not undergo the photoredox reaction) in 1:1 H_2O-CH_3CN (pH7) which showed only formation of the triplet excited state (430/570nm, $\tau \sim 5.0$ μs, quenched by oxgen, $\tau_{ox} \sim 0.35$ μs) without formation of the 450 nm species.

In pH 1, the triplet signals at 430 and 570 nm were shorter lived ($\tau \sim 5.4$ μs, compared to 10 μs at pH 7), consistent with acid catalysis of reaction. With decaying of the triplet state, a more intense new band (twice stronger than at pH 7) at 450 nm was observed with a long lifetime ($\tau \sim 60$ μs). Its yield was reduced greatly by the presence of oxygen, but its decay rate was not affected (Figure 4.7). In addition, the observed decay rate of the 450 nm transient was dependent on pH (k_{pH7}:$k_{pH1} \sim 6$:1), consistent with ketonation of enols generated from p-benzoylphenylacetic acid (k_{pH7}:$k_{pH1} \sim 100$:1).[98] The faster decay at pH 7 is associated with base catalysis of ketonization.[98] Thus we tentatively assign the 450 nm transient to an enol intermediate. LFP studies of the methyl compound **4.1a** also supported the assignment. LFP studies of **4.1a** in 1:1 H_2O-CH_3CN (pH1) showed only the

formation of the triplet excited state (430 and 570 nm, $\tau \sim 0.8$ μs, quenched by oxgen, $\tau_{ox} \sim 0.18$ μs) without observation of the 450 nm species.

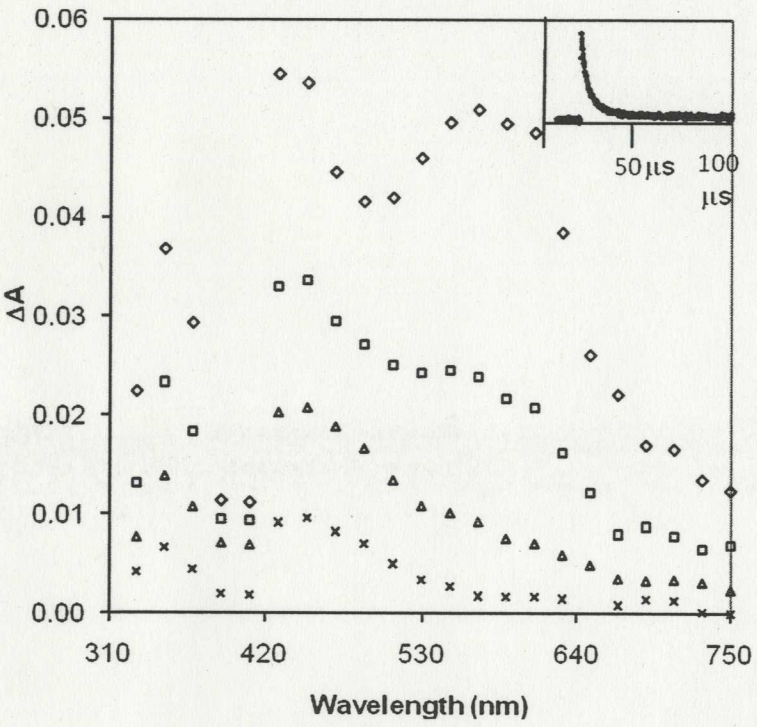

Figure 4.7 Transient absorption spectra of **4.1** in 1:9 H_2O-CH_3CN (pH 1, nitrogen-saturated) after the 266 nm pulse, 2.04 μs(◊),5.5 μs (□), 12.2 μs (Δ), 72.5 μs (×). Inset: triplet decay at 550 nm. (5.4 μs). Measurement error is about ± 10%.

4.4.3 HOMO/LUMO Calculations

We have carried out calculations of HOMO's and LUMO's (Chem 3D, AM1) for all of the compounds studied in this chapter in an attempt to predict reactivity on excitation. For all the reactive acenequinones (**HMAQ**, **4.1- 4.3**), examination of HOMO and LUMO coefficients (some of which are shown in Figure 4.8) show that there is significant to substantial migration of charge from at least the ring with CH_2OH substituent to the carbonyl and to the other ring(s) in the compound. This charge transfer (migration) would make the carbonyl oxygen more basic. On trapping of this charge transfer state with a proton (protonation of the carbonyl oxygen), one can assume that

some of the residual positive charge (sites of electron deficiency) will be localized on the ring with the CH_2OH substituent, making the CH proton on the CH_2OH more acidic. At this level of calculation, there is also evidence to suggest that the C-H bond (of the CH_2OH) moiety also donates electron density for compounds **HMAQ** and **4.2**. This would have the added effect of making this proton even more acidic. Indeed, **HMAQ** and **4.2** were the most reactive compounds and reacted without the need for acid. For pentacenequinone **4.1**, the HOMO/LUMO characteristics do not display this effect: for this compound, the reaction was only observable below pH 3. The presence of the OH group is also particularly crucial: it provides a further inductive acidifying effect and also makes the whole group readily oxidizable (to the aldehyde). For the unreactive compound **4.4** (Figure 4.8), the same calculations show that the charge transfer is in the *opposite direction*, that is, from the rings without the CH_2OH group (the "naphthalene" ring) to the carbonyl and to the ring containing the CH_2OH group. Although this charge transfer will still make the carbonyl oxygen more basic in the excited state and hence undergo protonation, one would not anticipate the same reactivity of the CH_2OH group since the ring in which it is attached is now more electron rich than in the ground state. Indeed, this compound proved to be photochemically inert! Thus simple semi-empirical MO calculations at the AM1 level are useful for the prediction of qualitative reactivity patterns for these compounds.

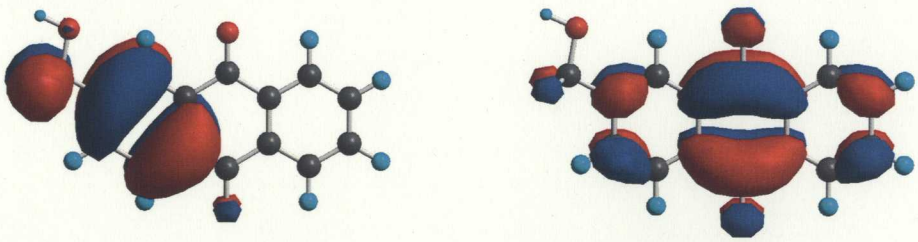

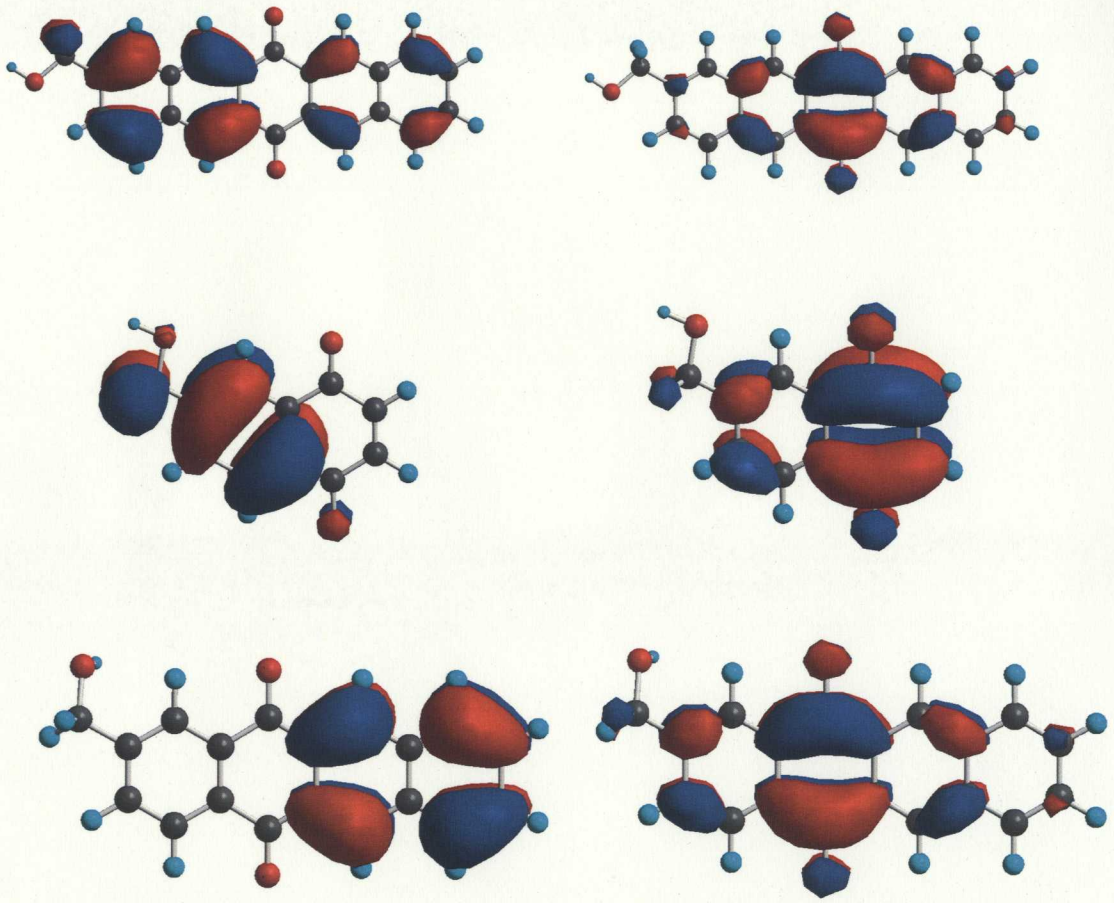

Figure 4.8 Calculated (Chem 3D, AM1) HOMOs (left) and LUMOs (right) for Acenequinones (top to bottom) **HMAQ** (reactive), **4.1** (reactive), **4.2** (reactive) and **4.4** (unreactive).

4.4.4 Proposed Mechanism

We believe that the observed formal intramolecular photoredox reactions of the present acenequinones, including the "parent" anthraquinone[62] and "simple" benzophenone[49] systems, are closely related to the acid-catalyzed photohydration of benzophenone (**1.47**) reported by Wirz and coworkers[41] (Scheme 1.8). They discovered that protonation (at the carbonyl) of triplet benzophenone results in an overall *photohydration* reaction, to give water-adducts **1.49** and **1.50** with a preference for **1.49**, i.e., hydration at the *meta* position. This reaction was unexpected and has missed detection in the past due to the

instability of the hydration products (**1.49** and **1.50**), which readily revert back to **1.47**. Wirz and coworkers[41] assigned a pK_a of -0.4 for the protonated triplet excited state. The mechanism[41] of photohydration presumably involves initiation protonation of the carbonyl oxygen of triplet excited benzophenone, to generate an excited triplet state conjugate acid **1.48** that has its positive charge significantly delocalized to the ortho and meta positions of the benzene ring (Scheme 1.8), as would be anticipated based on the Zimmerman "ortho-meta" effect for benzene ring site activation in photochemical reactions[43]. Attack by water at these sites of positive charge would lead to the observed hydration products which upon deactivation to their ground states would not be expected to be long-lived and readily returns to benzophenone (**1.47**) by dehydration (with re-aromatization). Although the above acid-catalyzed photohydration of benzophenone reported by Wirz and coworkers[41] gave no isolable *stable* product, it seemed reasonable to assume that the protonation of triplet excited benzophenone and aromatic ketones and related compounds such as acenequinones might lead to other types of acid-catalyzed chemistry, a prime example of which was the photoredox reaction of benzophenone **1.51** to give **1.52** in acidic aqueous solution reported by Wan and coworkers[49] (eqn. 1.11).

In view of this background and the fact that acenequinones also tend to react via triplet excited state with photochemical behaviour[59a] that is closely allied to what is known for benzophenones and our LFP studies of **4.1**, we believed that the photoredox reaction of the acenequinones involves a triplet excited state. In addition, photoredox reactions of acenequinones **4.1-4.3** only occur in the presence of water and **4.1** requires acid. Thus, we proposed that the mechanism of photoredox reaction of the acenequinones reported in this work also start with lowest π,π^* as for **HMAQ** (presented in Section 2.4.7). The

lowest π,π^* reactive state is sufficiently basic to be protonated at pH 7 or at pH < 3, depending on the substrate. Intramolecular photoredox reaction requires protonation of the ketone (by acid or by water) and deprotonation of the C-H proton at the CH_2OH moiety. This is a unique mechanism in photochemistry in that two very different types of excited state proton transfers are required (simultaneously or sequentially).

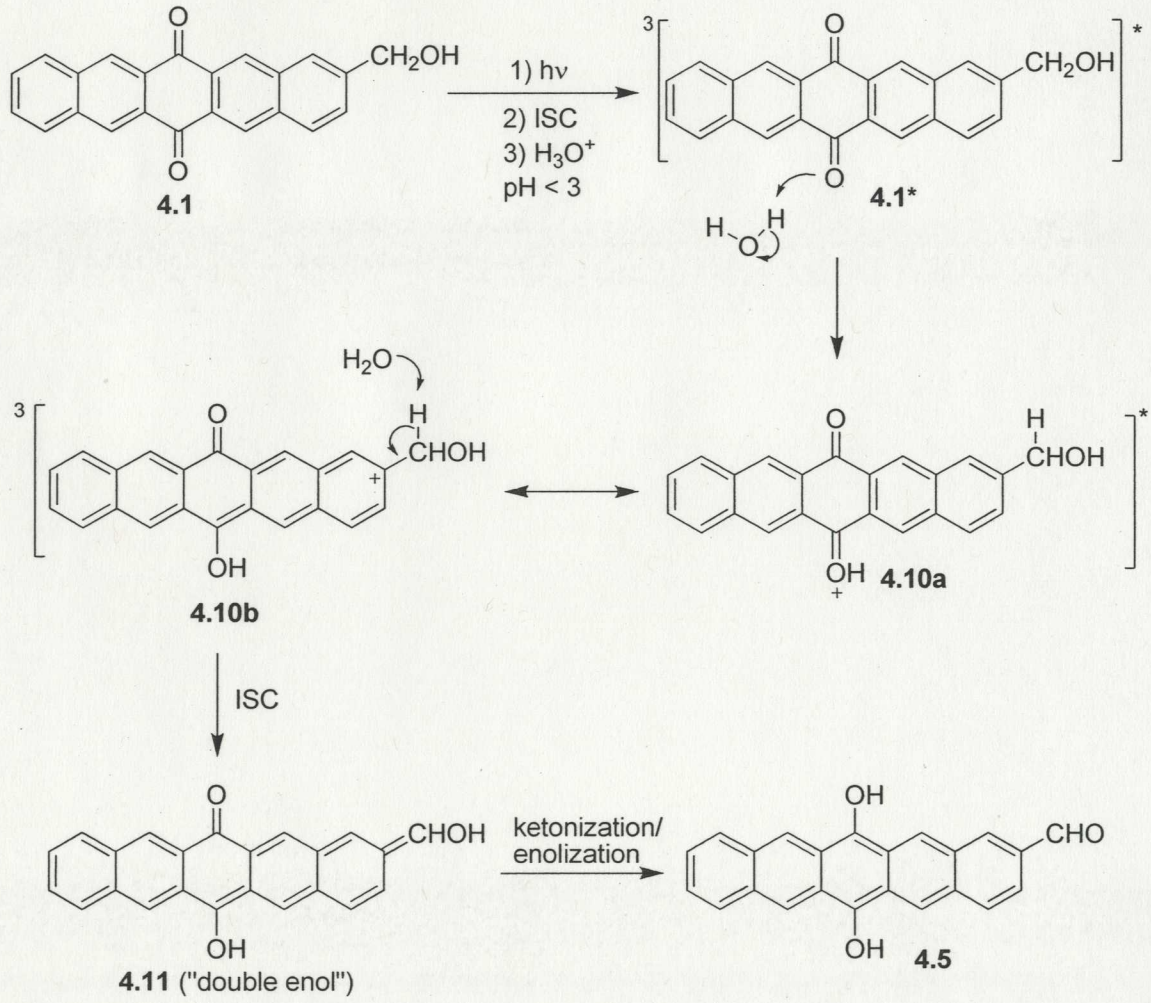

Scheme 4.4 Proposed mechanism for the intramolecular photoredox reaction of **4.1**

A working mechanism is shown for pentacenequinone **4.1** (Scheme 4.4). A highly polarized tripet excited state **4.1*** undergoes protonation to give **4.10a**. This results in a net positive charge on the benzene ring with the attached hydroxymethyl group (**4.10b**).

Subsequent deprotonation of the C-H proton in the CH_2OH moiety gives the double enol **4.11** which upon ketonization/enolization would give the redox product **4.5**.

4.5 Summary

The photoredox reaction of **HMAQ** (Chapter 2) has been extended to acenequinones **4.1-4.4**. Design of these compounds concerns not only the effect of electronic communication as for phenyl anthraquinone **3.1-3.4** (Chapter 3), but also the effect of a benzannelation (adding or removing a benzene ring to the anthraquinone moiety) on the efficiency of photoredox reactions of **4.1-4.4**. Results show that acenequinone **4.1-4.3** undergo the photoredox reaction and **4.4** is photoinert. Table **4.1** lists the experimental conditions and quantum yields of **HMAQ** and **4.1-4.4**. The photoredox reaction of **HMAQ** is the most efficient among these compounds and **4.2** is the second efficient.

Table 4.1 Comparison of efficiency of photoredox reactions of HMAQ and 4.1-4.4

Compounds	Solvent	pH	Quantum Yield (Φ)
HMAQ	1:1 H_2O-CH_3CN	7	0.8
4.1	1:3 H_2O-CH_3CN	1	0.1
4.2	1:1 H_2O-CH_3CN	7	0.4
4.3	1:1 H_2O-CH_3CN	7	0.01
4.4	1:1 H_2O-CH_3CN	7 or 1	0

All of these results suggest that a highly polarized triplet excited state leads to the intramolecular redox reaction in highly benzannelated systems. Adding or removing a benzene ring to the anthraquinone moiety affects the degree and orientation of electronic distribution on both the ground and electronically excited states. This explains why compound **4.4** is photoinert while **4.1-4.3** are photoreactive. All of these results confirm

that charge polarization of the π system plays an important role in the photoredox reaction.

4.6 Experimental

4.6.1 General

Details are the same as those shown in Section 2.6.1.

4.6.2 UV-Vis Studies

UV-Vis studies (~10^{-5} M in H_2O-CH_3CN, pH 7 or pH1) were carried out in 3.0 mL quartz cuvette. Details are reported in Section 2.6.2.

4.6.3 Product Studies

Compounds were photolyzed in 100 mL quartz tubes using a Rayonet RPR 100 photochemical reactor equipped with 300 nm or 350 nm lamps. Typically, a solution of the compound (10^{-4}-10^{-5} M, H_2O-CH_3CN (1:1 or 1:3), pH7 or 1) was bubbled with argon for 15 min and then irradiated under argon purge. The irradiated solution was extracted by 3 × 50 mL CH_2Cl_2 in air and the collected organic extracts was dried over anhydrous $MgSO_4$. The solvent was removed under reduced pressure and the photolysate analyzed by NMR, MS and IR.

In order to monitor the initially formed redox product, photolyses were carried out in NMR tubes which allowed characterization of the first formed redox products. NMR tubes were filled with 1 mL of the appropriate solution (10^{-3} M, 10% D_2O-CD_3CN). Solutions were bubbled using a fine needle through rubber stoppers with argon for 15 min before irradiation then irradiated with 300 nm or 350 nm lamps.

4.6.4 Quantum Yield Measurements

Quantum yields were measured using NMR and the reaction of 2-(hydroxymethyl)anthraquinone (**HMAQ**) as a secondary actinometer ($\Phi = 0.8$).[62] A solution of the compound (**4.1-4.3**, 10^{-4} M, in H_2O-CH_3CN (1:1 or 1:3), pH 7 or 1) was purged with argon for 15 min and irradiated for 1 min at 300 nm (2 lamps) under argon purge. After irradiation, the conversion to product was determined by ^{1}H NMR and compared to an identical run using **HMAQ**. All converions were kept below 30% and repeated twice.

4.6.5 Nanosecond Laser Flash Photolysis Studies of HMAQ

LFP studies were conducted at the University of Victoria LFP facility employing a Spectra Physics Quanta-Ray YAG laser, model GSR-11, with a pulse width of ~ 10 ns and excitation wavelength 266 nm. Quartz flow cells were used and solutions were purged with nitrogen or oxygen for 20 min prior to measurement. Optical densities at 266 nm were ~ 0.6.

4.6.6 Syntheses of 4.1-4.4

Preparation of 6-(hydroxymethyl)-1,4-anthraquinone **4.3**)[99]

2-(Bromomethyl)-1,4-anthraquinone was obtained in 50 % yield via the literature procedure[99] and hydroxylated by silver trifluoroacetate in 4:1 dioxane and water at room temperature to give **4.3** in 90% yield (yellow powder, m.p. 180-182 °C, lit.[99] 178-179°C). ^{1}H-NMR (300MHz, $CDCl_3$) δ: 8.59 (s, 2H), 8.05 (d, 1H, J = 8.80 Hz), 8.03 (s, 1H), 7.68 (d, 1H, J = 8.80 Hz), 6.05 (s, 2H), 4.92 (s, 2H); ^{13}C NMR (DMSO-d_6, 75 MHz) 184.4, 184.3, 144.6, 134.0, 139.9, 134.3, 133.4, 130.0, 128.8, 128.2, 127.9, 127.7 (2C), 126.3, 62.7; MS (EI), *m/z* 239 (M^+, 15), 238 (M^+, 100), 221 (10); IR (KBr) 3498, 3070, 2817, 1670, 1650 cm^{-1}.

Preparation 2-(hydroxymethyl)-6, 13-pentacenequinone (**4.1**)

A mixture of **4.3** (0.43 g, 1.8 mmol), α,α,α',α'-tetrabromo-o-xylene (1.14 g, 2.7 mmol) and NaI (2.70 g, 18 mml) were heated in 5 mL DMF for 3 h at 80 °C to give a dark brown mixture. After cooling, 50 mL of cold water was added followed by the addition of 10 mL 10 % $NaHSO_3$ dropwise until the dark brown colour was bleached. The mixture was extracted with 3 × 25 mL CH_2Cl_2 and dried over anhydrous $MgSO_4$. Removal of the solvent gave a brown solid, which upon separation by column chromatography (silica gel; CH_2Cl_2 and ethyl acetate as eluents) gave 0.13 g of **4.1** (21 %, yellow powder), m.p. (decomp) 286 °C; ^{1}H NMR (DMSO-d_6, 500 MHz) δ 8.95 (s, 1H), 8.94 (s, 1H), 8.93 (s, 1H), 8.89 (s, 1H), 8.38-8.33 (m, 2H), 8.31 (d, 1H, J = 8.54 Hz), 8.23 (s, 1H), 7.84-7.79 (m, 2H), 7.75 (d, 1H, J = 8.54 Hz), 5.54 (t, OH, J = 5.56 Hz), 4.75 (d, 2H, J = 5.56 Hz); ^{13}C NMR (DMSO-d_6, 125 MHz) 182.2, 182.1, 144.7, 134.8 (2C), 134.74, 134.72, 133.9, 130.4, 130.3, 130.1 (2C), 129.9 (2C), 129.8 (2C), 129.1 (2C), 129.0, 128.9, 128.8, 126.2, 62.7; MS (EI), m/z 338 (M^+, 100), 321 (5); HRMS calculated for $C_{23}H_{14}O_3$ 338.0943; observed 338.0928; IR (KBr) 3403, 3054, 2924, 2854, 1691, 1676 cm^{-1}.

Preparation 2-methy-6,13-pentacenequinone (**4.1a**)

Following the method described for the synthesis of **4.1**, use of 6-methyl-1,4-anthraquinone (**4.3a**, from ref. 135) (0.12 g, 0.54 mmol), α,α,α',α'-tetrabromo-o-xylene (0.32 g, 0.81 mmol), NaI (0.81 g, 5.4 mmol) gave 60 mg (35%, yellow powder), m.p. (decomp) 307 °C; ^{1}H NMR ($CDCl_3$, 500 MHz) δ 8.92 (s, 2H), 8.89 (s, 1H), 8.83 (s, 1H), 8.13-8.09 (m, 2H), 8.01 (d, 1H, J = 8.44 Hz), 7.87 (s, 1H), 7.71-7.67 (m, 2H), 7.53 (d, 1H, J = 8.44 Hz), 2.58 (s, 3H); ^{13}C ($CDCl_3$, 125 MHz) 183.4, 183.3, 140.2, 135.8 (2C), 135.52, 135.49, 133.8, 132.1, 130.98, 130.94, 130.3 (2C), 130.2, 130.1, 129.96, 129.94, 129.8, 129.6

(2C), 129.3 (2C), 22.2; MS (EI), m/z 322 (M^+, 100); HRMS calculated for $C_{23}H_{14}O_2$ 322.0994; observed 322.0993IR (KBr) 3051, 2920, 1676, 1615 cm^{-1}.

Preparation 6-(hydroxymethyl)-1,4-naphthoquinone (**4.2**)

This compound was synthesized according to the published procedure[100], except for the last hydrolysis step involving 6-(bromomethyl)-1,4-naphthoquinone, in which 1.5 equiv of silver trifluoacetate was used instead of 5 equiv of $CaCO_3$. Upon column chromatography (silica gel; CH_2Cl_2), 0.2 g (70 %, yellow powder) was obtained, m.p. 80-82°C, lit.[100] 81-82°C; ^{1}H-NMR (300MHz, $CDCl_3$) δ: 8.07 (d, 1H, J = 8.07 Hz), 8.05 (s, 1H), 7.76 (d, 1H, J = 8.07 Hz), 6.96 (s, 2H), 4.85 (s, 2H); ^{13}C (75 MHz, $CDCl_3$) 185.3, 185.1, 147.7, 139.0, 138.8, 132.2, 131.9, 131.3, 127.1, 124.4, 64.5; MS (EI), *m/z* 189 (M^+, 10), 188 (M^+, 100), 160 (90); IR (KBr) 3447, 3064, 2864, 1662, 1598 cm^{-1}.

Preparation 2-(hydroxymethyl)-5,12-naphthacenequinone (**4.4**)

A mixture **4.2** (0.22 g, 1.2 mmol), NaI (1.76 g, 11.7 mmol) and α,α,α',α'-tetrabromo-o-xylene (0.74 g, 1.76 mmol) in 4 mL DMF was heated to 80 °C overnight. After work-up and purification (as described for **4.1**), 0.29 g (85%) of a yellow powder was obtained, m.p. (decomp) 190 °C; ^{1}H NMR (300 MHz, $CDCl_3$) δ 8.84 (s, 2H), 8.40 (d, 1H, J = 8.08 Hz), 8.38 (s, 1H), 8.13-8.05 (m, 2H), 7.83 (d, 1H, J = 8.08 Hz), 7.73-7.64 (m, 2H), 4.91 (s, 2H); ^{13}C NMR (DMSO-d_6, 75 MHz) 182.2, 181.9, 149.8, 134.5 (2C), 133.7, 132.5, 131.9, 130.0 (2C), 129.6 (2C), 129.3, 128.9, 128.8 (2C), 127.0, 124.1, 62.2; MS (EI), m/z 288 (M^+, 100), 259 (50); HRMS calculated for $C_{19}H_{12}O_3$ 288.0786; observed 288.0792; IR (KBr) 3327, 3052, 2926, 1675, 1621, 1603 cm^{-1}.

4.6.7 Photolysis Procedures for 4.1-4.4 and Characterization of Products

Photolysis of (**4.1**)

Compound **4.1** (3 mg in 75 mL CH_3CN and 25 mL H_2O, pH 1) was irradiated (350 nm, 16 lamps) for 1 minute to give 18% yield of **4.6** (2-formyl-6,13-pentacenequinone) which was subsequently isolated in pure form, ^{1}H-NMR (300MHz, $CDCl_3$) δ 10.2 (s, 1H), 9.10 (s, 1H), 8.97 (s, 1H), 8.95 (s, 2H), 8.93 (d, 1H, J = 8.6 Hz), 8.58 (s, 1H), 8.23 (d, 1H, J = 8.6 Hz), 8.19-8.05 (m, 2H), 7.78-7.64 (m, 2H); m/z 336 (M^+, 100), 307 (10); HRMS calculated for $C_{23}H_{12}O_3$ 336.0786; observed 336.0787; IR (KBr) 3054, 1698, 1675 cm^{-1}

Photolysis of (**4.1a**)

Photolysis of **4.1a** as for **4.1** gave no reaction. The NMR of the isolated material was identical to starting materal.

Photolysis of (**4.2**)

Photolysis of **4.2** (5 mg in 50 mL CH_3CN and 50 mL H_2O, pH 7; 4 lamps, 1 minute) gave **4.8** (6-formyl-1,4-naphthoquinone, 44% yield by NMR), which was subsequently isolated in pure form, ^{1}H-NMR (300MHz, $CDCl_3$) δ: 10.17 (s, 1H), 8.57 (s, 1H), 8.25 (s, 2H), 7.07 (ss, 2H); ^{13}C NMR (CD_3Cl, 75 MHz) 190.8, 184.4, 184.1, 139.9, 139.2, 139.1, 135.4, 133.4, 132.8, 128.7, 127.6; MS (EI), m/z 186 (M^+, 100), 157 (40); HRMS calculated for $C_{11}H_6O_3$ 186.0317; observed 186.0322 ; IR 3051, 1697, 1664, 1597 cm^{-1}.

Photolysis of (**4.3**)

A solution of **5** (3 mg in 50 mL CH_3CN and 50 mL H_2O, pH 7, 16 lamps) was irradiated for 1 minute which gave an aldehyde product in < 2% conversion. Upon photolysis for 30 min, 30% conversion to 6-formyl-1,4-anthraquinone (**4.9**) could be achieved; ^{1}H-NMR (300MHz, $CDCl_3$) δ 10.22 (s, 1H), 8.78 (s, 1H), 8.67 (s, 1H), 8.54 (s, 1H), 8.16 (dd, 2H, J = 8.10 Hz), 7.11 (s, 2H); ^{13}C-NMR ($CDCl_3$, 75 MHz) 191.5, 184.5, 184.3, 140.3 (2C), 137.9, 136.7, 135.7, 134.5, 131.5, 130.6, 130.3, 129.5, 128.8, 126.5.

MS (EI), m/z 236 (M^+, 100), 207 (20); HRMS calculated for $C_{15}H_8O_3$ 236.0473; observed 236.0466; IR (KBr, cm^{-1}) 3071, 1706, 1668, 1589 cm^{-1}.

Photolysis of (**4.4**)

Photolysis of **4.3** (3 mg in 50 mL CH_3CN and 50 mL H_2O, pH 7 and pH 7, up to 30 min irradiation) gave no reaction. The NMR of the isolated material was identical to starting materal **4.3**.

4.6.8 Trapping the Photoredox Product of 4.2

Photolysis of **4.2** was also carried out in which the initially formed photoredox product **4.7** was trapped with Ac_2O, to give **4.7-OAc**, as follows (all carried out under argon): A solution of **4.2** (10 mg in 50 mL CH_3CN and 50 mL pH 7 H_2O) was irradiated for 5 min. Upon photolysis, sufficient solid NaOH was added to turn the yellow brown solution to red. This was followed by the addition of 1 mL of Ac_2O, which turned the solution to a brown colour. After work-up in air, the crude material was characterized with ^1H NMR which was consistent with 50% conversion to **4.7-OAc** (6-formyl-1,4-diacetoxynaphthalene). Further separation and purification was achieved by prep. TLC (silica gel, CH_2Cl_2), ^1H-NMR (300MHz, $CDCl_3$) δ 10.15 (s, 1H), 8.38 (s, 1H), 7.99 (s, 2H), 7.39 (dd, 2H, J = 8.08 Hz, J = 8.08 Hz,), 2.50 (s, 3H), 2.47 (s, 3H); ^{13}C-NMR ($CDCl_3$, 75 MHz) 191.9, 169.4 (2C), 145.5, 144.4, 134.8, 130.5, 127.9, 127.4, 124.3, 123.2, 121.4, 119.3, 21.4, 21.2; m/z 272 (M^+, 5), 230 (15), 188 (100), 43 (40); HRMS calculated for $C_{15}H_{12}O_5$ 272.0685; observed 272.0687; IR (KBr, cm^{-1}) 3070, 2942, 2817, 1754, 1699 cm^{-1}.

4.6.9 pH Effects of Photolysis of 4.1

A solution of **4.1** (2.5 mg in 10 mL CH_3CN, diluted 20-fold with 25% H_2O / CH_3CN, pH from 1 to 7, respectively) in a 3 mL quartz cuvette was purged with argon for 2 minutes prior to photolysis and the cuvette was covered by a cap and sealed with parafilm after the argon purge. The deoxygenated solutions were irradiated with UV light (350 nm, 16 lamps, 50s) for **4.1** to give photoredox products **4.5**, which was recorded by UV-Vis spectroscopy.

5. Summary

5.1 Intramolcular Photoredox Reaction of Anthraquinones

Results presented in this Thesis showed that the intramolecular photoredox reaction originally reported for **HMAQ** is a general reaction for a variety of anthraquinone derivatives in aqueous solution. Suitably designed anthraquinones with distal benzyl alcohol moieties and related acenequinones undergo an efficient and clean intramolecular redox reaction in acidic aqueous solution. Based on all of these studies, a better understanding of the intramolecular photoredox reaction of anthraquinone derivatives has been achieved. The photoredox reaction of anthraquinon-2-yl system possesses the following properties:

- Dramatical visible colours changes in this family of the photoredox reaction
- Unimolecular reaction in the anthraquinone molecule
- Water is an essential medium for reaction
- Product forming step probably involves C-H bond breaking at the CH_2OH moiety
- Competes effectively with simple photoreduction
- Highly polarized and photoreactive triplet excited state (lowest π,π^* configuration)
- Unusual dienol intermediate generated from the excited state

5.2 Potential Applications of the Intramolecular Photoredox Reaction of Anthraquinones

5.2.1 Photodeprotecting group

Based on the above studies, the anthraquinon-2-yl chromophore can be used for photocaging of alcohols, aldehydes and ketones. It has the following advantages:

- Photoprotected compounds are readily synthesized
- High yields of photorelease (90% conversion in one hour) upon irradiation.

- The photorelease reaction works in water with excitation wavelengths above 300 nm
- Clean photoreaction and with photoinert products

5.2.2 Oxygen Sensor

The photoredox reaction of anthraquinons generally exhibits a dramatical visible colour change. For example, photolysis of **HMAQ** undergoes a series of colour changes from yellowish (starting material) to orange (photoredox product) to yellowish (oxidized product). These colour changes can be used for oxygen sensing. Indeed, such an application has been reported by Scaiano and his coworkers using **HMAQ**.[101] The oxygen sensor was designed based on the intramolecular photoredox reaction of **HMAQ** adsorbed within zeolite cavities.

5.2.3 Manufacture of H_2O_2

In the Introduction, it was noted that in the manufacture industry of H_2O_2, anthraquinones are used, based on an initial thermal autoxidation. The intramolecular photoredox reaction of anthraquinones can open up a photochemical way to produce H_2O_2. The photoredox products of anthraquinones are oxidized by O_2 to produce H_2O_2 (eqn. 5.1). In order to make this a process useful, a selective reductant that will reduce the aldehyde back to the alcohol is required without reacting with the anthraquinone. This ultimately will be challenging.

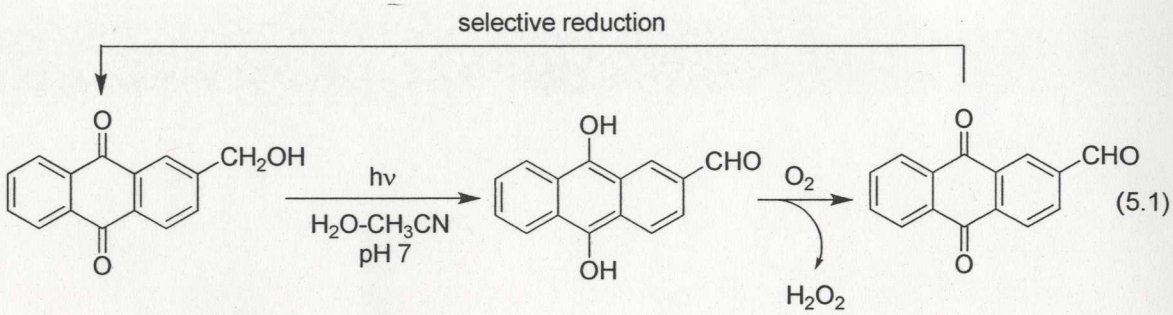

(5.1)

5.2.3 Solar Energy Storage

The overall photoredox reaction requires the formal movement of π electrons from one end (CH_2OH) of the molecule to the other (C=O). Since some of the studied compounds absorb visible light, such as **4.1** (up to 450 nm), the photochemical transformation could be a way of storing solar energy, in the form of the high energy dihydroxyacenes, which are compounds capable of reducing other molecules. Activation of O_2 has already been discussed above, but other activation can be envisaged, such as readily reducible quinones, etc.

Bibliography

1. (a)T. J. Donohue, Oxidation and Reduction in Organic Synthesis, Oxford University Press, USA, **2000**; (b) J. M. Grill, J. W. Ogle, and S. A. Miller, An Efficient and Practical System for the Catalytic Oxidation of Alcohols, Aldehydes, and α,β-Unsaturated Carboxylic Acids, *J. Org. Chem.*, **2006**, 71, 9291–9296; (c) F. A. Carey and R. J. Sundberg, Advanced Organic Chemistry: Part B: Reaction and Synthesis, Springer; 5th ed. **2007**.

2. (a)A. Osyczka, C. C. Moser, F. Daldal, and P. L. Dutton, Reversible Redox Energy Coupling in Electron Transfer Chains, *Nature*, **2004**, 427, 607-612; (b) D. Walz, Thermodynamics of Oxidatio Reduction Reactions and Its Application to Bioenergetics, *Bioehimica et Biophysica Acta*, **1979**, 505, 279-353.

3. (a) D. Walz, Thermodynamics of Oxidation-Reduction Reactions and Its Application to Bioenergetics, *Bioehimica et Biophysica Acta*, **1979**, 505, 279-353; (b) L. Michaelis, Semiquinones, the Intermediate Steps of Reversible Organic Oxidation-Reduction, *Chem. Rev.*, **1935**, 16, 243-286; (c) V. K. Deuchert, and S. Hiinig, Mehrstufige Organische Redoxsysteme-Ein allgemeines Strukturprinzip, *Angew. Chem.*, **1978**, 90, 927-938.

4. K. E. McMartin, G. Martin-Amat, P. E. Noker, and T. R. Tephly, Lack of a Role for Formaldehyde in Methanol Poisoning in the Monkey, *Biochemical Pharmacology*, **1979**, 28, 645-649.

5. L. R. Goldfrank, N. E. Flomenbaum, N. A. Lewin, R. S. Weisman, M. A. Howland, and R. S. Hoffman, eds. Goldfrank's Toxicologic Emergencies. 6th ed. Stamford, CT: Appleton & Lange; **1998**.

6. M. J. Casavant, Fomepizole in the Treatment of Poisoning, *Pediatrics*, **2001**, 107, 170-171.

7. A. Jablonski, Über den Mechanismus der Photolumineszenz von Farbstoffphosphoren, *Z. Phys.*, **1935**, 94, 38–46

8. (a) D. R. Kearns, Physical and Chemical Properties of Singlet Molecular Oxygen, *Chem. Rev.*, **1971**, 71, 395–427; (b) C. S. Foote, and S.Wexler, Singlet Oxygen. A Probable Intermediate in Photosensitized Autoxidations, *J. Am. Chem. Soc.*, **1964**, 86, 3880–3881.

9. P. Klán, and J. Wirz, Photochemistry of Organic Compounds: from Concepts to Practice, Wiley, New York, **2009**.

10. P. H Raven, R. F. Evert, and S. E. Eichhorn, Biology of Plants, 7th Edition. New York: W.H. Freeman and Company Publishers, **2005**.

11. (a) Supplement F2: the Chemistry of Amino, Nitroso, Nitro and Related Groups, S. Patai Eds. John Wiley & Sons, Ltd, 1996; (b) N.Ono, the Nitro Group in Organic Synthesis, Wiley-VCH, **2001**.

12. D. Döpp, Photochemical Reactivity of the Nitro Group,in *CRC Handbook of Organic Photochemistry and Photobiology*, Horspool, W. M., Song, P.-S. Eds.; CRC Press: Boca Raton, **1995**, 1019-1062.

13. (a) D. Döpp, Reactions of Aromatic Nitro Compounds via Excited Triplet States, *Top. Curr. Chem.*, **1975**, 55, 49-85; (b) H. A. Morrison, The Chemistry of the Nitro and Nistroso groups. Edited by H. Feuer. Wiley, New York, **1969**; (c) Y. L. Chow, In the Chemistry of the Amino, Nitro, and Nitroso Compounds and Their Derivatives. Edited by S. Patai. Wiley, New York. **1982**. Chapter. 6; (d) A. N. Frolov, N. A. Kuznetsova, and A.V. El'tsov, Intermolecular photoreduction of aromatic nitro compounds, *Russ. Chem. Rev. Eng. Trans.*, **1976**, 45, 1024-1034.

14. R. W. Yip, D. K. Sharma, R. Giasson, and D. Gravel, Photochemistry of the *o*-Nitrobenzyl System in Solution:Evidence for Singlet State Intramolecular Hydrogen Abstraction, *J. Phys. Chem.*, **1985**, 89, 5328-5330.

15. (a) G. Ciamician, and P. Silber, Chemieche Lichtwirkungen, *Chem. Ber.*, **1901**, 34, 2040-2046; (b) P. De Mayo and S. T. Reid, Photochemical Rearrangements and Related Transformations, *Quart. Rev.*, **1961**, 15, 393-417.

16. M. V. George, and J. C. Scaiano, Photochemistry of *o*-Nitrobenzaldehyde and Related Studies, *J. Phys. Chem.*, **1980**, *84*, 492–495.

17. G. W. Wubbels, R. R. Hautala, and R. L. Letsinger, Photoisomerization of *p*-Nitrobenzaldehyde, *Tetrahedron Lett.*, **1970**, 11, 1689-1691.

18. G. G. Wubbels, T. F. Kalhorn, D. E. Johnson, and D. Campbell, Mechanism of the Water-Catalyzed Photoisomerization of *p*–Nitrobemaldehyde, *J. Org. Chem.*, **1982**,47, 4664-4670.

19. (a) N. J. Turro, Modern Molecular Photochemistry, Benjamin/Cummings Publishing Co., Menlo Park, California, **1978**; b) P. Wan, and G. Zhang, Proton Transfer To Photoexcited Aromatic Compounds in Solution, *Res. Chem. Intermed.*, **1993**, 19, 119-129.

20. P. Wan, and K. Yates, Photoredox Chemistry of Nitrobenzyl Alcohols in Aqueous Solution. Acid and Base Catalysis of Reaction, *Can. J. Chem.*, **1986**, 64, 2076-2086.

21. (a) M. B. Rubin, Photoinduced Intermolecular Hydrogen Abstraction Reactions of Ketones. In W. M. Horspool and P.-S. Song (eds), CRC Handbook of Organic Photochemistry and Photobiology, CRC Press, Boca Raton, FL, **1995**, 430–436; (b) P. J. Wagner, and B.-S. Park, Photoinduced Hydrogen Atom Abstraction by Carbonyl Compounds. In A. Padwa (ed), Organic Photochemistry, Vol. 11, Marcel Dekker, New York, **1991**, 227–366; (c) W. M. Nau, and U. Pischel, Photoreactivity of n,π*-

Excited Azoalkanes and Ketones. In V. Ramamurthy and K. S. Schanze (eds), Organic Photochemistry and Photophysics, Vol. 14, CRC Press, Boca Raton, FL, **2006**, 75–129; (c) J. Mattay, and A. G. Griesbeck (eds), Carbonyl Compounds. In Photochemical Key Steps in Organic Synthesis, VCH, Weinheim, **1994**, 11–118.

22. (a) M. A. Garcia-Garibay, and L. M. Campos, Photochemical Decarbonylation of Ketones: Recent Advances and Reactions in Crystalline Solids. In W. M. Horspool and F. Lenci (eds), CRC Handbook of Organic Photochemistry and Photobiology, 2nd edn, CRC Press LLC, Boca Raton, FL, **2004**, Chapter 48, 1–41; (b) C. Bohne, Norrish Type I Processes of Ketones: Basic Concepts. In W. M. Horspool and P.-S. Song (eds), CRC Handbook of Organic Photochemistry and Photobiology, CRC Press, Boca Raton, FL, **1995**, 416–422.

23. (a) P. J. Wagner, and P. Klán, Norrish Type II Photoelimination of Ketones: Cleavage of 1,4-Biradicals Formed by a-Hydrogen Abstraction. In W. M. Horspool, and F. Lenci (eds), CRC Handbook of Organic Photochemistry and Photobiology, 2nd edn, CRC Press LLC, Boca Raton, FL, **2004**, Chapter 52, 1–31; (b) R. G. Weiss, Norrish Type II Processes of Ketones: Influence of Environment. In W. M. Horspool and P.-S. Song (eds), CRC Handbook of Organic Photochemistry and Photobiology, CRC Press, Boca Raton, FL, **1995**, 471–483; (c) J. C. Scaiano, Laser Flash-photolysis Studies of the Reactions of Some 1,4- Biradicals, *Acc. Chem. Res.*, **1982**, 15, 252–258.

24. (a) P. J. Wagner, Yang Photocyclization: Coupling of Biradicals Formed by Intramolecular Hydrogen Abstraction of Ketones. In W. M. Horspool and F. Lenci (eds), CRC Handbook of Organic Photochemistry and Photobiology, 2nd edn, CRC Press LLC, Boca Raton, FL, **2004**, Chapter 58, 1–70; (b) P. Wessig, and O. Mühling, Abstraction of ($\gamma \pm$ n)-Hydrogen by Excited Carbonyls. In A. G. Griesbeck and J. Mattay (eds), Synthetic Organic Photochemistry, Vol. 12, Marcel Dekker, New York, **2005**, 41–87.

25. (a) F. Muller, and J. Mattay, Photocycloadditions – Control by Energy and Electron Transfer, *Chem. Rev.*, **1993**, 93, 99–117; (b) A.G. Griesbeck, Photocycloadditions of Alkenes to Excited Carbonyls. In A.G. Griesbeck and J. Mattay (eds), Synthetic Organic Photochemistry, MarcelDekker, NewYork, **2005**, 89–139; (c) S. C. Freilich, and K. S. Peters, Observation of the 1,4-Biradical in the Patermò–Bùchi Reaction, *J.Am. Chem. Soc.*, **1981**, 103, 6255–6257; (d) S. C. Freilich, and K. S. Peters, Picosecond Dynamics of the Patermò–Bùchi Reaction, *J. Am. Chem. Soc.*, **1985**, 107, 3819–3822.

26. J. A. Barltrop, and J. D. Coyle, Excited States in Organic Chemistry, Jone Wiley & Sons, New York, **1975**.

27. (a) N. C. Yang, and C. J. Rivas, A New Photochemical Primary Process, The Photochemical Enolization of o-Substituted Benzophenones, *J. Am. Chem. Soc.*, **1961**, 83, 2213; (b)P. G. Sammes, Photoenolisation, *Tetrahedron*, **1976**, 32, 405-422.

28. W. M. Nau, F. L. Cozens, and J. C. Scaiano, Reactivity and Efficiency of Singlet- and Triplet-Excited States in Intermolecular Hydrogen Abstraction Reactions, *J. Am. Chem. Soc.,* **1996**, *118*, 2275-2282.

29. R. Haag, J. Wirz, and P. J.Wagner, The Photoenolization of 2-Methylacetophenone and Related, Compounds, *Helv. Chim. Acta*, **1977**, 60, 2595–2607; P. K. Das, M. V. Encinas, R. D. Small, and J. C. Scaiano, Photoenolization of *o*-Alkyl-substituted Carbonyl Compounds – Use of Electron Transfer Processes to Characterize Transient Intermediates, *J. Am. Chem. Soc.*, **1979**, 101, 6965–6970.

30. F. Ilhan, D. S. Tyson, and M. A.Meador, Phenacenes from Diels - Alder Trapping of Photogenerated o-Xylylenols: Phenanthrenes and Benzo[e]pyrene Bisimide, *Org. Lett.*, **2006**, 8, 577-580.

31. (a)J. Pika, A. Konosonoks, R. M. Robinson, P. N. D. Singh, and A. D. Gudmundsdottir, Photoenolization as A Means to Release Alcohols, *J. Org. Chem.*, **2003**, 68, 1964-1972; (b) J. Literák, L. Hroudná, and P. Klán, 1-Oxoindan-2-yl and 1,3-Dioxoindan-2-yl Esters as Photoremovable Protecting Groups, *J. Photochem. Photobio. A: Chemistry*, **2008**, 194, 59-66.

32. M. Zabadal, A. P. Pelliccioli, P. Klán, and J. Wirz, 2,5-Dimethylphenacyl Esters: A Photoremovable Protecting Group for Carboxylic Acids, J. *of Phys. Chem. A*, **2001**, 105, 10329-10333.

33. T. Förster, Deutung Erdmagnetischer Sturmvariationen Durch Stoßionisation, *Naturwissenschaften*, **1949**, 36, 186-187.

34. A. Weller, Fast Reactions of Excited Molecules, *Prog. React. Kinet.*, **1961**, 187-214.

35. J. F. Ireland, and P. A. H. Wyatt, Acid-base Properties of Electronically Excited States of Organic Molecules, *Adv. Phys. Org. Chem.*, **1976**, 12, 131-221.

36. (a) P. Wan, and B. Chak, Structure-Reactivity Studies and Catalytic Effects in the Photosolvolysis of Methoxy-substituted Benzyl Alcohols, *J. Chem. Soc., Perkin Trans. 2*, **1986**, 1751-1756. (b) P. Wan, and D. Shukla, Utility of Acid-Base Behavior of Excited States of Organic Molecules, *Chem. Rev.*, **1993**, 93, 571-584.

37. N. J. Turro, and P. Wan, Fluorescence quenching of methoxybenzyl alcohols by the hydronium ion in aqueous solution: acid-catalyzed formation of methoxybenzyl cations from the singlet excited state, *J. Photochem.,* **1985**, 28, 93-102.

38. (a) P. Wan, and B. Chak, Structure-Reactivity Studies and Catalytic Effects in the Photosolvolysis of Methoxy-substituted Benzyl Alcohols, *J. Chem. Soc., Perkin Trans. 2*, **1986**, 1751-1756. (b) P. Wan and D. Shukla, Utility of Acid-Base Behavior of Excited States of Organic Molecules, *Chem. Rev.*, **1993**, 93, 571-584.

39. (a) P. Wan, E. Krogh, and B. Chak, Enhanced formation of 8.pi.(4n) conjugated cyclic carbanions in the excited state: first example of photochemical C-H bond

heterolysis in photoexcited suberene, *J. Am. Chem. Soc.*, **1988**, 110, 4073-4074; (b) D. Budac, and P. Wan, Excited-state carbon acids. Facile benzylic carbon-hydrogen bond heterolysis of suberene on photolysis in aqueous solution: a photogenerated cyclically conjugated eight .pi. electron carbanion, *J. Org. Chem.*, **1992**, 57, 887-894.

40. J. F. Ireland, and P. A. H. Wyatt, Similar Excited State pK Behaviour of Xanthone and the Benzophenones, *J. Chem. Soc., Faraday Trans 1*, **1973**, , 69, 161-168.

41. M. Ramseier, P. Senn, and J. Wirz, Photohydration of Benzophenone in Aqueous Acid, *J. Phys. Chem. A*, **2003**, 107, 3305-3315.

42. J. C. Scaiano, Intermolecular Photoreductions of Ketones, *J. Photochem.*, **1973**, 2, 81-118.

43. H. E. Zimmerman, and D. I. Schuster, Mechanistic Organic Photochemistry. IV. Photochemical Rearrangements of 4,4-Diphenylcyclohexadienone, *J. Am. Chem. Soc.*, **1962**, 84, 4527-4540

44. N. J. Turro, *Modern Molecular Photochemistry*; University Science Books: Mill Valley, CA, **1991**.

45. W. Horspool, and D. Armesto, *Organic Photochemistry, A Comprehensive Treatment*; Ellis Horwood Limited: Chichester, England, **1992**, Chapter 3.

46. N. Filipescu, and F. L. Minn, Photoreduction of Benzophenone in Isopropyl Alcohol, *J. Am. Chem. Soc.*, **1968**, 90, 1544-1547.

47. Y. M. A. Nagulb, C. Steel, and S. G. Cohen, Photoreduction of Benzophenone by Acetonitrile: Correlation of Rates of Hydrogen Abstraction from RH with the Ionization Potentials of the Radicals R *J. Phys. Chem.*, **1987**, 91, 3033-3036.

48. D. M. Schuster, and T. M. Weil, Photochemistry of Ketones in Solution. XXXVIII. Mechanism for Photoreduction of Benzophenone in Benzene. Evidence for Self-quenching of Benzophenone triplets in Solution and for Hydrogen Abstreuction from Benzophenone Ground State, *J. Am. Chem. Soc.*, **1973**, 95, 4091-4092.

49. D. Mitchell, M. Lukeman, D. Lehnherr, and P. Wan, Formal Intramolecular Photoredox Chemistry of Meta-Substituted Benzophenones, *Org. Lett.*, **2005**, 7, 3387-3389.

50. R. H. Thomson, Naturally Occurring Quinones. III. Recent Advances. Chapman and Hall, London, **1987**.

51. M. Phillips, Chemistry of anthroquinone. *Chemical Reviews*, **1929**, 6, 157-174.

52. J. L. Gomide, Anthraquinone - an Effective Additive in Soda Pulping, *Papel*, **1980**, 41, 39-48.

53. (a) W. T. Thomson, Agricultural Chemicals, Book III -Fumigants, Growth Regulators, Repellents, and Rodenticides. Thomson Publishing, Fresno, CA, **1988**. (b) M. L. Avery, J. S. Humphrey, T. M. Primus, D. G. Decker, and A. P. McGrane, Anthraquinone Protects Rice Seed from Birds, *Crop Protection*, **1998**, 17, 225-230.

54. J. M. Campos-Martin, G. Blanco-Brieva, and J. L. G. Fierro, Hydrogen Peroxide Synthesis: An Outlook beyond the Anthraquinone Process, *Angew. Chem. Int. Ed.*, **2006**, 45, 6962-6984.

55. B. Fuchs, W.J.W. Mayer, and S. Abramson, *J. Chem. Soc., Chem. Commun.*, **1985**, 1711-1713.

56. (a) M. Shah, N. S. Allen, M. Edge, S. Navaratnam, and F. Catalina, Photochemistry and Photoiniation Activity of Radical Polymerization of 2-Substituted Anthraquinone Derivatives. III. Nanosecond Laser Flash Photolysis Study, *J. Appl. Poly. Sci.*, **1996**, 62, 319-340; (b) I. Loeff, A. Treinin, and H. Linschitz, Photochemistry of 9,10-Anthraquinone-2-Sulfonate in Solution. 1. Intermediates and Mechanism, *J. Phys. Chem.*, **1983**, 87, 2536-2544; (c) S. A. Carlson, and D. M. Hercules, Studies of Some Intermediates and Products of the Photoreduction of 9,10-Anthraquinone, *Photochem. Photobiol.*, **1973**, 17, 123-131; (d) H. Gan, and D. G. Whitten, A Sterically Controlled Recyclable System: Reversible Photoredox Reactions Between Anthraquinone and Hindered Tertiary Amines, *J. Am. Chem. Soc.*, **1993**, 115, 8031-8037.

57. (a) F. Wilkinson, Transfer of Triplet State Energy and the Chemistry of Excited States, *J. Phys. Chem.*, **1962**, 66, 2569-2574.

58. K. Tickle, and F. Wilkinson, Photoreduction of Anthraquinone in Isopropanol, *Trans. Faraday Soc.*, **1965**, 61, 1981-1990.

59. (a) H. G ̄rner, Photoreduction of 9,10-Anthraquinone Derivatives: Transient Spectroscopy and Effects of Alcohols and Amines on Reactivity in Solution, *Photochem. Photobiol.*, **2003**, 77, 171-179; (b) H. G ̄rner, Photoreactions of p-Benzo, p-Naphtho, and p-Anthraquinones with Ascorbic Acid, *Photochem. Photobiol. Sci.*, **2004**, 3, 933-938; (c) H. G ̄rner, Photoinduced Oxygen Uptake for 9,10-Anthraquinone in Air-Saturated Aqueous Acetonitrile in the Presence of Formate, Alcohols, Ascorbic Acid or Amines, *Photochem. Photobiol. Sci.*, **2006**, 5, 1052-1058.

60. (a) M. Kumbhakar, S. Nath, M. C. Rath, T. Mukherjee, and H. Pal, Electron Transfer Interaction of Dihydroxyquinones with Amine Quenchers: Dependence of the Quenching Kinetics on the Aliphatic and Aromatic Nature of the Amine Donors, *Photochem. Photobio.*, **2004**, 79(1): 1–10; (b) M. Kumbhakar, S. Nath, T. Mukherjee, and H. Pal, Kinetics and Mechanism of Bimolecular Electron Transfer Reaction in Quinone-Amine Systems in Micellar Solution, *J. Chem. Phys.*, **2005**, 122, 084512 (1-11).

61. (a) G. B. Schuster, Long-range Charge Transfer in DNA: Transient Structural Distortions Control the Distance Dependence, *Acc. Chem. Res.*, **2000**, 33, 253–260. (b) A. Gosh, A. Joy, G. B. Schuster, T. Douki, and J. Cadet, Selective One-electron Oxidation of Duplex DNA Oligomers: Reaction at Thymines, *Org. Biomol. Chem.* **2008**, 6, 916–928.

62. M. Lukeman, M. Xu, and P. Wan, Excited State Intramolecular Redox Reaction of 2-(Hydroxymethyl)anthraquinone in Aqueous Solution, *Chem. Commun.*, **2002**, 136-137.

63. (a) R. W. Binkley, and T. W. Flechtner, Synthetic Organic Photochemistry-Photoremovable Protecting Groups, New York, **1984**; (b) C. G. Bochet, Photolabile Protecting Groups and Linkers, *J. Chem. Soc. Perkin Trans. 1*, **2002**, 2, 125-142.

64. (a) G. Dorman, and G. D. Prestwich, Using Photolabile Ligands in Drug Discovery and Development, *Trends Biotechnol*, **2000**, 18, 64-77; (b) Y. Shigeri, Y. Tatsu, and N. Yumoto, *Pharmacol. Ther.*, **2001**, 91, 85-92; (c) S. R. Adams, and R. Y. Tsien, Synthesis and Application of Caged Peptides and Proteins, *Annu. Rev. Physiol.*, **1993**, 55, 755-784.

65. A. P. Pellicuioli, and J. Wirz, Photoremovable Protecting Groups: Reaction Mechanisms and Applications, *Photochem. Photobio. Sci.*, **2002**, 1, 441-458.

66. (a) U. Zehavi, B. Amit, and A. Patchornik, Light-sensitive Glycosides. I. 6-Nitroveratryl β-D-Glucopyranoside and 2-Nitrobenzyl β-D-Glucopyranoside, *J. Org. Chem.*, **1972**, 37, 2285-2288; (b)S. Watanabe, T. Sueyoshi, M. Ichihara, C. Uehara, and M. Iwamura, Reductive Ring Opening of *o*-Nitrobenzylidene Acetals of Monosaccharides: Synthesis and Photolysis of Some Photolabile Sugars, *Org. Lett.*, **2001**, 3, 255-257.

67. (a) J. Hébert, and D. Gravel, *o*-Nitrophenylethylene Glycol. Photosensitive Protecting Group for Aldehydes and Ketones, *Can. J. Chem.*, **1974**, 52, 187-189; (b) A. Blanc, and C. G. Bochet, Bis(o-nitrophenyl)ethanediol: A Practical Photolabile Protecting Group for Ketones and Aldehydes, *J. Org. Chem.*, **2003**, 68, 1138-1141; (c) S. Kantevari, C.V. Narasimhaji, and H. B. Mereyala, Bis(4,5-dimethoxy-2-nitrophenyl)ethylene Glycol: a New and Efficient Photolabile Protecting Group for Aldehydes and Ketones, *Tetrahedron*, **2005**, 61, 5849–5854.

68. (a) A. Patchornik, B. Amit, and R. B. Woodward, Photosensitive Protecting Groups, *J. Am. Chem. Soc.*, **1970**,92, 6333-6335; (b) J. F. Cameron, and J. M. J. Fréchet, Photogeneration of Organic Bases from *o*-Nitrobenzyl-derived Carbamates, J. *Am. Chem. Soc.*, **1991**, 113, 4303-4313.

69. K. R. Gee, L. Niu, K. Schaper, V. Jayaraman, and G. P. Hess, Synthesis and Photochemistry of a Photolabile Precursor of N-Methyl-D-aspartate (NMDA) that is Photolyzed in the Microsecond Time Region and is Suitable for Chemical Kinetic Investigations of the NMDA Receptor, *Biochem.*, **1999**, 38, 3140-3147;

70. J. H. Kaplan, B. Forbush III, and J. F. Hoffman, Rapid Photolytic Release of Adenosine 5'-Triphosphate from a Protected Analog – Utilization by Na–K Pump of Human Red Blood-cell Ghosts, *Biochem.*, **1978**, 17, 1929-1935.

71. J. W. Walker, G. P. Reid, J. A. McCray, and D. R. Trentham, Photolabile 1-(2-nitrophenyl)ethyl Phosphate Esters of Adenine Nucleotide Analogs – Synthesis and Mechanism of Photolysis, *J. Am. Chem. Soc.*, **1988**, 110, 7170-7177.

72. Y. V. Il'ichev, M. A. Schworer, and J. Wirz, Photochemical Reaction Mechanisms of 2-Nitrobenzyl Compounds: Methyl Ethers and Caged ATP, *J. Am. Chem. Soc.*, **2004**, 126, 4581–4595.

73. (a) R. S. Givens, A. Jung, C.-H. Park, J. Weber, and W. Bartlett, New Photoactivated Protecting Groups. 7. *p*-Hydroxyphenacyl: A Phototrigger for Excitatory Amino Acids and Peptides, New Photoactivated Protecting Groups. 6. *p*-Hydroxyphenacyl: A Phototrigger for Chemical and Biochemical Probes, *J. Am. Chem. Soc.*, **1997**, 119, 8369-8370; (b) C.-H. Park, and R. S. Givens, *J. Am. Chem. Soc.*, **1997**, 119, 2453-2463.

74. R. S. Rock, and S. I. Chan, Synthesis and Photolysis Properties of a Photolabile Linker Based on 3'-Methoxybenzoin, *J. Org. Chem.*, **1996**, 61, 1526-1529.

75. (a) T. Furuta, H. Torigai, M. Sugimoto, and M. Iwamura, Photochemical Properties of New Photolabile cAMP Derivatives in a Physiological Saline Solution, *J. Org. Chem.*, **1995**, 60, 3953-3956; (b) B. Schade, V. Hagen, R. Schmidt, R. Herbich, E, Krause, T. Echardt, and J. Bendig, Deactivation Behavior and Excited-State Properties of (Coumarin-4-yl)methyl Derivatives. 1. Photocleavage of (7-methoxycoumarin-4-yl)methyl-Caged Acids with Fluorescence Enhancement, *J. Org. Chem.*, **1999**, 64, 9109-9117.

76. T. Furata, Y. Hirayama, and M. Iwamura, Anthraquinon-2-ylmethoxycarbonyl (Aqmoc): a new photochemically removable protecting group for alcohols, *Org. lett.*, **2001**, 3, 1809-1812.

77. J.-Y. Yu, W.-J. Tang, H.-B. Wang, and Q.-H. Song, Anthraquinon-2-ylethyl-1',2'-diol (Aqe-diol) as a New Photolabile Protecting Group for Aldehydes and Ketones, *J. Photochem. Photobiol., A: Chemistry*, **2007**, 185, 101-105.

78. (a) R. L. Blankespoor, R. Hsung, and D. L. Schutt, Photodemethylation of methoxy-substituted 9,10-anthraquinones in methanol, *J. Org. Chem.*, **1988**, 53, 2877-2878; (b) R. L. Blankespoor, R. L. De Jong, R. Dykstra, D. A. Hamstra, D. B. Rozema, D. P. VanMeurs, and P. Vink, Photochemistry of 1-alkoxy- and 1-(Benzyloxy)-9,10-anthraquinones in Methanol: a δ -Hydrogen Atom Abstraction Process That Exhibits a Captodative Effect, *J. Am. Chem. Soc.*, **1991**, 113, 3507-3513; (c) R. L. Blankespoor, R. P. Smart, E. D. Batts, A. A. Kiste, R. E. Lew, and M. E. Vasnder Vilet, Photochemistry of 1-alkoxy- and 1-(benzyloxy)-9,10-anthraquinones in methanol: A facile process for the preparation of aldehydes and ketones, *J. Org.*

Chem., **1995**, 60, 6852-6859; (d) R. P. Smart, T. J. Peelen, R. L. Blankespoor, and D. L. Ward, Short-Lived 1,5-Biradicals Formed from Triplet 1-Alkoxy- and 1-(Benzyloxy)-9,10-anthraquinones, *J. Am.Chem. Soc.*, **1997**, 119, 461-465. (e) R. L. Blankespoor, T. DeVries, E. Hansen, J. M. Kallemeyn, A. M. Klooster, J. A. Mulder, R. P. Smart, and D. A. Vander Griend, Photochemical Synthesis of Aldehydes in the Solid Phase, J. *Org. Chem.*, **2002**, 67, 2677-2681.

79. J. M. Ruxer, and G. Solladie, Synthesis and Optical Resolution of Substituted Dibenzo[*b,f*][1,4]diazocines, *J. Chem.Res. Synopses*, **1978**, 10, 408-409.

80. C. G. Bochet, Photolabile Protecting Groups and Linkers, *J. Chem. Soc., Perkin Trans. 1*, **2002**, 125-142.

81. N. P. Gritsan, I. V. Khmelinski, and O. M. Usov, Experimental and Theoretical Study of Photoenolization Mechanism of 1-Methylanthraquinone, *J. Am. Chem. Soc.*, **1991**, 113, 9615-9620.

82. M.-G. Ren, N.-M. Bi, M. Mao, and Q.-H. Song, 2-(1'-Hydroxyethyl)-anthraquinone as a Photolabile Protecting Group for Carboxylic Acids, J. *Photochem. Photobio., A: Chemistry,* **2009**, 204, 13-18.

83. (a) J. Olmsted III, and T. Akashah, Photooxidation of Isobenzofurans, *J. Am. Chem. Soc.*, **1973**, 95, 6211-6215; (b) T. Sasaki, K. Kanematsu, K. Hayakawa, and M. Sugiura, Photochemical and Thermal Cycloaddition Reactions of 1,3-Diphenylisobenzofuran with Cycloheptatriene, *J. Am. Chem. Soc.*, **1975**, 97, 355-359; (c) R. N. Warrener, I. G. Pitt, and R. A. Russell, *Aust. J. Chem.*, **1993**, 46, 1515-1534.

84. D. Budac, and P. Wan, Excited State Carbon Acids. Facile Benzylic C-H Bond Heterolysis of Suberene on Photolysis in Aqueous Solution: A Photogenerated Cyclically Conjugated Eight π Electron Carbanion, *J. Org. Chem.*, **1992**, 57, 887-894.

85. J. Morrison, H. Osthoff, and P. Wan, Photoredox, Photodecarboxylation and Photo-Retro-Aldol Chemistry of p-Nitrobiphenyls, *Photochem. Photobiol. Sci.*, **2002**, 1, 384-394.

86. S. L. Murov, I. Carmichael, and G. L. Hug, Handbook of Photochemistry, Second Edition, Published by Marcel Dekker, **1993**.

87. I. Carmichael, and G. L. Hug, In Handbook of Organic Photochemistry; Scaiano, J. C., Ed.; CRC Press: Boca Raton, **1989**, Vol. 1.

88. S. L. Murov, Handbook of Photochemistry, Marcel Dekker, New York, **1973**.

89. (a) I. Loeff, A. Treinin, and H. Linschitz, Photochemistry of 9,10-Anthraquinone-2-Sulfonate in Solution. 1. Intermediates and Mechanism, *J. Phys. Chem.*, **1983**, 87, 2536-2544; (b) S. A. Carlson, and D. M. Hercules, Studies of Some Intermediates and Products of the Photoreduction of 9,10-Anthraquinone, *Photochem. Photobiol.*, **1973**, 17, 123-131; (c) H. Gan, and D. G. Whitten, A Sterically Controlled Recyclable

System: Reversible Photoredox Reactions Between Anthraquinone and Hindered Tertiary Amines, *J. Am. Chem. Soc.*, **1993**, 115, 8031-8037.

90. G. Porter, and P. Suppan, Some Aspects of Transitions between Electronic Levels, *Pure Appl. Chem.*, **1964**, 9, 499-505.

91. (a) E. A. Jefferson, J. R. Keeffe, and A. J. Kresge, Characterization of the Indan-1-one Keto–enol System *J. Chem. Soc., Perkin Trans. 2*, **1995,** 2041–2046; (b) j. R. Keeffe and A. J. Kresge, in The Chemistry of Enols, ed. Z. Rappoport, Wiley, New York, **1997**.

92. (a) Y. Shi, and P. Wan, Solvolysis and Ring Closure of Quinone Methides Photogenerated from Biaryl Systems, *Can. J. Chem.*, **2005**, 83, 1306-1323; (b) M. Xu, C. Z. Chen, and P. Wan, Intramolecular Charge Transfer in Photoexcited Hydroxyterphenyls: Evidence for Formation of Terphenyl Quinone Methides in Aqueous Solution, *J. Photochem. Photobiol. A,* **2008**, 198, 26-33.

93. (a) N. S. Kudryashev, G. A. Val'kova, and D. N. Shigorin, Quantum Chemistry and Molecular Structure, *Russ. J. Phys. Chem.*, **1992**, 66, 1587-1589; (b) N. A. Shcheglova, D. N. Shigorin, and A. M. Sergeev, The Influence of Conformational Changes in Molecules on Their Electronic Spectra, *Russ. J. Phys. Chem.*, **1978**, 52, 1259-1263; (c) N. A. Shcheglova, D. N. Shigorin, and N. S. Dokunikhin, The Luminescence and Absorption Spectra of α-and β-Alkyl- and – Aryl-derivatives of Anthraquinone in Solution. II. Luminescence Spectra at 77 K, *Russ. J. Phys. Chem.*, **1966**, 40, 564-569.

94. Y. Chiang, A. J. Kresge, I. Onyido, J. P. Richard, P Wan, and M. Xu, Ketonization of the Remarkably Strongly Acidic Elongated Enol Generated by Flash Photolytic Decarboxylation of *p*-Benzoylphenylacetic Acid in Aqueous Solution, *Chem. Commun.*, **2005**, 4231-4233.

95. F. Wηrthner, Plastic Transistors Reach Maturity for Mass Applications in Microelectronics, *Angew. Chem., Int. Ed.*, **2001**, 40, 1037-1039.

96. (a) J. Jiang, B. R. Kaafarani, and D. C. Neckers, Design, Synthesis, and Properties of New Derivatives of Pentacene, *J. Org. Chem.*, **2006**, 71, 2155-2158; (b) C. R. Swartz, S. R. Parkin, J. E. Bullock, J. E. Anthony, A. C. Mayer, and G. G. Malliaras, Synthesis and Characterization of Electron-Deficient Pentacenes, *Org. Lett.*, **2005**, 7, 3163-3166; (c) E. J. Hwang, Y. E. Kim, C. J. Lee, and J. W. Park, Synthesis and Luminescent Properties of Pentacene Derivatives Having a Chromophore, *Thin Solid Films*, **2006**, 499, 185-191; (d) K. Kobayashi, R. Shimaoka, M. Kawahata, M. Yamanaka, and K. Yamaguchi, Synthesis and Cofacial π-Stacked Packing Arrangement of 6,13-Bis(alkylthio)pentacene, *Org. Lett.*, **2006**, 8, 2385-2388; (e) S. H. Chan, H. K. Lee, Y. M. Wang, N. Y. Fu, X. M. Chen, Z. W. Cai, and H. N. C. Wong, A Soluble Pentacene: Synthesis, EPR and Electrochemical Studies of 2,3,9,10-Tetrakis(trimethylsilyl)pentacene, *J. Chem. Soc., Chem. Comm.*, **2005**, 66-68.

97. K. P. Weidkamp, A. Afzali, R. M. Tromp, and R. J. Hamers, A Photopatternable Pentacene Precursor for Use in Organic Thin-Film Transistors, *J. Am. Chem. Soc.*, **2004**, 126, 12740-12741.

98. H. Yamada, Y. Yamashita, M. Kikuchi, H. Watanabe, T. Okujima, H. Uno, T. Ogawa, K. Ohara, and N. Ono, Photochemical Synthesis of Pentacene and its Derivatives, *Chem. Eur. J.*, **2005**, 11, 6212-6220.

99. D. H. Hua, K. Lou, J. Havens, E. M. Perchellet, Y. Wang, J. P. Perchellet, and T. Iwamoto, Synthesis and in vitro antitumor activity of substituted anthracene-1,4-diones, *Tetrahedron*, **2004**, 60, 10155-10163

100. E. Torres, C. A. Panetta, N. E. Heimer, B. J. Clark, and C. L. Hussey, Synthesis and properties of 6-(hydroxymethyl)-9,9,10,10-tetracyanonaphthoquinodimethane, *J. Org. Chem.*, **1991**, 56, 3737-3739.

101. Katherine L. McGilvray, Michelle N. Chre´tien, **Matthew Lukeman** and J. C. Scaiano, A simple and smart oxygen sensor based on the intrazeolite reactions of a substituted anthraquinone, *Chem. Commun.*, **2006**, 4401–4403

Appendix A: ^{1}H, ^{13}C NMR Spectra

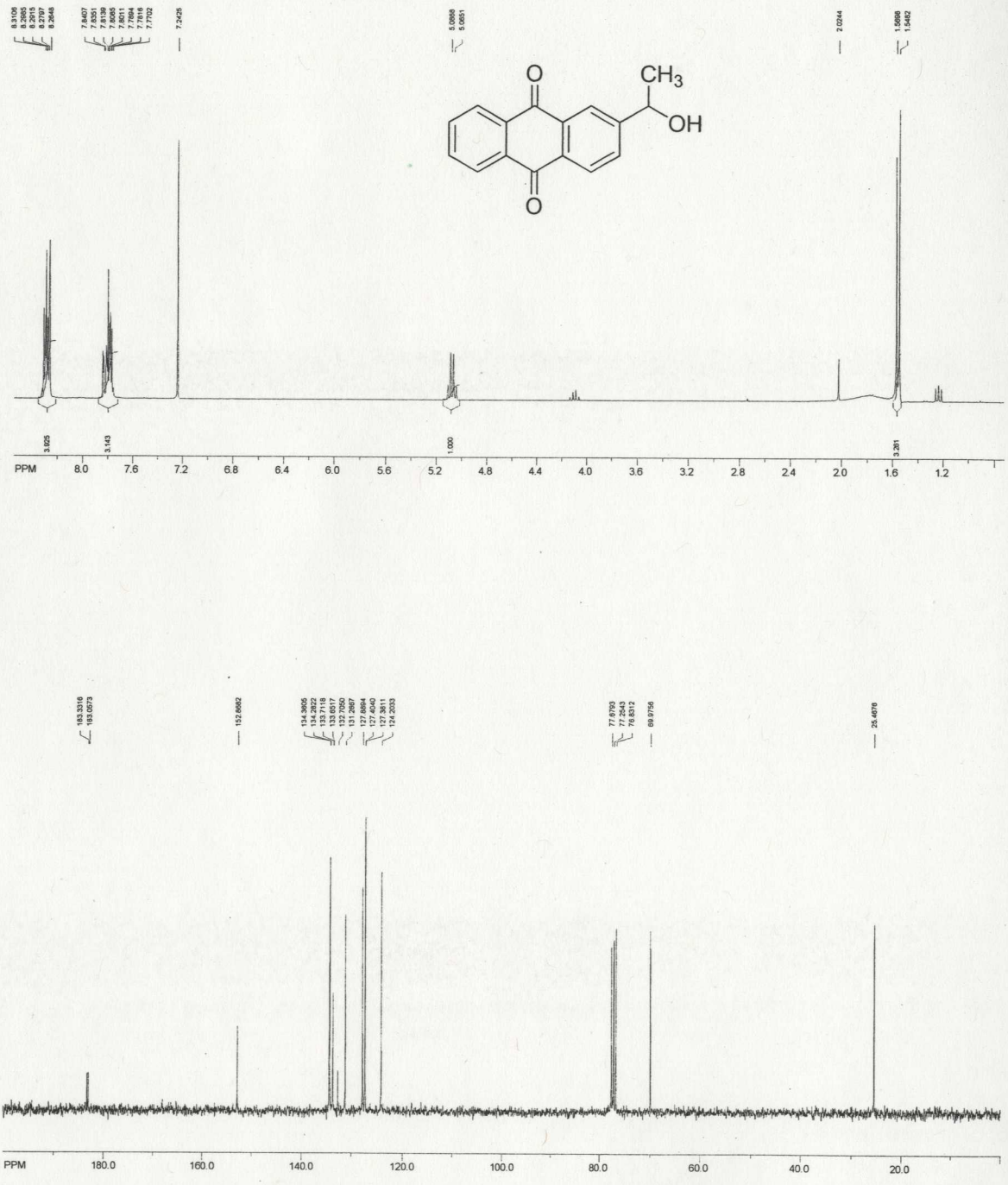

Figure A - 1 ^{1}H (top) and ^{13}C NMR (bottom) for 2-(1-hydroxyethyl)-9,10-anthraquinone (2.1) in $CDCl_3$ at 300 K

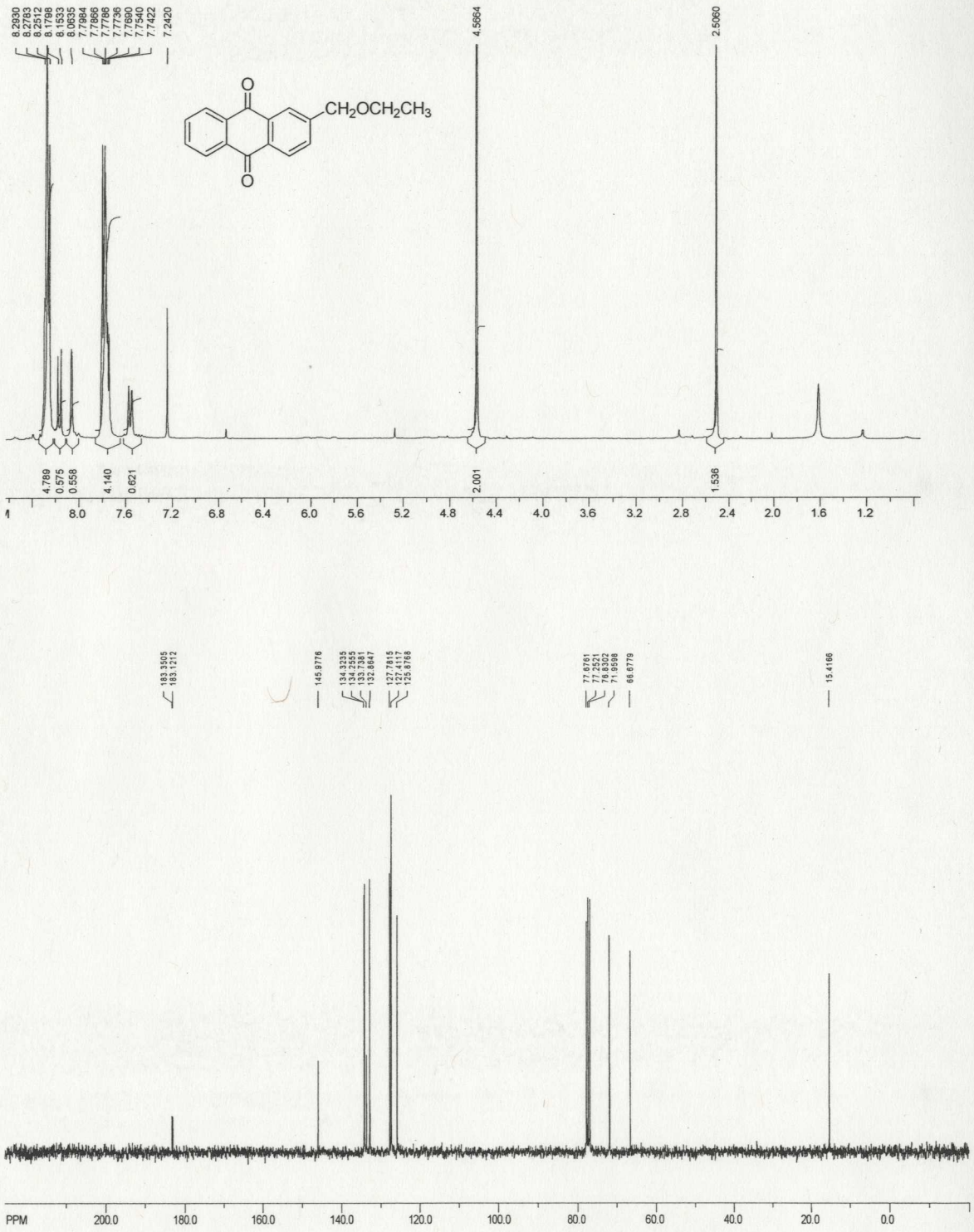

Figure A - 2 ^{1}H (top) and ^{13}C NMR (bottom) for 2-(ethoxymethyl)-9,10-anthraquinone (**2.2**) in $CDCl_3$ at 300 K

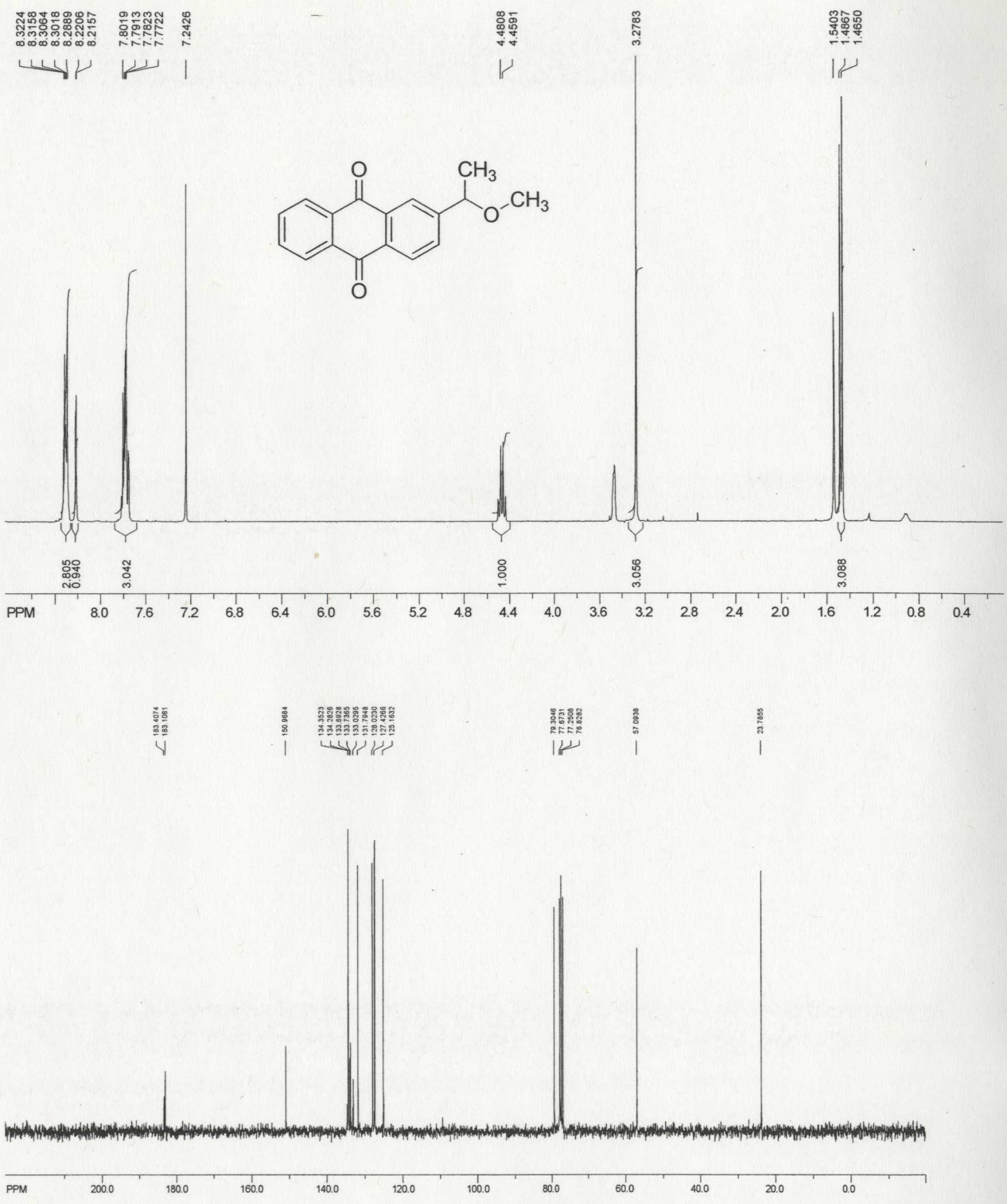

Figure A - 3 ^{1}H (top) and ^{13}C NMR (bottom) for 2-(1-methoxyethyl)-9,10-anthraquinone (**2.3**) in $CDCl_3$ at 300 K

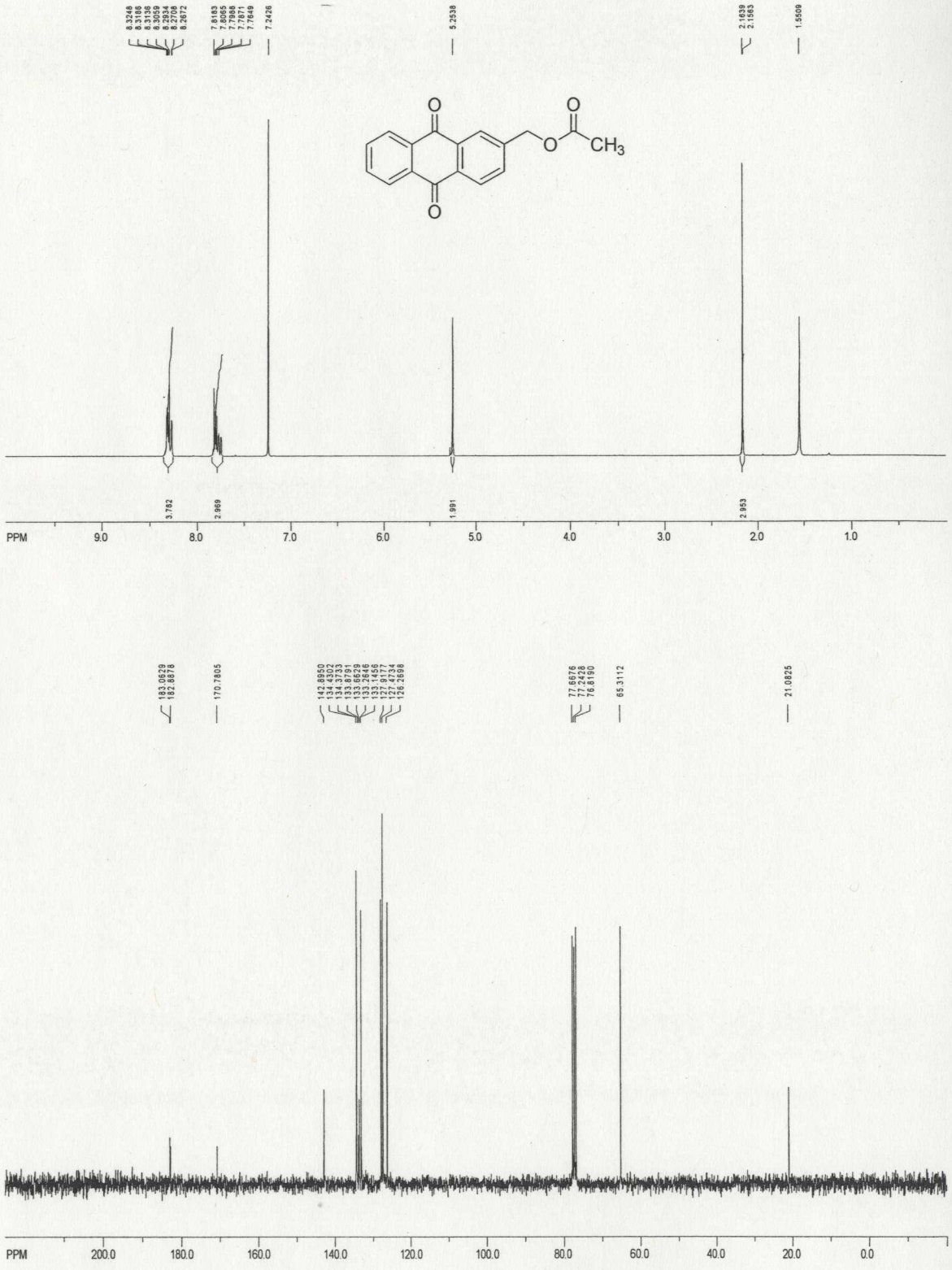

Figure A - 4 ^{1}H (top) and ^{13}C NMR (bottom) for 2-(acetoxymethyl)-9,10-anthraquinone (**2.4**) in $CDCl_3$ at 300 K

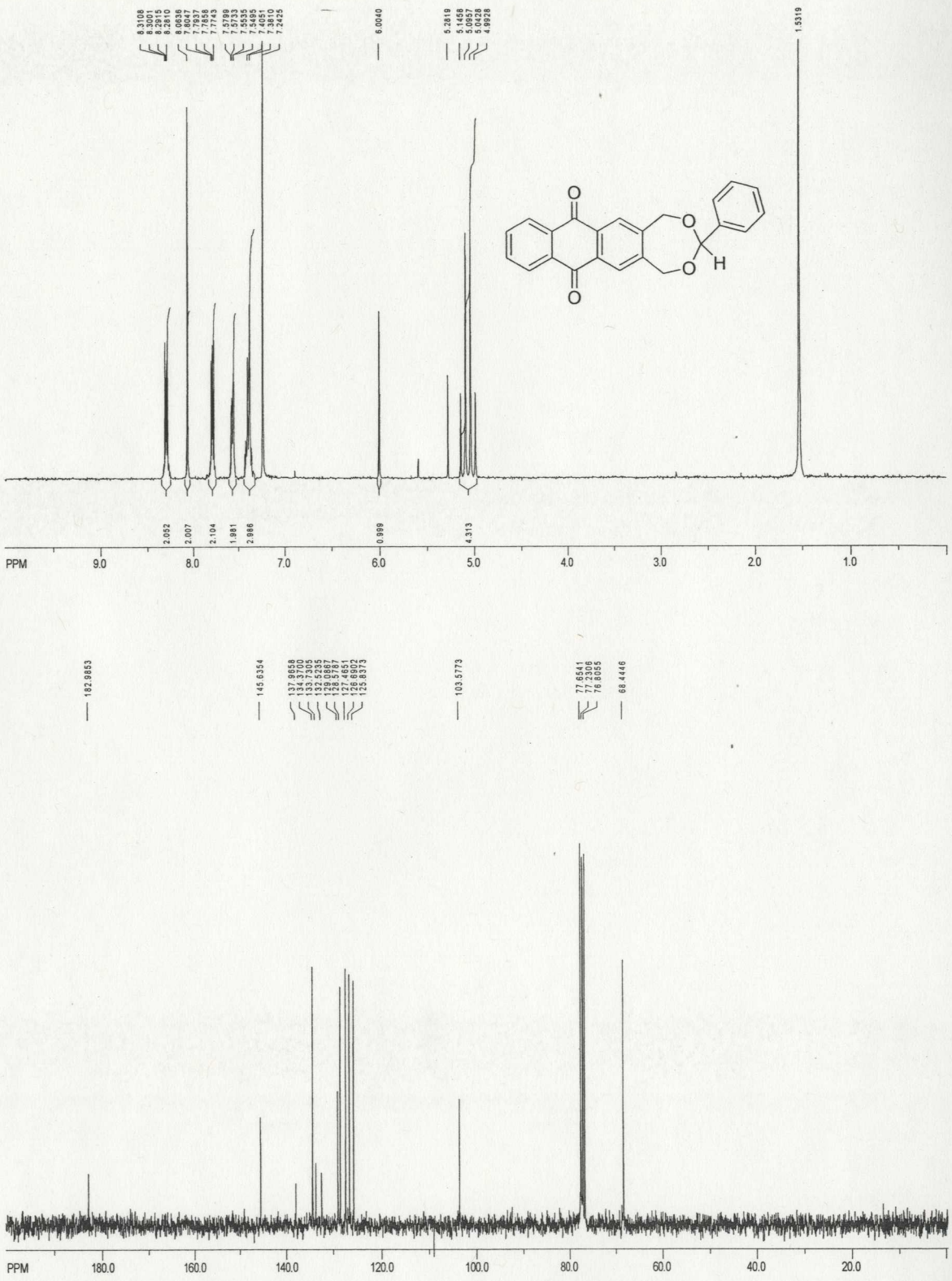

Figure A - 5 ^{1}H (top) and ^{13}C NMR (bottom) for 9-phenyl-7,11-dihydro-8,10-dioxa-cyclohepta [b]anthracene-5,13-dione (**2.5**) in $CDCl_3$ at 300 K.

Figure A - 6 ^{1}H (top) and ^{13}C NMR (bottom) for 9-methyl-9-phenyl-7,11-dihydro-8,10-dioxa-cyclohepta [b]anthracene-5,13-dione (**2.6**) in $CDCl_3$ at 300 K.

Figure A - 7 ^{1}H (top) and ^{13}C NMR (bottom) for 2,3-di(hydroxymethyl)-9,10-anthraquinone (**2.7**) in Acetone-d_6 at 300 K.

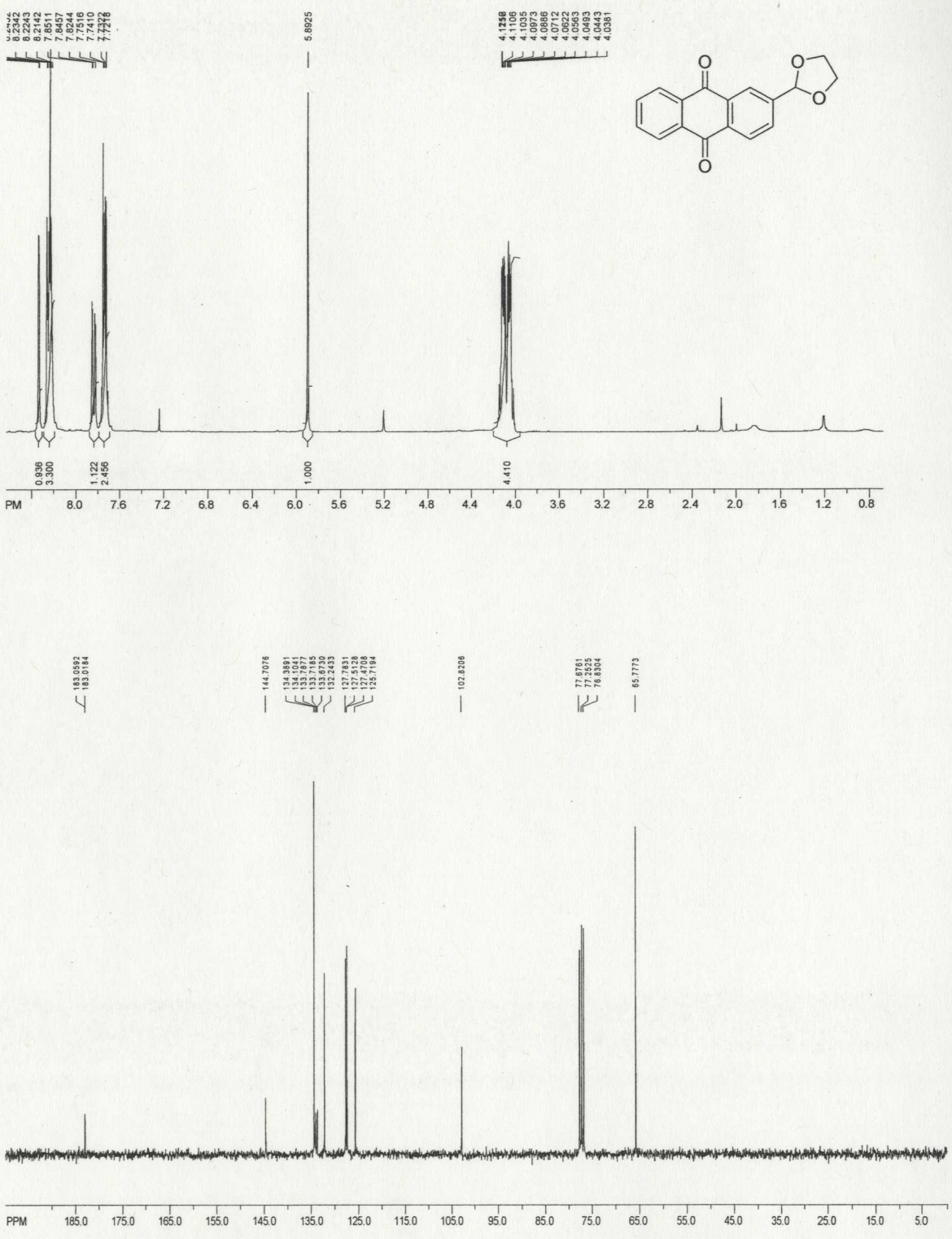

Figure A - 8 ^{1}H (top) and ^{13}C NMR (bottom) for 2-[1,3]dioxolan-2-yl-9,10-anthraquinone (**2.8**) in $CDCl_3$ at 300 K

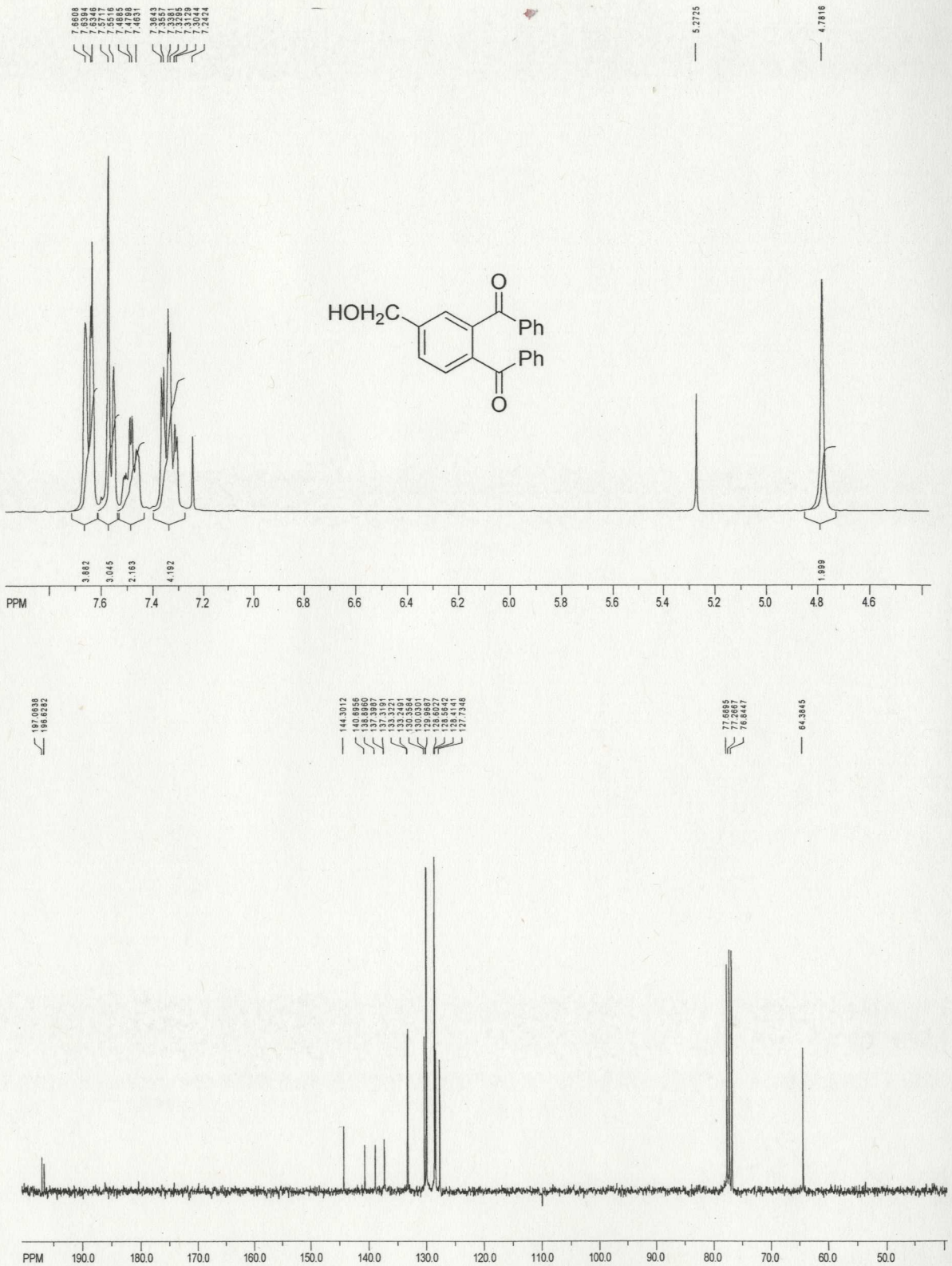

Figure A - 9 ^{1}H (top) and ^{13}C NMR (bottom) for 1,2-dibenzoyl-4-methylbenzene (**2.9**) in $CDCl_3$ at 300 K.

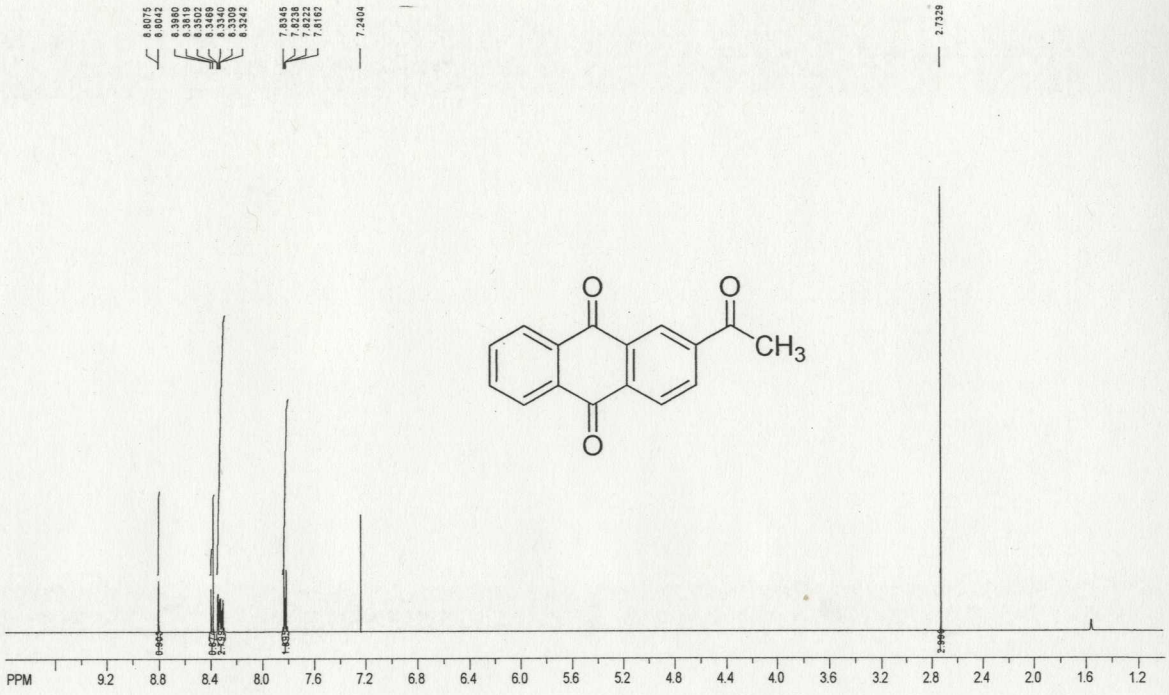

Figure A - 10 ^{1}H for 2-acetyl-9,10-anthraquinone (**2.11**) in $CDCl_3$ at 300 K.

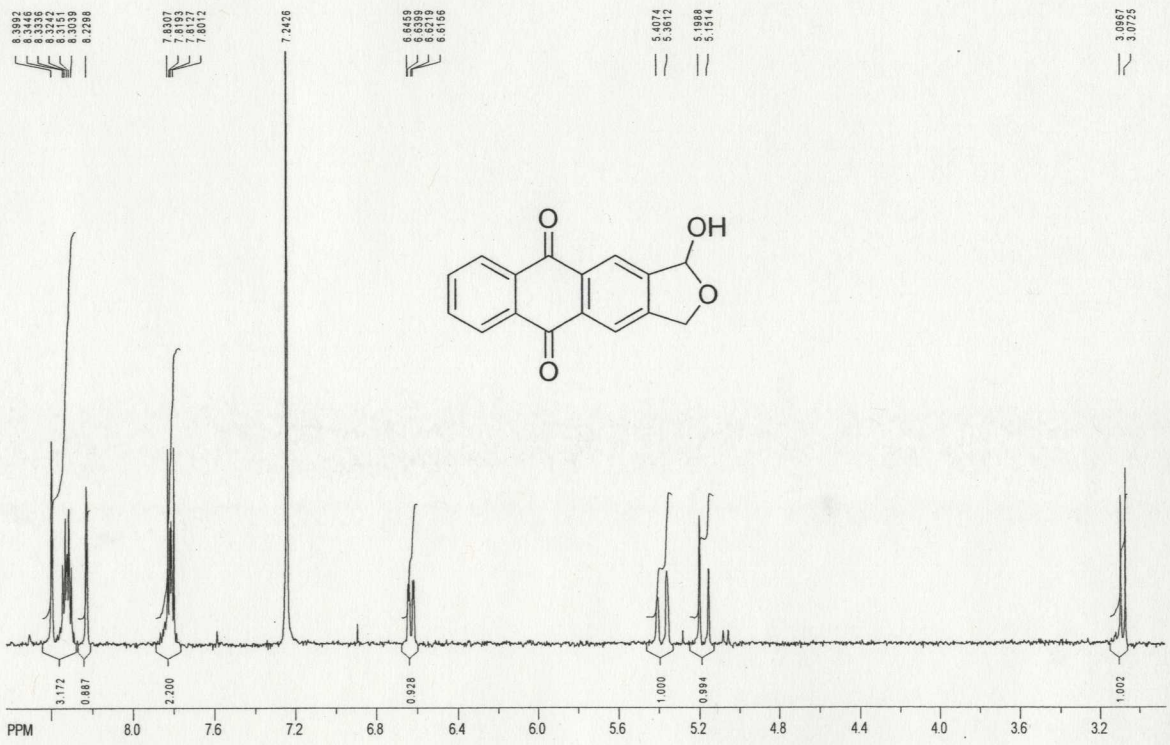

Figure A - 11 ^{1}H for 1-hydroxy-1,3-dihydro-anthra[2,3-*c*]furan-5,10-dione (**2.14**) in $CDCl_3$ at 300 K.

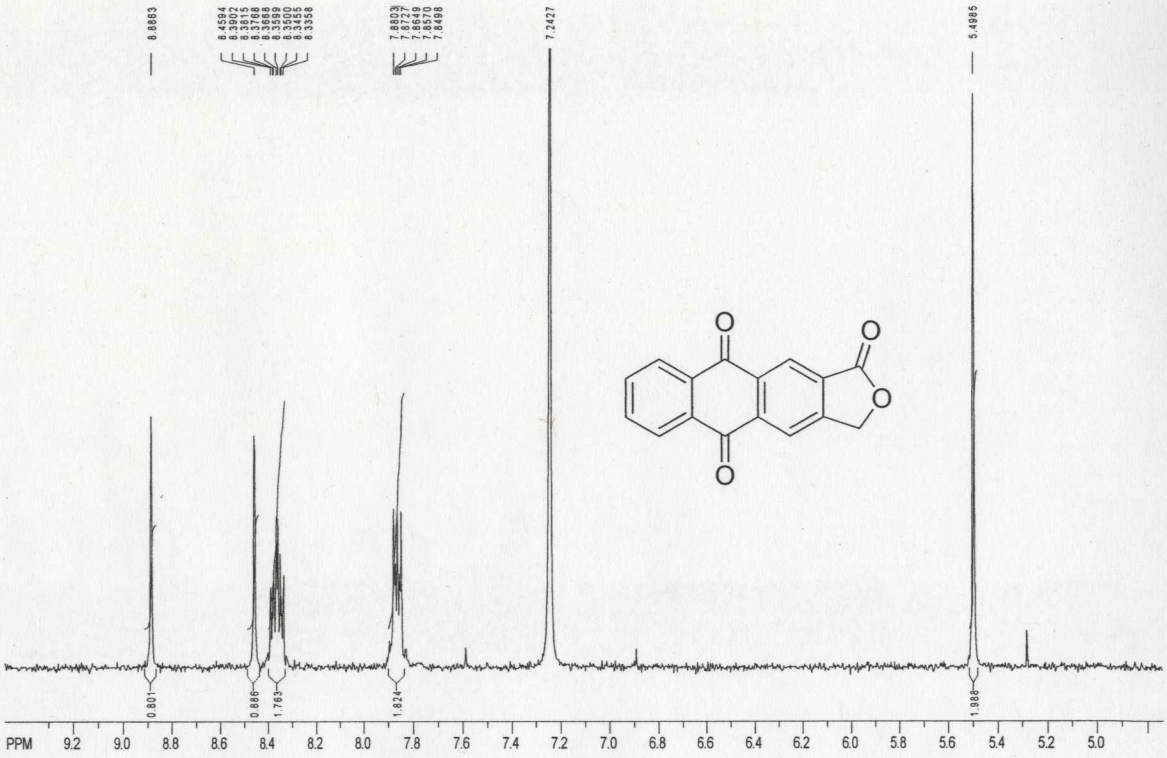

Figure A - 12 ^{1}H for 3*H*-anthra[2,3-*c*]furan-1,5,10-trione **(2.16)** in $CDCl_3$ at 300 K.

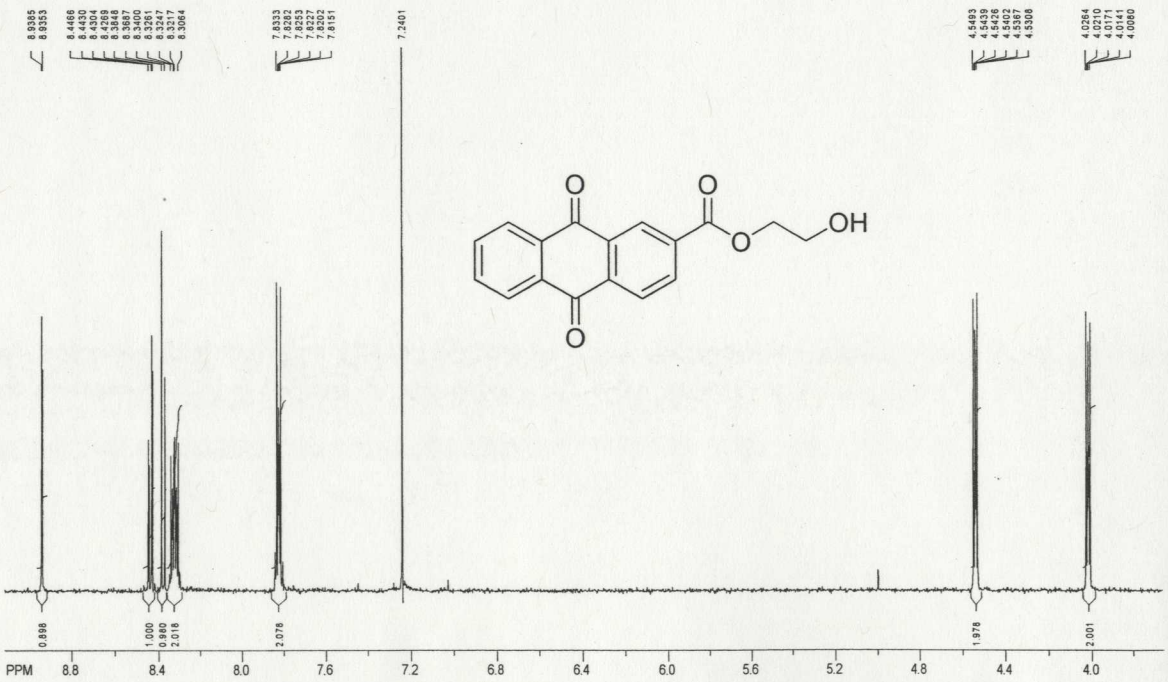

Figure A - 13 ^{1}H for 9,10-dioxo-9,10-dihydroanthracene-2-carboxylic acid 2-hydroxy-ethyl ester **(2.18)** in $CDCl_3$ at 300 K.

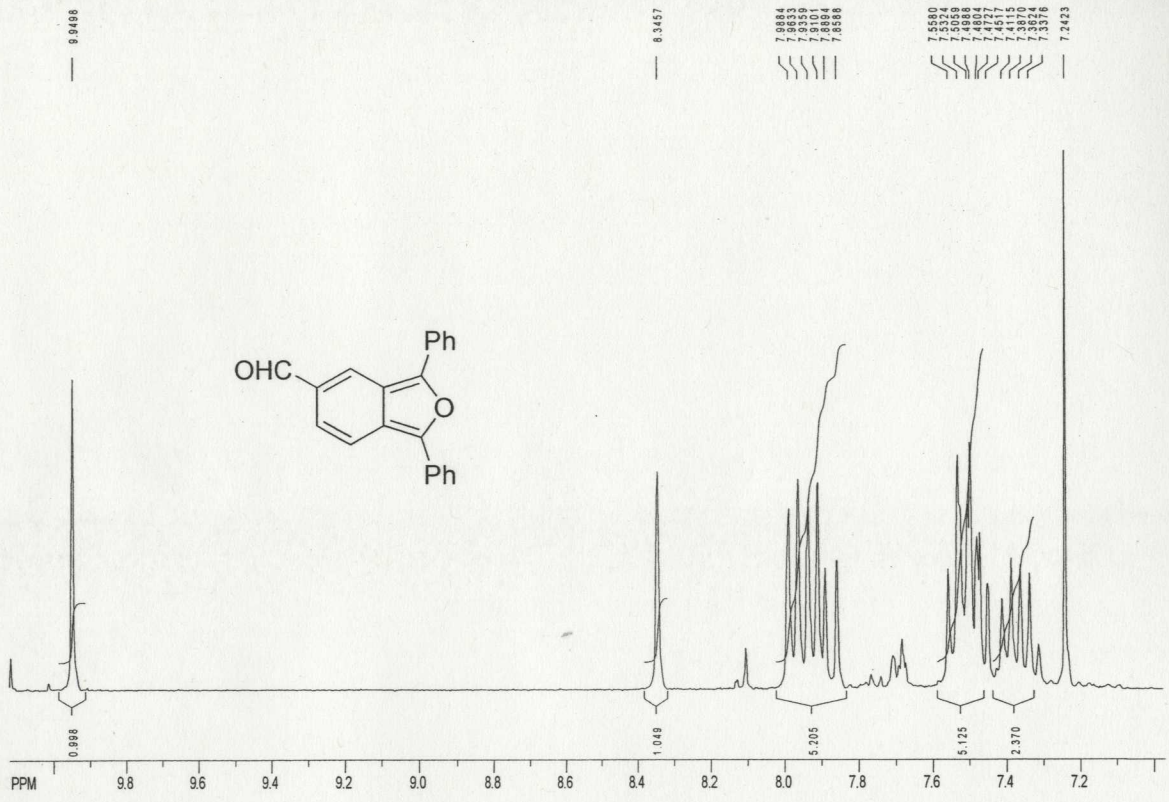

Figure A - 14 ^{1}H for 1,3-diphenyl-isobenzofuran-5-carbaldehyde (**2.29**) in $CDCl_3$ at 300 K.

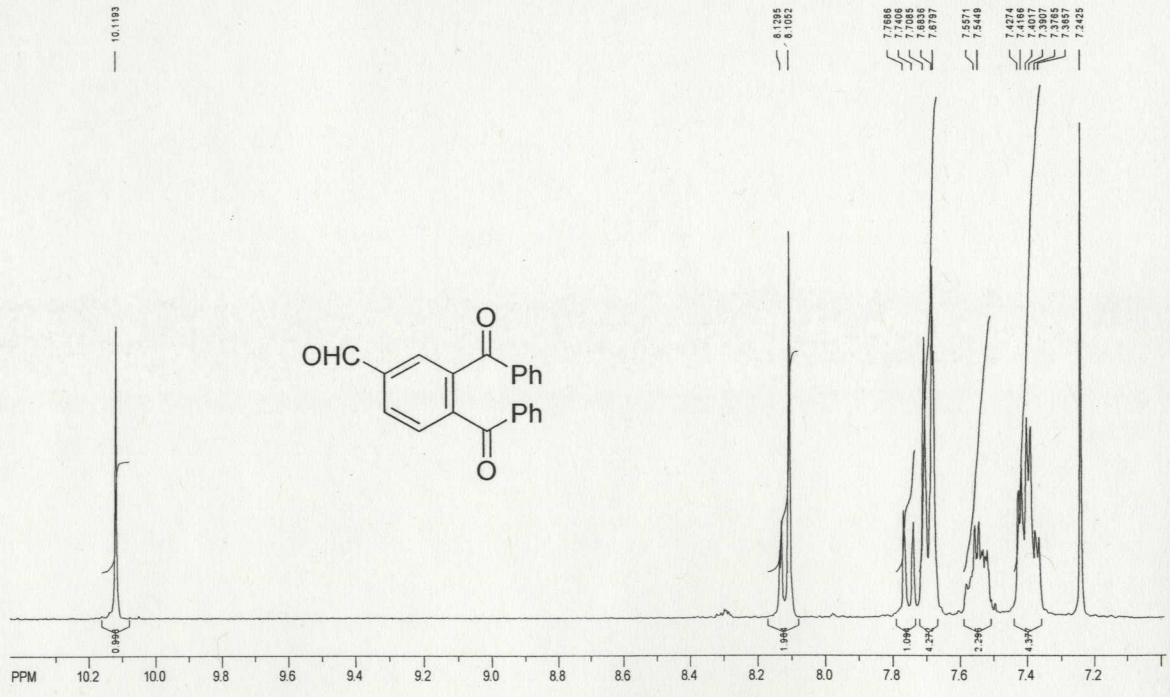

Figure A - 15 ^{1}H for 1,2-dibenzoyl-4-formylbenzene (**2.30**) in $CDCl_3$ at 300 K.

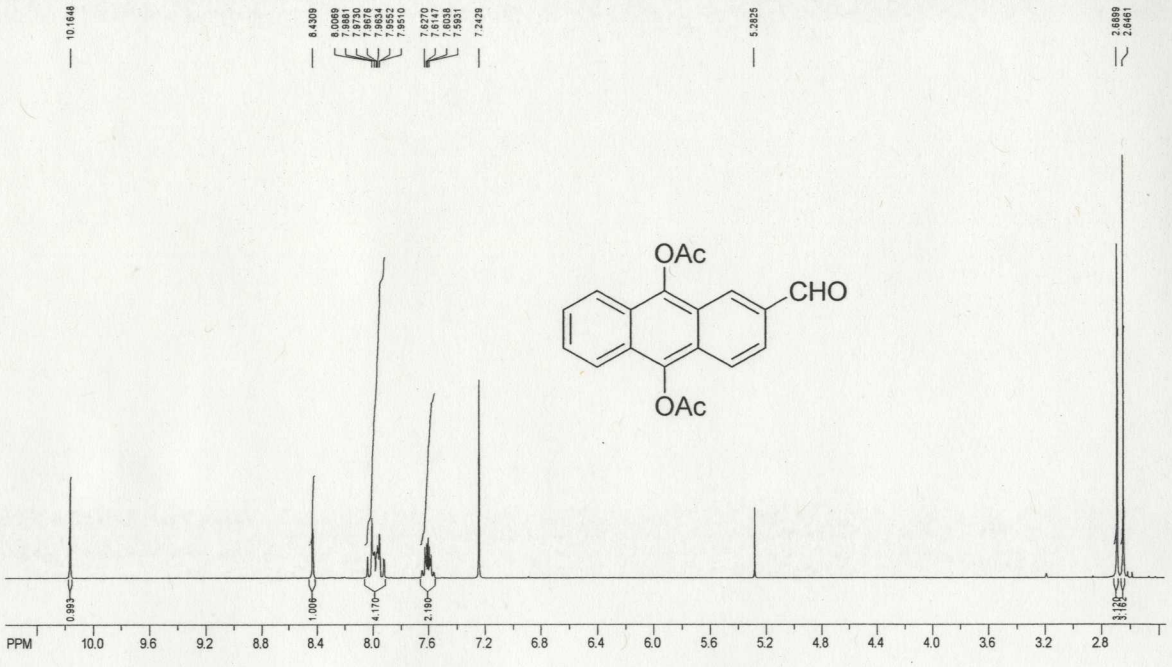

Figure A - 16 ^{1}H for 2-formyl-9,10-diacetoxyanthracene (**2.34**) in $CDCl_3$ at 300 K.

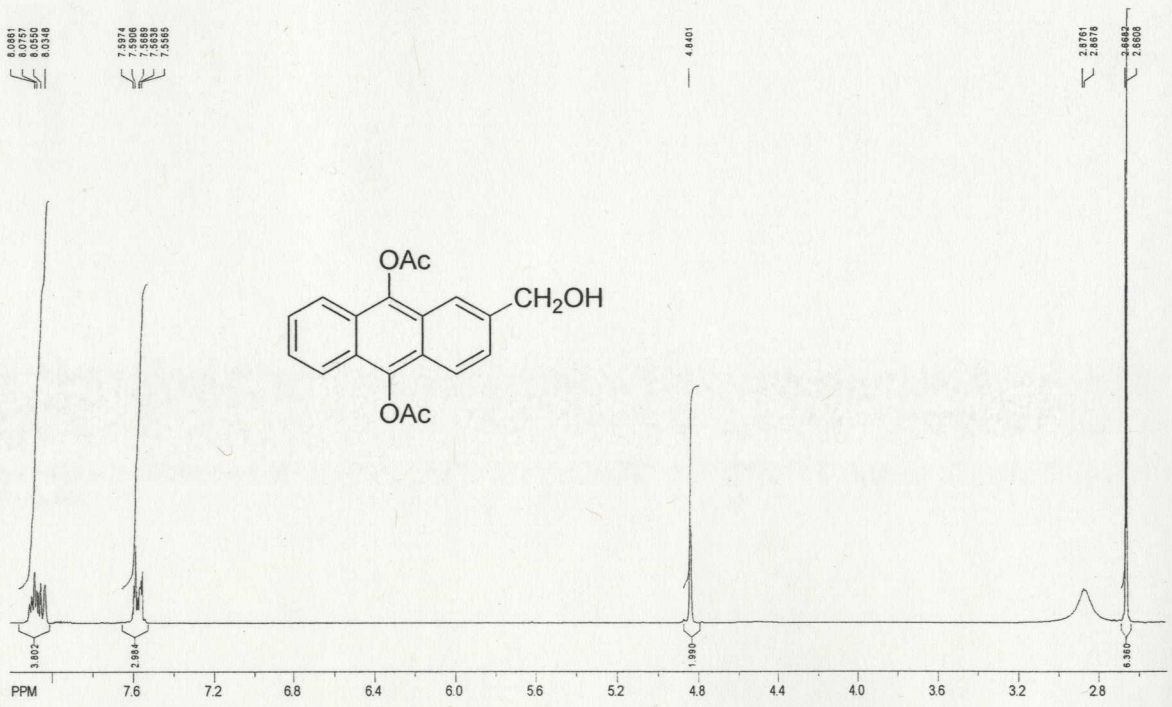

Figure A - 17 ^{1}H for 2-(hydroxymethyl)-9,10-diacetoxyanthracene (**2.35**) in Acetone-d_6 at 300 K.

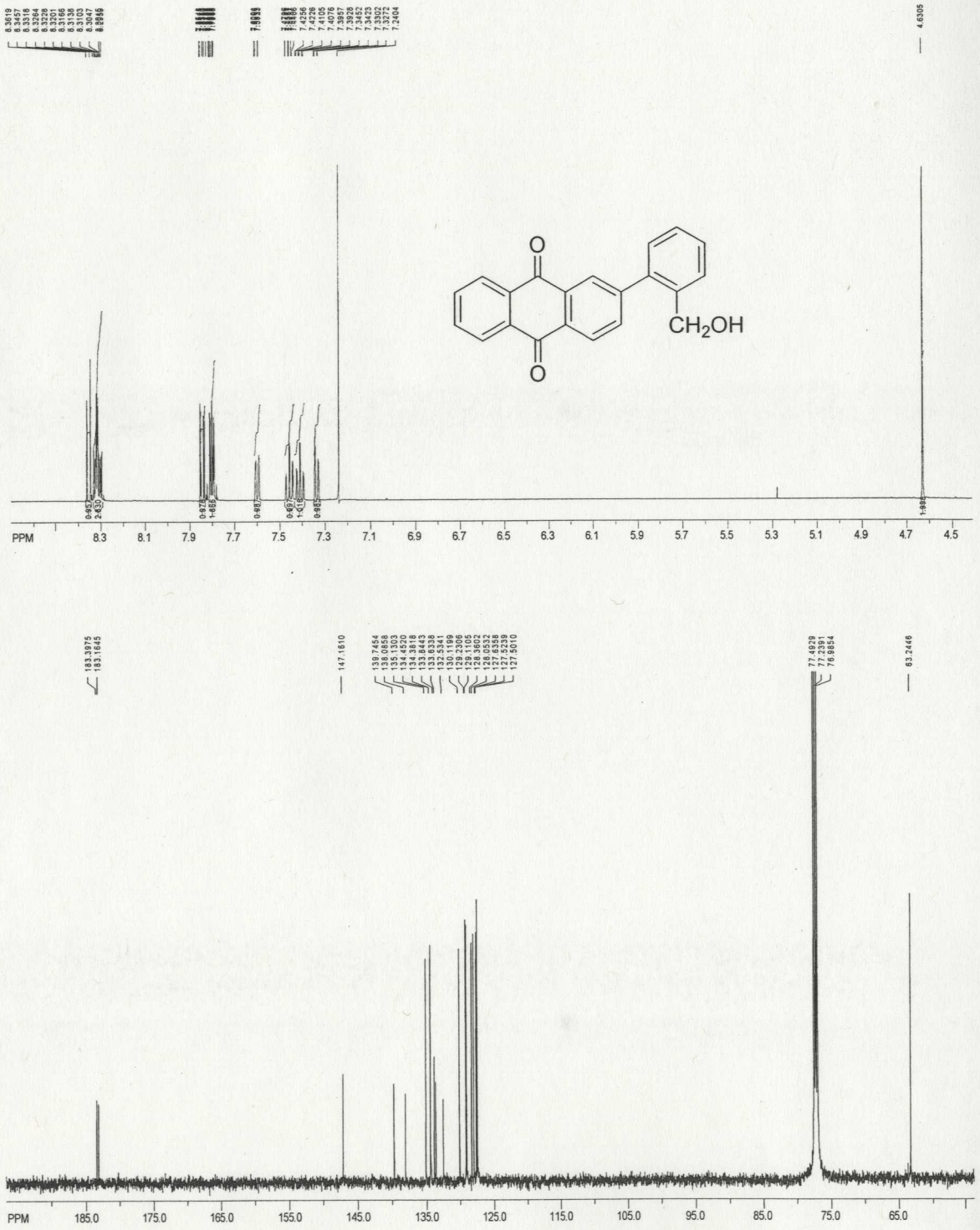

Figure A - 18 ^{1}H (top) and ^{13}C NMR (bottom) for 2-(*o*-hydroxymethylphenyl)-9,10-anthraquinone (**3.1**) in $CDCl_3$ at 300 K.

Figure A - 19 ^{1}H (top) and ^{13}C NMR (bottom) for 2-(*o*-methylphenyl)-9,10-anthraquinone (**3.1a**) in $CDCl_3$ at 300 K

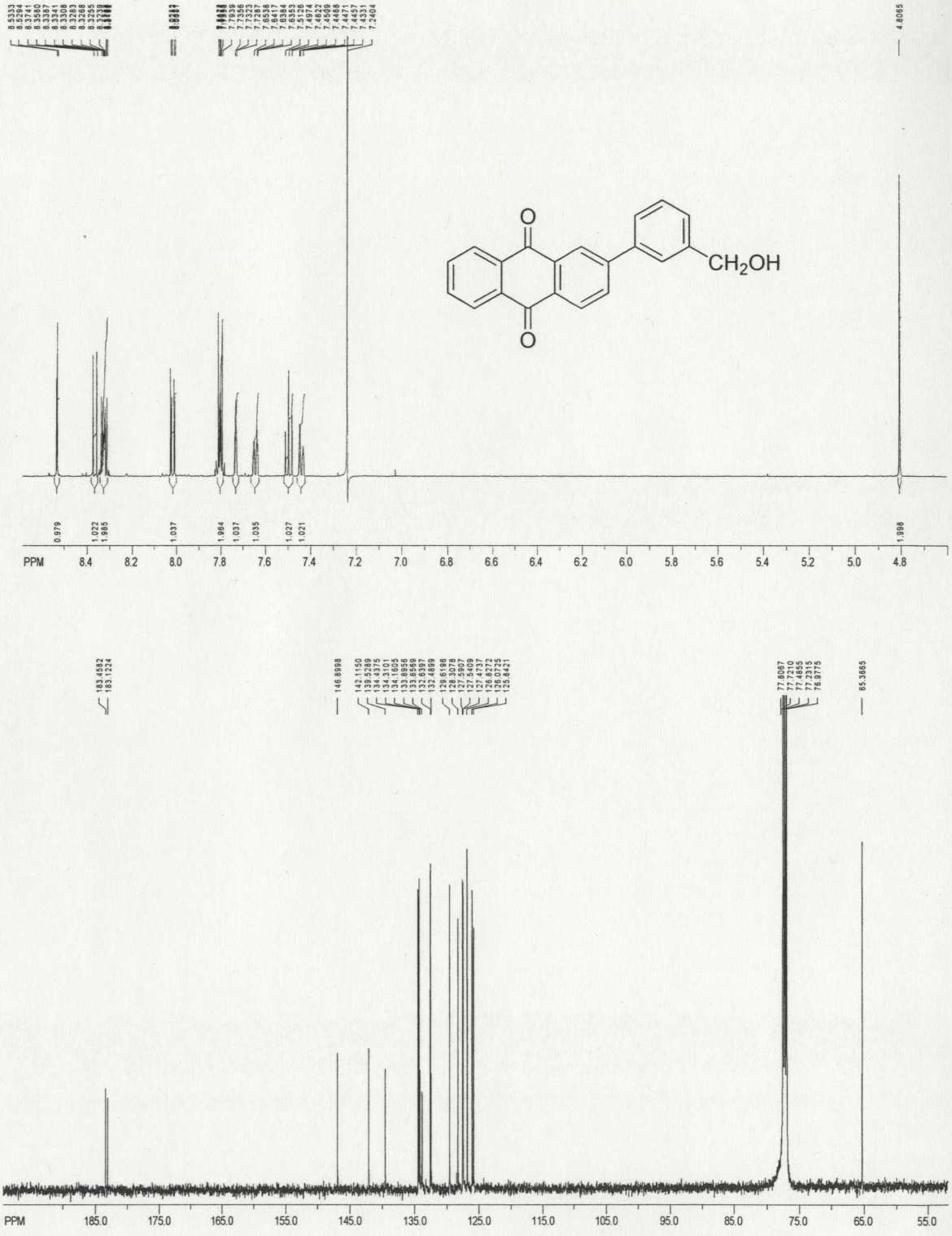

Figure A - 20 ^{1}H (top) and ^{13}C NMR (bottom) for 2-(*m*-hydroxymethylphenyl)-9,10-anthraquinone (**3.2**) in $CDCl_3$ at 300 K.

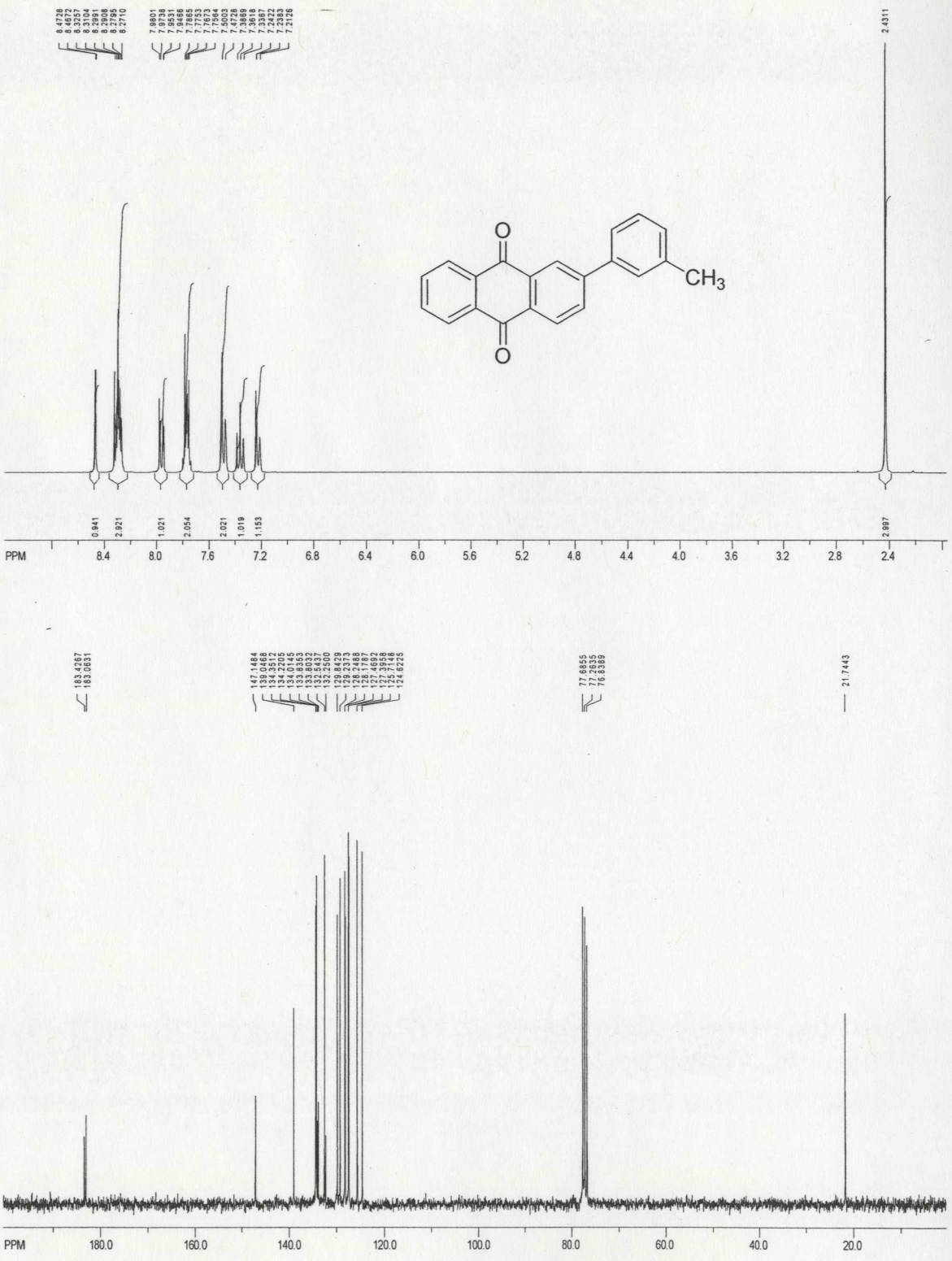

Figure A - 21 ^{1}H (top) and ^{13}C NMR (bottom) for 2-(*m*-methylphenyl)-9,10-anthraquinone (**3.2a**) in $CDCl_3$ at 300 K.

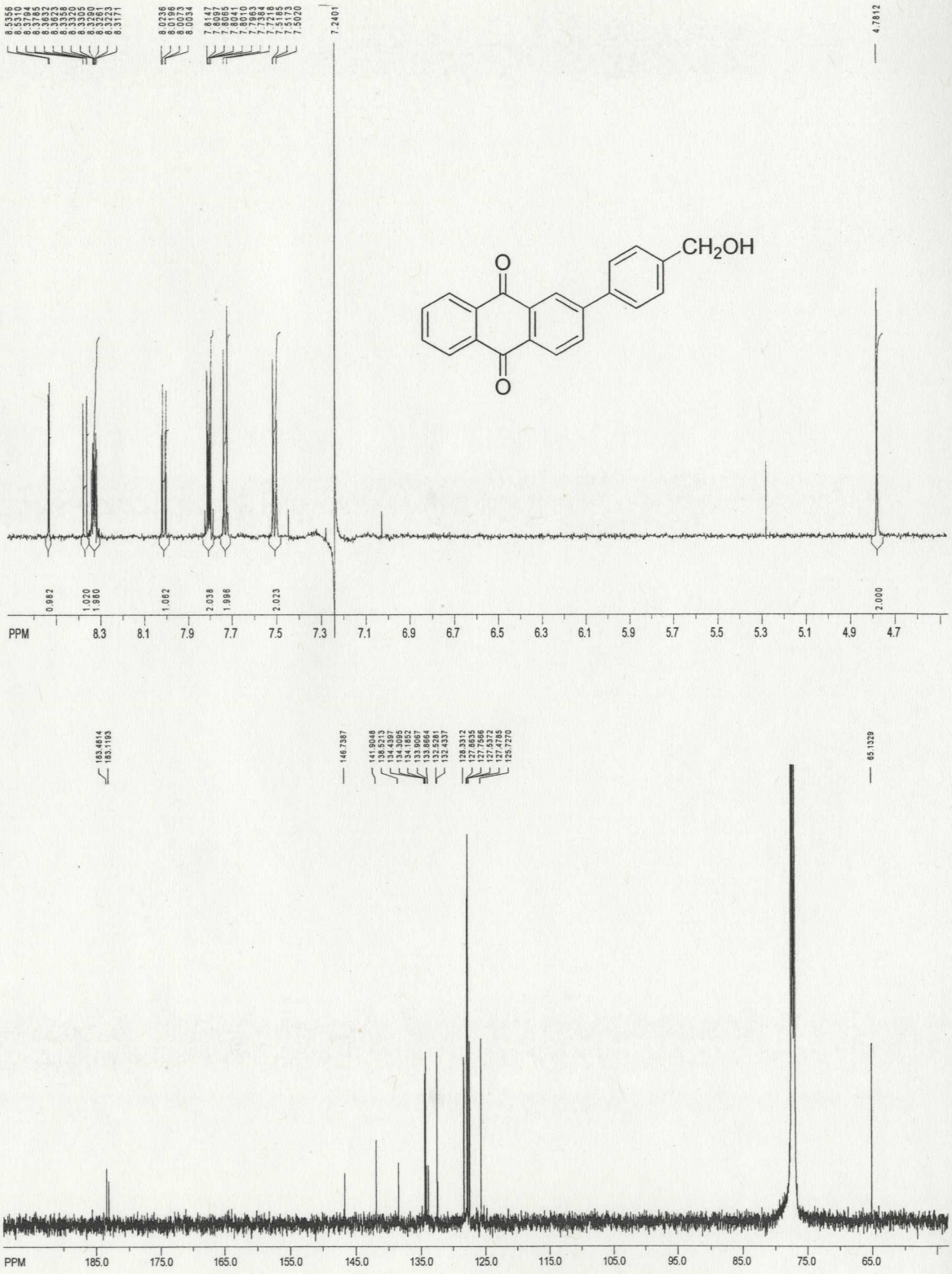

Figure A - 22 ^{1}H (top) and ^{13}C NMR (bottom) for 2-(*p*-hydroxymethylphenyl)-9,10-anthraquinone (**3.3**) in $CDCl_3$ at 300 K.

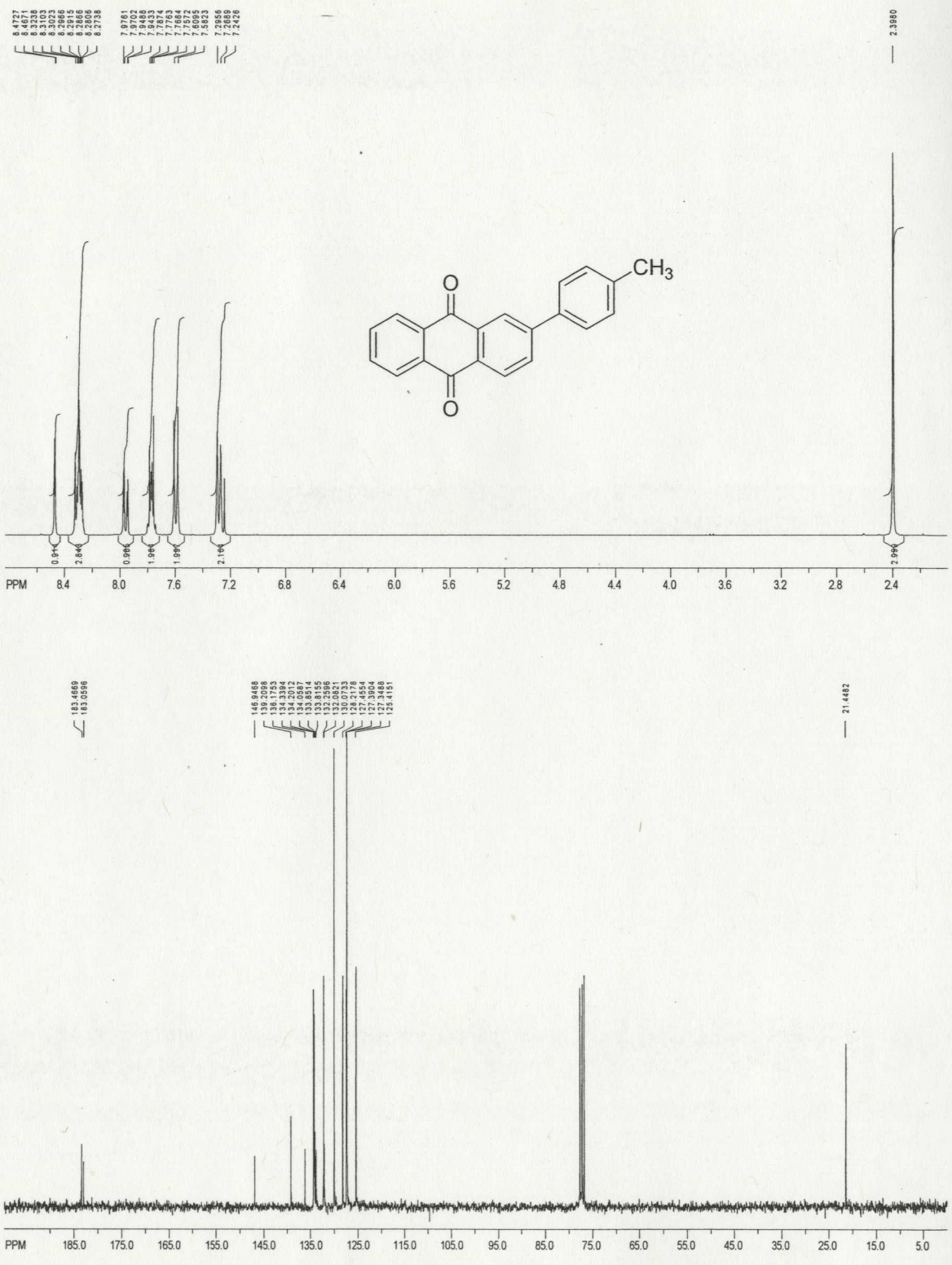

Figure A - 23 ^{1}H (top) and ^{13}C NMR (bottom) for 2-(*p*-methylphenyl)-9,10-anthraquinone (**3.3a**) in $CDCl_3$ at 300 K

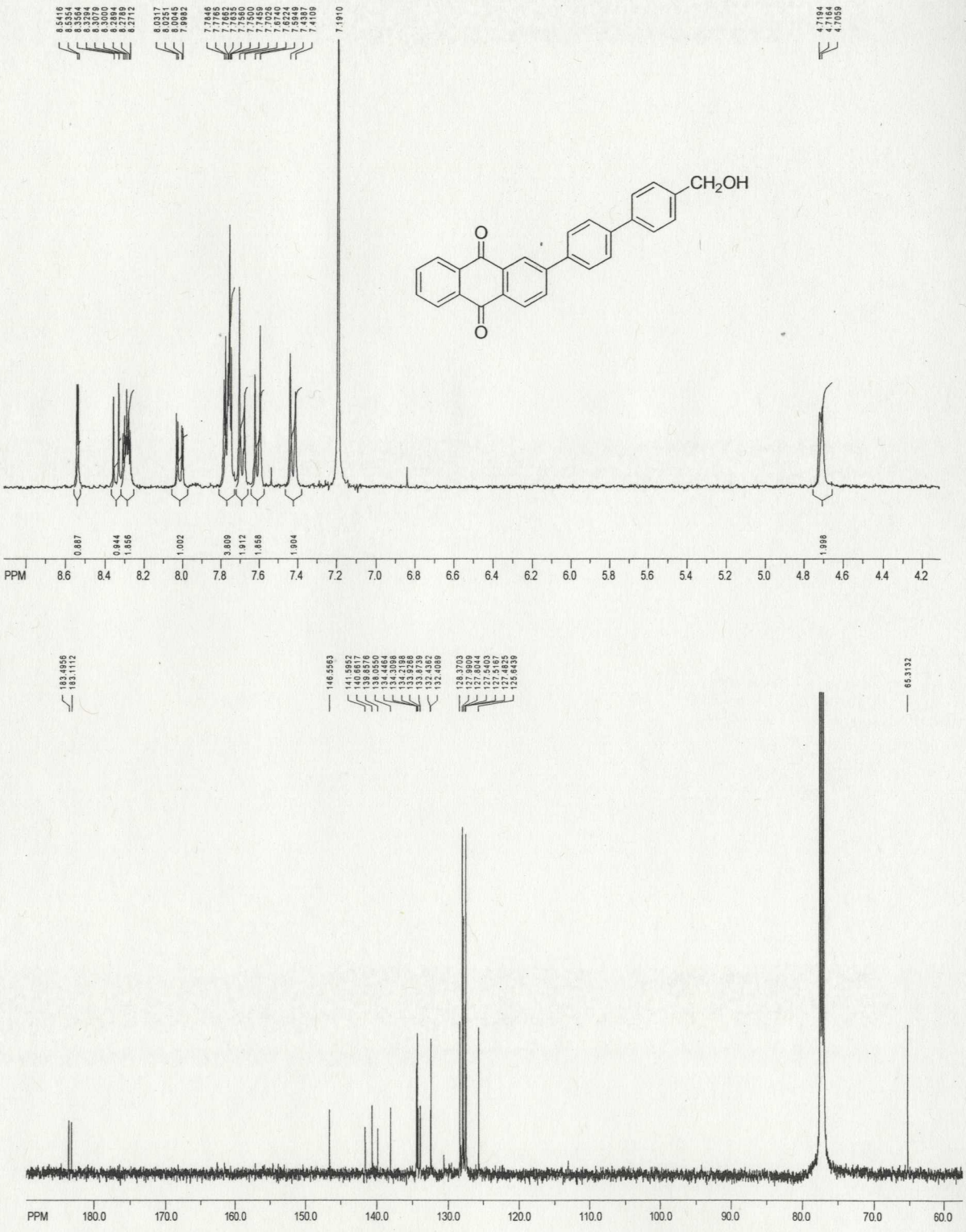

Figure A - 24 ^{1}H (top) and ^{13}C NMR (bottom) for 2-(*p*-hydroxymethylbiphenyl)-9,10-anthraquinone (**3.4**) in $CDCl_3$ at 300 K.

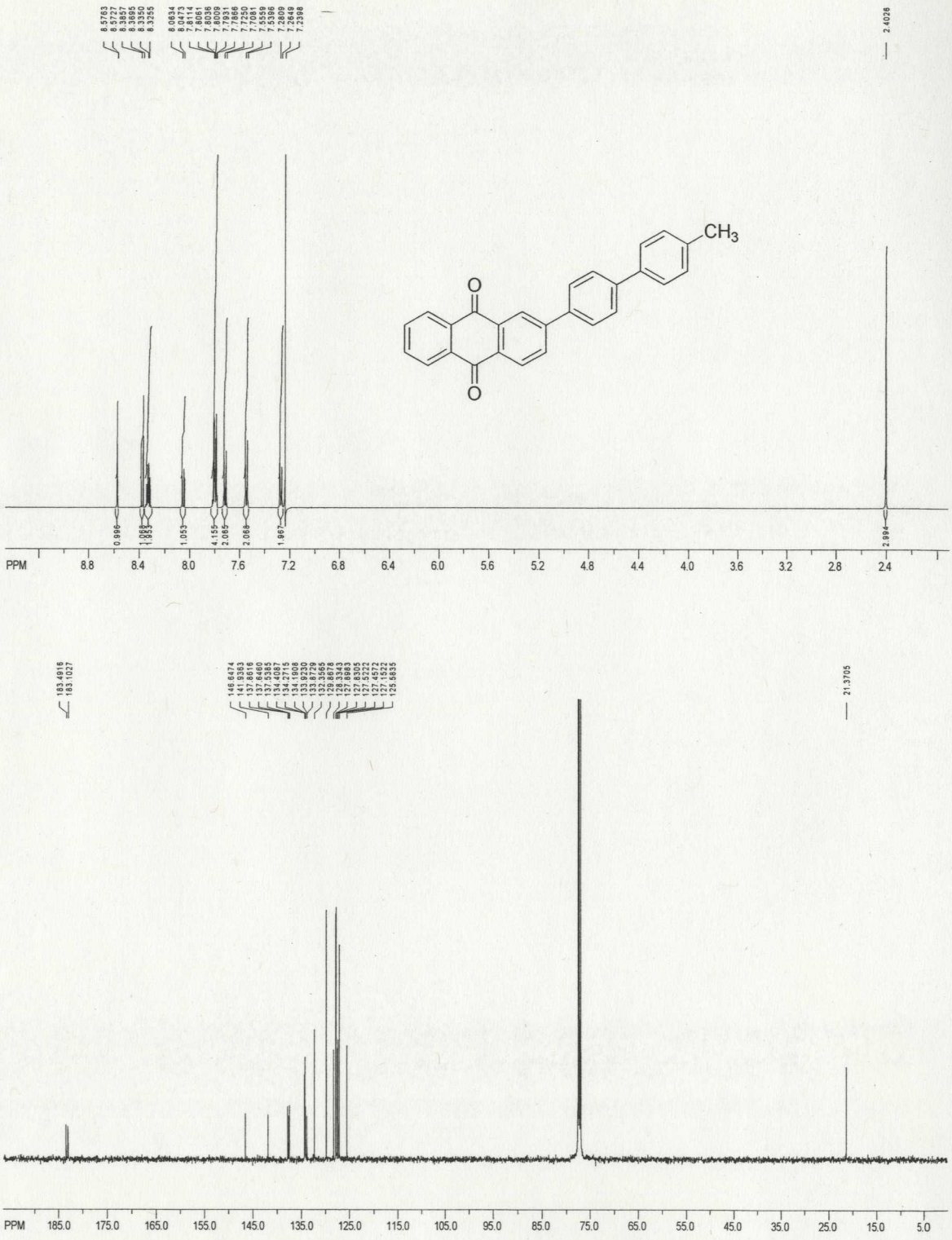

Figure A - 25 ^{1}H (top) and ^{13}C NMR (bottom) for 2-(*p*-methylbiphenyl)-9,10-anthraquinone (**3.4a**) in $CDCl_3$ at 300 K.

Figure A - 26 ^{1}H (top) and ^{13}C NMR (bottom) for 2-(*o*-formylphenyl)-9,10-anthraquinone (**3.8**) in $CDCl_3$ at 300 K.

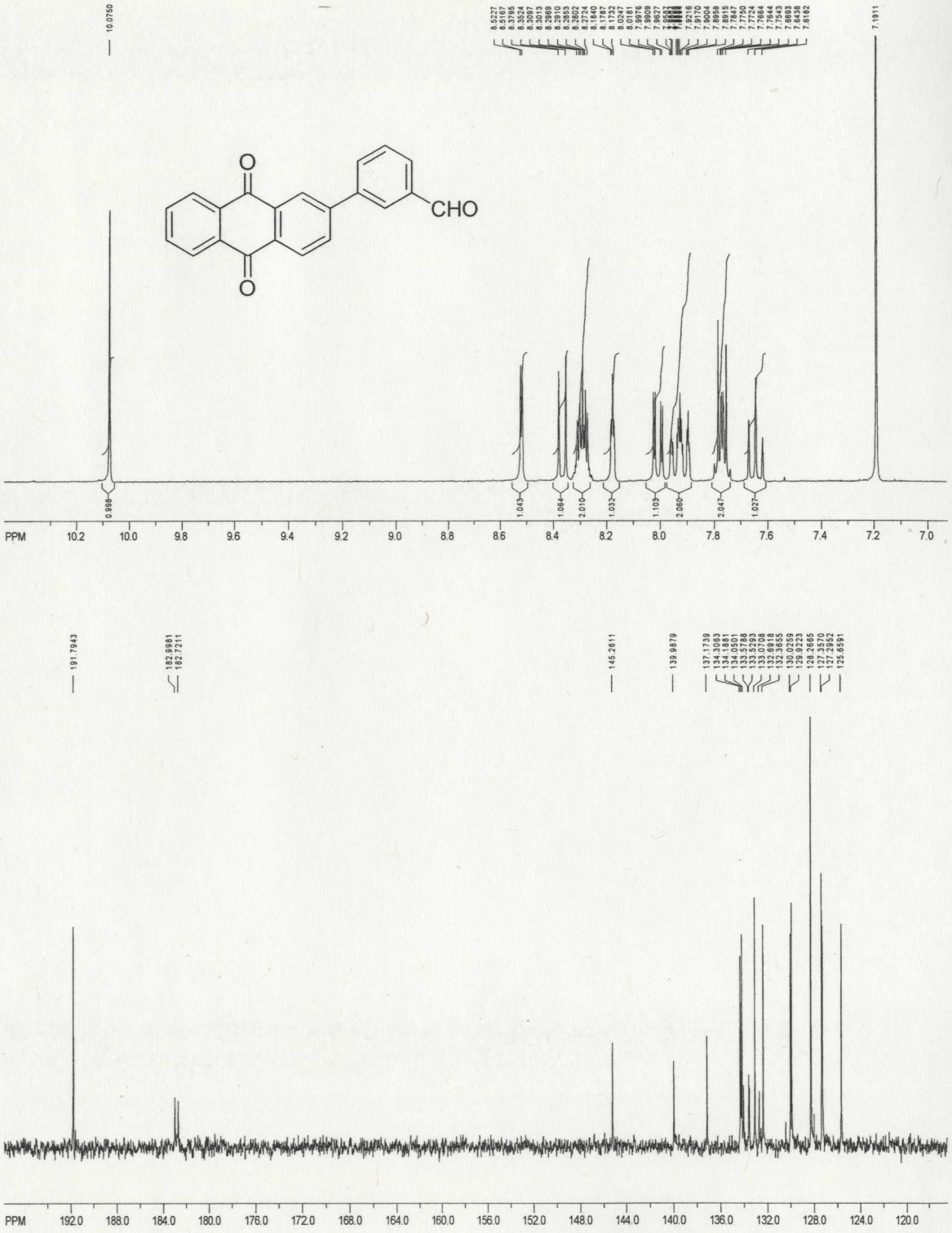

Figure A - 27 ^{1}H (top) and ^{13}C NMR (bottom) for 2-(*m*-formylphenyl)-9,10-anthraquinone (**3.9**) in $CDCl_3$ at 300 K.

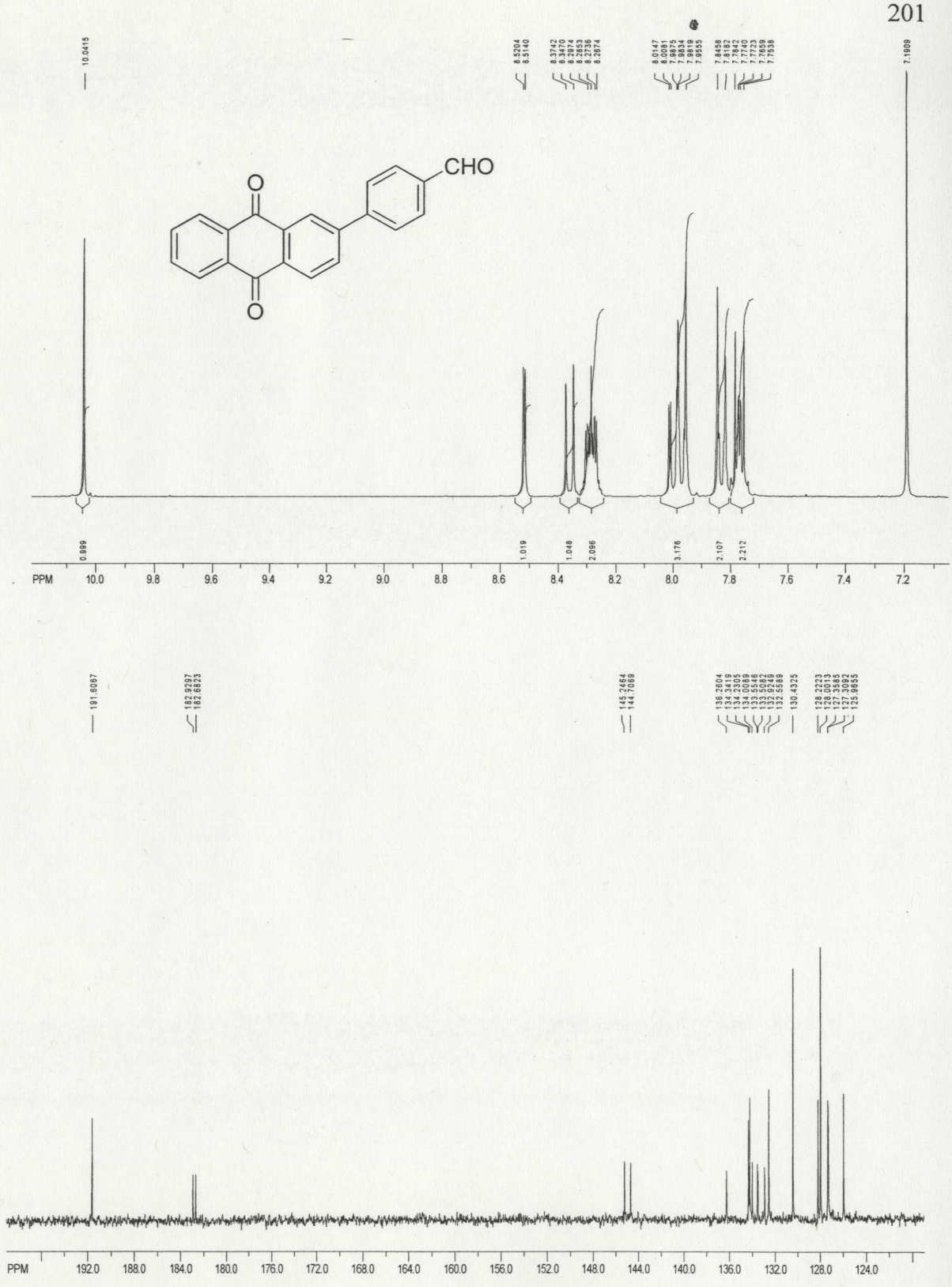

Figure A - 28 ^{1}H (top) and ^{13}C NMR (bottom) for 2-(*p*-formylphenyl)-9,10-anthraquinone (**3.10**) in $CDCl_3$ at 300 K.

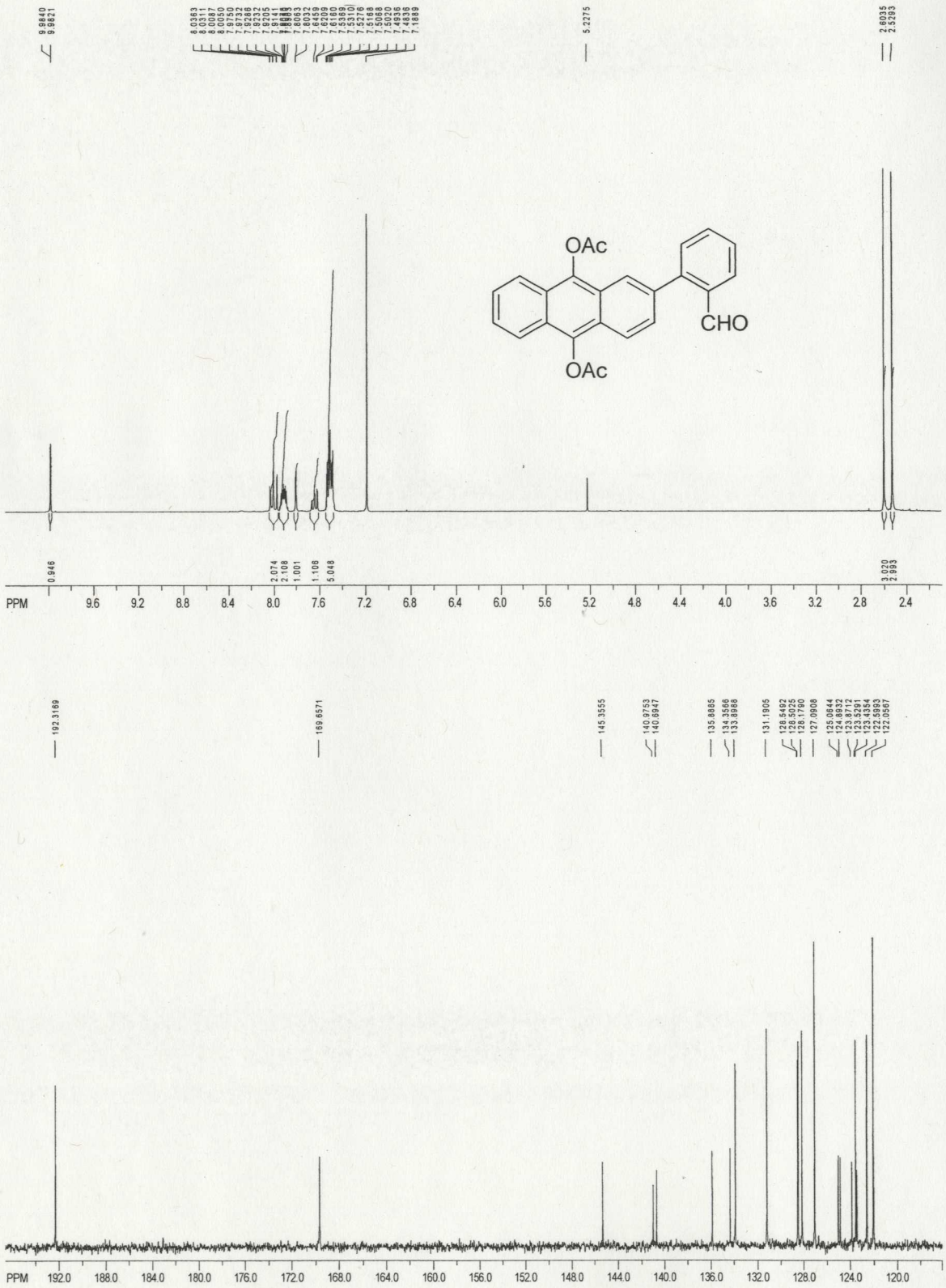

Figure A - 29 ^{1}H (top) and ^{13}C NMR (bottom) for 2-(*o*-formylphenyl)-9,10-diacetoxyanthracene (**3.11-OAC**) in $CDCl_3$ at 300 K.

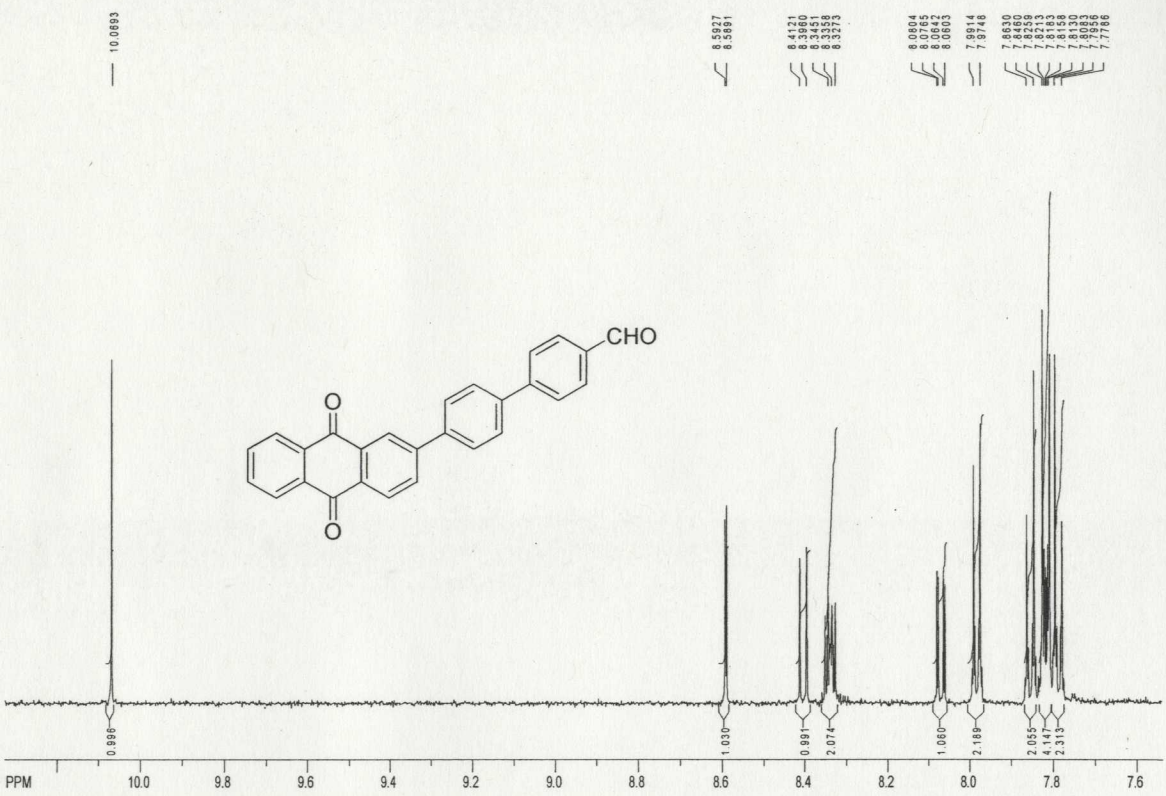

Figure A - 30 ^{1}H (top) and ^{13}C NMR (bottom) for 2-(*p*-formylbiphenyl)-9,10-anthraquinone (**3.14**) in $CDCl_3$ at 300 K.

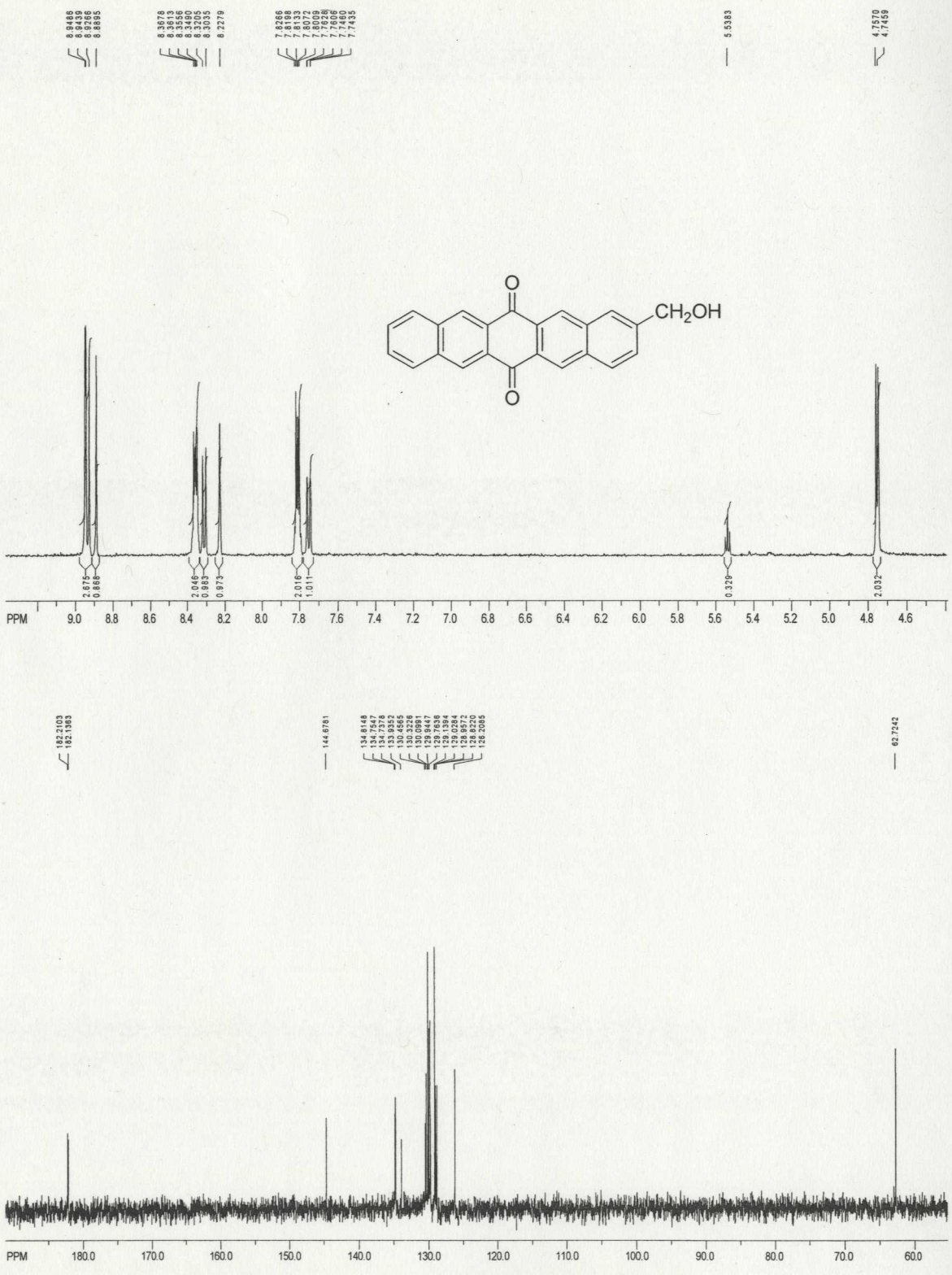

Figure A - 31 ^{1}H (top) and ^{13}C NMR (bottom) for 2-(hydroxymethyl)-6,13-pentacenequinone (**4.1**) in DMSO-d_6 at 300 K.

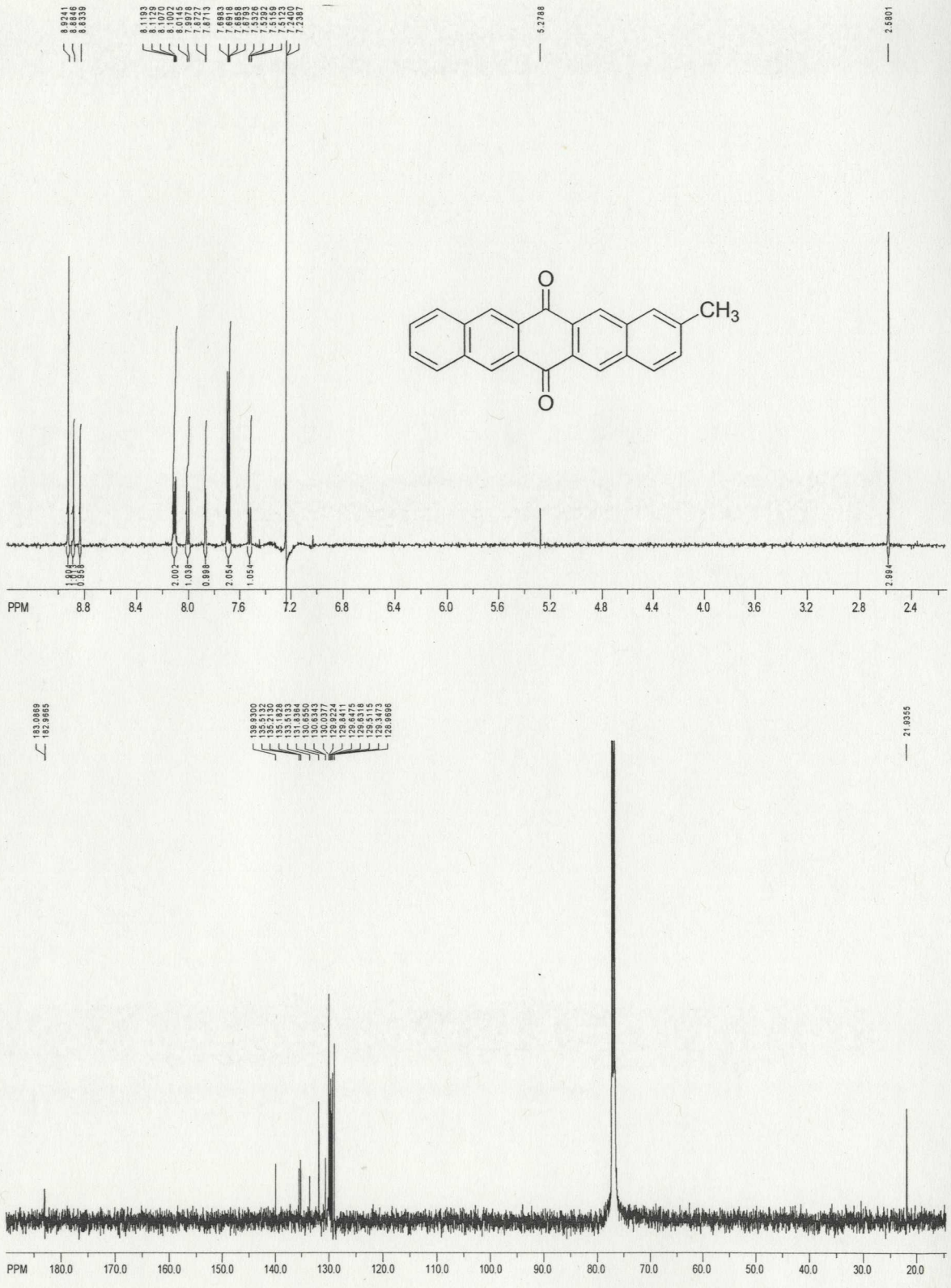

Figure A - 32 ^{1}H (top) and ^{13}C NMR (bottom) for 2-methyl-6,13-pentacenequinone (**4.1a**) in $CDCl_3$ at 300 K.

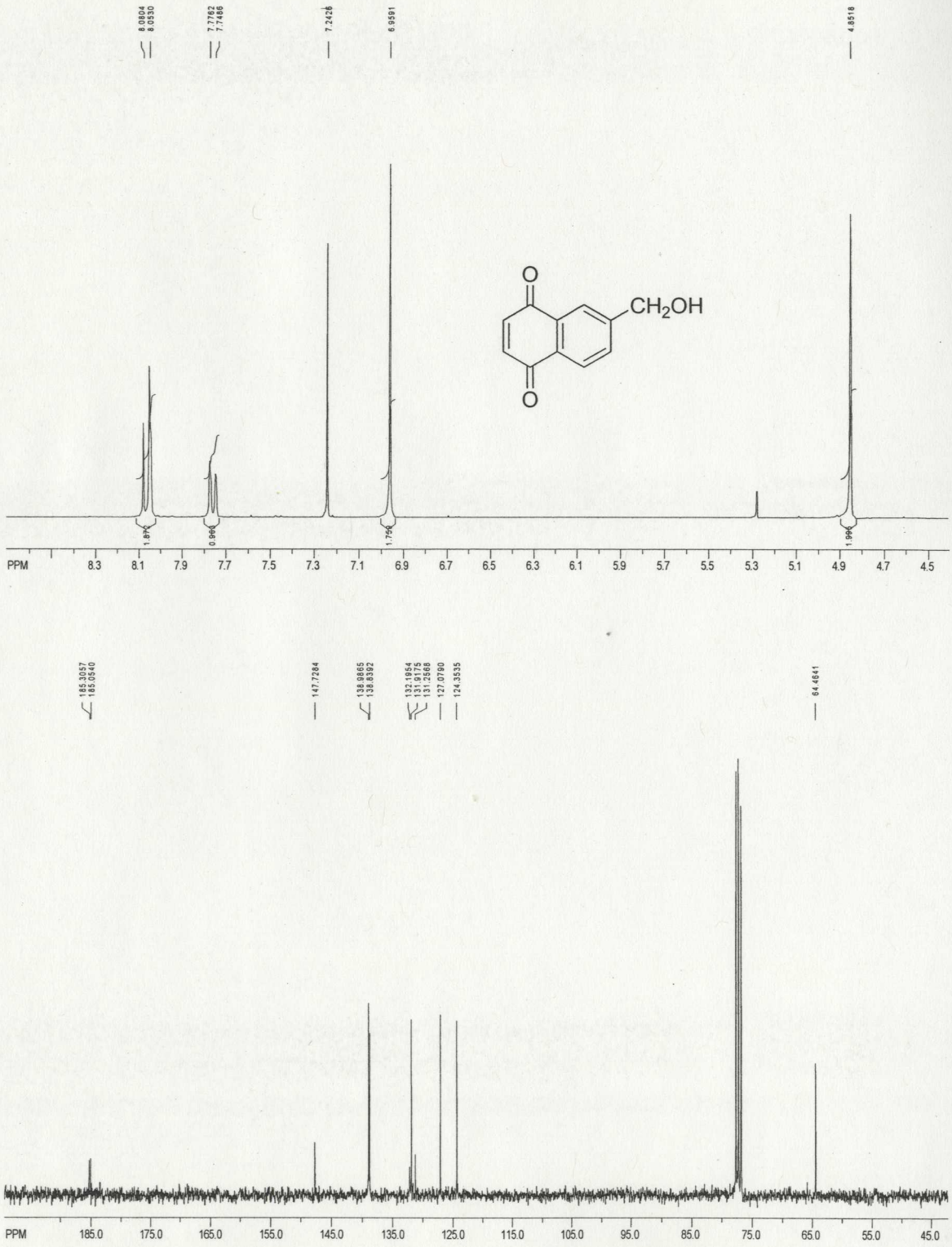

Figure A - 33 ^{1}H (top) and ^{13}C NMR (bottom) for 6-(hydroxymethyl)-1,4-naphthoquinone (**4.2**) in $CDCl_3$ at 300 K.

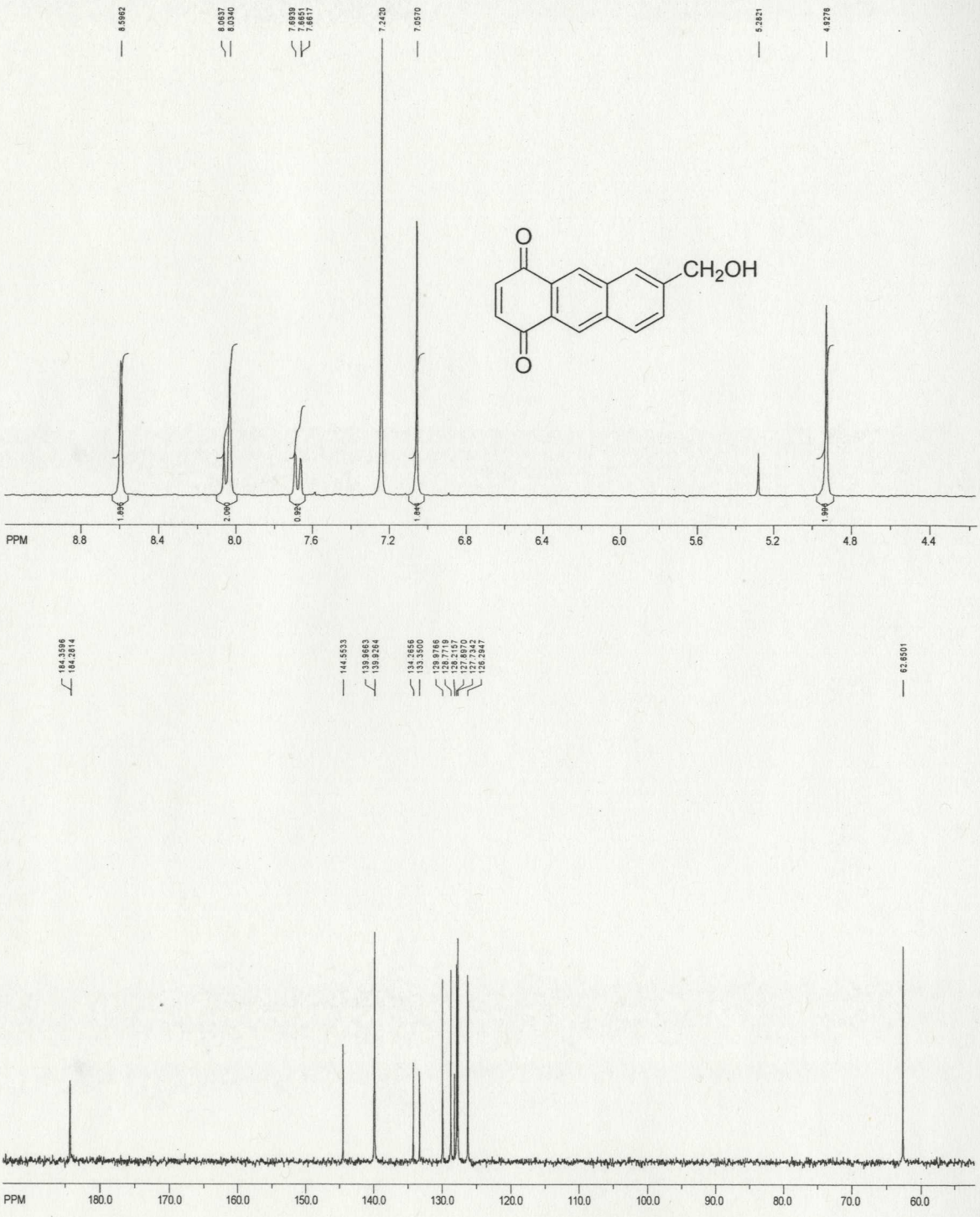

Figure A - 34 ^{1}H (top) and ^{13}C NMR (bottom) for 6-(hydroxymethyl)-1,4-anthraquinone (**4.3**) in $CDCl_3$ at 300 K.

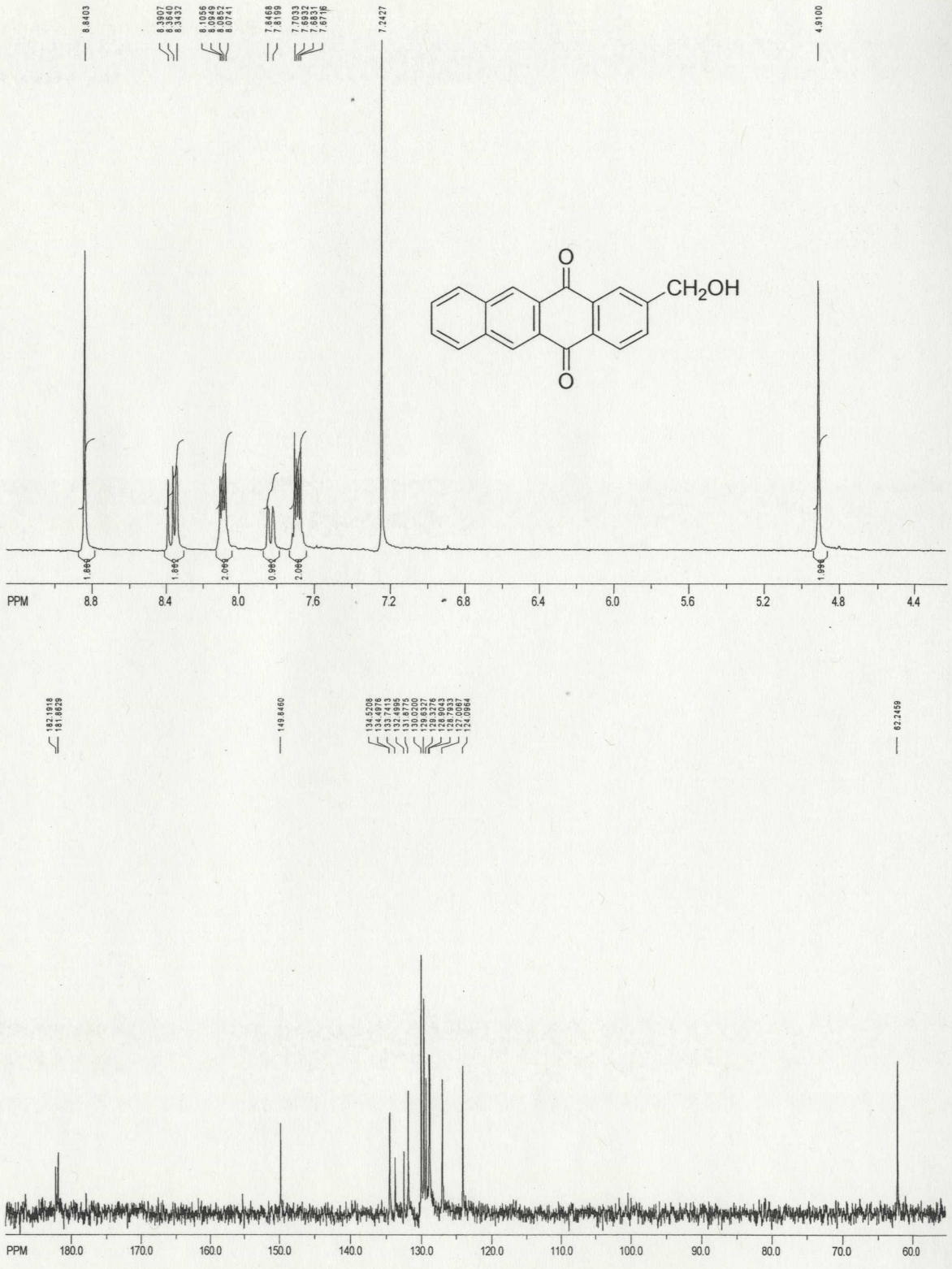

Figure A - 35 ^{1}H (in $CDCl_3$, top) and ^{13}C NMR (in DMSO-d_6, bottom) for 2-(hydroxymethyl)-5,12-naphthacenequinone (**4.4**) at 300 K.

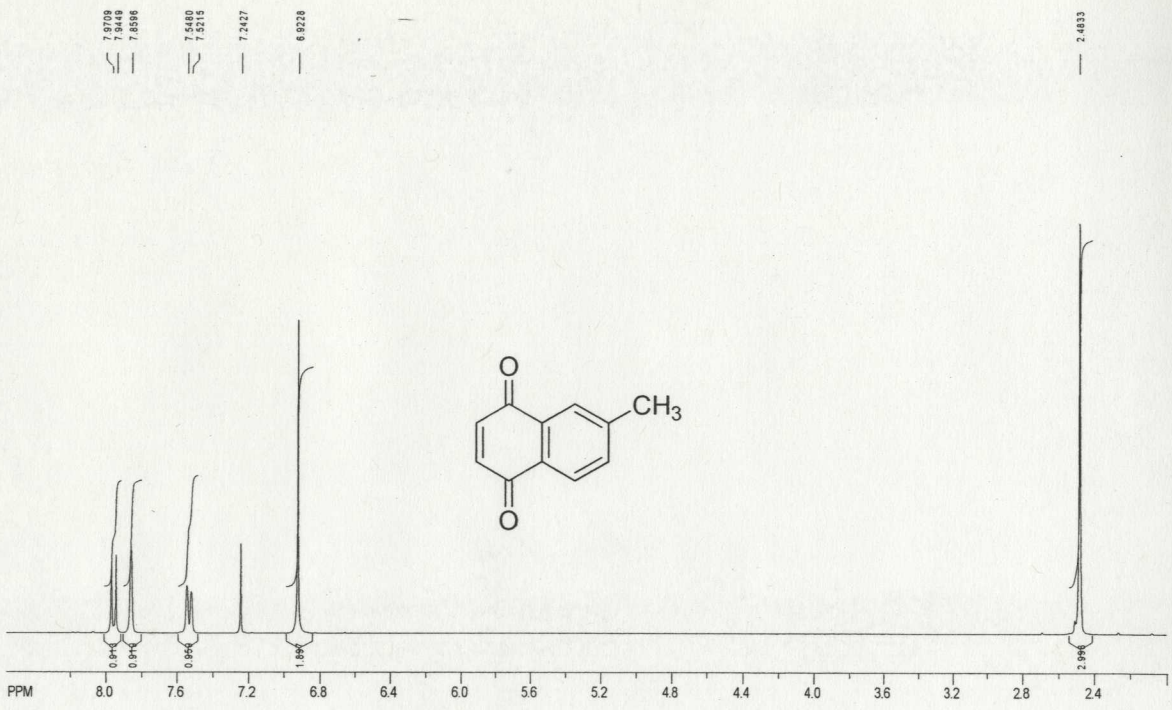

Figure A - 36 ^{1}H (top) and ^{13}C NMR (bottom) for 6-methyl-1,4-naphthoquinone (**4.2a**) in $CDCl_3$ at 300 K.

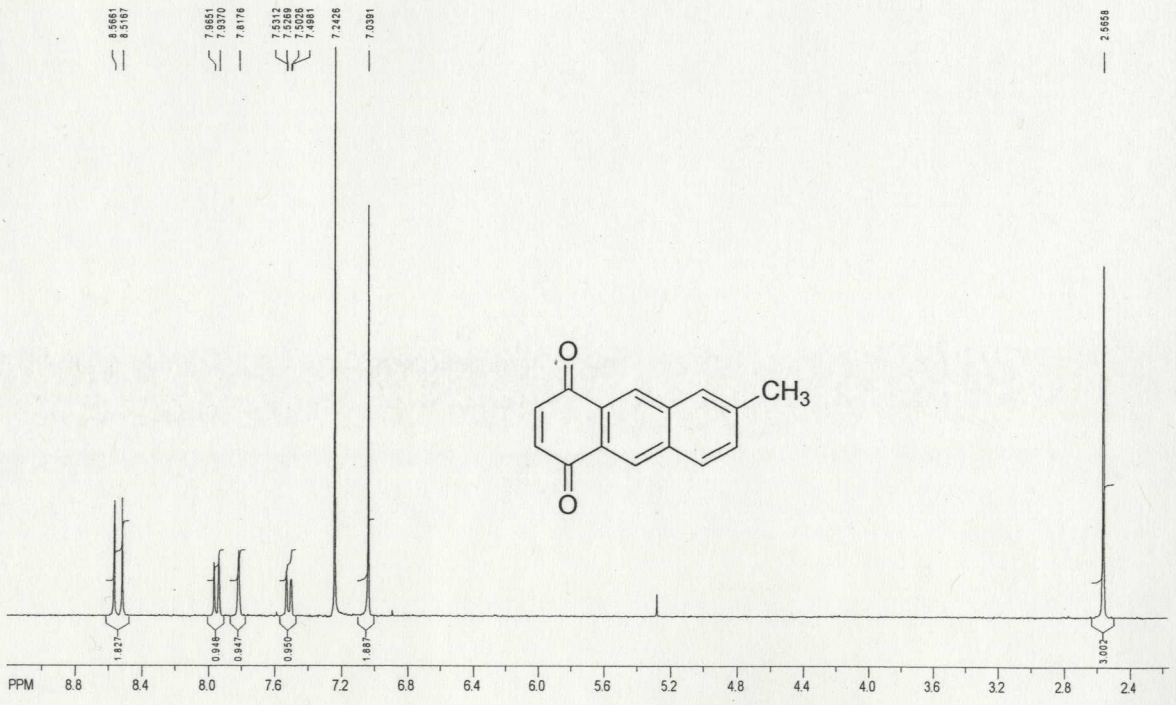

Figure A - 37 ^{1}H (top) and ^{13}C NMR (bottom) for 6-methyl-1,4-anthraquinone (**4.3a**) in $CDCl_3$ at 300 K.

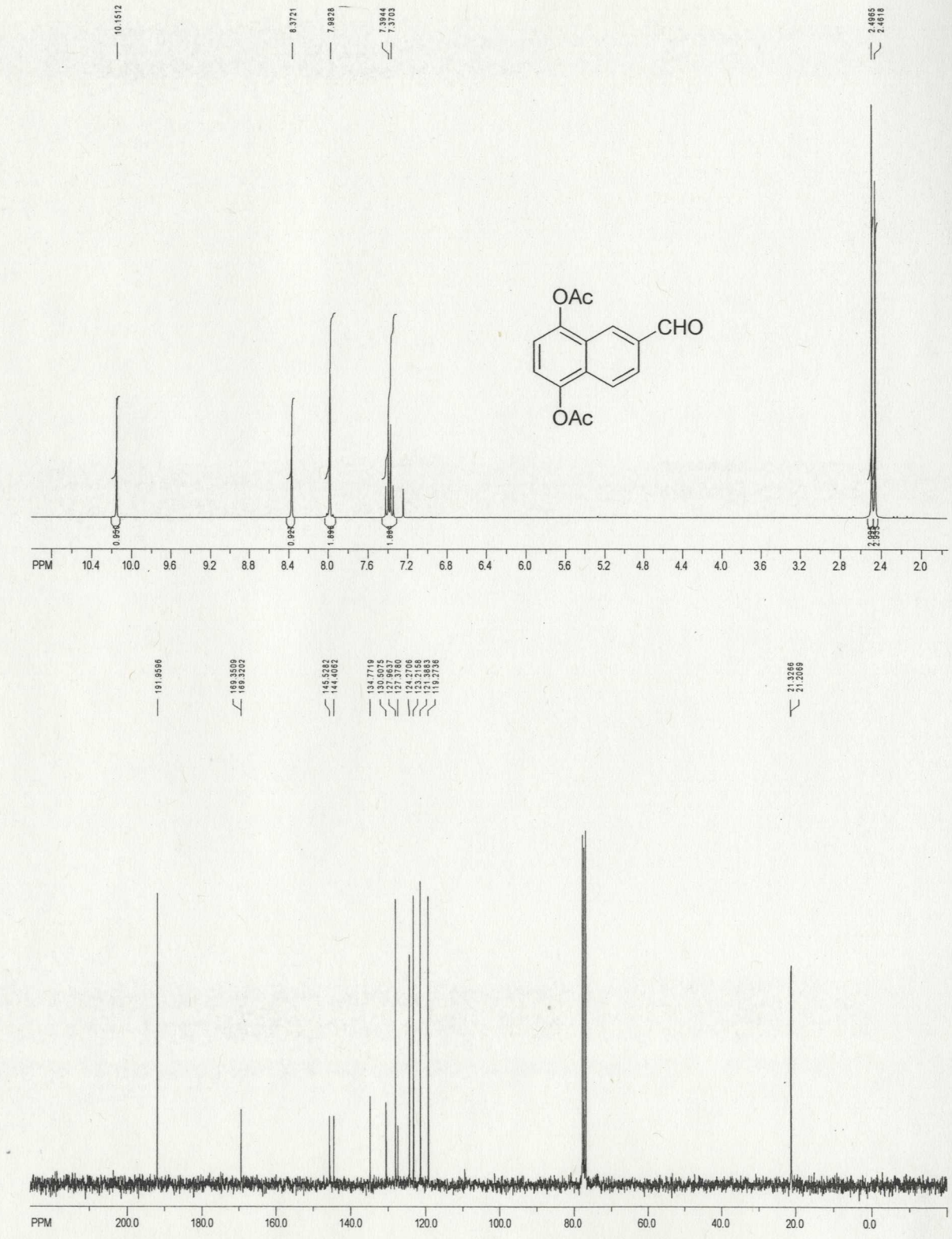

Figure A - 38 ^{1}H (top) and ^{13}C NMR (bottom) for 6-formyl-1,4-diacetoxynaphthalene (**4.7-OAc**) in $CDCl_3$ at 300 K.

Figure A - 39 ^{1}H (top) and ^{13}C NMR (bottom) for 6-formyl-1,4-naphthoquinone (**4.8**) in $CDCl_3$ at 300 K.

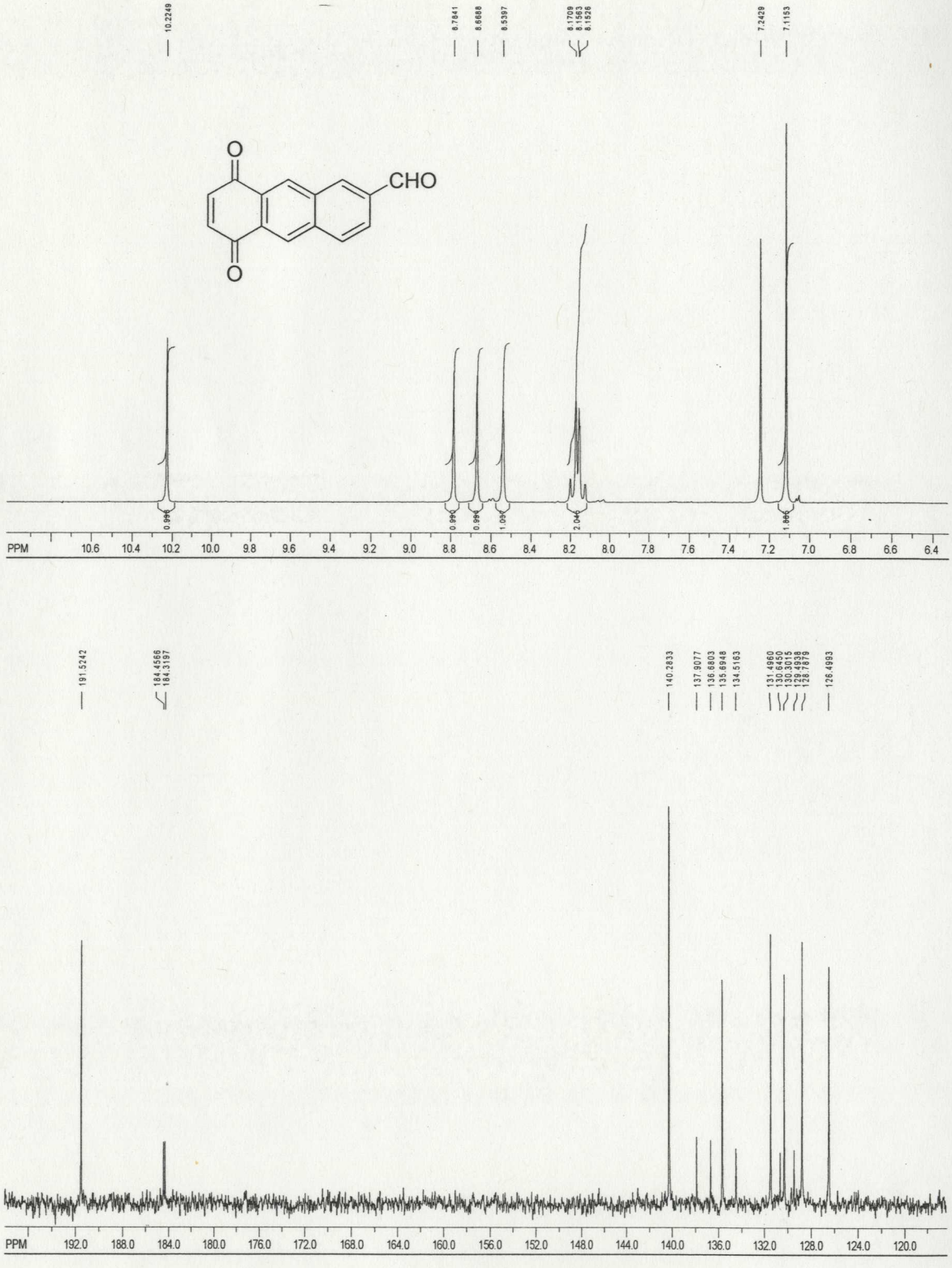

Figure A - 40 ^{1}H (top) and ^{13}C NMR (bottom) for 6-formyl-1,4-anthraquinone (**4.9**) in $CDCl_3$ at 300 K.

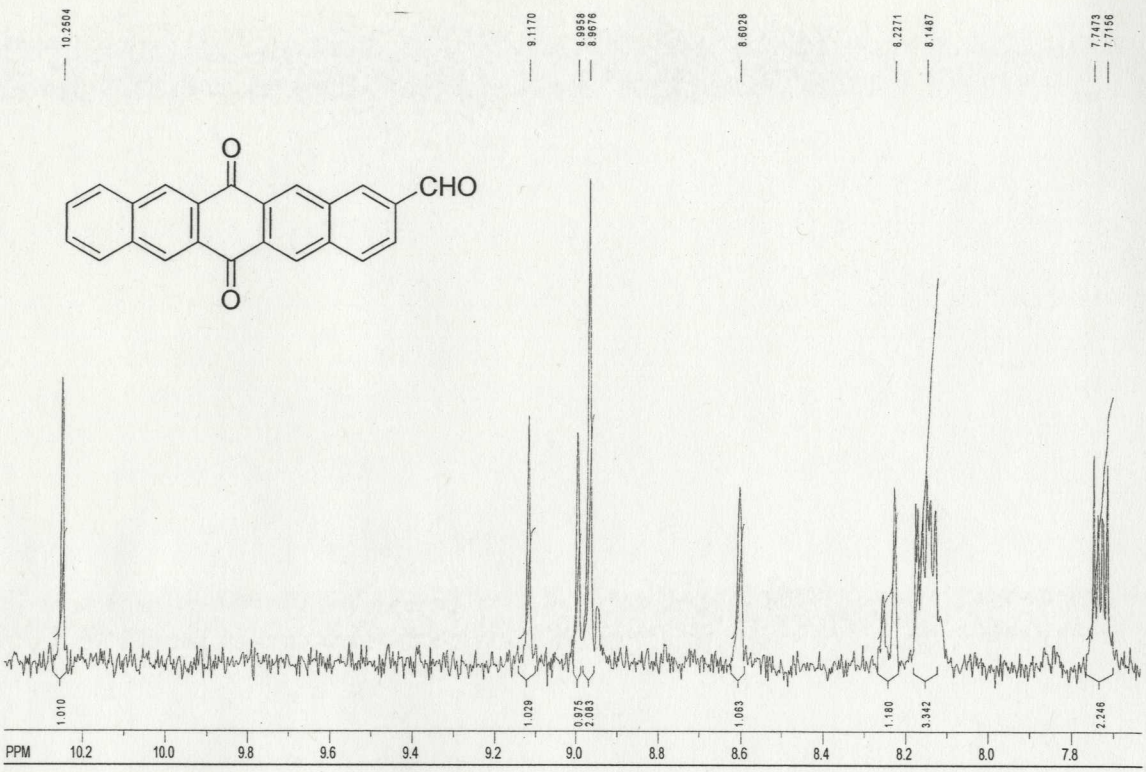

Figure A - 41 ^{1}H (top) and ^{13}C NMR (bottom) for 2-formyl-6,13-pentacenequinone (**4.6**) in $CDCl_3$ at 300 K.

Appendix B: UV-Vis Traces

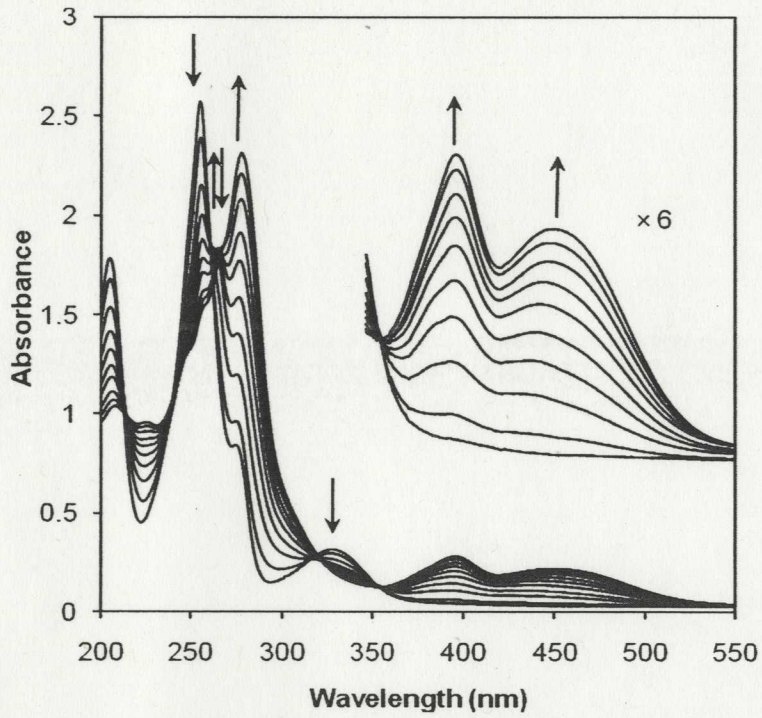

Figure B - 1 UV-Vis traces of the photoredox reaction of **2.3** in 1:1 H_2O-CH_3CN (λ_{ex} = 300 nm). Each trace represents 10 s of photolysis. Early photolysis resulted in loss of absorption (due to photoreaction of **2.3**) at 256 and 328 nm with formation of an observable intermediate (269 and 398 nm). This is subsequently transformed to **DHA** (over a 10 min period; loss of 269 nm band, formation of 280, 400 and 456 nm bands). Insert: six-fold expansion of the long wavelength region.

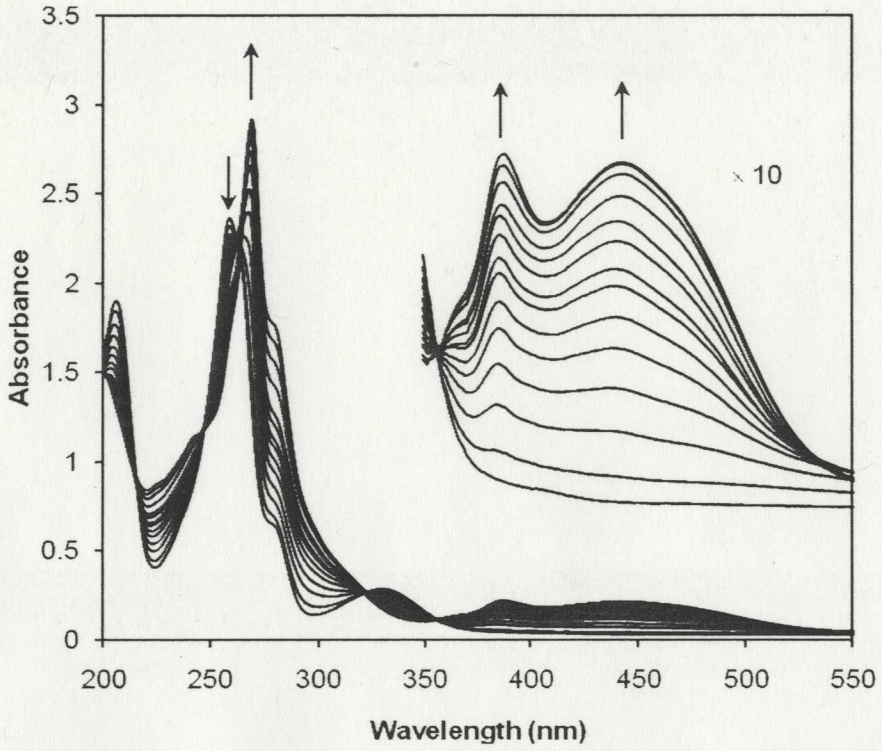

Figure B - 2 UV-Vis traces of the photoredox reaction of **2.6** in 1:1 H_2O-CH_3CN (λ_{ex} = 300 nm). Each trace represents 20 s of photolysis. Photolysis resulted in the loss of absorption (due to photoreaction of **2.3**) at 264 and 324 nm with formation of **2.13** (270 nm, 391 nm and 448 nm). Insert: ten-fold expansion of the long wavelength region

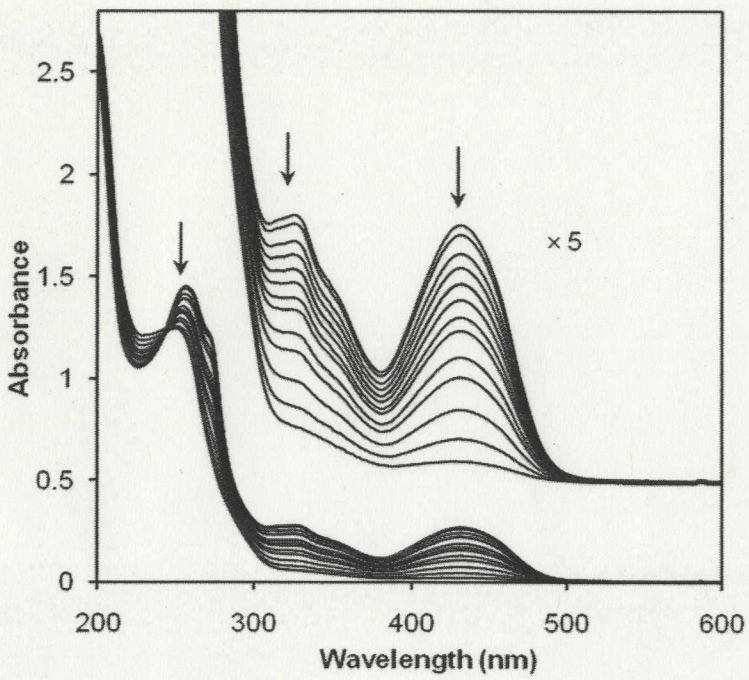

Figure B - 3 Decay of the photolysis product of diketone, diphenylisofuran **2.29** (1: 1 H_2O-CH_3CN, pH 0, 0-15min, 2 lamps, 300 nm in the presence of air). Each trace represents 1 min of photolysis. Photolysis resulted in the loss of absorption (due to the photoreaction of **2.29**) at 331 nm and 441 nm with formation of the photoredox product **2.30** (259 nm). Insert: five-fold expansion of the long wavelength region.

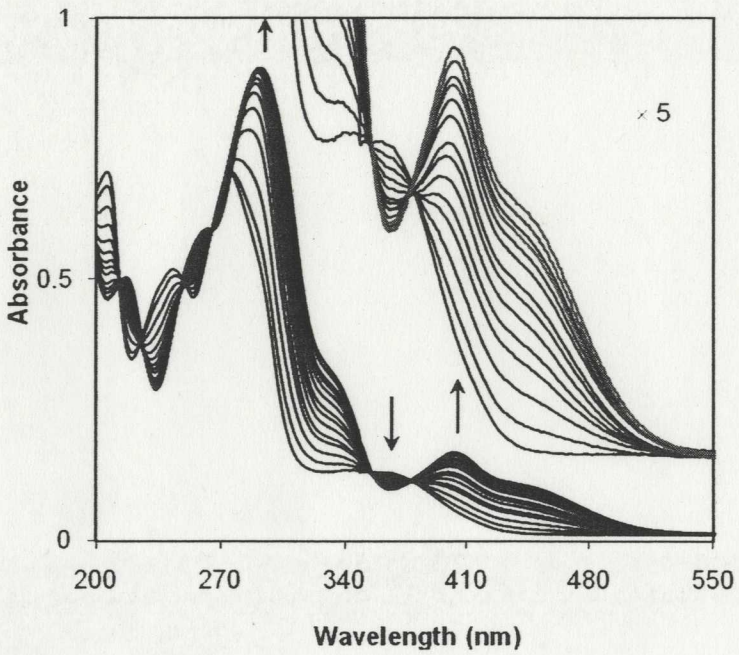

Figure B - 4 UV-Vis traces of photolysis of **3.3** in 1:1 H_2O-CH_3CN, pH 1 (λ_{ex} = 300 nm; argon purged). Each trace represents 5 s of photolysis. Photolysis resulted in the loss of absorption (due to the photoreaction of **3.3**) at 275 nm and 359 nm with formation of the photoredox product **3.10** (297, 408 and 457 nm). Inset: five-fold expansion of the long wavelength region.

Appendix C: Excitation and Fluorescence Spectrum

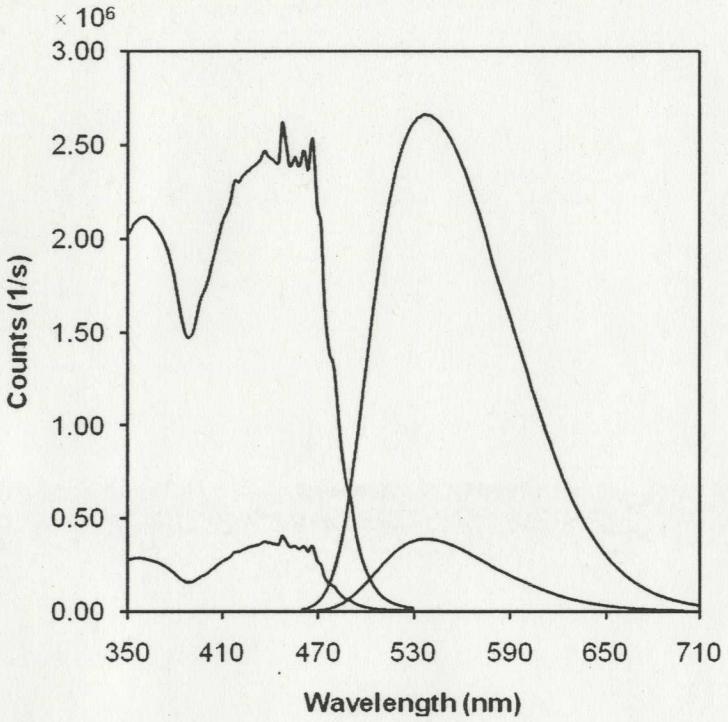

Figure C - 1 Excitation spectrum (left, λ_{em} = 550 nm) and fluorescence spectrum (right, λ_{ex} = 440 nm) of **2.29** (15 μmol/L in neat CH_3CN) before photolysis (top) and after photolysis in the presence of air (bottom).

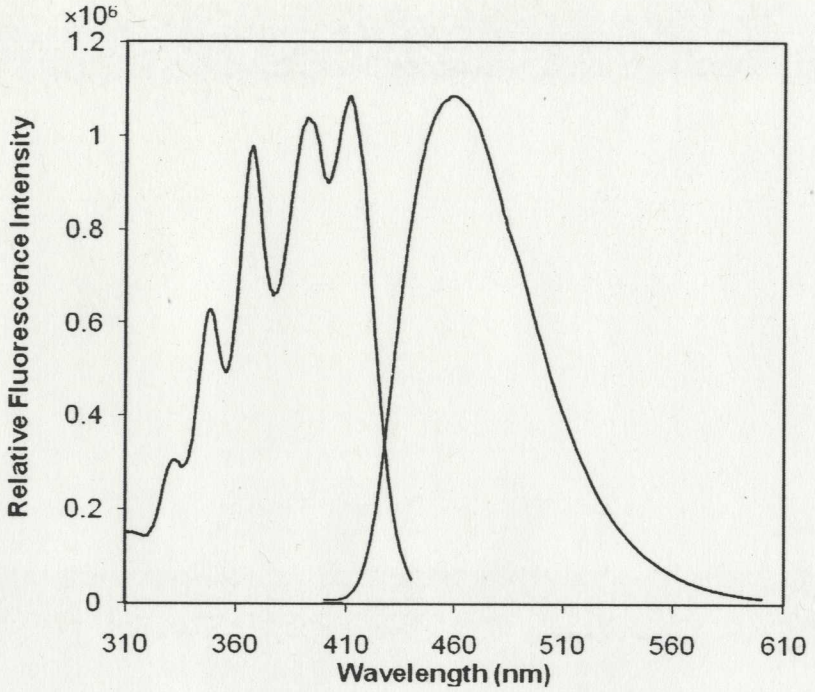

Figure C - 2 Excitation (left) and fluorescence spectrum (right) of **2.34** (23 μmol/L in neat CH_3CN). Emission wavelength:430 nm and excitation wavelength: 390 nm.

Appendix D: Others

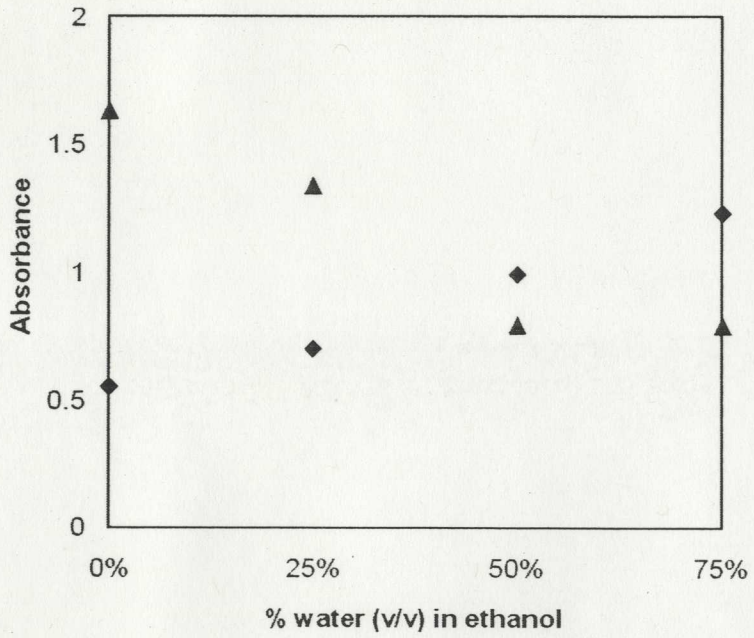

Figure D - 1 Solvent effect on the competition between intramolecular photoredox (formation of **DHA**) and simple photoreduction (formation of **2.33**) on photolysis of **HMAQ** in H_2O-CH_3CH_2OH mixtures; ■ absorption due to **DHA** at 280 nm; ▲ absorption due to **2.33** at 267 nm. Measurement error is about ± 5%.

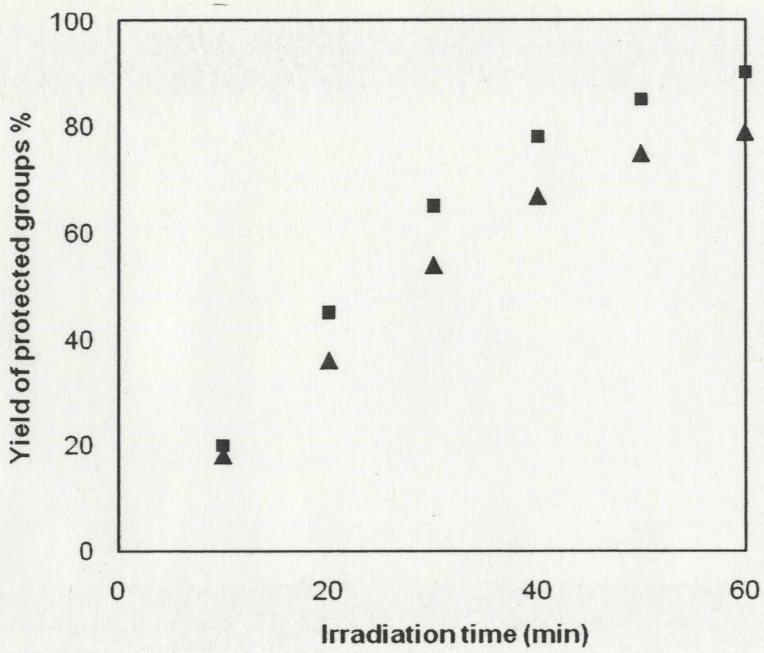

Figure D - 2 Yield of benzaldehyde (▲) and acetophenone (■) from photolysis of **2.5** and **2.6**, respectively, in 10% D_2O-CD_3CN (λ_{ex} 300 nm), as determined by ^1H NMR (relative to starting material). Measurement error is about ± 5%

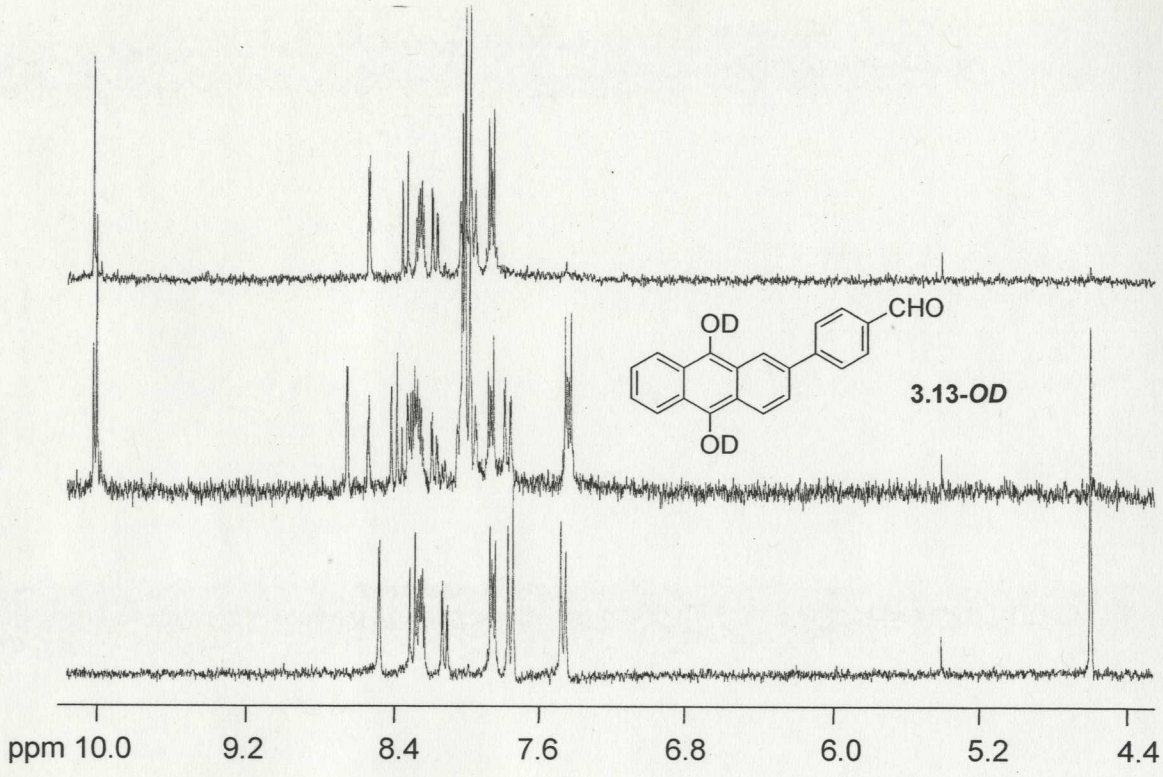

Figure D - 3 Proton NMR studies of photolysis of **3.3** in 10% D_2O-CD_3CN (pD 1, argon saturated). Bottom spectrum is **3.3** prior to photolysis, middle spectrum is **3.13-*OD***, and top spectrum is that of **3.10** (formed upon aeration of **3.13-*OD***).

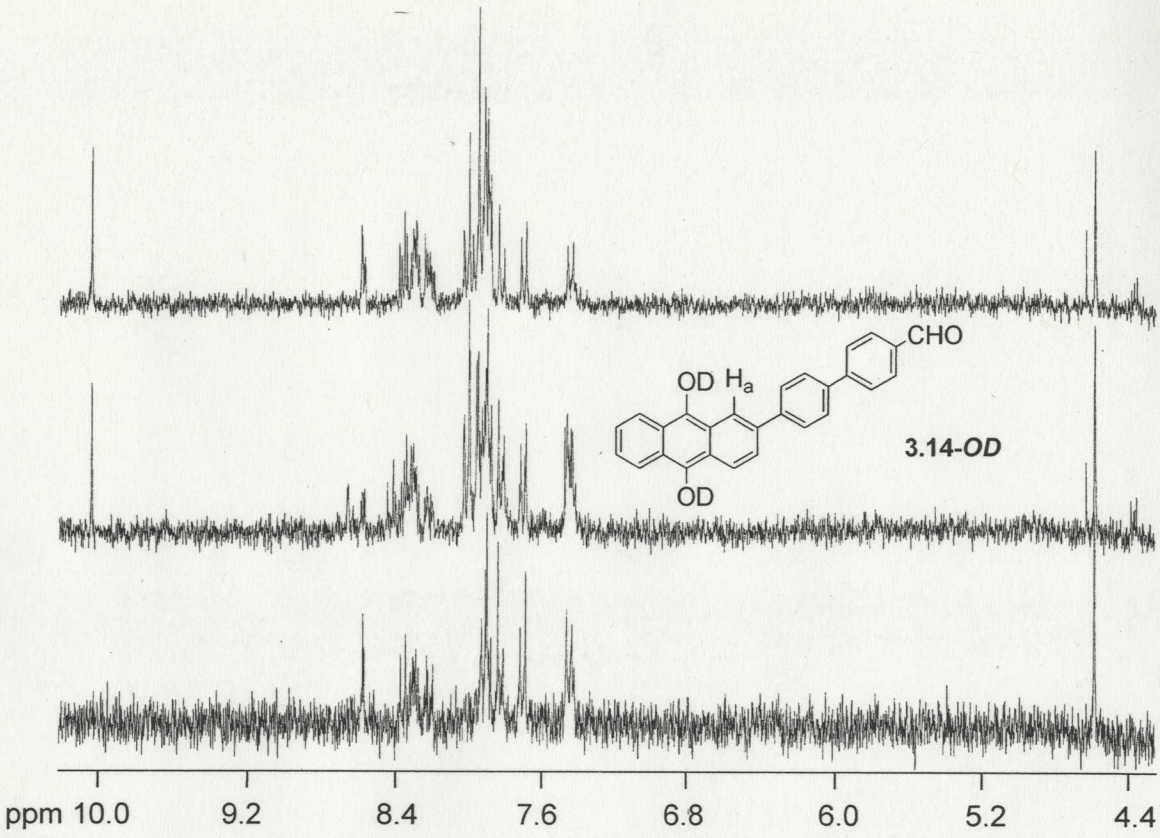

Figure D - 4 Proton NMR studies of photolysis of **3.4** in 10% D_2O-CD_3CN (pD 1, argon saturated). Bottom spectrum is **3.4** prior to photolysis, middle spectrum is **3.15-*OD***, and top spectrum is that of **3.14** (formed upon aeration of **3.15-*OD***).

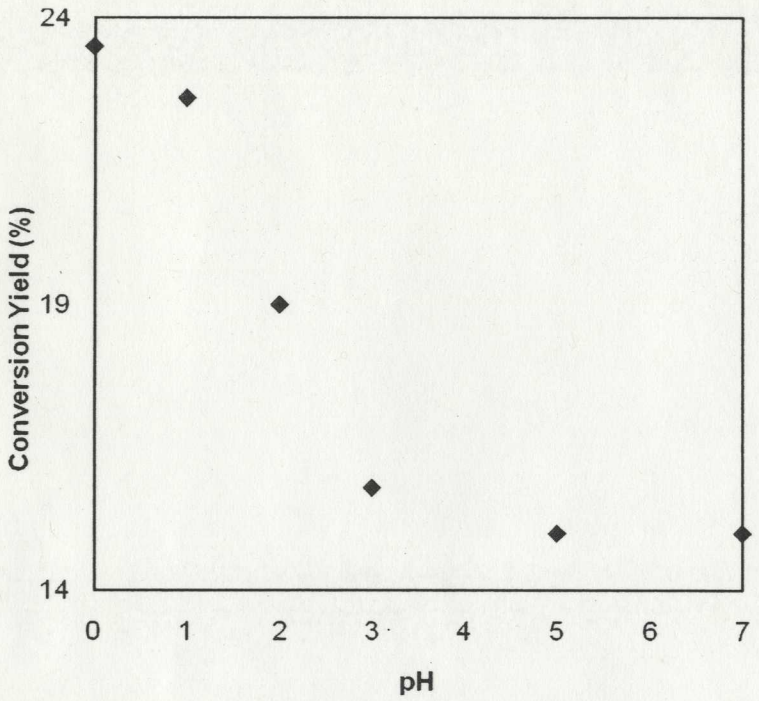

Figure D - 5 pH Dependence of intramolecular photoredox efficiency for **3.4** in 1:3 H_2O-CH_3CN, ~ 10^{-4}M, N_2 (pH refers to the aqueous portion). Measurement error is about ± 5%.